United States Environmental Protection Agency | Office of Air Quality Planning and Standards Research Triangle Park, NC 27711 | EPA-453/R-96-013c
October 1996

Air

EPA

Study of Hazardous Air Pollutant Emissions from Electric Utility Steam Generating Units -- Interim Final Report

Volume 3. Appendices H - M

TABLE OF CONTENTS

Appendix H—Summary of Speciation, Environmental Chemistry, and Fate of Eight HAPs Emitted from Utility Boiler Stacks

Appendix H is followed by Appendix H-1, List of Utility Boiler Test Reports, and Appendix H-2, Utility Boiler Stack Emisisons of Furans/Dioxins, PAHs, and Six Trace Metals.

This page is intentionally blank.

H.1 INTRODUCTION

Under Section 112(n)(1)(A) of the 1990 Clean Air Act Amendments (CAAA), Congress mandates that the U.S. Environmental Protection Agency (EPA) study the hazards to public health reasonably anticipated to occur as a result of emissions of hazardous air pollutants (HAPs) by electric utility steam generating units (utilities). EPA was to present the results of this study in a Report to Congress by November 15, 1995.

As part of this study, the EPA is conducting direct and indirect human exposure modeling. This document was prepared as part of EPA's indirect exposure modeling effort. It discusses the environmental chemistry, speciation, and fate of eight HAPs: arsenic, cadmium, chromium, lead, mercury, nickel, dioxins/furans, and polycyclic aromatic hydrocarbons (PAHs). The eight HAPs were investigated as to their form when emitted from a utility boiler stack (Section H.2) and their reactions (if any) and fate in the atmosphere, water, and soils (Section H.3) to better understand what HAPs or reaction products of HAPs humans are most likely to be exposed to via various routes of exposure (e.g., oral [ingestion], inhalation, dermal [skin]) as a result of emissions from utilities. This document summarizes the available information.

In preparing this report, test reports, published and unpublished literature, and other readily available information such as government documents (e.g., Agency for Toxic Substances and Disease Registry [ATSDR] toxicological profiles) and reference books were reviewed to identify information on the physical state, species, oxidative state, and anticipated aquatic and soil reaction products of the eight HAPs.

H.2 UTILITY TEST RESULTS

As part of a Congressionally mandated study of HAPs from electric steam generating units (utilities), the Department of Energy (DOE), the Northern States Power Company (NSP), and the Electric Power Research Institute (EPRI) conducted emissions tests at over 40 power plants for a variety of HAPs potentially present. Nine of the tests were performed for DOE, eight for NSP, and the remainder for EPRI. The EPRI sites were identified only by a site number; the other sites were identified by name. Of the tests performed, 33 were on coal-fired boilers, 12 were on oil-fired boilers, and 2 were on gas-fired boilers. The Agency reviewed test reports from 47 recent tests performed at 43 utility boiler sites. (Appendix H-1 lists the 47 test reports.)

Emission control systems tested for the coal-fired boilers included 13 electrostatic precipitators (ESPs), 3 fabric filters (FFs), 5 combined ESP flue-gas desulfurization (FGD) units, 6 combined FF FGD units, and one each of the following: a combined hot-side, cold-side ESP, an ESP with ammonia injection, a combined ESP and pulse-jet FF, and a fluidized-bed combustor (FBC) boiler with FF. Emission control systems for the oil-fired units were one ESP, one FF, one pulse-jet FF, two units that combined magnesium oxide (MgO) slurry fuel additive and an ESP, and one unit using MgO fuel additive and a selective catalytic reduction (SCR) nitrogen oxides/sulfur oxides (NO_x/SO_x) removal process. Seven of the oil-fired units had no emission control, and neither of the gas-fired units had emission controls. For some sites, more than one emission control system was tested, either as a pilot unit in parallel with an existing system or after replacement of an existing system with a new system. The representativeness of the data should allow the descriptive statistics presented here to withstand scrutiny.

All of the tests discussed here were performed in 1990 or later, with most of them performed in 1992 and 1993. The timing of the testing is important because of test method validity. For example, mercury tests performed before the introduction of new test methods in 1990 may provide suspect results.

The type of fuel, boiler, and emission controls can affect HAP emissions from a boiler stack. The data presented in this report could be analyzed to determine the qualitative effects of each of these variables for the trace metals and possibly for the dioxins/furans and PAHs.

H.2.1 Frequency of HAPs Occurrence

Appendix H-2 contains air emissions for the 6 trace metals (including some speciation for mercury, arsenic, chromium, and nickel), 16 individual polychlorinated dioxins and furan isomers and 9 congeners, and 29 PAHs (classified as polycyclic organic matter [POM] on the CAAA HAPs list) measured during the testing at utility boiler stations discussed in Section 2.0. These tables are based on 47 tests and 59 HAPs. Unlike other industries that measure emissions as metric weight per dry standard cubic meter (e.g., ng/dscm), the unit of measure in Appendix H-2 is $lb/10^{12}$ British thermal unit (Btu). This unit of measure is commonly used in the utility industry to report emissions relative to the amount of fuel burned.

At least one of the metals was measured in all of the 47 tests reported. In addition, mercury was measured in speciated forms in 10 emission tests, speciated chromium in

11 tests, speciated nickel in 2 tests, and speciated arsenic in 2 tests at one site. Dioxins and furans were measured at 12 test sites, but many of the reported averages contained one or more values below the detection limit. Of the 25 individual dioxin and furan isomers and congeners, most were found at 10 of the test sites. One or more of the 29 PAHs were found at 24 of the tests. However, measurements were scattered among sites and among individual PAHs. The most frequently measured PAHs were 2-methylnaphthalene, fluorene, fluoranthene, phenanthrene, and pyrene. All 29 PAHs except 1-chloronaphthalene, dibenz(a,j)acridine, 3-methylcholene, 7,12-dimethylbenz(a)anthracene, nitranthracene, and perylene were measured at least once.

H.2.2 Data Quality

The eight HAPs discussed in this report are present only in trace quantities in utility boiler stacks. In many cases, concentrations are near the detection limit of the analytical method being used. Additionally, the sampling process is carried out in large ducts (up to about 40 or 50 feet wide) carrying hot, particulate-laden gas streams that usually have irregular flow patterns. The combustion process may be irregular as to fuel characteristics and will change with load changes in the generating system. For example, coal fired on one day may be mined from the center of a seam rich in a trace metal, while coal fired on another day may be mined from a different area of the seam that is less rich in the trace metal. When power demand on a boiler is reduced, less fuel is fired and the combustion zone changes in dimension. However the size of the combustion chamber remains the same. This situation might change the distribution of combustion products in the flue gas and the partitioning of elements between fly ash and bottom ash. All of these factors combine to produce final analytical results that should be accepted with caution.

Additional uncertainties associated with combining measured concentrations of an analyte with averages of measured flow rates in a series of tests made over several days need to be considered when using these data. For example, the heating value of a coal feed may be measured on a Monday, but the concentration of a compound in the flue gas may not be measured until Tuesday. A resulting value of emission rate in $lb/10^{12}$ Btu will contain errors caused by the time difference in measurements.

Because of low or nonexistent concentrations of analytes, many measurements resulted in nondetects. Nondetects occurred when concentration values were so low that the analytical method could not determine if the analytes were present. For such

situations, the presence of an analyte in any individual test of a series (as shown by a concentration above the detection limit) was taken to mean that the analyte was present. The question then arose as to what concentration value to assign to any other measurement in the series when the measurement was below the detection limit. Common choices have been zero, half the detection limit, or the detection limit. For this report, tests showing nondetects were assumed to have an analyte concentration equal to half the detection limit.

In Tables H-2-1 through H-2-3 of Appendix H-2, essentially all values are calculated averages of more than one measurement. If all measurements forming one average are above the detection limit, the average is shown in an open box. If the average contains one or more nondetect values, the box is shaded. All averages contain at least one value above the detection limit, either at the stack or at some point prior to the stack.

H.2.3 Speciation Data

For the HAPs examined in this report, all 25 isomers and congeners of dioxins and furans are reported, as are most of the individual compounds listed as PAHs. Species within the trace metals are available for 20 tests and only for mercury, chromium, nickel, and arsenic. Each of the three categories of HAPs is discussed below. Numerical emission values are given in Tables H-2-1 through H-2-3 of Appendix H-2.

H.2.3.1 Dioxins and Furans. Table H-1 summarizes Appendix H-2 emissions of dioxins and furans measured at utility boilers.

In general, 2,3,7,8-TCDD and 2,3,7,8-TCDF emissions were approximately 10^{-6} lb/10^{12} Btu. With a few exceptions at 10^{-5} lb/10^{12} Btu and 10^{-4} lb/10^{12} Btu and one exception at 10^{-3} lb/10^{12} Btu, other forms had similar values.

H.2.3.2 PAHs. Eight of the PAHs are of particular interest due to their probable carcinogenicity under EPA's category B2 (weight of evidence from animal testing). These are benz(a)anthracene, benzo(b)fluoranthene, benzo(b and k)fluoranthene, benzo(k)fluoranthene, benzo(a)pyrene, chrysene, dibenz(a,h)anthracene, and indeno(1,2,3-c,d)pyrene. Table H-2 shows median values and ranges for each of the eight as well as other frequently measured PAHs.

Table H-1. Emissions of Dioxins/Furans from Utility Boilers ($lb/10^{12}$ Btu)

Specific Dioxin or Furan	Median	Maximum / Minimum
2,3,7,8-Tetrachlorodibenzo-p-dioxin	2.30×10^{-6}	6.51×10^{-6} / 3.50×10^{-7}
1,2,3,7,8-Pentachlorodibenzo-p-dioxin	4.38×10^{-6}	6.51 x 10-6 / 6.03 x 10-7
1,2,3,4,7,8-Hexachlorodibenzo-p-dioxin	1.05×10^{-5}	1.52 x 10-5 / 1.21 x 10-6
1,2,3,6,7,8-Hexachlorodibenzo-p-dioxin	5.44×10^{-6}	1.83 x 10-5 / 6.03 x 10-7
1,2,3,7,8,9-Hexachlorodibenzo-p-dioxin	8.34×10^{-6}	1.92 x 10-5 / 6.03 x 10-7
1,2,3,4,6,7,8-Heptachlorodibenzo-p-dioxin	1.23×10^{-5}	3.27 x 10-4 / 5.99 x 10-7
Octachlorodibenzo-p-dioxin	4.07×10^{-5}	1.71 x 10-3 / 4.79 x 10-6
2,3,7,8-Tetrachlorodibenzofuran	3.94×10^{-6}	4.55×10^{-5} / 6.68×10^{-7}
1,2,3,7,8-Pentachlorodibenzofuran	2.89×10^{-6}	2.09×10^{-5} / 6.89×10^{-7}
2,3,4,7,8-Pentachlorodibenzofuran	6.51×10^{-6}	4.83×10^{-5} / 1.62×10^{-6}
1,2,3,4,7,8-Hexachlorodibenzofuran	8.08×10^{-6}	2.56×10^{-4} / 2.79×10^{-6}
1,2,3,6,7,8-Hexachlorodibenzofuran	3.99×10^{-6}	8.77×10^{-5} / 7.33×10^{-7}
1,2,3,7,8,9-Hexachlorodibenzofuran	6.30×10^{-6}	1.75×10^{-5} / 6.03×10^{-7}
2,3,4,6,7,8-Hexachlorodibenzofuran	1.05×10^{-5}	1.88×10^{-4} / 9.99×10^{-7}
1,2,3,4,6,7,8-Heptachlorodibenzofuran	1.67×10^{-5}	1.18×10^{-3} / 1.36×10^{-6}
1,2,3,4,7,8,9-Heptachlorodibenzofuran	1.01×10^{-5}	5.67×10^{-4} / 1.21×10^{-6}
Octachlorodibenzofuran	1.39×10^{-5}	8.21×10^{-3} / 7.99×10^{-7}
Tetrachlorodibenzo-p-dioxin	6.61×10^{-6}	5.97×10^{-5} / 1.24×10^{-6}
Pentachlorodibenzo-p-dioxin	5.76×10^{-6}	4.22×10^{-5} / 6.89×10^{-7}
Hexachlorodibenzo-p-dioxin	1.60×10^{-5}	1.80×10^{-4} / 8.76×10^{-7}
Heptachlorodibenzo-p-dioxin	2.56×10^{-5}	6.00×10^{-4} / 2.34×10^{-6}
Tetrachlorodibenzofuran	9.68×10^{-6}	1.49×10^{-4} / 1.37×10^{-6}
Pentachlorodibenzofuran	1.16×10^{-5}	2.89×10^{-4} / 2.89×10^{-6}
Hexachlorodibenzofuran	1.50×10^{-5}	7.62×10^{-4} / 3.85×10^{-6}
Heptachlorodibenzofuran	1.91×10^{-5}	2.63×10^{-3} / 2.54×10^{-6}

Btu = British thermal unit.

Table H-2. Emissions of Selected PAHs from Fossil-Fuel-Fired Utility Boilers

PAH[a]	Frequency of detection (from up to 47 individual tests)	Median (lb/10^{12} Btu)	Maximum/minimum (lb/10^{12} Btu)
Benz(a)anthracene (c)	9	3.53×10^{-3}	1.41×10^{-1} / 1×10^{-3}
Pyrene (f)	14	1.26×10^{-2}	1.60×10^{-1} / 1.21×10^{-3}
Benzo(b)fluoranthene (c)	1	808×10^{-3}	only one value
Benzo(b and k)fluoranthene (c)	5	6.65×10^{-3}	4.79×10^{-2} / 1.61×10^{-3}
Benzo(k)fluoranthene (c)	1	3.56×10^{-3}	only one value
Benzo(a)pyrene (c)	8	1.02×10^{-3}	3.67×10^{-2} / 2.27×10^{-4}
Chrysene (c)	9	3.56×10^{-3}	5.99×10^{-2} / 3.30×10^{-4}
Dibenz(a,h)anthracene (c)	4	2.70×10^{-3}	1.32×10^{-2} / 3.30×10^{-4}
Indeno(1,2,3-c,d)pyrene (c)	6	6.40×10^{-3}	3.59×10^{-2} / 1.65×10^{-3}
2-Methylnaphthalene (f)	12	2.34×10^{-2}	2.15×10^{-2} / 1.72×10^{-3}
Fluorene (f)	13	1.35×10^{-2}	1.72×10^{-1} / 1.29×10^{-3}
Fluoranthene (f)	15	9.89×10^{-3}	2.81×10^{-3} / 9.58×10^{-2}
Phenanthrene (f)	17	2.66×10^{-2}	3.08×10^{-1} / 9.37×10^{-3}

Btu = British thermal unit.
[a] (c) indicates suspected carcinogen; (f) indicates measured frequency greater than 10.

With one exception, all of the median values are on the order of 10^{-3} lb/10^{12} Btu. The exception, pyrene, is approximately 1.3 x 10^{-2} lb/10^{12} Btu. Ranges run from 10^{-4} lb/10^{12} Btu to 10^{-1} lb/10^{12} Btu.

Of the PAHs not listed in Table H-2, all, with the exception of biphenyl, have median values in the 10^{-2} lb/10^{12} Btu or 10^{-3} lb/10^{12} Btu range. Biphenyl has a median value of about 1.8 x 10^{-1} lb/10^{12} Btu. Ranges generally run from about 10^{-4} lb/10^{12} Btu to 10^{-1} lb/10^{12} Btu.

H.2.3.3 Trace Metals. Four of the metals (mercury, chromium, nickel, and arsenic) had speciation data (see Table H-3). All of the metals were measured in nonspeciated form at nearly all sites. Most of the measurements were made in the test site stack or ductwork ahead of the stack. However, a few measurements were made at the outlet of a pilot or full-scale device operating in parallel with ductwork or other control devices. All of the measurements represent values that, in the absence of chemical reaction, should be found being emitted to the atmosphere after passing through the control device indicated in Table H-2-3 (Appendix H-2).

The median value for lead was 3.78 lb/10^{12} Btu, with a range of 1.1 x 10^{-1} lb/10^{12} Btu to 176 lb/10^{12} Btu. The median value for cadmium was 1.24 lb/10^{12} Btu with a range of 2.33 x 10^{-2} lb/10^{12} Btu to 28.5 lb/10^{12} Btu. The four speciated metals are discussed separately.

H.2.3.3.1 Mercury. Although total mercury was measured at most of the sites, elemental mercury and ionic mercury were measured at only 10 sites. Several of the sites attempted measuring methyl mercury with the Bloom method.[1] However, the method does not provide consistently accurate methyl mercury measurements. A resolution to this problem is to add reported methyl mercury values to reported ionic mercury values (for the same test) and report the sum as ionic mercury. This procedure is followed here.

Total mercury had a median value of 3.44 lb/10^{12} Btu, with a range of 6.60 x 10^{-2} lb/10^{12} Btu to 22.9 lb/10^{12} Btu. The sum of the median values for elemental mercury (1.44 lb/10^{12} Btu) and ionic mercury (1.93 lb/10^{12} Btu) was about the same value as for total mercury. This agreement is surprisingly good, considering

Table H-3. Emissions of Selected Trace Metals from Fossil-Fuel-Fired Utility Boilers

Trace metal	Frequency of detection (from up to 47 individual tests)	Average		Median		Standard deviation	5th percentile[a]	
		lb/10^{12} BTU	Percent of Species	lb/10^{12} BTU	Percent of Species	lb/10^{12} BTU	lb/10^{12} BTU	Percent of Species
Lead in coal and oil	43	13.5	NA	3.78	NA	14.8		
Lead in coal	30	10.3	NA	3.78	NA	16.6		
Lead in oil	10	8.61	NA	6.32	NA	8.83		
Mercury in coal and oil	38	4.53	NA	3.44	NA	5.02		
Elemental mercury in coal and oil	10[b,c]	3.40	62	1.44[d]	43	4.54	0.170	62
Ionic mercury in coal and oil	10[b,c]	2.12	38	1.93[e]	57	1.89	0.106	38
Mercury in coal	33	5.43	NA	3.93	5.12	5.12		
Elemental mercury in coal	9[b]	3.40	59	1.44	40	4.54	0.170	59
Ionic mercury coal	9[b]	2.35	41	2.16	60	1.85	0.118	41
Mercury in oil	5	0.658	NA	0.400	NA	0.825		
Elemental mercury in oil	0	f	f	f	f	f	f	f
Ionic mercury in oil	1[b]	0.027	NA	0.027	NA	NA	NA	NA
Cadmium in coal and oil	40	2.79	NA	1.24	NA	4.89		
Cadmium in coal	30	3.21	NA	1.49	NA	5.55		
Cadmium in oil	10	1.51	NA	0.970	NA	1.41		

Table H-3. (continued)

Trace metal	Frequency of detection (from up to 47 individual tests)	Average		Median		Standard deviation	5th percentile[a]	
		lb/10^{12} BTU	Percent of Species	lb/10^{12} BTU	Percent of Species	lb/10^{12} BTU	lb/10^{12} BTU	Percent of Species
Arsenic in coal and oil	47	9.98	NA	2.25	NA	21.4		
Arsenic in coal	36	11.8	NA	15.8	NA	24.6		
Trivalent arsenic in coal	2[b,g]	0.486	39	4.86×10^{-1}[h]	39	0.258	0.0243	39
Pentavalent arsenic in coal	2[b,g]	0.772	61	7.72×10^{-1}[i]	61	0.852	0.0386	61
Arsenic in oil	11	6.25	NA	3.63	NA	7.80		
Nickel in coal and oil	46	165	NA	5.45	NA	397		
Nickel in coal	34	19.4	NA	4.54	NA	60.4		
Nickel in oil	12	581	NA	372	NA	616		
Soluble nickel in oil	2[b,j]	628	58	6.28×10^{2}[k]	58	616	31.5	58
Sulfidic nickel in oil	2[b,j]	37.8	3	3.78×10^{1}[l]	3	49.8	1.89	3
Metallic nickel in oil	0	f	f	f	f	f	f	f
Nickel oxides in oil	2[b,j]	422	39	4.22×10^{2}[m]	39	584	21.1	39
Chromium in coal and oil	45	13.4	89	6.42	88	22.9	0.67	89
Hexavalent chromium in coal and oil	11[b,n]	1.63	11	8.89×10^{-1}[o]	12	1.9	0.082	11
Chromium in coal	34	15.8	89	7.00	90	25.9	0.792	89
Hexavalent chromium in coal	4[b]	1.90	11	0.772	10	2.78	0.095	11
Chromium in oil	11	5.94	80	3.48	77	5.49	0.297	80
Hexavalent chromium in oil	7[b]	1.48	20	1.04	23	1.44	0.074	20

Table H-3. (continued)

Trace metal	10th percentile[a]		90th percentile[a]		95th percentile[a]		Maximum/minimum (lb/10^{12} BTU)
	lb/10^{12} BTU	Percent of Species	lb/10^{12} BTU	Percent of Species	lb/10^{12} BTU	Percent of Species	
Lead in coal and oil							1.76×10^{2} / 1.1×10^{-1}
Lead in coal							76.5 / 0.110
Lead in oil							27.8 / 0.300
Mercury in coal and oil							2.29×10^{1} / 6.6×10^{-2}
Elemental mercury in coal and oil	0.340	62	9.23	67	10.9	68	1.47×10^{1} / 4.6×10^{-1}
Ionic mercury in coal and oil	0.212	38	4.55	33	5.24	32	5.49 / 2.72×10^{-2}
Mercury in coal							22.9 / 0.350
Elemental mercury in coal	0.340	59	9.23	66	10.9	67	5.35 / 0.460
Ionic mercury coal	0.235	41	4.73	34	5.40	33	5.49 / 0.075
Mercury in oil							2.11 / 0.066
Elemental mercury in oil	f	f	f	f	f	f	f
Ionic mercury in oil	NA	NA	NA	NA	NA	NA	NA
Cadmium in coal and oil							2.85×10^{1} / 2.33×10^{-2}
Cadmium in coal							28.5 / 0.0023
Cadmium in oil							3.97 / 0.130
Arsenic in coal and oil							1.04×10^{2} / 4×10^{-2}

Table H-3. (continued)

Trace metal	10th percentile[a]		90th percentile[a]		95th percentile[a]		Maximum/minimum (lb/10^{12} BTU)
	lb/10^{12} BTU	Percent of Species	lb/10^{12} BTU	Percent of Species	lb/10^{12} BTU	Percent of Species	
Arsenic in coal							
Trivalent arsenic in coal	0.0486	39	0.818	30	0.911	30	6.69×10^{-1} / 3.03×10^{-1}
Pentavalent arsenic in coal	0.077	61	1.87	70	2.17	70	1.38 / 1.7×10^{-1}
Arsenic in oil							27 / 0.040
Nickel in coal and oil							2.15×10^{3} / 3×10^{-2}
Nickel in coal							340 / 0.003
Nickel in oil							2,150 / 0.640
Soluble nickel in oil	63.1	58	1,740	58	2,050	58	1.24×10^{3} / 2.13×10^{1}
Sulfidic nickel in oil	3.78	3	102	3	120	3	7.3×10^{1} / 2.6
Metallic nickel in oil	f	f	f	f	f	f	f
Nickel oxides in oil	42.2	39	1,170	39	1,380	39	8.35×10^{2} / 9.0
Chromium in coal and oil	1.34	89	42.8	91	51.1	91	1.38×10^{2} / 4.11×10^{-1}
Hexavalent chromium in coal and oil	0.163	11	4.07	9	4.76	9	6.04 / 2.37×10^{-2}
Chromium in coal	1.58	89	49.1	90	58.4	90	138 / 0.411
Hexavalent chromium in coal	0.190	11	5.48	10	6.48	10	6.40 / 0.024
Chromium in oil	0.594	80	13.0	80	15.0	80	19.9 / 1.70
Hexavalent chromium in oil	0.148	20	3.33	20	3.85	20	3.78 / 0.186

Table H-3. (continued)

BTU = British thermal unit.

NA = not applicable.
Open cells indicate nonspeciated elements.

a Percentiles were found as areas under a normal curve constructed from the average and standard deviation of each sample population. Where the 5th and 10th percentiles were negative numbers, they were replaced by finding the 5th and 10th percent values between zero and the population average.
b Tests for speciated metals were only performed for a portion of the 47 tests.
c Nine coal-fired boilers; one oil-fired boiler. Elemental and ionic mercury were measured at the same 10 sites.
d Represents 43 percent of total speciated mercury for the 10 sites, on average. Percentages ranged from 9 to 96.
e Represents 57 percent of total speciated mercury for the 10 sites, on average. Percentages ranged from 4 to 91.
f Elemental mercury not detected in the one sample of oil tested. Metallic nickel not detected in the two samples of oil tested.
g Coal-fired boilers; species measured at the same two sites.
h Represents 39 percent of total speciated arsenic for the two sites, on average. Percentages ranged from 33 to 64.
i Represents 61 percent of total speciated arsenic for the two sites, on average. Percentages ranged from 36 to 67.
j Oil-fired boilers; species measured at the same two sites. Examples of soluble nickel include water-soluble salts such as nickel sulfate and nickel sulfide. Examples of sulfidic nickel include Ni_3S_2, NiS, and Ni_3S_4. Examples of nickel oxides include NiO, complex oxides, and silicates. Most of these compounds have a valence state of 2.
k Represents 58 percent of total speciated nickel for the two sites, on average. Percentages ranged from 58 to 65.
l Represents 3 percent of total speciated nickel for the two sites, on average. Percentages ranged from 3 to 8.
m Represents 39 percent of total speciated nickel for the two sites, on average. Percentages ranged from 27 to 39.
n Four coal-fired boilers; seven oil-fired boilers.
o Represents 10 percent of total speciated chromium for the 11 sites, on average. Percentages ranged from 0.4 to 34.

that different test methods were used for measuring total mercury and for measuring species. Ranges for elemental and ionic mercury (mercury (+2)) were 4.60×10^{-1} lb/10^{12} Btu to 14.7 lb/10^{12} Btu and 2.72×10^{-2} lb/10^{12} Btu to 5.49 lb/10^{12} Btu, respectively. The split between elemental and ionic mercury was not consistent from one site to another. About half the sites had more ionic mercury, while the rest have more elemental mercury. The average proportion of elemental mercury from 10 test sites was 62 percent, while the ionic mercury was 38 percent. When median values are used, 43 percent was elemental and 57 percent was ionic. For coal only, the average values from 9 samples were 59 percent for elemental mercury and 41 percent for ionic mercury (median percentages were 40 and 60 for elemental and ionic, respectively). For oil, only one sample was found to contain ionic mercury; elemental mercury was not detected. Statistics on a percentage basis for mercury are given in Table H-4.

H.2.3.3.2 Chromium. Total chromium was measured at most sites. The median value was 6.42 lb/10^{12} Btu, with a range of 4.11×10^{-1} lb/10^{12} Btu to 13.8 lb/10^{12} Btu. The median value for the 11 tests showing chromium (VI) was 8.89×10^{-1} lb/10^{12} Btu with a range of 2.37×10^{-2} lb/10^{12} Btu to 6.04 lb/10^{12} Btu. The amount of chromium (VI) for these 11 test sites averaged 11 percent (median 12 percent) of all speciated chromium, with a range of 0.4 percent to 34 percent. Separate tests for chromium (III) were not made. When divided between coal- and oil-fired utilities, chromium (VI) averaged 11 percent (median 10 percent) for the four coal-fired sites, with a range from 0.4 percent to 23 percent. Seven oil-fired boilers averaged 20 percent chromium (VI) (median 23 percent), with a range from 5 percent to 34 percent. No other sites were available for testing.

It should be noted that chromium (VI) is easily reduced to chromium (III) when in reducing conditions. Stack conditions lead to rapid reduction of existing chromium (VI), as experienced during field testing.[2] This factor may influence (reduce) the levels of chromium (VI) measured in the stack and downwind from the stack while the chromium (VI) remains in reducing conditions. Even in ambient conditions, the half-life of chromium (VI) is about 15 hours. Table H-5 gives statistics on a percentage basis for speciated chromium.

Table H-4. Mercury Emissions from Fossil-Fuel-Fired Utility Boilers

Species	Frequency of detection (from up to 47 individual tests)	Range, (percent of species)	Average (percent of species)	Median (percent of species)	5th percentile (percent of species)	10th percentile (percent of species)	90th ercentile (percent of species)	95th percentile (percent of species)	Maximum % /minimum %
Elemental mercury in coal and oil	10	87	62	43	62	62	67	68	96/9
Ionic mercury in coal and oil	10	79	38	57	38	38	33	32	91/12
Elemental mercury in coal	9	87	59	40	59	59	66	67	96/9
Ionic mercury coal	9	79	41	60	41	41	34	33	91/12
Elemental mercury in oil	0	a	a	a	a	a	a	a	a
Ionic mercury in oil	1	NA	100	100	NA	NA	NA	NA	NA

a Elemental mercury not detected in the one sample of oil tested.
NA means not applicable.

H.2.3.3.3 Arsenic. Total arsenic was measured at nearly all sites, but only one site provided data on the presence of arsenic (III) and arsenic (V). Two tests were made at that site. Total arsenic had a median value of 2.25 $lb/10^{12}$ Btu and a range of 4×10^{-2} $lb/10^{12}$ Btu to 10^{4} $lb/10^{12}$ Btu. The median value for arsenic (III) was 4.86×10^{-1} $lb/10^{12}$ Btu and for arsenic (V) was 7.72×10^{-1} $lb/10^{12}$ Btu, or about half again as much arsenic (V). The discrepancy between the median value for total arsenic and the sum of the median values for arsenic (III) and arsenic (V) may be due to using different test methods for total and for speciated arsenic. High and low values for arsenic (III) and (V) were 3.03×10^{-1} $lb/10^{12}$ Btu and 6.69×10^{-1} $lb/10^{12}$ Btu, and 1.70×10^{-1} $lb/10^{12}$ Btu and 1.38 $lb/10^{12}$ Btu, respectively.

H.2.3.3.4 Nickel. Total nickel was measured at nearly all sites, but only two sites provided data on speciated nickel. The species measured were soluble nickel (water-soluble salts such as nickel sulfate and nickel chloride), sulfidic nickel (such as Ni_3S_2, NiS, and Ni_3S_4), metallic nickel (including alloys), and oxidic nickel (including NiO, complex oxides, and silicates). Total nickel had a median value of 5.45 $lb/10^{12}$ Btu and a range of 3.00×10^{-2} $lb/10^{12}$ Btu to 2.15×10^{3} $lb/10^{12}$ Btu. Metallic nickel was not detected at either site; the distribution of the remaining three types of species, in $lb/10^{12}$ Btu and in percent of total nickel species, is shown in Table H-6.

H.2.3.3.5 Individual Test Site Data for Mercury and Chromium Data. Individual test site data for mercury and chromium data for each test contributing species information to this report are given in Tables H-7 and H-8 for mercury and Tables H-9 through H-11 for chromium.

When the one value of divalent mercury found in an oil-fired boiler is removed, the percentiles for coal-fired boilers change slightly, as shown in Table H-8.

Table H-10 shows the chromium data for four coal-fired boilers. Table H-11 shows Chromium data for seven oil-fired boilers.

Table H-5. Chromium Statistics for Coal- and Oil-Fired Boilers

Species	Frequency of detection (from up to 47 individual sets)	Range (percent of species)	Average (percent of species)	Median (percent of species)	5th percentile (percent of species)	10th percentile (percent of species)	90th percentile (percent of species)	95th percentile (percent of species)	Maximum percent /Minimum percent
Chromium in coal and oil	45	34	89	88	89	89	91	91	100/66
Hexavalent chromium in coal and oil	11	34	11	12	11	11	9	9	34/0.4
Chromium in coal	34	23	89	90	89	89	90	90	100/77
Hexavalent chromium in coal	4	8	11	10	11	11	10	10	8.8/0.4
Chromium in oil	11	29	80	77	80	80	80	80	95/66
Hexavalent chromium in oil	7	29	20	23	20	20	20	20	34/5

Table H-6. Emission Statistics for Nickel Species From Two Oil-Fired Utility Boilers (lb/10^{12} BTU/Percent of Species)

Statistic	Soluble nickel	Sulfidic nickel	Nickel oxides
Average	628/58	37.8/3	422/39
Maximum	1,240/58	73/3	835/39
Minimum	21.3/65	2.60/8	9.00/27
Standard deviation	616/NA	49.8/NA	584/NA
Range	1,219/7	70/5	826/12
5th percentile	31.5/58	1.89/3	21.1/39
10th percentile	63.1/58	3.78/3	42.2/39
90th percentile	1,740/58	102/3	1,170/39
95th percentile	2,050/58	120/3	1,380/39

Note: Data from two sites. Metallic nickel not detected. Examples of soluble nickel include water-soluble salts such as nickel sulfate and nickel sulfide. Examples of sulfidic nickel include Ni_3S_2, NiS, and Ni_3S_4. Examples of nickel oxides include NiO, complex oxides, and silicates. Most of these compounds have a valence state of 2.

Table H-7. Mercury Data for Nine Coal- and 1 Oil-Fired Boilers

Test site	Fuel	Elemental mercury (%)	Divalent mercury (%)
1	Coal	31	69
2	Coal	24	76
3	Coal	85	15
4	Coal	71	29
5	Coal	18	82
6	Coal	9	91
7	Coal	54	46
8	Coal	88	12
9	Coal	96	4
10	Oil	Not detected	up to 100
Summary Statistics			
Average (%)a		62	38
Standard deviation (%)a		33	33
Range (%)a		87	87
Maximum (%)a		96	91
Minimum (%)a		9	4
5th percentile (lb/10^{12} Btu)a		0.170	0.106
10th percentile (lb/10^{12} Btu)a		0.340	0.212
90th percentile (lb/10^{12} Btu)a		9.23	4.55
95th percentile (lb/10^{12} Btu)a		10.9	5.24

[a] Results from Site 10 are excluded.

Table H-8. Mercury Percentiles for Coal-Fired Boilers

Percentile	Elemental mercury	Divalent mercury
5th percentile (lb/1012 Btu)	0.170	0.118
10th percentile (lb/1012 Btu)	0.340	0.235
90th percentile (lb/1012 Btu)	9.23	4.73
95th percentile (lb/1012 Btu)	10.9	5.40

Table H-9. Chromium Data for Four Coal- and Seven Oil-fired Boilers

Test site	Fuel	Elemental chromium (%)	Hexavalent chromium (%)
1	Coal	99.6	0.4
2	Coal	90	10
3	Coal	91	9
4	Coal	77	23
5	Oil	95	5
6	Oil	91	9
7	Oil	77	23
8	Oil	83	17
9	Oil	66	34
10	Oil	83	17
11	Oil	Not detected	up to 100
Summary Statistics			
Average (%)[a]		85	15
Standard deviation (%)[a]		10	10
Range (%)[a]		34	34
Maximum (%)[a]		99.6	34.2
Minimum (%)[a]		65 .8	0.4
5th percentile ($lb/10^{12}$ Btu)[a]		0.67	0.082
10th percentile ($lb/10^{12}$ Btu)[a]		1.34	0.163
90th percentile ($lb/10^{12}$ Btu)[a]		42.8	4.07
95th percentile ($lb/10^{12}$ Btu)[a]		51.1	4.76

[a] Results from Site 11 are excluded

Table H-10. Chromium Data for Four Coal-Fired Boilers

Test site	Elemental chromium (%)	Hexavalent chromium (%)
1	99.6	0.4
2	90	10
3	91	9
4	77	23
Summary Statistics		
Average (%)	89	11
Standard deviation (%)	9	9
Range (%)	22	22
Maximum (%)	99.6	22.5
Minimum (%)	77.5	0.4
5th percentile (lb/10^{12} Btu)	0.792	0.095
10th percentile (lb/10^{12} Btu)	1.58	0.190
90th percentile (lb/10^{12} Btu)	49.1	5.48
95th percentile (lb/10^{12} Btu)	58.4	6.48

Table H-11. Chromium Data for Seven Oil-Fired Boilers

Test site	Elemental chromium (%)	Hexavalent chromium (%)
5	95	5
6	91	9
7	77	23
8	83	17
9	66	34
10	83	17
11	Not detected	up to 100
Summary Statistics		
Average (%)[a]	82	18
Standard deviation (%)[a]	10	10
Range (%)[a]	29	29
Maximum (%)[a]	95	34
Minimum (%)[a]	66	5
5th percentile (lb/10^{12} Btu)[a]	0.297	0.074
10th percentile (lb/10^{12} Btu)[a]	0.594	0.148
90th percentile (lb/10^{12} Btu)[a]	13.0	3.33
95th percentile (lb/10^{12} Btu)[a]	15.0	3.85

[a] Results from Site 11 are excluded.

H.3 ENVIRONMENTAL CHEMISTRY AND FATE

The following sections provide a summary of the environmental chemistry and fate of HAPs associated with emissions from utilities. HAPs of interest include selected PAHs, dioxins and furans, and trace metals.

H.3.1 Dioxins and Furans

This subsection discusses the processes that affect the fate, degradation, and transformation of chlorinated dibenzodioxins (CDDs) and chlorinated dibenzofuran (CDFs) in the environment. In general, the discussion presented here focuses on CDDs and CDFs as a group and not on individual dioxin and furan congeners. Information is also presented on the homologue groups of dioxins and furans (i.e., hexa-, hepta-, octa-chlorodibenzodioxins, etc.) with discussion of congener-specific fate and transformation processes limited to 2,3,7,8-TCDD.

H.3.1.1 Transportation and Fate. CDDs and CDFS are widely dispersed throughout the environment by atmospheric transport and deposition. During transport CDDs and CDFs partition between the vapor and the particle-bound phase.[3] Vapor pressure greatly influences the extent to which CDD/CDF congeners are found in the vapor phase. Table H-12 lists the vapor pressures and other chemical properties of homologue groups of CDDs and CDFs. The ratio of vapor- to particulate-bound CDDs and CDFs ranges from 6.69 for tetra-CDD (relatively high vapor pressure) to 0.02 for octa-CDDs (relatively low vapor pressure)[4]

CDDs and CDFs can be physically removed from the atmosphere through wet deposition, particle dry deposition, and gas phase dry deposition.[5] Wet deposition is very effective at removing CDDs and CDFs from the atmosphere and can dominate removal processes in areas of low suspended particulate matter. However, in areas with high total suspended particulate matter, dry deposition (gravity settling of particles) can dominate.[6]

As seen Table H-12, CDDs and CDFs have low water solubilities and vapor pressures and high octanol water partition coefficients (K_{ow}) and organic carbon partition coefficients

Table H-12. Summary of Physical and Chemical Properties of Dioxin and Furan Congener Groups at 25 °C[7]

Congener group	Molecular weight (g/mol)	Vapor pressure (mm Hg)[a]	Solubility (mg/L)b	Log K_{ow}	Log K_{oc}	Henry's law constant (atm-m^3/mol)
2,3,7,8-TCDD	322.0	7.4×10^{-10}	1.93×10^{-5}	6.64	6.4	1.6×10^{-5}
PeCDD	356.4	7.3×10^{-10}	1.2×10^{-4}	6.6	5.7	2.6×10^{-6}
HxCDD	390.9	5.9×10^{-11}	4.4×10^{-6}	7.3	5.9	1.2×10^{-5}
HpCDD	425.3	3.2×10^{-11}	2.4×10^{-6}	8.2	--	7.5×10^{-6}
OCDD	460.8	8.25×10^{-13}	7.4×10^{-8}	7.59	--	7.0×10^{-9}
TCDF	306.0	2.5×10^{-8}	4.2×10^{-4}	6.2	--	8.6×10^{-6}
PeCDF	340.4	2.7×10^{-9}	2.4×10^{-4}	6.4	--	6.2×10^{-6}
HxCDF	374.9	2.8×10^{-10}	1.3×10^{-5}	--	--	1.0×10^{-5}
HpCDF	409.3	9.9×10^{-11}	1.4×10^{-6}	7.9	--	5.3×10^{-5}
OCDF	444.8	3.75×10^{-12}	1.2×10^{-6}	8.78	--	1.9×10^{-6}

[a] The vapor pressures and Henry's law constants for the congener groups were classified as low based on scales developed for US EPA (1988).[8]
[b] The solubilities presented here were measured at temperatures ranging from 20 °C to 25 °C.

(K_{oc}).[a],[9,10] These chemical properties indicate that CDDs/CDFs are strongly sorbed in soils.[11] In subsurface soils—particularly in soils with high organic carbon content—CDDs/CDFs show little or no vertical migration, as they are resistant to both leaching and volatilization. However, the mobility of CDDs/CDFs in soil has been shown to increase with a carrier solution such as waste oil or diesel fuel, although he research in this area is ambiguous.[12] Because CDDs/CDFs are resistant to leaching and volatilization, they are mainly transported to surface waters through soil erosion.[13]

In the aquatic environment, CDDs and CDFs remain sorbed to particulate matter, and dissolved CDDs/CDFs entering surface waters will partition to suspended solids or dissolved organic matter.[14] Volatilization is not expected to be a significant loss mechanism for the higher chlorinated CDDs/CDFs under normal conditions.[15] The primary removal mechanism for removing CDDs/CDFs from the water column is through sedimentation and, ultimately, burial in sediments. Research has shown that concentration of solids settling through the water column was an order of magnitude higher than the concentration in the suspended particulate matter. This difference in the concentrations indicates that the solids tend to scavenge CDDs/CDFs as they settle. Once buried, little recirculation of CDDs/CDFs occurs within the water column.[16]

Aquatic organisms are shown to bioaccumulate CDDs/CDFs when exposed to contaminated sediments and to bioconcentrate CDDs/CDFs dissolved in water.[b,17,18,19,20,21] Although the pathways for

---

[a] The K_{ow} is defined as the ratio of a chemical's concentration in the octanol phase to its concentration in the aqueous phase of a two-phase octanol/water system. A chemical's K_{ow} gives a strong indication of its behavior in the environment. Chemicals with low K_{ow} values are considered hydrophilic and tend to have high water solubilities and small soil/sediment adsorption coefficients and bioconcentration factors. Conversely, chemicals with large K_{ow} values are considered hydrophobic and have the opposite tendencies.[9] The K_{oc} defines the extent to which an organic chemical partitions itself between the solid and solution phases of a water-saturated soil, runoff water, or sediment. It is the ratio of the amount of chemical adsorbed per unit weight of organic carbon in the soil or sediment to the concentration of the chemical in solution at equilibrium. K_{oc} is a useful parameter because the degree of soil adsorption can affect a chemical's mobility in the environment and other fate processes.[10]

[b] Bioconcentration refers to the accumulation of a chemical from direct exposure to water. In aquatic organisms, bioconcentration involves uptake via gills and skin; elimination via gills, skin, urine, and feces; and metabolic transformation.[17] Bioconcentration is important because a chemical that bioconcentrates in an organism may affect ecological processes at aquatic concentrations that appear safe for the organism according to bioassay criteria for acute or chronic exposure.[18] A bioconcentration factor (BCF) describes a chemical's tendency to bioconcentrate in an organism and is defined as the ratio of chemical concentration in an aquatic

(continued...)

accumulation are not fully understood, the accumulation may be primarily food-chain-based since most of the CDDs/CDFs are associated with sediments and dissolved organic matter. Most likely, uptake starts with benthic organisms (e.g., mussels, chironomids, etc.) through ingestion or filtering, and those organisms (e.g., crabs, suckers, etc.) consuming benthic organisms would then pass the contaminant up the food chain.[22]

H.3.1.2 Transformation and Degradation. CDDs and CDFs are extremely stable in the environment under normal conditions. CDDs/CDFs do not hydrolyze appreciably,[23] and 2,3,7,8-TCDD is recalcitrant to microbial degradation.[24] 2,3,7,8-TCDD is also stable to oxidation in the ambient environment.[25] The most significant natural degradation of CDDs/CDFs is by photodegradation.[26] Photodegradation is slow in water and on dry surfaces but increases in the presence of organic solvents.[27] CDDs and CDFs photodegrade to lower chlorinated CDDs and CDFs. In general, the rate of photolysis increases as the degree of chlorination decreases and, within a congener group, as the degree of ortho substitution decreases. Research has shown that CDFs degrade much more rapidly than CDDs.[28] In the soil, photodegradation is limited to only the soil surface and is not significant below the first few millimeters of soil depth.[29]

Atmospheric photodegradation of CDDs/CDFs is not well characterized but appears to be the most significant mechanism for degradation of CDDS/CDFs in the vapor phase. However, measuring the rate of atmospheric photodegradation is difficult because of the low volatility of CDDs/CDFs. For airborne CDDs/CDFs sorbed to particles, photolysis appears to proceed very slowly, and sorption of CDDs onto airborne particulate matter may even act to stabilize CDDs from photodegradation. Research has shown that the half-life of gaseous 2,3,7,8-TCDD was several hours under simulated sunlight. When the 2,3,7,8-TCDD was sorbed onto fly ash particles, Mill observed only an 8 percent loss of 2,3,7,8-TCDD after 40 hours of illumination.[30]

---

[b] (...continued)
organism to that in water.[19] Bioaccumulation also describes increases in the concentration of chemicals in organisms. However, bioaccumulation may be distinguished from bioconcentration in that it encompasses accumulation of a chemical from all routes of exposure, including ingestion, and is not limited to direct exposure to water or soil.[20] Biomagnification is a related term and is the systematic increase of a chemical in tissue concentrations at higher levels in the food chain.[21]

H.3.2 Polycyclic Aromatic Hydrocarbons

This section discusses the processes that affect the fate, degradation, and transformation of selected PAHs in the environment. PAHs selected were those that are probable carcinogens and those that are present most frequently in utility emissions. Probable carcinogens include benzo(a)anthracene, benzo(b)fluoranthene, benzo(k)fluoranthene, benzo(b and k)fluoranthene,[c] chrysene, benzo(a)pyrene, dibenzo(a,h)anthracene, and indeno(1,2,3-c,d)pyrene; the most frequently emitted PAHs are 2-methylnaphthalene, fluoranthene, fluorene, pyrene, and phenanthrene.

H.3.2.1 Transportation and Fate. Transport and fate of PAHs in the environment are determined to a large extent by the physical and chemical properties of the individual PAH. Table H-13 summarizes the properties of selected PAHs as described in section H.3.2. Some of the properties correlate roughly to the molecular weights of the PAHs, which can be grouped into the following categories:

- Low-molecular-weight compounds (142-178 g/mol)--2-methylnaphthalene, fluorene, and phenanthrene;
- Medium-molecular-weight compounds (202 g/mol)--fluoranthene and pyrene; and
- High-molecular-weight compounds (228-278 g/mol)--benzo(a)anthracene, benzo(b)fluoranthene, benzo(k)fluoranthene, chrysene, benzo(a)pyrene, dibenz(a,h)anthracene, and indeno(1,2,3-c,d)pyrene.

Much of the discussion of the transport and fate of PAHs is based on these categories.[31]

PAHs in the atmosphere are present in the gaseous phase or sorbed onto particles. The ratio of particulate to gaseous PAHs varies for different PAHs. For example, the results of a study of air samples collected in Antwerp, Belgium, indicated that the ratio of particulate to gas phase PAHs ranged from 0.03 for anthracene to 11.5 for benzo(a)fluoranthene and benzo(b) fluoranthene combined. Additionally, atmospheric residence time and transport distance depend on the size of particles to which PAHs are sorbed. Larger particles released from urban sources deposit close to their source of origin and can become part of urban runoff. Conversely, smaller submicron-diameter soot

[c] Information on the environmental chemistry and fate of benzo(b and k)fluoranthene was not readily available from the literature for this study.

Table H-13. Summary of Physical and Chemical Properties of Selected PAHs at 25 °C[32,33]

PAH[a]	Molecular weight[b] (g/mol)	Vapor pressure[b] (mm Hg)	Solubility (mg/L)	Log K_{ow}	Log K_{oc}	Henry's law constant (atm-m^3/mol)
Benz(a)anthracene (c)	228.3[c]	2.1x10-7[c]	0.011[c]	5.91[c]	5.30[d]	5.7×10^{-6} [c,e]
Benzo(b)fluoranthene (c)	252.32[c]	~10-11 to 10^{-6} [c]	0.0015[c]	5.80[c]	5.74[d]	1.22×10^{-5} [d]
Benzo(k)fluoranthene (c)	252.32[c]	3.9×10^{-10} [c]	0.0008[c]	6.06[c]	5.74[d]	1.6×10^{-7} [c,e]
Chrysene (c)	228.3[c]	4.3×10^{-9} [c]	$1.5-2.2\times10^{-3}$ [d]	1.65[c]	5.30[d]	6.4×10^{-7} [c,e]
Benzo(a)pyrene (c)	252.32[c]	5.3×10^{-9} [c]	0.0038[c]	6.04[c]	6.74[d]	4.5×10^{-7} [c,e]
Dibenz(a,h)anthracene(c)	278.36[c]	2.8×10^{-12} [c]	0.0006[c]	6.75[c]	6.52[d]	7.3×10^{-8} [c,e]
Indeno (1,2,3-c,d)pyrene(c)	276.38[d]	~10-10 at 20°C[d]	0.062[d]	6.58[d]	6.20[d]	6.95×10^{-8} [d]
2-Methylnaphthalene (f)	142.2[c]	0.078[c]	25[c]	3.86[c]	3.4, 3.93[c]	5.05×10^{-4} [c,e]
Fluorene (f)	166.2[c]	6.75×10^{-4} [c]	1.90[c]	4.18[c]	3.86[d]	7.77×10^{-5} [c,e]
Pyrene (f)	202.26[c]	4.5×10^{-6} [c]	0.132[c]	5.18[c]	4.58[d]	9.1×10^{-6} [c,e]
Fluoranthene (f)	202.6[c]	9.2×10^{-6} [c]	0.26[c]	5.22[c]	4.58[d]	1.02×10^{-5} [c,e]
Phenanthrene (f)	178.24[c]	1.5×10^{-4} [c]	1.10[c]	4.57[c]	4.15[d]	3.2×10^{-5} [c,e]

[a] (c) indicates suspected carcinogen; (f) indicates measured frequency of detection greater than 10. (See Table H-2.)

[b] The vapor pressures and Henry's law constants for the selected PAHs were classified as moderate to low based on scales developed for U.S. EPA (1988).[8]

[c] Reference 32.

[d] Reference 33.

e Calculated.

particles associated with urban air have residence times of weeks and are subject to long-range transport. PAHs can be removed from the atmosphere by wet and dry deposition, and the relative importance of each removal process varies according to the PAHs involved. For example, dry deposition of benzo(a)pyrene accounts for three to five times more removal than does wet deposition.[34]

In water, PAHs can be removed by volatilization to the atmosphere and by sorption onto suspended and bottom sediment. Low-molecular-weight PAHs, which have Henry's law constants ranging from 10^{-3} to 10^{-5} atm-m^3/mol, are associated with significant volatilization from water. Only limited volatilization occurs for medium- to high-molecular-weight PAHs, which have Henry's law constants of less than 10^{-5}. However, as exhibited by their K_{oc} values in Table H-13, high-molecular-weight PAHs strongly sorb onto the organic carbon present in the suspended and bottom sediments. Low-and medium-weight PAHs have only a moderate potential for sorption onto organic carbon.[35]

PAHs in soil can be removed by volatilization. Volatilization of low-molecular-weight PAHs may be substantial. In one study, volatilization was found to account for 20 percent of 1-methylnaphthalane and 30 percent of the loss of naphthalene; both compounds are low molecular weight PAHs. Volatilization of higher molecular weight PAHs is not expected to be a significant removal process from soil.[36]

Because of the tendency of high-molecular-weight PAHs to sorb strongly to soil, they are resistant to leaching. However, leaching can occur in the lower-weight PAHs. In a study conducted on land cleared by burning, PAHs were found to move into the soils by partitioning and leaching. Phenanthrene and fluoranthene at the site were incorporated into the soil to a greater extent than the higher-molecular-weight PAHs, such as indeno(1,2,3-c,d)pyrene.[37]

Plants and animals can bioconcentrate PAHs. Table H-14 provides BCFs of selected species for the PAHs chosen due to suspected carcinogenicity and frequency of occurrence in emission tests. Generally, bioconcentration factors (BCFs) are larger for the higher-molecular-weight PAHs. In water, bioconcentration and bioaccumulation of PAHs vary greatly depending on the type of aquatic organism. Fish and crustaceans readily bioaccumulate PAHs from contaminated food, whereas mollusks and polychaete worms have limited assimilation. Biomagnification is the systematic increase in tissue concentrations at higher levels in

Table H-14. PAH Bioconcentration Factors (BCF) for Selected Species[a,b]

PAHs[c]	BCF	Species
Benz(a)anthracene (c)	10,233	*Daphnia magna*
	10,000	Fathead minnow
Benzo(b)fluoranthene (c)	9.1	*polychaet sp*
	10,000	*daphnia magna*
Benzo(k)fluoranthene (c)	14.1	*polychaet sp*
	13,183	*daphnia magna*
Chrysene (c)	14.8	*Polychaet sp*
	6,095	*Daphnia magna*
	20,417	*P. hoyi*
Benzo(a)pyrene (c)	2,818	*Daphnia magna*
	12,882	*Daphnia magna*
	54,954	*P. hoyi*
	8,912,509, 3,235,936	*P. hoyi*
	13.8	*Polychaet sp*
Dibenz(a,h)anthracene (c)	10,000	*daphnia magna*
	2,399	algae
2-Methylnaphthalene (f)	407, 447	None cited
Fluorene (f)	502	*Daphnia magna*
Pyrene (f)	5.20	*Polychaet sp*
	2,692	*Daphnia magna*
	44,668	*P. hoyi*
Fluoranthene (f)	5.7	*Polychaet sp*
	1,738	*Daphnia magna*
	79,433	*P. hoyi*
Phenanthrene (f)	5.6	*Polychaet sp*
	324	*Daphnia magna*
	15,136, 19,055	*P. hoyi*

[a] No BCF was available for indeno(1,2,3-c,d)pyrene.
[b] All references cited are from Mackay, et al, 1992 (Reference 32).
[c] (c) indicates suspected carcinogen; (f) indicates measured frequency of detection greater than 10. (See Table H-2) (Reference 8).

the food chain, and because many aquatic animals such as mollusks rapidly eliminate PAHs, biomagnification of PAHs has not been reported in aquatic animals.[38]

Some terrestrial plants can uptake PAHs through the roots or foliage. Factors that influence the uptake rate of plants include concentration of PAH in soil, the solubility and the molecular weight of PAHs, and the plant species. Evidence suggests that plant uptake of PAHs from deposition on foliage greatly exceeds uptake from roots. Research has shown that about 30 percent to 70 percent of atmospheric PAHs deposited into a forest were sorbed onto the leaves and needles of the trees and then deposited as litterfall. Furthermore, PAHs can accumulate in terrestrial animals through the food change or by soil ingestion.[39]

H.3.2.2 Transformation and Degradation. PAHs in the atmosphere react with a variety of pollutants such as ozone, NO_x, SO_2, and peroxyacetylnitrate. Reactions of PAHs with ozone or peroxyacetylnitrate yield diones[40] (compounds having two ketone groups). Nitro and dinitro PAHs are formed from reactions with NO_x. SO_2 reacts with PAHs to form sulfonic acids.[41] Additionally, some PAHs have been shown to degrade by oxidation reactions.[42]

Photodegradation of many atmospheric PAHs forms nitrated PAHs, quinones, phenols, and dihydrodiols. Some degradation products are mutagenic. PAHs absorbed onto particulates with high organic carbon are more resistant to photodegradation than the pure compounds. The dark, high-organic-content particulates on which the PAHs sorb may absorb more light, thereby making less light available for photodegradation.[43]

Photodegradation is also an important degradation process of PAHs in water. The rate and extent of photodegradation vary widely among PAHs. For example, one study reported that anthracene, phenanthrene, and benzo(a)anthracene were susceptible to photodegradation in water, while chrysene, benzo(a)pyrene, fluorene, and pyrene were resistant and are also dependent on water depth, temperature, and turbidity. The most common products of PAH photodegradation in water are peroxides, quinones, and diones.[44]

PAHs can be chemically oxidized in water by chlorination. Research has shown that pyrene and benzo(a)anthracene degrade rapidly upon chlorination. Indeno(1,2,3-c,d)pyrene has an intermediate degradation rate. Of the chemicals considered in this study, benzo(k)fluoranthene and fluoranthene were the

slowest to degrade. The byproducts of PAH chlorination are not fully known but include anthraquinone, a chlorohydration of fluoranthene, and monochloro derivatives of fluorene and phenanthrene.[45]

PAHs in water can also be oxidized by ozonation. However, ozonation is generally slower and less efficient than chlorination in degrading PAHs. Some products of PAH ozonation include benzo(a)anthracene to 7,12-quinone; benzo(a)pyrene to 3,6-, 1,6-, and 4,5-diones; and fluorene to fluorenone.[46]

Biodegradation is another removal process of PAHs from water. Bacteria degrade PAHs into cis-dihydrodiol via a dioxetane intermediate, and trans-dihydrodiols are formed through arene oxide intermediates in fungi. Arene oxides have been linked to the carcinogenicity of PAHs. Additionally, algae were found to transform benzo(a)pyrene to oxides, peroxides, and dihydrodiols.[47]

Microbial metabolism is the major degradation process of PAHs in soil. Photolysis, hydrolysis, and oxidation are not as significant. However, evidence suggests that photolysis and volatilization may be important for PAHs containing fewer than four aromatic rings.[48]

The rate and extent of biodegradation in soil are affected by environmental factors, the physical and chemical properties of the PAHs, and the level of contamination at the site. Environmental factors include temperature, pH, oxygen content, soil type, moisture, and the presence of nutrients and other substrates that can act as cometabolites. In one study, the type of PAH and its properties also influenced the biodegradation rate. Biodegradation half-lives of PAHs composed of two and three aromatic rings ranged from 2 to 60 days, while PAHs with four and five aromatic rings had half-lives greater than 300 days.[49] In another study, the mean half-lives correlated positively with K_{ow}. The rate of biodegradation may also be altered by the degree of contamination at the site. Half-lives may be longer at highly contaminated sites, since other contaminants may be lethal to microbes.[50] Table H-15 gives half-lives of selected PAHs in soils and other environmental compartments.

For some PAHs, the products of microbial degradation in soil are well known, while for others only limited information is available. As in water, bacteria degrade PAHs in soil to cis-dihydrodiols through dioxetane intermediates, and fungal

Table H-15. Environmental Half-Lives in Days or Hurs for Selected PAHs in Various Compartments[32]

	Air		Water		Soil	
PAHs[a]	Value	Type/conditions	Value	Type/conditions	Value	Type/conditions
Benz(a)anthracene (c)	1-3 h	Based on estimated photolysis half-life in air	1-3 h	Based on estimated photolysis in water	4-6,250 d	Not specified
	0.4 h	For adsorption to wood soot	0.034 h	Direct photolysis	2,448 - 16,320 h	Based on aerobic soil die-away test
			0.20 d	No sediment water partitioning/direct photolysis	261 d	Kinman sandy loam soil
			0.95 d	Sediment water partitioning/direct photolysis	162 d	McLaurin sandy loam soil
			4,896-32, 640 h	Groundwater, based on aqueous aerobic biodegradation half-life		
Benzo(b)fluoranthene (c)	1.43-14.3 h	Based on estimated photooxidation half-life	8.7 - 720 h	Based on photolysis half-life in water	294 d	Kinman sandy loam soil
Benzo(b)fluoranthene (c)	1.3 h	For adsorption to wood soot	17,280-29, 280 h	Ground water, based on aqueous aerobic biodegradation half-life	211 d	McLaurin sandy loam soil
Benzo(k)fluoranthene (c)	1.1 - 11 h	Based on estimated photooxidation half-life	3.8 - 499 h	Based on photolysis half-life in water	21,840 - 51,360 h	Based on aerobic soil die-away test
	0.8 h	For adsorption to wood soot	42,680 - 102,720 h	Ground water, based on aqueous aerobic biodegradation half-life		

Table H-15. (continued).

	Air		Water		Soil	
PAHs[a]	Value	Type/conditions	Value	Type/conditions	Value	Type/conditions
Chrysene (c)	0.802-8.02 h	Based on estimated photooxidation half-life	4.4 h	Direct photolysis	>5.5 d	Not specified
	1.3 h	For adsorption to wood soot	13 h	No sediment water partitioning/direct photolysis	371 d	Kinman sandy loam soil
			68 d	Sediment water partitioning/direct photolysis	387 d	McLaurin sandy loam soil
			17,808-48,000 h	Groundwater, based on aqueous aerobic biodegradation half-life	8,904-24,000 h	Based on aerobic soil die-away test
Benzo(a)pyrene	0.37—1.1 h	Based on estimated photolysis half-life in air	3.2 d	No sediment partitioning	>2 d	Not specified
	0.5 h	For adsorption on soot particles	13 d	With sediment partitioning	309 d	Kidman sandy loam soils
			0.37—1.1 h	Based on photolysis half-life in water	229 d	McLaurin sandy loam soils
			2,736—25,440 h	Based on estimated aqueous aerobic biodegradation half-life	1,368—12,720 h	Based on aerobic soil die-away test

Table H-15. (continued).

	Air		Water		Soil	
PAHs[a]	Value	Type/conditions	Value	Type/conditions	Value	Type/conditions
Dibenz(a,h)anthracene (c)	0.428-4.28 h	Based on estimated photooxidation half-life	6 -782 h	Based on photolysis half-life in water	361 d	Kinman sandy loam soil
			17,328- 45,120 s	Ground water, based on aqueous aerobic biodegradation half-life	420 d	McLaurin sandy loam soil
					8,664 - 22,560 h	Based on aerobic soil die-away test
2-Methylnaphthalene (f)	No data	No data	54 h	Direct photolysis	No data	No data
			410 d	No sediment water partitioning/direct photoly sis		
			440 d	Sediment water partitioning/ direct photolysis		
Fluorene (f)	6.81-68.1 h	Based on estimated photooxidation half-life	768-1440 h	Surface water, based on aerobic soil dieaway test	768- 1,440 h	Based on aerobic soil die-away test
			1536- 2880 h	Ground water, based on aqueous aerobic biodegradation half-life		

Table H-15. (continued).

	Air		Water		Soil	
PAHs[a]	Value	Type/conditions	Value	Type/conditions	Value	Type/conditions
Pyrene (f)	0.68-2.04 h	Based on estimated photolysis half-life in water	0.58 h	Direct photolysisis	3-35 h	Not specified
			4.2 d	No sediment water partitioning/direct photolysis	5,040-45,600 h	Based on aerobic soil die-away test
			5.9 d	Sediment water partitioning/direct photolysis	260 d	Kinman sandy loam soil
			10,080-91,200 h	Groundwater, based on aqueous aerobic biodegradation half-life	199 d	McLaurin sandy loam soil
Fluoranthene (f)	2.02-20.2 h	Based on estimated sunlight photolysis half-life in water	21 h	Direct photolysis	44-182 d	Not specified
			160 d	No sediment water partitioning/direct photolysis	3,360-10,560 h	Based on aerobic soil die-away test
			200 d	Sediment water partitioning/ direct photolysis	377 d	Kinman sandy loam soil
			6,720-21,120 h	Groundwater, based on aqueous aerobic biodegradation half-life	268 d	McLaurin sandy loam soil

Table H-15. (continued).

	Air		Water		Soil	
PAHs[a]	Value	Type/conditions	Value	Type/conditions	Value	Type/conditions
Phenanthrene (f)	2.01-20.1 h	Based on estimated photooxidation half-life	8.4 h	Direct photolysis	2.5-26 d	Not specified
			59 d	No sediment water partitioning/direct photolysis	384-4,800 h	Based on aerobic soil die-away test
			69 d	Sediment water partitioning/direct photolysis	35 d	Kinman sandy loam soil
			768-9600 h	Groundwater, based on aqueous aerobic biodegradation half-life	11 d	McLaurin sandy loam soil

a (c) indicates suspected carcinogen, (f) indicates measured frequency of detection greater than 10. (See Table H-2.)

degradation produces trans-dihydrodiols through arene oxide intermediates. Arene oxides have been linked to the carcinogenicity of PAHs.[51]

H.3.3 Trace Metals

The environmental chemistry and fate of trace metals emitted from utility boiler stacks are discussed in the following sections. Trace metals include arsenic, cadmium, chromium, lead, mercury, and nickel.

H.3.3.1 Arsenic. This section discusses the processes that affect the fate, degradation, and transformation of arsenic in the environment.

H.3.3.1.1 Transportation and Fate. Arsenic is found as a component of sulfidic ores and as arsenides or diarsenides of metals. Trace levels of arsenic are found in soils and rocks.[52] In the environment, arsenic can be transported by wind or water erosion of small particles and by leaching into rainfall or snowmelt. However, leaching transports arsenic only short distances, because many arsenic compounds readily absorb to soils and sediments.[53]

Arsenic in the atmosphere exists as particulate matter, primarily with diameters less than 2 μm. A typical residence time of particulate arsenic is 9 days, depending on the particle size and meteorological data. Arsenic is removed from the atmosphere by wet or dry deposition.[54]

Transport and partitioning of arsenic in water depend upon the chemical form of arsenic and on its interactions with other substances in the water. Soluble forms of arsenic can be transported long distances in rivers and water. However, arsenic can be adsorbed onto suspended and bottom sediments in water. Chemical and biological interconversions of sediment-bound arsenic may return arsenic to the water.[55]

Bioconcentration of arsenic occurs in aquatic organisms, primarily in algae and lower invertebrates. The BCFs for several arsenic compounds have been shown to range from 0 to 17 for freshwater invertebrates and fish, and a BCF of 350 was observed in marine oysters. Although some fish and invertebrates contain high levels of arsenic, biomagnification in aquatic food chains does not appear to be significant. Terrestrial plants accumulate arsenic by root uptake from soil or by absorption of airborne arsenic deposited on the leaves, and certain species may accumulate substantial levels.[56]

H.3.3.1.2 Transformation and Degradation. Arsenic is released into the atmosphere primarily as arsenic trioxide and, less frequently, in arsines or in one of several other volatile organic compounds. Atmospheric arsenic is typically a mixture of trivalent and pentavalent arsenic. Trivalent arsenic and methyl arsenic oxidizes to the pentavalent state in the atmosphere. Photolysis of atmospheric arsenic compounds is insignificant.[57]

Arsenic in water can undergo a complex series of transformations, including oxidation-reduction reaction, ligand exchange, and biotransformation. Rate constants for these various reactions are not readily available, but the factors that most strongly influence fate processes in water include the oxidation-reduction potential, pH, metal sulfide and sulfide ion concentrations, iron concentrations, temperature, salinity, and distribution and composition of the aquatic biota. Arsenic in water exists predominantly as arsenate, but aquatic microorganisms may reduce the arsenate to arsenite and a variety of methylated arsenicals.[57] As in the atmosphere, trivalent arsenic in aerated surface waters can be oxidized to pentavalent arsenic, while pentavalent arsenic in the aquatic environment can be reduced to trivalent arsenic in the presence of an oxidizing agent at acidic conditions.[58]

Transformations of arsenic in soil are similar to those occurring in aquatic systems. Pentavalent arsenic predominates in aerobic soils, and trivalent arsenic predominates in slightly reduced soils, such as temporarily flooded areas. Arsine, methylated arsenic, and elemental arsenic are the predominant forms found in extremely reduced soils such as swamps and bogs.[59]

H.3.3.2 Cadmium. This section discusses the processes that affect the fate, degradation, and transformation of cadmium in the environment.

H.3.3.2.1 Transportation and Fate. Cadmium released from the combustion of coal and petroleum products is usually associated with small particles that are in the respirable range of less than 10 μm in diameter.[d,60] These small particles are persistent in the atmosphere and can be transported great distances, with typical residence times from 1 to 10 days. Wet and dry deposition (gravitational setting) are the primary removal mechanisms for cadmium in the atmosphere.[60] Cadmium compounds usually found in the atmosphere are oxide, sulfide, sulfate, and chloride.[61]

---

[d] Only limited data were analyzed for this report concerning the size distribution of cadmium emitted from utility boilers. As a result, comparing the current data to the value cited in the reference (reference 60) is not appropriate.

Cadmium is relatively mobile in water when compared to other heavy metals. Most cadmium in water exists as the hydrated ion ($Cd(+2) \cdot 6H_2O$). Cadmium complexed with humic substance is another important form of cadmium in water. The concentration of cadmium in water is usually inversely related to the pH value and the amount of organic material present. Cadmium is removed from water by sorption onto organic materials and mineral surfaces, and sediment bacteria may assist in the partitioning of cadmium from water to sediments. Cadmium does not volatilize from the aquatic environment.[62]

Cadmium is readily released from acidic soils and is susceptible to leaching. Soil particles containing bound cadmium also may erode into air or water.[63]

Cadmium is bioaccumulated at all levels of the food chain in the aquatic environment. Cadmium accumulates in freshwater and marine organisms at concentrations hundreds and thousands of times greater than in the water. Bioconcentration of cadmium is greatest for invertebrates, followed by fish and aquatic plants. BCFs range from 113 to 18,000 for invertebrates and from 3 to 2,213 for fish.[64] In terrestrial animals, cadmium accumulates at all levels of the food chain. However, data on the biomagnification of cadmium are not conclusive.[65]

H.3.3.2.2 Transformation and Degradation. Limited information is available on cadmium reactions in the atmosphere. Cadmium compounds in the atmosphere (oxide, sulfate, chloride) are stable and do not undergo chemical reactions quickly. Photodegradation is insignificant for atmospheric cadmium. However, atmospheric cadmium compounds can be transformed by solubility in water and dilute acids.[66]

Because cadmium is present predominantly in the 2+ oxidative state in water, aqueous cadmium is not strongly influenced by the oxidation or reduction potential of water.[67] However, cadmium sulfide, which is formed under reducing conditions, has a low solubility and tends to precipitate out in water.[68] Photolysis and biological methylation of cadmium is not likely to occur in water.[69]

Transformation of cadmium in soil includes precipitation, dissolution, complexation, and ion exchange. Transformation is affected by the pH; the soil content of clay, minerals, and organic matter; and the presence of carbonated materials, oxides, and oxygen.[70]

H.3.3.3 Chromium. This subsection discusses the processes that affect the fate, degradation, and transformation of chromium in the atmosphere.

H.3.3.3.1 Atmospheric Transportation and Fate. Chromium exists in the atmosphere primarily in particulate form. The mass mediam diameter of particulate chromium is approximately 1 μm in the ambient atmosphere. Chromium is removed from the atmosphere by wet and dry deposition. However, the size of the chromium particles and chromium's mean deposition velocity of 0.5 cm/s favor dry deposition. Wet deposition can occur, and acid rain may facilitate removal of acid-soluble chromium compounds. Chromium in water cannot be volatilized into the atmosphere, but chromium in soil may be transported to the atmosphere as an aerosol.[71]

H.3.3.3.2 Transformation and Degradation in the Atmosphere. Chromium occurs in the atmosphere primarily in two oxidative states, chromium (III) and chromium (VI).[72] In natural systems these are also the two most stables forms of chromium.[73] Chromium released from combustion processes and ore processing industries is present mainly as chromium (III) oxide (Cr_2O_3),[74] and reports show that chromium (VI) makes up approximately 0.2 percent of the total chromium emitted from power plants.[75]

Chromium (VI) is readily reduced to chromium (III) by vanadium (V^{2+}, V^{3+}, or VO^{2+}), iron (Fe^{2+}), hydrogen sulfite (HSO_3^-), and arsenic (As(III)). Conversely, the oxidation of Cr(III) to Cr(VI) may occur at a significant rate in the atmosphere only if chromium is found in a salt other than Cr_2O_3, in the presence of manganese oxide.[76] The time required for these reactions to occur is unknown, given all the other species present.[77]

H.3.3.4 Lead. This section discusses the processes that affect the fate, degradation, and transformation of lead in the environment.

H.3.3.4.1 Transportation and Fate. Atmospheric lead exists primarily as lead sulfate ($PbSO_4$) and lead carbonate ($PbCO_3$),[78] and it is predominantly found in the particulate phase. The transport of lead in the atmosphere is affected by the size distribution of lead particles. Particles larger than 2 μm in diameter tend to settle out of the atmosphere quickly and are deposited near their source of origin. Smaller particles can be transported great distances and can also coagulate into larger particles.[79]

Wet and dry deposition is the primary removal mechanism of lead from the atmosphere. Of the two types, wet deposition is more important, with approximately 40 to 70 percent of removal

resulting from wet deposition. For instance, the ratios of wet to dry deposition were calculated as 1.63, 1.99, and 2.50 in a study conducted at various sites in Canada.[80]

The concentration of dissolved lead is low in most surface waters. At the proper pH, lead will readily react with anions, such as hydroxides, carbonates, sulfates, and phosphates, to form compounds that precipitate out of water (section H.3.3.4.2), which limits its soluability. Lead is also removed frcm water by binding with mineral particles in suspended sediment. The ratio of lead in suspended solids to dissolved lead varies from 4:1 in rural streams to 27:1 in urban streams.[81]

Lead readily adsorbs to the organic matter in soils. Generally, lead is strongly retained in soils and resistant to leaching, so that little is transported into surface or groundwater. However, lead can enter water as a result of erosion of soil particles containing lead, and leaching of lead can occur in acidic soils. As in water, lead can form many different complexes in soil depending, in part, on the soil type and pH, and the mobility of the different forms of lead in soil varies. At a pH of 6 to 8 and in high-organic soils, lead may form insoluble organic lead complexes. In acidic soils, these organic lead complexes can become soluble and are subject to leaching. In soils with less organic mater and a pH of 6 to 8, lead can form hydrous lead oxide complexes or may precipitate out with carbonate or phosphate ions. Additionally, lead at the soil surface may be converted to lead sulfate, which is relatively soluble when compared to lead carbonate or phosphate.[82]

Lead bioconcentrates in plants and animals. Terrestrial plants uptake lead via roots and foliage, and animals can intake lead via inhalation or ingestion of plants or soil. In the aquatic environment, higher BCFs are usually found in algae and benthic organisms. Low BCFs are associated with upper-level predators, such as carnivorous fish. Thus, biomagnification of lead does not occur. In terms of toxicity to organisms, organolead compounds are more toxic than inorganic forms of lead.[83]

H.3.3.4.2 Transformation and Degradation. Only limited information is available concerning the chemistry of lead in air. Lead oxides in the atmosphere form lead carbonates and sulfates. Trialkyl and dialkyl lead compounds can decompose into organic lead by a combination of photolysis and reactions with hydroxyl radicals and ozone.[84]

The chemistry of lead in water is complex because lead can be found in a multiplicity of forms. At the proper pH, lead can produce insoluble compounds with many of the anions found in

natural waters. Hydroxide, carbonate, sulfide, and sulfate may act as solubility controls in precipitating lead from water. Lead forms lead sulfate in the presence of sulfate ions at pH less than 5.4, while lead carbonates form at pH greater than 5.4. As noted previously, these lead compounds are insoluble and tend to precipitate out of solution.[85]

Organic lead compounds undergo a variety of degradation and transformation reactions in water. In anaerobic lakes, biological alkylation of organic and inorganic lead by microorganisms may form the volatile organometal lead compound and tetramethyl lead. In aerobic waters, the tetramethyl lead oxidizes, thereby reducing its volatilization from sediment. Tetraalkyl lead compounds photodegrade to trialkyl compounds, and degradation proceeds to dialkyl lead and then to inorganic lead. Tetraethyl lead is also susceptible to photodegradation in the water.[86]

In soil, evidence suggests that atmospheric lead is deposited on the soil as lead sulfate or is converted rapidly to lead sulfate at the soil surface. As noted previously, lead forms different compounds depending on the soil type and the pH (section H.3.3.4.1).[87]

H.3.3.5 Mercury. This subsection discusses the processes that affect the fate, degradation, and transformation of mercury in the environment.

H.3.3.5.1 Transportation and Fate. Mercury can exist in three oxidation states in the environment: Hg^0 (elemental), Hg_2^{2+} (mercurous ion), Hg^{2+}, (mercury II, divalent mercury). An analysis of stack test results conducted for this report shows that mercury is found in stack emissions in both the elemental and ionic form (See Appendix H-2). Mercury in all three oxidative states can be methylated by natural process in the environment to form organic compounds, such as monomethylmercury (methylmercury).[88]

In the atmosphere, between 95 percent and 99 percent of mercury exists as gaseous Hg^0. The remainder generally comprises methylmercury and mercury associated with particles. The latter category includes Hg^{2+}, which is thought to occur primarily as mercuric chloride. Gaseous Hg^{2+} may also exist in the atmosphere, especially near mercury emission sources.[89]

The form of mercury affects both the rate and mechanisms by which mercury is removed from the atmosphere. Although Hg^0 is found more abundantly in the atmosphere than either methylmercury or Hg^{2+}, these two forms of mercury make up a higher proportion of the mercury that is deposited. Methylmercury is probably more

effectively removed by dry deposition than is Hg^0. Additionally, Hg^{2+} and methylmercury are more soluble and are scavenged by precipitation more easily than Hg^0, with Hg^{2+} being the predominant form in precipitation. Wet deposition is apparently the primary mechanism for transporting mercury from the atmosphere to the surface waters and land.[90]

Once in the surface water, mercury can exist in dissolved or particulate form. Elemental mercury and dimethylmercury can be easily volatilized from the surface waters to the atmosphere. Mercury can also undergo transformations as discussed below. An important reservoir for mercury is contaminated sediments. Sediment-bound mercury can recycle back into the aquatic ecosystem for decades or longer.[91]

Mercury bound to soil forms compounds that can limit mercury's mobility and its availability for uptake by living organisms. Mercury has long retention times in soil, and accumulated mercury may continue to be released to surface waters for long periods of time.[92]

H.3.3.5.2 Transformation and Degradation. The chemical transformation and movement of mercury within and among the air, surface water, and soil is termed mercury cycling. A discussion of the movement of mercury in the environment was discussed above. This subsection focuses on the transformations of mercury that occur during the cycling of mercury in the environment.

In the environment, mercury reacts to form inorganic compounds (e.g., $HgCl_2$, mercuric chloride) and organic compounds (methylmercury). Mercury in all three oxidative states can be methylated by natural process in the environment to form methylmercury. Methylmercury is of special concern because if it is stable, it can readily accumulate in fish due to efficient uptake from dietary sources and to low rates of elimination. Methylmercury is also the most toxic form of mercury.[93]

Hg^{2+} in the surface waters can be reduced to Hg^0, and the volatile Hg^0 can be released to the atmosphere.[94] Hg^{2+} can also be methylated in sediments and, to a lesser extent, the water column to form methylmercury.[95] Each of these reactions is also reversible, and the net rate of production of each species of mercury depends on balance between forward and reverse reactions.[96]

Methylation of mercury in sediments by anaerobic sulfur-reducing bacteria is a major source of methylmercury in many aquatic environments. The rate of mercury methylation varies with physical and chemical factors, including mercury

loadings, the amount of suspended sediment, nutrient content, pH and redox conditions, temperature, and other variables.[97]

As in water, mercury in soil can be transformed to other forms of mercury. Hg^{2+} deposited from the air can bind with the top layer of forest soils or form stable complexes with soils particles of high organic or sulfur content and with humic and fulvic acids.[98] Bacteria or organic substances can reduce Hg^{2+} to Hg^0, releasing volatile inorganic mercury into the atmosphere. The various forms of mercury can also be methylated by bacteria or organic substances. Demethylation of mercury by bacteria can occur depending on soil conditions.[99]

H.3.3.6 Nickel. This section discusses the processes that affect the fate, degradation, and transformation of nickel in the atmosphere.

H.3.3.6.1 Atmospheric Transportation and Fate. Nickel is released to the atmosphere mainly as particulates and aerosols that cover a broad spectrum of sizes. For instances, a study conducted in Ontario showed that nickel is associated with relatively large particles, 5.6±2.5 μm, while another study conducted in six U.S. cities in 1970 demonstrated that the mass median diameter of nickel was ≈ 1.0 μm. The latter study, however, may have underestimated larger nickel particles.[100] Additionally, particulate nickel emitted from power plants tend to be smaller than that emitted from smelters.[101]

Once in the atmosphere, nickel can be removed by wet and dry deposition. Researchers disagree as to which type of deposition is more significant for nickel. One study found the same percentage of wet and dry deposition for nickel, while in a study conducted in the Ontario providence, the wet deposition was found to be 2.2 times greater than dry deposition.[102] In general, though, the importance of wet deposition relative to dry deposition increases with decreasing particle size.[103]

Small nickel particles in the atmosphere can have atmospheric half-lives of up to 30 days and can be transported over large distances. Evidence for long-range transport of nickel is provided by the fact that emission sources in North America, Greenland, and Europe are responsible for elevated atmospheric nickel concentrations in the Norwegian arctic during both summer and winter.[104]

H.3.3.6.2 Atmospheric Transformation and Degradation. Little information is available on the speciation and chemical and physical transformations of nickel in the atmosphere, due to limitations in the analytical methods. In the absence of specific information, elements of anthropogenic origin,

especially those emitted from combustion sources, are assumed to be present as the elemental oxide, and nickel oxide has been identified in industrial emissions.[105]

H.4 SUMMARY AND CONCLUSIONS

EPA's study of the health effects from indirect exposure to the seven aforementioned HAPs requires information on (1) the various chemical species of each HAP as it is emitted from a utility stack, (2) how each species behaves chemically once it is released to the atmosphere, and (3) what the ultimate fate of the HAP is as it is transported through the atmosphere, water, and soil. This section summarizes the information collected on these three topics and provides conclusions that will be considered for input to EPA's Indirect Exposure Model (IEM) and the Agency's long-range transport modeling. The results of this modeling--in conjunction with results of EPA's Human Exposure Model (HEM) for the direct inhalation of these and other selected HAPs--will be used to assess the potential risk to public health of HAP air emissions from utilities. The following paragraphs contain summaries and conclusions drawn about HAP air emissions and their environmental chemistry and fate.

H.4.1 Dioxins and Furans

Dioxins and furans leave utility boiler stacks at concentrations near the detection limit for present analytical methods. Median values are on the order of 10^{-6} lb/10^{12} Btu. Most of the 25 dioxin and furan congeners were found at 10 test sites. Emissions of 2,3,7,8-TCDD from the utility boilers reported here had a maximum value of 6.51×10^{-6} lb/10^{12} Btu. Emissions of 2,3,7,8-TCDF had a maximum value of 4.55×10^{-5} lb/10^{12} Btu.

In general, dioxins and furans have low water solubilities and vapor pressures and high K_{ow}s and K_{oc}s. They tend to sorb strongly to soils and sediments.[106] In soils, they resist leaching and are transported to surface water via soil erosion.[107,108] In the aquatic environment, dioxins and furans are removed from the water column via sedimentation and burial.[109] Dioxins and furans are stable under normal conditions, and photodegradation appears to be the most significant degradation of these compounds.[110,111] Aquatic organisms bioaccumulate dioxins and furans.[112]

H.4.2 PAHs

PAHs were measured at concentrations on the order of 10^{-3} or 10^{-2} lb/10^{12} Btu. The PAHs measured most frequently in the tests were 2-methyl naphthalene, fluorene, fluroanthrene, phenanthrene, and pyrene. Pyrene was detected with the greatest frequency (14 times), having a maximum measured emission value of 0.16 lb/10^{12}

Btu. Benz(a)anthracene was second, having nine measured values with a maximum of 0.144 lb/10^{12} Btu.

The PAHs discussed above have low to moderate molecular weights when compared to the other PAHs considered in this report. As such, they tend to have a moderate to high potential for volatilization from soil and water and a moderate potential for adsorption to soil.[113] These PAHs are similar to other PAHs in that they are subject to photodegradation, chlorination, and ozonation in the environment. Monochloro derivatives are formed from the chlorination of fluorene and phenanthrene in water, and fluorene forms fluorenone due to ozonation in water.[114,115,116,117] Environmental half-lives of PAHs range from less than 1 hour to more than 300 days depending on the type of PAH and the environmental conditions (Table H-14).[118] Microbial metabolism is the major degradation process of PAHs in soil.[119]

H.4.3 Trace Metals

Nearly all of the trace metals were measured in their total element category at all 43 test sites. The trace metals examined had median concentrations of about 1 to 6 lb/10^{12} Btu. Trace metals, especially when sorbed to small particles (less than about 1 or 2 μm), may persist in the atmosphere. For larger particles, or as particles agglomerate, they may also leave the atmosphere by wet or dry deposition and may bioaccumulate. The trace metals generally sorb to soil or mud particles, but may be leached or transformed depending on pH conditions and the surrounding environment.

Total mercury was measured 38 times with values as high as 22.9 lb/10^{12} Btu. In 10 speciation tests, elemental mercury was measured at a maximum of 14.7 lb/10^{12} Btu, and ionic mercury had a maximum measured value of 3.17 lb/10^{12} Btu.

Chromium was detected at 40 test sites with a maximum value of 138 lb/10^{12} Btu. Chromium (VI) was measured in 11 tests and had values as high as 6.04 lb/10^{12} Btu. The most important states of chromium in the atmosphere are chromium (III), and (VI). Chromium (VI) can be reduced to chromium (III) in the atmosphere.[120,121,122]

Total arsenic was detected in tests at 43 sites, with values as high as 10^4 lb/10^{12} Btu. In speciation tests, its trivalent species was measured at a maximum of 6.69 lb/10^{12} Btu; its pentavalent species was measured at 1.38 lb/10^{12} Btu. In the atmosphere, arsenic usually exists as a mixture of trivalent and pentavalent states, and trivalent arsenic can oxidize to the pentavalent state.[123] The predominant species of arsenic in soils varies, with As (V) dominating in aerobic soils, As (III) dominating in slightly reduced soils, and arsine, methylated

arsenic, and elemental arsenic dominating extremely reduced conditions.[124] In water, arsenic can undergo complex transformations, but the predominant form of arsenic is usually arsenate.[125]

Total nickel was detected at 41 sites, with values as high as 2.15 $lb/10^{12}$ Btu. In speciation tests, soluble nickel compounds (such as sulfates and chlorides) were measured at the maximum of 1.24×10^{3} $lb/10^{12}$, sulfidic nickel compounds were measured 7.3×10^{1} $lb/10^{12}$, and nickel oxides were measured at 8.35×10^{2} $lb/10^{12}$. Metallic nickel was not detected.

Lead and cadmium were not measured in their speciated forms; however, total lead and cadmium were measured at nearly all of the more than 43 test sites. Lead was measured at a maximum of 176 $lb/10^{12}$ Btu, and cadmium's highest value measured was 28.5 lb/1012 Btu. The predominant forms of lead in the atmosphere are lead carbonate and lead sulfate.[126] Limited information is available on the chemistry of atmospheric lead.[127] In water, lead undergoes many complex reactions. At pHs above 5.4, lead tends to form lead carbonates, and at pHs below 5.4, lead sulfates are formed.[128]

Lead in soil can form many different complexes depending on the pH and the soil type. Different soil pHs also affect the mobility of lead in soil.[129,130] Additionally, plants and animals bioconcentrate lead, but biomagnification of lead has not been detected.[131]

Cadmium compounds are stable in the atmosphere. The most common cadmium compounds are oxide, sulfate, sulfide, and chloride.[132] In water, cadmium is found only in the 2+ oxidative state and can exist as the hydrated ion or as ionic complexes with other inorganic or organic material.[133] The mobility of cadmium in soil dependens upon the soil pH, with cadmium compounds' being prone to leaching in acidic soils. Cadmium is not reduced or methylated by microorganisms in water).[134]

H.5 REFERENCES

1. Bloom, N., and W. Fitzgerald. Determination of Volatile Mercury Species at the Picogram Level by Low-Temperature Gas Chromatography with Cold-Vapor Atomic Fluorescence Detection. Analytica Chimica Acta, 208 151-161. 1988.

2. Grohse, P., Research Triangle Institute (RTI). Personal communication with J. Turner. RTI. 1995.

3. U.S. Environmental Protection Agency. Estimating Exposure to Dioxin-Like Compounds. Volume II. Properties, Sources, Occurrences, and Background Exposures. Draft. EPA/600/6-88/005Cb. Office of Research and Development, Washington, D.C. 1994a. p. 2-22.

4. Reference 3, p. 2-23.

5. Reference 3, p. 2-24.

6. Reference 3, p. 2-26.

7. Reference 3, pp. 2-8 to 2-11.

8. U.S. Environmental Protection Agency. Hazardous Waste TSDF. Background Information for Proposed RCRA Air Emission Standards. Office of Air Quality Planning and Standards, RTP, NC. 1988. p. D-53 to D-57.

9. Lyman, W., W.F. Reehl, and D.H. Rosenblatt. 1982. Handbook of Chemical Property Estimation Methods. McGraw Hill, Inc., New York, NY. 1982. pp. 1.1 to 1.3.

10. Reference 9, pp. 4.1 to 4.1.

11. Reference 3, p. 2-21.

12. Reference 3, pp. 2-26 to 2-28.

13. Reference 3, p. 2-28.

14. Reference 3, p. 2-28.

15. Reference 3, p. 2-30.

16. Reference 3, p. 2-29.

17. U.S. Environmental Protection Agency. 1993. Interim Report on Data and Methods for Assessment of 2,3,7,8-Tetrachorordibenzo-p-dioxin Risks to Aquatic Life and Associate Wildlife. EPA/600/R-93155. Office of Research

and Development, Duluth, MN. 1993. p. 3-1.

18. Reference 9, p. 5-1.

19. Reference 19 , p. 3-2.

20. Suter, G.W., L.W. Barnthouse, S.M. Bartell, T. Mill, D. Mackay, and S. Peterson. Ecological Risk Assessment. Lewis Publishers, Boca Raton, FL. 1993. p. 498.

21. Reference 9, p. 5-2.

22. Reference 3, p. 2-30.

23. Reference 3, p. 2-21.

24. Reference 3, p. 2-36.

25. Reference 3, p. 2-35.

26. Reference 3, p. 2-30.

27. Reference 3, p. 2-31.

28. Reference 3, p. 2-34.

29. Reference 3, p. 2-33.

30. Reference 3, pp. 2-34 to 2-35.

31. Reference 3, p. 147.

32. Mackay, D., W.Y. Shiu, K.C. Ma. Illustrated Handbook of Physical-Chemical Properties and Environmental Fate for Organic Chemicals. Volume II. Polynuclear Aromatic Hydrocarbons, Polychlorinated Dioxins, and Dibenzofurans. Lewis Publishers, Boca Raton, FL. 1992. pp. 76-79, 125-129, 132-140, 163-177, 182-186, 195-203, 206-208, and 236-238.

33. U.S. Public Health Service. Toxicological Profile for Polycyclic Aromatic Hydrocarbons. Agency for Toxic Substances and Disease Registry, Atlanta, GA. 1993e. pp. 132-137.

34. Reference 33, pp. 147-148.

35. Reference 33, p. 148.

36. Reference 33, pp. 148-149.

37. Reference 33, p. 148.

38. Reference 33, p. 149.

39. Reference 33, p. 150.

40. Reference 33, p. 150.

41. Reference 33, p. 150.

42. Reference 33, p. 151.

43. Reference 33, pp. 150 to 151.

44. Reference 33, p. 151.

45. Reference 33, p. 151.

46. Reference 33, p. 151.

47. Reference 33, p. 152.

48. Reference 33, p. 152.

49. Reference 33, p. 152.

50. Reference 33, p. 153.

51. Reference 33, p. 152.

52. U.S. Environmental Protection Agency. Health Assessment Document for Inorganic Arsenic. Final Report. EPA-600/8-83-021F. Office of Health and Environmental Assessment, Washington, D.C. 1984. p. 3-1.

53. U.S. Public Health Service. Toxicological Profile for Arsenic. Agency for Toxic Substances and Disease Registry, Atlanta, GA. 1993b. p. 103.

54. Reference 53, p. 103.

55. Reference 53, p. 103.

56. Reference 53, p. 103.

57. Reference 53, p. 103.

58. Reference 52, p. 3-13.

59. Reference 53, p. 104.

60. U.S. Public Health Service. Toxicological Profile for Cadmium. Agency for Toxic Substances and Disease Registry, Atlanta, GA. 1993. p. 89.

61. Reference 60, p. 90.

62. Reference 60, pp. 89 to 90.

63. Reference 60, P. 90.

64. Reference 60, p. 90.

65. Reference 60, p. 90.

66. Reference 60, p. 90.

67. Reference 60, p. 89.

68. Reference 60, p. 91.

69. Reference 60, p. 91.

70. Reference 60, p. 91.

71. U.S. Public Health Service. Toxicological Profile for Chromium. Agency for Toxic Substances and Disease Registry, Atlanta, GA. 1993. p. 151.

72. U.S. Environmental Protection Agency. Noncarcinogenic Effects of Chromium. Update to Health Assessment Document. EPA-600/8-87/048F. Office of Health Effects and Assessment, RTP, NC. 1990. p. 3-6.

73. Reference 71, p. 129.

74. Reference 71, p. 145.

75. Reference 72, p. 3-13.

76. Reference 71, p. 153.

77. Reference 71, p. 3-13.

78. U.S. Public Health Service. Toxicological Profile for Lead. Agency for Toxic Substances and Disease Registry, Atlanta, GA. 1993. p. 190.

79. Reference 78, p. 188.

80. Reference 78, p. 188.

81. Reference 78, p. 189.

82. Reference 78, p. 189.

83. Reference 78, p. 190.

84. Reference 78, pp. 190 to 191.

85. Reference 78, p. 191.

86. Reference 78, p. 191.

87. Reference 78, p. 191.

88. U.S. Environmental Protection Aagency. An Ecological Assessment for Anthropogenic Mercury Emissions in the United States. EPA 452/R-96-003. Office of Air Quality Planning and Standards and the Office of Research and Development, Research Triangle Park, NC. 1994. P. 2-1.

89. Reference 88, p. 2-3.

90. Reference 88, pp. 2-3 to 2-4.

91. Reference 88, p. 2-4.

92. Reference 88, pp. 2-4 to 2-5.

93. Reference 88, pp. 2-2 to 2-3.

94. Reference 88, p. 2-4.

95. Reference 88, p. 2-2.

96. Reference 88, p. 2-4.

97. Reference 88, p. 2-2.

98. Reference 88, p. 2-4.

99. Reference 88, p. 2-5.

100. U.S. Public Health Service. Toxicological Profile for Nickel. Agency for Toxic Substances and Disease Registry, Atlanta, GA. 1993. pp. 89 to 90.

101. Reference 100, p. 81.

102. Reference 100, p. 90.

103. Reference 100, p. 89.

104. Reference 100, p. 89.

105. Reference 100, p. 93.

106. Reference 3, p. 2-22.

107. Reference 3, pp. 2-26 to 2-28.

108. Reference 3, p. 2-28.

109. Reference 3, p. 2-29.

110. Reference 3, p. 2-21.

111. Reference 3, pp. 2-34 to 2-35.

112. Reference 3, p. 2-30.

113. Reference 32, pp. 76 to 79, 125 to 129, 132 to 140, 163 to 177, 182 to 186, 195 to 203, 206 to 208, and 236 to 238.

114. Reference 33, pp. 132 to 137.

115. Reference 33, pp. 150 to 151.

116. Reference 33, p. 151.

117. Reference 33, p. 151.

118. Reference 32, pp. 76 to 79, 125 to 129, 132 to 140, 163 to 177, 182 to 186, 195 to 203, 206 to 208, and 236 to 238.

119. Reference 33, p. 152.

120. Reference 72, p. 3-6.

121. Reference 72, p. 129.

122. Reference 71, p. 153.

123. Reference 53, p. 103.

124. Reference 53, P. 104.

125. Reference 53, p. 103.

126. Reference 78, p. 190.

127. Reference 78, pp. 190 to 191.

128. Reference 78, p. 191.

129. Reference 78, p. 189.

130. Reference 78, p. 191.

131. Reference 78, p. 190.

132. Reference 60, p. 90.

133. Reference 60, pp. 89 to 90.

134. Reference 60, p. 91.

APPENDIX H-1

LIST OF UTILITY BOILER TEST REPORTS

TABLE H-1-1. List of Utility Boiler Test Reports

Provider	Site	Contractor	Report date
DOE	Baldwin	Roy F. Weston	12/93
DOE	Boswell	Roy F. Weston	12/93
DOE	Cardinal	Energy and Environmental Research Corp.	12/93
DOE	Coal Creek	Battelle	12/93
DOE	Niles	Battelle	12/93
DOE	Nile/NO_x	Battelle	12/93
DOE	Springerville	Southern Research Institute	12/93
DOE	Yates	Radian	12/93
NSP	A.S. King	Interpoll	11/91
NSP	Black Dog 1,3,4	Interpoll	1/92
NSP	Black Dog 2	Interpoll	5/92
NSP	HB 3,4,5,6	Interpoll	1/92
NSP	Riverside 6,7	Interpoll	2/92
NSP	Riverside 8	Interpoll	9/92
NSP	Sherburne 1,2	Interpoll	7/90, 10/91
NSP	Sherbourne 3	Interpoll	6/90, 10/91
EPRI	Site 10	Radian	10/92
EPRI	Site 102	Radian	2/93
EPRI	Site 11	Radian	10/92, 10/93
EPRI	Site 110	Southern Research Institue	10/93
EPRI	Site 110A	Southern Research Institute	10/93
EPRI	Site 111	Radian	1/94
EPRI	Site 112	Carnot	12/93, 3/94
EPRI	Site 114	NA	NA
EPRI	Site 115	Carnot	NA
EPRI	Site 117	Carnot	1/94
EPRI	Site 118	Carnot	1/94
EPRI	Site 119	Carnot	1/94

TABLE H-1-1. (continued)

Provider	Site	Contractor	Report date
EPRI	Site 12	Radian	11/92, 10/93
EPRI	Site 120	NA	NA
EPRI	Site 121	NA	NA
EPRI	Site 13	Radian	2/93
EPRI	Site 14	Radian	11/92
EPRI	Site 15	Radian	10/92
EPRI	Site 16/OFA	Radian	11/93
EPRI	Site 16/OFA/LONOX	Radian	11/93
EPRI	Site 18	Radian	4/93
EPRI	Site 19	Radian	4/93
EPRI	Site 21	Radian	5/93
EPRI	Site 22	Radian/Carnot	3/93, 2/94
EPRI	Site 103	Radian	3/93
EPRI	Site 104	Radian	3/93
EPRI	Site 105	Radian	3/93
EPRI	Site 106	Radian	3/93
EPRI	Site 107	Radian	3/93
EPRI	Site 108	Radian	3/93
EPRI	Site 109	Radian	3/93

NA = Not available

APPENDIX H-2

UTILITY BOILER STACK EMISSIONS OF FURANS/DIOXINS, PAHS, AND SIX TRACE METALS

The following tables give utility boiler emissions, in lb/1012 Btu, for furans/dioxins, PAHs, arsenic, cadmium, chromium, lead, mercury, and nickel. Limited speciation data are given for arsenic, chromium, mercury, and nickel.

The data in the tables are taken from a series of 47 test reports (resulting in 48 lines of data) provided by the Department of Energy (DOE), the Electric Power Research Institute (EPRI), and Northern States Power Company (NSP). The tests were performed at 43 sites. A legend and notes are provided at the end of the table. The table structure gives each test site in the first column, succeeded by type of emission control and stack emission values (in lb/1012 Btu) in the remaining columns. Dioxins/furans are given first, followed by PAHs and trace metals.

Table H-2-1. Speciation Data from Utility Boiler Tests for Dioxins and Furans (lb/10^{12} Btu)

Test Site	Fuel	Control	2378 TCDD	12378 PeCDD	123478 HxCDD	123678 HxCDD	123789 HxCDD
DOE Baldwin	Coal	ESP	2.30E-06				
DOE Boswell	Coal	FF	3.50E-07	6.03E-07	1.21E-06	6.03E-07	6.03E-07
DOE Cardinal	Coal	ESP					
DOE Creek	Coal	ESP/FGD					
DOE Niles2	Coal	ESP				2.87E-06	2.71E-06
DOE NilesNox2 (FF)	Coal	FF/SCR					
DOE NilesNox2 (WSA)	Coal	FF/SCR/WSA					
DOE Spring	Coal	SDA/FF					
DOE Yates	Coal	ESP/JBR			1.52E-05		
NSP-A.S. King	Coal	ESP	2.30E-06	4.26E-06	1.05E-05	8.72E-06	1.19E-05
NSP-BD-1-3-4	Coal	ESP					
NSP-BD-2	Coal	ESP					
NSP-HB-3-4-5-6	Coal	ESP					
NSP-Riv-6-7	Coal	FF					
NSP-Riv-8	Coal	ESP					
NSP-Sher-1-2	Coal	FGD					
NSP-Sher-3	Coal	SDA/FF	9.78E-07	4.38E-06	8.83E-06	1.83E-05	1.92E-05
Site 10	Coal	FBC/FF					
Site 102	Coal	ESP					
Site 11	Coal	ESP/FGD					
Site 110	Coal	HESP/CESP					
Site 110A	Coal	HESP/CESP					
Site 111	Coal	SDA/FF					
Site 112 (a)	Oil	ESP					
Site 114	Coal	ESP					
Site 115	Coal	FF					
Site 117 (a)	Oil	SCR					
Site 118	Oil	ESP		5.01E-06	1.24E-05	5.24E-06	8.73E-06
Site 119 (a)	Oil	ESP	6.51E-06	6.51E-06		5.64E-06	7.95E-06
Site 12	Coal	ESP/FGD					
Site 120	Gas	None					
Site 121	Gas	None					
Site 13	Oil	PJFF					
Site 14	Coal	SDA/PJFF					
Site 15	Coal	ESP					
Site 16/OFA	Coal	ESP					
Site 16/OFA/LNB (b)	Coal	ESP					
Site 18	Coal	ESP/COHPAC					
Site 19	Coal	ESP					
Site 21	Coal	ESP/FGD					
Site 22	Coal	ESP					
EPRI-103/Oil	Oil	None					
EPRI-104/Oil	Oil	None					
EPRI-105/Oil	Oil	None					
EPRI-106/Oil	Oil	None					
EPRI-107/Oil	Oil	None					
EPRI-108/Oil	Oil	None					
EPRI-109/Oil	Oil	None					
Average			2.49E-06	4.15E-06	9.63E-06	6.90E-06	8.52E-06
Median			2.30E-06	4.38E-06	1.05E-05	5.44E-06	8.34E-06
Max			6.51E-06	6.51E-06	1.52E-05	1.83E-05	1.92E-05
Min			3.50E-07	6.03E-07	1.21E-06	6.03E-07	6.03E-07
See notes at the end of table							

2378-TCDD = 2,3,7,8-Tetrachlorodibenzo-p-dioxin
12378-PeCDD = 1,2,3,7,8-Pentachlorodibenzo-p-dioxin
123478-HxCDD = 1,2,3,4,7,8-Hexachlorodibenzo-p-dioxin
123678-HxCDD = 1,2,3,6,7,8-Hexachlorodibenzo-p-dioxin
123789-HxCDD = 1,2,3,7,8,9-Hexachlorodibenzo-p-dioxin

(continued....)

Table H-2-1. Speciation Data from Utility Boiler Tests for Dioxins and Furans (lb/10^{12} Btu)

Test Site	Fuel	Control	1234678 HpCDD	OCDD	2378 TCDF	12378 PeCDF	23478 PeCDF
DOE Baldwin	Coal	ESP	1.19E-06	8.29E-06	1.15E-06	6.89E-07	1.62E-06
DOE Boswell	Coal	FF	5.99E-07	4.79E-06	2.59E-06	2.39E-06	2.19E-06
DOE Cardinal	Coal	ESP	2.28E-06		6.68E-07		
DOE Creek	Coal	ESP/FGD	3.21E-06	1.50E-05	9.51E-06		
DOE Niles2	Coal	ESP	1.67E-05	1.83E-05	4.63E-06		1.04E-05
DOE NilesNox2 (FF)	Coal	FF/SCR					
DOE NilesNox2 (WSA)	Coal	FF/SCR/WSA					
DOE Spring	Coal	SDA/FF					
DOE Yates	Coal	ESP/JBR	2.60E-05	1.29E-04	3.25E-06		
NSP-A.S. King	Coal	ESP	1.21E-04	1.99E-04	4.55E-05	2.09E-05	4.83E-05
NSP-BD-1-3-4	Coal	ESP					
NSP-BD-2	Coal	ESP					
NSP-HB-3-4-5-6	Coal	ESP					
NSP-Riv-6-7	Coal	FF					
NSP-Riv-8	Coal	ESP					
NSP-Sher-1-2	Coal	FGD					
NSP-Sher-3	Coal	SDA/FF	3.27E-04	1.71E-03	2.75E-05	1.26E-05	2.92E-05
Site 10	Coal	FBC/FF					
Site 102	Coal	ESP		2.56E-04			
Site 11	Coal	ESP/FGD					
Site 110	Coal	HESP/CESP					
Site 110A	Coal	HESP/CESP					
Site 111	Coal	SDA/FF					
Site 112 (a)	Oil	ESP					
Site 114	Coal	ESP					
Site 115	Coal	FF					
Site 117 (a)	Oil	SCR					
Site 118	Oil	ESP	2.74E-05	2.32E-05	1.97E-06	2.89E-06	3.11E-06
Site 119 (a)	Oil	ESP	1.23E-05		7.23E-06	5.79E-06	6.51E-06
Site 12	Coal	ESP/FGD					
Site 120	Gas	None					
Site 121	Gas	None					
Site 13	Oil	PJFF					
Site 14	Coal	SDA/PJFF					
Site 15	Coal	ESP					
Site 16/OFA	Coal	ESP					
Site 16/OFA/LNB (b)	Coal	ESP					
Site 18	Coal	ESP/COHPAC					
Site 19	Coal	ESP					
Site 21	Coal	ESP/FGD					
Site 22	Coal	ESP	5.73E-06	5.82E-05		2.44E-06	
EPRI-103/Oil	Oil	None					
EPRI-104/Oil	Oil	None					
EPRI-105/Oil	Oil	None					
EPRI-106/Oil	Oil	None					
EPRI-107/Oil	Oil	None					
EPRI-108/Oil	Oil	None					
EPRI-109/Oil	Oil	None					
Average			4.94E-05	2.42E-04	1.04E-05	6.81E-06	1.45E-05
Median			1.23E-05	4.07E-05	3.94E-06	2.89E-06	6.51E-06
Max			3.27E-04	1.71E-03	4.55E-05	2.09E-05	4.83E-05
Min			5.99E-07	4.79E-06	6.68E-07	6.89E-07	1.62E-06
See notes at the end of table							
1234678-HpCDD = 1,2,3,4,6,7,8-Heptachlorodibenzo-p-dioxin							
OCDD = Octachlorodibenzo-p-dioxin							
2378-TCDF = 2,3,7,8-Tetrachlorodibenzofuran							
12378-PeCDF = 1,2,3,7,8-Pentachlorodibenzofuran							
23478-PeCDF = 2,3,4,7,8-Pentachlorodibenzofuran						(continued....)	

Table H-2-1. Speciation Data from Utility Boiler Tests for Dioxins and Furans (lb/10^{12} Btu)

Test Site	Fuel	Control	123478 HxCDF	123678 HxCDF	123789 HxCDF	234678 HxCDF	1234678 HpCDF
DOE Baldwin	Coal	ESP	6.58E-06	7.33E-07		1.38E-06	1.36E-06
DOE Boswell	Coal	FF	2.79E-06	9.59E-07	6.03E-07	9.99E-07	1.99E-06
DOE Cardinal	Coal	ESP					
DOE Creek	Coal	ESP/FGD					3.96E-05
DOE Niles2	Coal	ESP	9.57E-06	3.99E-06	6.30E-06		1.67E-05
DOE NilesNox2 (FF)	Coal	FF/SCR					
DOE NilesNox2 (WSA)	Coal	FF/SCR/WSA					
DOE Spring	Coal	SDA/FF					
DOE Yates	Coal	ESP/JBR	1.62E-05			1.62E-05	2.27E-05
NSP-A.S. King	Coal	ESP	2.56E-04	8.77E-05	1.75E-05	1.88E-04	1.18E-03
NSP-BD-1-3-4	Coal	ESP					
NSP-BD-2	Coal	ESP					
NSP-HB-3-4-5-6	Coal	ESP					
NSP-Riv-6-7	Coal	FF					
NSP-Riv-8	Coal	ESP					
NSP-Sher-1-2	Coal	FGD					
NSP-Sher-3	Coal	SDA/FF	1.55E-04	5.30E-05	1.06E-05	1.14E-04	7.12E-04
Site 10	Coal	FBC/FF					
Site 102	Coal	ESP					
Site 11	Coal	ESP/FGD					
Site 110	Coal	HESP/CESP					
Site 110A	Coal	HESP/CESP					
Site 111	Coal	SDA/FF					
Site 112 (a)	Oil	ESP					
Site 114	Coal	ESP					
Site 115	Coal	FF					
Site 117 (a)	Oil	SCR					
Site 118	Oil	ESP	6.30E-06	3.34E-06	6.30E-06		
Site 119 (a)	Oil	ESP	5.79E-06	4.34E-06	5.35E-06	4.77E-06	9.40E-06
Site 12	Coal	ESP/FGD					
Site 120	Gas	None					
Site 121	Gas	None					
Site 13	Oil	PJFF					
Site 14	Coal	SDA/PJFF					
Site 15	Coal	ESP					
Site 16/OFA	Coal	ESP					
Site 16/OFA/LNB (b)	Coal	ESP					
Site 18	Coal	ESP/COHPAC					
Site 19	Coal	ESP					
Site 21	Coal	ESP/FGD					
Site 22	Coal	ESP					4.70E-06
EPRI-103/Oil	Oil	None					
EPRI-104/Oil	Oil	None					
EPRI-105/Oil	Oil	None					
EPRI-106/Oil	Oil	None					
EPRI-107/Oil	Oil	None					
EPRI-108/Oil	Oil	None					
EPRI-109/Oil	Oil	None					
Average			5.73E-05	2.20E-05	7.78E-06	5.42E-05	2.21E-04
Median			8.08E-06	3.99E-06	6.30E-06	1.05E-05	1.67E-05
Max			2.56E-04	8.77E-05	1.75E-05	1.88E-04	1.18E-03
Min			2.79E-06	7.33E-07	6.03E-07	9.99E-07	1.36E-06
See notes at the end of table							
123478-HxCDF = 1,2,3,4,7,8-Hexachlorodibenzofuran							
123678-HxCDF = 1,2,3,6,7,8-Hexachlorodibenzofuran							
123789-HxCDF = 1,2,3,7,8,9-Hexachlorodibenzofuran							
234678-HxCDF = 2,3,4,6,7,8-Hexachlorodibenzofuran							
1234678-HpCDF = 1,2,3,4,6,7,8-Heptachlorodibenzofuran						(continued....)	

Table H-2-1. Speciation Data from Utility Boiler Tests for Dioxins and Furans (lb/10^{12} Btu)

Test Site	Fuel	Control	1234789 HpCDF	OCDF	TCDD	PeCDD	HxCDD
DOE Baldwin	Coal	ESP		3.85E-06	1.24E-06	6.89E-07	8.76E-07
DOE Boswell	Coal	FF	1.21E-06	7.99E-07	4.00E-06	1.99E-06	8.96E-07
DOE Cardinal	Coal	ESP		9.12E-06			2.25E-05
DOE Creek	Coal	ESP/FGD		1.39E-05			
DOE Niles2	Coal	ESP	3.67E-06	1.91E-05	7.10E-06	2.47E-06	9.57E-06
DOE NilesNox2 (FF)	Coal	FF/SCR					
DOE NilesNox2 (WSA)	Coal	FF/SCR/WSA					
DOE Spring	Coal	SDA/FF			5.97E-05		
DOE Yates	Coal	ESP/JBR		1.29E-04	6.61E-06		2.59E-05
NSP-A.S. King	Coal	ESP	5.67E-04	5.10E-04	1.40E-05	1.72E-05	6.24E-05
NSP-BD-1-3-4	Coal	ESP					
NSP-BD-2	Coal	ESP					
NSP-HB-3-4-5-6	Coal	ESP					
NSP-Riv-6-7	Coal	FF					
NSP-Riv-8	Coal	ESP					
NSP-Sher-1-2	Coal	FGD					
NSP-Sher-3	Coal	SDA/FF	3.43E-04	8.21E-03	2.35E-05	4.22E-05	1.80E-04
Site 10	Coal	FBC/FF					
Site 102	Coal	ESP		6.60E-04	1.21E-05	2.56E-05	5.68E-05
Site 11	Coal	ESP/FGD					
Site 110	Coal	HESP/CESP					
Site 110A	Coal	HESP/CESP					
Site 111	Coal	SDA/FF					
Site 112 (a)	Oil	ESP					
Site 114	Coal	ESP					
Site 115	Coal	FF					
Site 117 (a)	Oil	SCR					
Site 118	Oil	ESP			4.78E-06	5.01E-06	7.52E-06
Site 119 (a)	Oil	ESP	1.01E-05	1.01E-05	6.51E-06	6.51E-06	8.68E-06
Site 12	Coal	ESP/FGD					
Site 120	Gas	None					
Site 121	Gas	None					
Site 13	Oil	PJFF					
Site 14	Coal	SDA/PJFF					
Site 15	Coal	ESP					
Site 16/OFA	Coal	ESP					
Site 16/OFA/LNB (b)	Coal	ESP					
Site 18	Coal	ESP/COHPAC					
Site 19	Coal	ESP					
Site 21	Coal	ESP/FGD					
Site 22	Coal	ESP		4.70E-06	5.26E-06		
EPRI-103/Oil	Oil	None					
EPRI-104/Oil	Oil	None					
EPRI-105/Oil	Oil	None					
EPRI-106/Oil	Oil	None					
EPRI-107/Oil	Oil	None					
EPRI-108/Oil	Oil	None					
EPRI-109/Oil	Oil	None					
Average			1.85E-04	8.70E-04	1.32E-05	1.27E-05	3.75E-05
Median			1.01E-05	1.39E-05	6.61E-06	5.76E-06	1.60E-05
Max			5.67E-04	8.21E-03	5.97E-05	4.22E-05	1.80E-04
Min			1.21E-06	7.99E-07	1.24E-06	6.89E-07	8.76E-07
See notes at the end of table							

1234789-HpCDF = 1,2,3,4,7,8,9-Heptachlorodibenzofuran
OCDF = Octachlorodibenzofuran
TCDD = Tetrachlorodibenzo-p-dioxin
PeCDD = Pentachlorodibenzo-p-dioxin
HxCDD = Hexachlorodibenzo-p-dioxin

(continued...)

Table H-2-1. Speciation Data from Utility Boiler Tests for Dioxins and Furans (lb/10^{12} Btu)

Test Site	Fuel	Control	HpCDD	TCDF	PeCDF	HxCDF	HpCDF
DOE Baldwin	Coal	ESP	2.34E-06	3.56E-06	3.69E-06	5.10E-06	2.93E-06
DOE Boswell	Coal	FF		2.59E-05	2.03E-05	9.59E-06	2.99E-06
DOE Cardinal	Coal	ESP					
DOE Creek	Coal	ESP/FGD		6.52E-05	1.07E-05		
DOE Niles2	Coal	ESP	2.55E-05	1.59E-05	1.83E-05	2.15E-05	1.91E-05
DOE NilesNox2 (FF)	Coal	FF/SCR					
DOE NilesNox2 (WSA)	Coal	FF/SCR/WSA					
DOE Spring	Coal	SDA/FF		1.37E-06			
DOE Yates	Coal	ESP/JBR		3.25E-06	6.51E-06	1.62E-05	2.91E-05
NSP-A.S. King	Coal	ESP	1.89E-04	1.18E-05	1.81E-05	6.72E-05	2.68E-04
NSP-BD-1-3-4	Coal	ESP					
NSP-BD-2	Coal	ESP					
NSP-HB-3-4-5-6	Coal	ESP					
NSP-Riv-6-7	Coal	FF					
NSP-Riv-8	Coal	ESP					
NSP-Sher-1-2	Coal	FGD					
NSP-Sher-3	Coal	SDA/FF	6.00E-04	1.49E-04	2.89E-04	7.62E-04	2.63E-03
Site 10	Coal	FBC/FF					
Site 102	Coal	ESP	2.06E-04	1.14E-05	2.13E-05	7.81E-05	2.91E-04
Site 11	Coal	ESP/FGD					
Site 110	Coal	HESP/CESP					
Site 110A	Coal	HESP/CESP					
Site 111	Coal	SDA/FF					
Site 112 (a)	Oil	ESP					
Site 114	Coal	ESP					
Site 115	Coal	FF					
Site 117 (a)	Oil	SCR					
Site 118	Oil	ESP	2.74E-05	1.97E-06	2.89E-06	5.47E-06	
Site 119 (a)	Oil	ESP	1.23E-05	7.95E-06	1.16E-05	1.37E-05	1.45E-06
Site 12	Coal	ESP/FGD					
Site 120	Gas	None					
Site 121	Gas	None					
Site 13	Oil	PJFF					
Site 14	Coal	SDA/PJFF					
Site 15	Coal	ESP					
Site 16/OFA	Coal	ESP					
Site 16/OFA/LNB (b)	Coal	ESP					
Site 18	Coal	ESP/COHPAC					
Site 19	Coal	ESP					
Site 21	Coal	ESP/FGD					
Site 22	Coal	ESP	1.13E-05	6.86E-06	8.08E-06	3.85E-06	2.54E-06
EPRI-103/Oil	Oil	None					
EPRI-104/Oil	Oil	None					
EPRI-105/Oil	Oil	None					
EPRI-106/Oil	Oil	None					
EPRI-107/Oil	Oil	None					
EPRI-108/Oil	Oil	None					
EPRI-109/Oil	Oil	None					
Average			1.34E-04	2.53E-05	3.73E-05	9.83E-05	3.61E-04
Median			2.65E-05	9.68E-06	1.16E-05	1.50E-05	1.91E-05
Max			6.00E-04	1.49E-04	2.89E-04	7.62E-04	2.63E-03
Min			2.34E-06	1.37E-06	2.89E-06	3.85E-06	1.45E-06
See notes at the end of table							
HpCDD = Heptachlorodibenzo-p-dioxin							
TCDF = Tetrachlorodibenzofuran							
PeCDF = Pentachlorodibenzofuran							
HxCDF = Hexachlorodibenzofuran							
HpCDF = Heptachlorodibenzofuran							

LEGEND AND NOTES TO TABLES H-2-1 through H-2-3

Chemical abbreviations are shown below. Numerical entries are averages of (usually) three measurments in $lb/10^{12}$ Btu. Shaded values in the table include one or more measurements below the detection limit. However, at least one mesurement in each average is above the detection limit. See Section H.2.2 for a further discussion of nondetects.

DIOXINS AND FURANS

2378	2,3,7,8-TETRACHLORODIBENZO-P-DIOXIN
12378P	1,2,3,7,8-PENTACHLORODIBENZO-P-DIOXIN
123478	1,2,3,4,7,8-HEXACHLORODIBENZO-P-DIOXIN
123678	1,2,3,6,7,8-HEXACHLORODIBENZO-P-DIOXIN
123789	1,2,3,7,8,9-HEXACHLORODIBENZO-P-DIOXIN
1234678H	1,2,3,4,6,7,8-HEPTACHLORODIBENZO-P-DIOXIN
OCTA DI	OCTACHLORODIBENZO-P-DIOXIN
2378T	2,3,7,8-TETRACHLORODIBENZOFURAN
12378P	1,2,3,7,8-PENTACHLORODIBENZOFURAN
23478P	2,3,4,7,8-PENTACHLORODIBENZOFURAN
123478	1,2,3,4,7,8-HEXACHLORODIBENZOFURAN
123678	1,2,3,6,7,8-HEXACHLORODIBENZOFURAN
123789	1,2,3,7,8,9-HEXACHLORODIBENZOFURAN
234678	2,3,4,6,7,8-HEXACHLORODIBENZOFURAN
1234678H	1,2,3,4,6,7,8-HEPTACHLORODIBENZOFURAN
1234789H	1,2,3,4,7,8,9-HEPTACHLORODIBENZOFURAN
OCTA F	OCTACHLORODIBENZOFURAN
TETRAPDI	TETRACHLORODIBENZO-P-DIOXIN
PENTAPDI	PENTACHLORODIBENZO-P-DIOXIN
HEXAPDI	HEXACHLORODIBENZO-P-DIOXIN
HEPTAPDI	HEPTACHLORODIBENZO-P-DIOXIN
TETRAF	TETRACHLORODIBENZOFURAN
PENTAF	PENTACHLORODIBENZOFURAN
HEXAF	HEXACHLORODIBENZOFURAN
HEPTAF	HEPTACHLORODIBENZOFURAN

PAHs

1CLNAPH	1-CHLORONAPHTHALENE
1MTHLNAPH	1-METHYLNAPHTHALENE
2CLNAPH	2-CHLORONAPHTHALENE
2MTHLNAPH	2-METHYLNAPHTHALENE
3MTCHOL	3-METHYCHOLANTHRENE
7,12DIMET	7,12-DIMETHYLBENZ(a)ANTHRACENE
ACENAPH	ACENAPHTHENE
ACENAPHY	ACENAPHTHYLENE
ANTHRACN	ANTHRACENE
BNZaANTH	BENZ(a)ANTHRACENE
BNZOaPYR	BENZO(a)PYRENE

BNZOePYR	BENZO(e)PYRENE
BENZObFLN	BENZO(b)FLUORANTHENE
BNZObkFLN	BENZO(b+k)FLUORANTHENE
BNZOkFLN	BENZO(k)FLUORANTHENE
BNZOghiPERY	BENZO(g,h,i)PERYLENE
BIPHENYL	BIPHENYL
CHRYSENE	CHRYSENE
DBNZajACR	DIBENZ(a,j)ACRIDINE
DBNZOahANT	DIBENZO(a,h)ANTHRACENE
FLURANTHN	FLUORANTHENE
FLUORENE	FLUORENE
INDNOPYRN	INDENO(1,2,3-c,d)PYRENE
NTRANTHRCN	NITRANTHRACENE/PHENANTHRENE
NTRBNZFLU	NITROBENZOFLUORANTHENE
NTROCHRYS	NITROCHRYSENE/BENZANTHRACENE
PERYLENE	PERYLENE
PHNANTREN	PHENANTHRENE
PYRENE	PYRENE

TRACE METALS AND ARSENIC

LEAD	TOTAL LEAD
MERCURY	TOTAL MERCURY
HG ELEM	ELEMENTAL MERCURY
HG ION	IONIC MERCURY
CADMIUM	TOTAL CADMIUM
ARSENIC	TOTAL ARSENIC
AS III	TRIVALENT ARSENIC
AS V	PENTAVALENT ARSENIC
CHROM	TOTAL CHROMIUM
CHROM6	HEXAVALENT CHROMIUM
NICKEL	TOTAL NICKEL
SOLY N	SOLUBLE NICKEL
SULF N	SULFIDIC NICKEL
MET N	METALLIC NICKEL
OX N	OXIDIZED NICKEL

Abbreviations under the "CONTROL" column are:

CESP	Cold-side electrostatic precipitator
COHPAC	Compact hybrid particulate collector
ESP	Electrostatic precipitator
FBC	Fluidized bed combustor
FF	Fabric filter
FGD	Flue-gas desulfurization
HESP	Hot-side electrostatic precipitator
JBR	Jet bubbling reactor [SO_2 control]
PJFF	Pulse-jet fabric filter
SCR	Selective catalytic reduction [NO_x control]
SDA	Spray drier absorber [SO_2 control]
WSA	Wet sulfuric acid [condenser]

Note 1. Magnesium oxide is added to the fuel oil. Because Site 112 had an apparently low-efficiency ESP (less than 4 percent), and sampling problems were found at the ESP outlet, reported values are taken from the ESP inlet.

Note 2. Ammonia is added to the flue gas to improve ESP performance.

Table H-2-2. Speciation Data from Utility Boiler Tests for PAHs (lb/10^{12} Btu)

Test Site	Fuel	Control	1MTHLNAPH	2CLNAPH	2MTHLNAPH	ACENAPH	ACENAPHY
DOE Baldwin	Coal	ESP		1.44E-04			
DOE Boswell	Coal	FF		8.07E-02	7.87E-02	7.37E-02	
DOE Cardinal	Coal	ESP					
DOE Creek	Coal	ESP/FGD					
DOE Niles2	Coal	ESP					
DOE Nilesnox2 (FF)	Coal	FF/SCR	5.55E-03		1.03E-02	7.85E-02	4.16E-03
DOE Nilesnox2 (WSA)	Coal	FF/SCR/WSA	1.14E-02		1.99E-02	5.35E-03	4.16E-03
DOE Spring	Coal	SDA/FF					
DOE Yates	Coal	ESP/JBR					
NSP-A.S. King	Coal	ESP					
NSP-BD-1-3-4	Coal	ESP					
NSP-BD-2	Coal	ESP					
NSP-HB-3-4-5-6	Coal	ESP					
NSP-RIV-6-7	Coal	FF					
NSP-RIV-8	Coal	ESP					
NSP-SHER-1-2	Coal	FGD					
NSP-SHER-3	Coal	SDA/FF					
Site 10	Coal	FBC/FF					
Site 102	Coal	ESP					
Site 11	Coal	ESP/FGD					
Site 110	Coal	HESP/CESP					
Site 110A	Coal	HESP/CESP					
Site 111	Coal	SDA/FF				7.76E-03	2.80E-02
Site 112 (a)	Oil	ESP					
Site 114	Coal	ESP					
Site 115	Coal	FF			2.72E-02		
Site 117 (a)	Oil	SCR			1.90E-02		
Site 118	Oil	ESP			2.70E-02		
Site 119 (a)	Oil	ESP					
Site 12	Coal	ESP/FGD					
Site 120	Gas	None					
Site 121	Gas	None					
Site 13	Oil	PJFF					
Site 14	Coal	SDA/PJFF					
Site 15	Coal	ESP					
Site 16/OFA	Coal	ESP					
Site 16/OFA/LNB (b)	Coal	ESP				8.10E-03	3.00E-03
Site 18	Coal	ESP/COHPAC					
Site 19	Coal	ESP					
Site 21	Coal	ESP/FGD					
Site 22	Coal	ESP				6.00E-03	3.40E-03
EPRI-103/Oil	Oil	None					
EPRI-104/Oil	Oil	None					
EPRI-105/Oil	Oil	None					
EPRI-106/Oil	Oil	None					
EPRI-107/Oil	Oil	None					
EPRI-108/Oil	Oil	None					
EPRI-109/Oil	Oil	None					
Average			8.48E-03	4.04E-02	3.03E-02	2.99E-02	8.55E-03
Median			8.48E-03	4.04E-02	2.34E-02	7.93E-03	4.16E-03
Max			1.14E-02	8.07E-02	7.87E-02	7.85E-02	2.80E-02
Min			5.55E-03	1.44E-04	1.03E-02	5.35E-03	3.00E-03

See notes at the end of table H-2-1

1MTHLNAPH = 1-Methylnaphthalene
2CLNAPH = 2-Chloronaphthalene
2MTHLNAPH = 2-Methylnaphthalene
ACENAPH = Acenaphthene
ACENAPHY = Acenaphthylene

(continued...)

Table H-2-2. Speciation Data from Utility Boiler Tests for PAHs (lb/10^{12} Btu)

Test Site	Fuel	Control	ANTHRACN	BNZaANTH	BNZOaPYR	BNZOePYR	BNZObFLN
DOE Baldwin	Coal	ESP			2.27E-04		
DOE Boswell	Coal	FF			3.67E-02		
DOE Cardinal	Coal	ESP					
DOE Creek	Coal	ESP/FGD					
DOE Niles2	Coal	ESP					
DOE Nilesnox2 (FF)	Coal	FF/SCR	1.72E-03	2.05E-03	6.60E-04	1.21E-03	
DOE Nilesnox2 (WSA)	Coal	FF/SCR/WSA		2.14E-03	9.40E-04		
DOE Spring	Coal	SDA/FF					
DOE Yates	Coal	ESP/JBR					
NSP-A.S. King	Coal	ESP					
NSP-BD-1-3-4	Coal	ESP					
NSP-BD-2	Coal	ESP					
NSP-HB-3-4-5-6	Coal	ESP					
NSP-RIV-6-7	Coal	FF					
NSP-RIV-8	Coal	ESP					
NSP-SHER-1-2	Coal	FGD					
NSP-SHER-3	Coal	SDA/FF					
Site 10	Coal	FBC/FF					
Site 102	Coal	ESP					
Site 11	Coal	ESP/FGD					
Site 110	Coal	HESP/CESP					
Site 110A	Coal	HESP/CESP					
Site 111	Coal	SDA/FF	2 15E-02	8 84E-03			8.08E-03
Site 112 (a)	Oil	ESP					
Site 114	Coal	ESP					
Site 115	Coal	FF					
Site 117 (a)	Oil	SCR					
Site 118	Oil	ESP					
Site 119 (a)	Oil	ESP					
Site 12	Coal	ESP/FGD					
Site 120	Gas	None					
Site 121	Gas	None					
Site 13	Oil	PJFF					
Site 14	Coal	SDA/PJFF					
Site 15	Coal	ESP					
Site 16/OFA	Coal	ESP					
Site 16/OFA/LNB (b)	Coal	ESP	3.70E-03		1.89E-03		
Site 18	Coal	ESP/COHPAC					
Site 19	Coal	ESP					
Site 21	Coal	ESP/FGD					
Site 22	Coal	ESP	4.60E-03	1.00E-03	1.10E-03		
EPRI-103/Oil	Oil	None					
EPRI-104/Oil	Oil	None					
EPRI-105/Oil	Oil	None					
EPRI-106/Oil	Oil	None					
EPRI-107/Oil	Oil	None					
EPRI-108/Oil	Oil	None					
EPRI-109/Oil	Oil	None					
Average			7.87E-03	3.51E-03	6.92E-03	1.21E-03	8.08E-03
Median			4.15E-03	2.10E-03	1.02E-03	1.21E-03	8.08E-03
Max			2.15E-02	8.84E-03	3.67E-02	1.21E-03	8.08E-03
Min			1.72E-03	1.00E-03	2.27E-04	1.21E-03	8.08E-03
See notes at the end of table H-2-1							
ANTHRACN = Anthracene							
BNZaANTH = Benz(a)anthracene							
BNZOaPYR = Benzo(a)pyrene							
BNZOePYR = Benzo(e)pyrene							
BNZObFLN = Benzo(b)fluoranthene							
						(continued...)	

Table H-2-2. Speciation Data from Utility Boiler Tests for PAHs (lb/10^{12} Btu)

Test Site	Fuel	Control	BNZObkFLN	BNZOkFLN	BNZOghiPERY	BIPHENYL	CHRYSENE
DOE Baldwin	Coal	ESP					
DOE Boswell	Coal	FF					
DOE Cardinal	Coal	ESP					
DOE Creek	Coal	ESP/FGD					
DOE Niles2	Coal	ESP					
DOE Nilesnox2 (FF)	Coal	FF/SCR	1.61E-03			3.43E-01	2.71E-03
DOE Nilesnox2 (WSA)	Coal	FF/SCR/WSA					
DOE Spring	Coal	SDA/FF					
DOE Yates	Coal	ESP/JBR					
NSP-A.S. King	Coal	ESP					
NSP-BD-1-3-4	Coal	ESP					
NSP-BD-2	Coal	ESP					
NSP-HB-3-4-5-6	Coal	ESP					
NSP-RIV-6-7	Coal	FF					
NSP-RIV-8	Coal	ESP					
NSP-SHER-1-2	Coal	FGD					
NSP-SHER-3	Coal	SDA/FF					
Site 10	Coal	FBC/FF					
Site 102	Coal	ESP					
Site 11	Coal	ESP/FGD					
Site 110	Coal	HESP/CESP					
Site 110A	Coal	HESP/CESP					
Site 111	Coal	SDA/FF		3.56E-03	4.20E-03		3.56E-03
Site 112 (a)	Oil	ESP					
Site 114	Coal	ESP					
Site 115	Coal	FF					
Site 117 (a)	Oil	SCR					
Site 118	Oil	ESP					
Site 119 (a)	Oil	ESP					
Site 12	Coal	ESP/FGD					
Site 120	Gas	None					
Site 121	Gas	None					
Site 13	Oil	PJFF					
Site 14	Coal	SDA/PJFF					
Site 15	Coal	ESP					
Site 16/OFA	Coal	ESP					
Site 16/OFA/LNB (b)	Coal	ESP					7.87E-04
Site 18	Coal	ESP/COHPAC					
Site 19	Coal	ESP					
Site 21	Coal	ESP/FGD					
Site 22	Coal	ESP			2.20E-03		2.50E-03
EPRI-103/Oil	Oil	None					
EPRI-104/Oil	Oil	None					
EPRI-105/Oil	Oil	None					
EPRI-106/Oil	Oil	None					
EPRI-107/Oil	Oil	None					
EPRI-108/Oil	Oil	None					
EPRI-109/Oil	Oil	None					
Average			1.61E-03	3.56E-03	3.20E-03	3.43E-01	2.39E-03
Median			1.61E-03	3.56E-03	3.20E-03	3.43E-01	2.61E-03
Max			1.61E-03	3.56E-03	4.20E-03	3.43E-01	3.56E-03
Min			1.61E-03	3.56E-03	2.20E-03	3.43E-01	7.87E-04
See notes at the end of table H-2-1							
BNZObkFLN = Benzo(b+k)fluoranthene							
BNZOkFLN = Benzo(k) Fluoranthene							
BNZOghiPERY = Benzo(g,h,i)perylene							
BIPHENYL = Biphenyl							
CHRYSENE = Chrysene							
						(continued...)	

Table H-2-2. Speciation Data from Utility Boiler Tests for PAHs (lb/10^{12} Btu)

Test Site	Fuel	Control	DBNZOahANT	FLURANTHN	FLUORENE	INDNOPYRN	NTRBNZFLU
DOE Baldwin	Coal	ESP		7.29E-03			
DOE Boswell	Coal	FF					
DOE Cardinal	Coal	ESP					
DOE Creek	Coal	ESP/FGD					
DOE Niles2	Coal	ESP			1.35E-02		
DOE Nilesnox2 (FF)	Coal	FF/SCR		5.13E-03	1.32E-02		
DOE Nilesnox2 (WSA)	Coal	FF/SCR/WSA					
DOE Spring	Coal	SDA/FF					
DOE Yates	Coal	ESP/JBR					
NSP-A.S. King	Coal	ESP					
NSP-BD-1-3-4	Coal	ESP					
NSP-BD-2	Coal	ESP					
NSP-HB-3-4-5-6	Coal	ESP					
NSP-RIV-6-7	Coal	FF					
NSP-RIV-8	Coal	ESP					
NSP-SHER-1-2	Coal	FGD					
NSP-SHER-3	Coal	SDA/FF					
Site 10	Coal	FBC/FF					
Site 102	Coal	ESP					
Site 11	Coal	ESP/FGD					
Site 110	Coal	HESP/CESP					
Site 110A	Coal	HESP/CESP					
Site 111	Coal	SDA/FF		2.91E-02	1.72E-01	4.20E-03	
Site 112 (a)	Oil	ESP					
Site 114	Coal	ESP					
Site 115	Coal	FF					
Site 117 (a)	Oil	SCR		5.12E-03			1.50E-02
Site 118	Oil	ESP					
Site 119 (a)	Oil	ESP					
Site 12	Coal	ESP/FGD					
Site 120	Gas	None					
Site 121	Gas	None					
Site 13	Oil	PJFF					
Site 14	Coal	SDA/PJFF					
Site 15	Coal	ESP					
Site 16/OFA	Coal	ESP					
Site 16/OFA/LNB (b)	Coal	ESP		4.72E-03	4.33E-03		
Site 18	Coal	ESP/COHPAC					
Site 19	Coal	ESP					
Site 21	Coal	ESP/FGD					
Site 22	Coal	ESP	3.30E-04	2.40E-02	1.20E-02	8.60E-03	
EPRI-103/Oil	Oil	None					
EPRI-104/Oil	Oil	None					
EPRI-105/Oil	Oil	None					
EPRI-106/Oil	Oil	None					
EPRI-107/Oil	Oil	None					
EPRI-108/Oil	Oil	None					
EPRI-109/Oil	Oil	None					
Average			3.30E-04	1.26E-02	4.30E-02	6.40E-03	1.50E-02
Median			3.30E-04	6.21E-03	1.32E-02	6.40E-03	1.50E-02
Max			3.30E-04	2.91E-02	1.72E-01	8.60E-03	1.50E-02
Min			3.30E-04	4.72E-03	4.33E-03	4.20E-03	1.50E-02

See notes at the end of table H-2-1

DBNZOahANT = Dibenzo(a,h)anthracene
FLURANTHN = Fluoranthene
FLUORENE = Fluorine
INDNOPYRN = Indeno (1,2,3-c,d)pyrene
NTRBNZFLU = Nitrobenzofluoranthene

(continued...)

Table H-2-2. Speciation Data from Utility Boiler Tests for PAHs ($lb/10^{12}$ Btu)

Test Site	Fuel	Control	NTROCHRYS	PHNANTREN	PYRENE		
DOE Baldwin	Coal	ESP					
DOE Boswell	Coal	FF					
DOE Cardinal	Coal	ESP		2.38E-02			
DOE Creek	Coal	ESP/FGD					
DOE Niles2	Coal	ESP					
DOE Nilesnox2 (FF)	Coal	FF/SCR		3.15E-02	1.21E-03		
DOE Nilesnox2 (WSA)	Coal	FF/SCR/WSA					
DOE Spring	Coal	SDA/FF					
DOE Yates	Coal	ESP/JBR					
NSP-A.S. King	Coal	ESP					
NSP-BD-1-3-4	Coal	ESP					
NSP-BD-2	Coal	ESP					
NSP-HB-3-4-5-6	Coal	ESP					
NSP-RIV-6-7	Coal	FF					
NSP-RIV-8	Coal	ESP					
NSP-SHER-1-2	Coal	FGD					
NSP-SHER-3	Coal	SDA/FF					
Site 10	Coal	FBC/FF					
Site 102	Coal	ESP					
Site 11	Coal	ESP/FGD					
Site 110	Coal	HESP/CESP					
Site 110A	Coal	HESP/CESP					
Site 111	Coal	SDA/FF		1.29E-01	1.29E-02		
Site 112 (a)	Oil	ESP					
Site 114	Coal	ESP					
Site 115	Coal	FF					
Site 117 (a)	Oil	SCR	1.60E-02	1.70E-02			
Site 118	Oil	ESP		1.20E-02			
Site 119 (a)	Oil	ESP					
Site 12	Coal	ESP/FGD					
Site 120	Gas	None					
Site 121	Gas	None					
Site 13	Oil	PJFF					
Site 14	Coal	SDA/PJFF					
Site 15	Coal	ESP					
Site 16/OFA	Coal	ESP					
Site 16/OFA/LNB (b)	Coal	ESP		2.01E-02	4.72E-03		
Site 18	Coal	ESP/COHPAC					
Site 19	Coal	ESP					
Site 21	Coal	ESP/FGD					
Site 22	Coal	ESP		6.90E-02	1.60E-01		
EPRI-103/Oil	Oil	None					
EPRI-104/Oil	Oil	None					
EPRI-105/Oil	Oil	None					
EPRI-106/Oil	Oil	None					
EPRI-107/Oil	Oil	None					
EPRI-108/Oil	Oil	None					
EPRI-109/Oil	Oil	None					
Average			1.60E-02	4.32E-02	4.47E-02		
Median			1.60E-02	2.38E-02	8.83E-03		
Max			1.60E-02	1.29E-01	1.60E-01		
Min			1.60E-02	1.20E-02	1.21E-03		
See other notes at the end of table H-2-1							
NTROCHRYS = Nitrochrysene/Benzanthracene							
PHNANTREN = Phenanthrene							
PYRENE = Pyrene							

Table H-2-3. Speciation Data from Utility Boiler Tests for Metals (lb/10^{12} Btu)

Test Site	Fuel	Control	Lead	Mercury	HG ELEM	HG ION	Cadmium
DOE Baldwin	Coal	ESP	2.86E+01	3.36E+00	1.44E+00	3.17E+00	2.69E+00
DOE Boswell	Coal	FF	2.44E+00	4.69E+00	5.34E-01	1.69E+00	1.10E+01
DOE Cardinal	Coal	ESP	3.78E+00	5.31E-01			8.00E-01
DOE Creek	Coal	ESP/FGD	6.63E-01	9.09E+00			
DOE Niles2	Coal	ESP	1.61E+00	1.45E+01			6.78E-02
DOE NilesNox2 (FF)	Coal	FF/SCR	3.66E-01	1.95E+01			6.30E-02
DOE NilesNox2 (WSA)	Coal	FF/SCR/WSA	5.22E-01	2.29E+01			1.07E-01
DOE Spring	Coal	SDA/FF	6.76E-01	3.93E+00			
DOE Yates	Coal	ESP/JBR	3.55E-01	3.07E+00	2.80E+00	5.10E-01	6.00E-01
NSP-A.S. King	Coal	ESP	2.76E+00	1.83E+00			1.13E-01
NSP-BD-1-3-4	Coal	ESP	1.40E+01	3.10E+00			1.06E+00
NSP-BD-2	Coal	ESP	5.08E+01	2.60E+00			6.55E+00
NSP-HB-3-4-5-6	Coal	ESP	2.60E+00	3.92E+00			5.70E+00
NSP-Riv-6-7	Coal	FF	6.80E+00	4.87E+00			2.85E+01
NSP-Riv-8	Coal	ESP	2.49E+00	3.52E+00			
NSP-Sher-1-2	Coal	FGD	5.90E+00	1.05E+01			8.23E+00
NSP-Sher-3	Coal	SDA/FF	7.07E+00	3.62E+00			8.07E+00
Site 10	Coal	FBC/FF	2.52E+00				
Site 102	Coal	ESP	2.70E+00	1.78E+00			2.12E-01
Site 11	Coal	ESP/FGD	6.78E+00	6.78E+00	5.35E+00	2.16E+00	1.26E+00
Site 110	Coal	HESP/CESP	1.83E+01	6.20E+00	1.24E+00	5.49E+00	1.74E+00
Site 110A	Coal	HESP/CESP	1.72E+01	4.99E+00	4.60E-01	4.43E+00	1.72E+00
Site 111	Coal	SDA/FF					2.13E+00
Site 112 (a)	Oil	ESP	2.61E+00	2.38E-01	ND	2.72E-02	3.23E-01
Site 114	Coal	ESP	7.56E+01	4.66E+00			1.81E+00
Site 115	Coal	FF	4.34E-01	3.50E-01			2.33E-02
Site 117 (a)	Oil	SCR	9.10E+00	4.80E-01			1.30E-01
Site 118	Oil	ESP	1.78E+00	4.00E-01			1.80E-01
Site 119 (a)	Oil	ESP					
Site 12	Coal	ESP/FGD	4.48E+00	1.33E+00			1.87E+00
Site 120	Gas	None	2.64E-01				
Site 121	Gas	None	4.68E-01	3.95E-01			
Site 13	Oil	PJFF	3.00E-01	6.60E-02			
Site 14	Coal	SDA/PJFF	2.82E+00	2.00E+00			9.60E-01
Site 15	Coal	ESP	4.75E+00	1.04E+00			3.05E+00
Site 16/OFA	Coal	ESP	3.33E+01	6.38E+00			5.02E-01
Site 16/OFA/LNB (b)	Coal	ESP	1.13E+01	4.85E+00	3.61E+00	3.05E+00	3.64E+00
Site 18	Coal	ESP/COHPAC		7.10E+00			3.10E+00
Site 19	Coal	ESP		6.20E+00			1.30E-01
Site 21	Coal	ESP/FGD	6.32E+00	8.40E-01	5.38E-01	7.47E-02	5.70E-01
Site 22	Coal	ESP	1.10E-01	3.80E+00	1.47E+01	5.99E-01	1.60E-01
EPRI-103/Oil	Oil	None	3.71E+00				3.19E+00
EPRI-104/Oil	Oil	None	2.23E+00				7.17E-01
EPRI-105/Oil	Oil	None	8.94E+00				7.03E-01
EPRI-106/Oil	Oil	None	2.78E+01				1.22E+00
EPRI-107/Oil	Oil	None					1.56E+00
EPRI-108/Oil	Oil	None	1.04E+01				3.97E+00
EPRI-109/Oil	Oil	None	1.92E+01	2.11E+00			3.11E+00
Average			1.35E+01	4.53E+00	3.40E+00	2.12E+00	2.79E+00
Median			3.78E+00	3.44E+00	1.44E+00	1.93E+00	1.24E+00
Max			1.76E+02	2.29E+01	1.47E+01	5.49E+00	2.85E+01
Min			1.10E-01	6.60E-02	4.60E-01	2.72E-02	2.33E-02
See notes at the end of table H-2-1							
LEAD = Total Lead							
MERCURY = Total Mercury							
HG ELEM = Elemental Mercury							
HG ION = Ionic Mercury							
CADMIUM = Total Cadmium						(continued...)	

Table H-2-3. Speciation Data from Utility Boiler Tests for Metals (lb/10^{12} Btu)

Test Site	Fuel	Control	ARSENIC	AS III	AS V	CHROM	CHROM6
DOE Baldwin	Coal	ESP	1.21E+01			4.63E+01	
DOE Boswell	Coal	FF	3.44E+01			2.04E+00	
DOE Cardinal	Coal	ESP	3.10E+00			6.17E+00	2.37E-02
DOE Creek	Coal	ESP/FGD	1.18E+00			5.88E+01	
DOE Niles2	Coal	ESP	4.23E+01			3.06E+00	
DOE NilesNox2 (FF)	Coal	FF/SCR	9.09E+00			1.18E+00	
DOE NilesNox2 (WSA)	Coal	FF/SCR/WSA	5.22E-01			2.10E+01	
DOE Spring	Coal	SDA/FF	1.37E-01			5.30E+00	
DOE Yates	Coal	ESP/JBR	1.20E+00			1.14E+00	
NSP-A.S. King	Coal	ESP	2.25E+00			8.68E+00	
NSP-BD-1-3-4	Coal	ESP	4.27E-01			1.84E+00	
NSP-BD-2	Coal	ESP	5.33E-01			6.66E+00	
NSP-HB-3-4-5-6	Coal	ESP	3.32E+00			7.00E+00	
NSP-Riv-6-7	Coal	FF	1.11E+00			1.38E+02	
NSP-Riv-8	Coal	ESP	3.91E-01			3.99E+00	
NSP-Sher-1-2	Coal	FGD	2.83E-01			5.62E+00	6.54E-01
NSP-Sher-3	Coal	SDA/FF	4.85E-02			9.21E+00	8.89E-01
Site 10	Coal	FBC/FF	7.45E-01			1.64E+00	
Site 102	Coal	ESP	2.91E+00			8.59E+00	
Site 11	Coal	ESP/FGD	6.04E-01			4.14E+00	
Site 110	Coal	HESP/CESP	1.40E+00	6.69E-01	1.38E+00	1.27E+01	
Site 110A	Coal	HESP/CESP	9.48E+00	3.03E-01	1.70E-01	3.04E+01	
Site 111	Coal	SDA/FF	2.13E-01			4.25E+00	
Site 112 (a)	Oil	ESP	2.46E+00			3.77E+00	
Site 114	Coal	ESP	7.13E+00			1.36E+01	
Site 115	Coal	FF	7.53E-01			6.61E-01	
Site 117 (a)	Oil	SCR	2.90E+00			1.99E+01	
Site 118	Oil	ESP	5.50E-01			3.30E+00	1.89E-01
Site 119 (a)	Oil	ESP				1.86E+00	1.86E-01
Site 12	Coal	ESP/FGD	1.77E+00			9.75E+00	
Site 120	Gas	None	1.58E-01				
Site 121	Gas	None	1.17E-01				
Site 13	Oil	PJFF	4.00E-02			1.70E+00	
Site 14	Coal	SDA/PJFF	5.00E-01			4.11E-01	
Site 15	Coal	ESP	1.34E+01			1.11E+01	
Site 16/OFA	Coal	ESP	9.45E+01			3.75E+01	
Site 16/OFA/LNB (b)	Coal	ESP	1.04E+02			2.08E+01	6.04E+00
Site 18	Coal	ESP/COHPAC	3.60E+01			2.50E+01	
Site 19	Coal	ESP	7.90E+00			1.30E+01	
Site 21	Coal	ESP/FGD	6.17E+00			2.74E+00	
Site 22	Coal	ESP	8.70E-02				
EPRI-103/Oil	Oil	None	3.63E+00			3.48E+00	1.04E+00
EPRI-104/Oil	Oil	None	6.53E+00			3.00E+00	ND
EPRI-105/Oil	Oil	None	4.13E+00			2.10E+00	4.20E-01
EPRI-106/Oil	Oil	None	2.70E+01			7.27E+00	3.78E+00
EPRI-107/Oil	Oil	None	1.27E+01			7.93E+00	1.67E+00
EPRI-108/Oil	Oil	None	7.76E+00			ND	3.05E+00
EPRI-109/Oil	Oil	None	1.01E+00			1.10E+01	
Average			9.98E+00	4.86E-01	7.72E-01	1.34E+01	1.63E+00
Median			2.25E+00	4.86E-01	7.72E-01	6.42E+00	8.89E-01
Max			1.04E+02	6.69E-01	1.38E+00	1.38E+02	6.04E+00
Min			4.00E-02	3.03E-01	1.70E-01	4.11E-01	2.37E-02
See notes at the end of table H-2-1							
ARSENIC = Total Arsenic							
AS III = Trivalent Arsenic							
AS V = Pentavalent Arsenic							
CHROM = Total Chromium							
CHROM6 = Hexavalent Chromium						(continued...)	

Table H-2-3. Speciation Data from Utility Boiler Tests for Metals (lb/10^{12} Btu)

Test Site	Fuel	Control	NICKEL	SOL Ni	SULF Ni	MET Ni	OX Ni
DOE Baldwin	Coal	ESP	2.21E+01				
DOE Boswell	Coal	FF	1.97E+00				
DOE Cardinal	Coal	ESP	4.72E+00				
DOE Creek	Coal	ESP/FGD	5.10E+00				
DOE Niles2	Coal	ESP	5.50E-01				
DOE NilesNox2 (FF)	Coal	FF/SCR	2.20E-01				
DOE NilesNox2 (WSA)	Coal	FF/SCR/WSA	2.20E+00				
DOE Spring	Coal	SDA/FF					
DOE Yates	Coal	ESP/JBR	4.01E+01				
NSP-A.S. King	Coal	ESP	3.00E-02				
NSP-BD-1-3-4	Coal	ESP	1.40E+00				
NSP-BD-2	Coal	ESP	3.29E+00				
NSP-HB-3-4-5-6	Coal	ESP	3.52E+00				
NSP-Riv-6-7	Coal	FF	3.40E-01				
NSP-Riv-8	Coal	ESP	4.53E+00				
NSP-Sher-1-2	Coal	FGD	4.55E+00				
NSP-Sher-3	Coal	SDA/FF	7.20E+00				
Site 10	Coal	FBC/FF					
Site 102	Coal	ESP	3.40E+02				
Site 11	Coal	ESP/FGD	2.60E+00				
Site 110	Coal	HESP/CESP	7.70E+00				
Site 110A	Coal	HESP/CESP	5.00E+00				
Site 111	Coal	SDA/FF	5.80E+00				
Site 112 (a)	Oil	ESP	3.03E+02				
Site 114	Coal	ESP	7.80E+01				
Site 115	Coal	FF	1.50E+00				
Site 117 (a)	Oil	SCR	8.09E+02				
Site 118	Oil	ESP	4.60E+01	2.13E+01	2.60E+00	ND	9.00E+00
Site 119 (a)	Oil	ESP	2.15E+03	1.24E+03	7.30E+01	ND	8.35E+02
Site 12	Coal	ESP/FGD	4.40E+00				
Site 120	Gas	None	3.60E+00				
Site 121	Gas	None	8.60E-01				
Site 13	Oil	PJFF	1.60E+00				
Site 14	Coal	SDA/PJFF	2.30E+00				
Site 15	Coal	ESP	5.90E+00				
Site 16/OFA	Coal	ESP	2.40E+01				
Site 16/OFA/LNB (b)	Coal	ESP	1.70E+01				
Site 18	Coal	ESP/COHPAC	1.60E+01				
Site 19	Coal	ESP	7.90E+00				
Site 21	Coal	ESP/FGD	1.68E+00				
Site 22	Coal	ESP	6.40E-01				
EPRI-103/Oil	Oil	None	3.48E+02				
EPRI-104/Oil	Oil	None	3.64E+02				
EPRI-105/Oil	Oil	None	5.10E+02				
EPRI-106/Oil	Oil	None	3.80E+02				
EPRI-107/Oil	Oil	None	4.20E+02				
EPRI-108/Oil	Oil	None	1.40E+03				
EPRI-109/Oil	Oil	None	2.40E+02				
Average			1.65E+02	6.28E+02	3.78E+01	0.00E+00	4.22E+02
Median			5.45E+00	6.28E+02	3.78E+01	0.00E+00	4.22E+02
Max			2.15E+03	1.24E+03	7.30E+01	0.00E+00	8.35E+02
Min			3.00E-02	2.13E+01	2.60E+00	0.00E+00	9.00E+00
See notes at the end of table H-2-1							
NICKEL = Total Nickel							
SOL Ni = Soluble Nickel							
SULF Ni = Sulfidic Nickel							
MET Ni = Metallic Nickel							
OX Ni = Oxidized Nickel							

Appendix I - SUMMARY OF EPRI'S UTILITY REPORT

This page is intentionally blank.

The industry (Electric Power Research Institute[EPRI]) produced its own exposure and risk assessment. The Executive Summary, from the report entitled "Electric Utility Trace Substances Synthesis Report"(November, 1994)[1], is included and quoted below.

BACKGROUND AND OVERVIEW

"This report by the Electric Power Research Institute (EPRI) is intended to provide information to electric utilities, and to EPA for its own utility study, as well as to the broader scientific and regulatory community. The key goal of the effort is to bring together the best scientific data and methods currently available to understand the potential magnitude and nature of human health risks due to trace emissions from electric utility steam-generating units in the United States. As such, the report summarizes the results of recent trace substance research, conducted by EPRI and others, addressing a range of critical issues such as trace substance emission rates from utility generating units, appropriate sampling and analytical methods for determining these rates, and the toxicity of specific substances found in utility emissions. Further, the report describes the risk assessment methodology developed to integrate this research and understand its implications with respect to a nationwide evaluation of potential human health risk.

"The data, methodologies, and analysis results presented in this report provide an understanding of utility trace substance emissions and the risks associated with these emissions, consistent with the best data and methodologies available at this time. The results of this research and analysis indicate that trace substance emissions from fossil-fired electric utility steam generating units, after compliance with other provisions of the Clean Air Act Amendments, will not pose significant long-term risks (either carcinogenic or noncarcinogenic) to human health.

SCOPE/APPROACH

"Two major projects served as the foundation for EPRI's trace substance research and provided much of the input and direction for this analysis. These projects were the Power Plant Integrated Systems: Chemical Emissions

Study (PISCES) project and the Comprehensive Risk Evaluation (CORE) project. PISCES conducted extensive method development and field measurement programs that provide a database for predicting airborne trace substance emissions throughout the utility industry. CORE developed the methodology to integrate the information from PISCES and other research results on emissions, fate, and health effects, into a nationwide assessment of health risks.

"As an initial step, these projects identified 16 trace substances as critical to include in an industry-wide risk assessment. The 16 were selected based on an evaluation of those trace substances 1) most likely to be found in utility stack emissions (based on a literature review and EPRI measurement data) *and* 2) for which health risk analysis could be readily performed using available toxicity factors. The substances identified as meeting both of these criteria include:

Arsenic	Chlorine	Lead	PAHs
Benzene	Chromium	Manganese	Radionuclides
Beryllium	Dioxins/Furans	Mercury	Selenium
Cadmium	Formaldehyde	Nickel	Toluene

The scope of the risk assessment presented in this report encompasses the potential chronic (i.e., long-term) health risks due to emissions of these 16 trace substances from approximately 600 power plants, encompassing roughly 1700 fossil-fired steam electric generating units. To predict emissions from these units, several scenarios were produced describing how the electric utility industry may be configured after all measures to achieve compliance with the SO_2 provisions of the CAAA are implemented (assumed to be 2010). These scenarios were augmented by additional data on particulate controls developed through an independent survey of utility operators regarding their plans to modify or upgrade particulate control equipment to meet other air pollution control requirements. These projections of power plant operations and control configurations were combined with characterizations of trace element concentrations in utility fuels to produce estimates of emissions in the year 2010 from the entire population of United

States electric utility steam generating units (with >25 MW nameplate capacity).

"Plant operating and design characteristics together with regional meteorological data were used to model the transport and dispersion of trace emissions and the resulting ground-level concentration within 50 kilometers of each plant. The EPA's Industrial Source Complex Long Term 2 (ISCLT2) model was selected for the dispersion modeling. The ISCLT2 model estimates annual-average concentrations, making it useful for evaluating chronic effects due to long-term exposures to chemicals, as well as allowing the efficient modeling of several hundred separate sources. In addition to evaluating the concentration levels due to individual plants, an 'overlapping plume' analysis was performed to account for the total exposure of populations living within 50 kilometers of more than one power plant.

"Population data from the 1990 United States census were used to assess the exposure levels of individuals living within 50 kilometers of electric utility generating units, based on electricity supply scenarios for the year 2010. Due to the initial atmospheric transport of these contaminants, the primary pathway evaluated for human exposure was through inhalation. The incremental increase in inhalation cancer risk due to utility emissions was computed for two exposure scenarios: the 'Maximally Exposed Individual' (or MEI) and a 'reasonably Exposed Individual' (or REI). The MEI represents a conservative estimate of possible exposure, assuming an individual breathes outside air, in the location with the highest concentrations of trace substances due to a single power plant's emissions, 24 hours per day for a 70-year lifetime.

"To provide a more realistic estimate of potential human exposures, and in keeping with recent recommendations by EPA and the National Academy of Sciences, EPRI developed the REI. The REI incorporates data on the amount of time individuals spend indoors and outdoors in various activities and on indoor reductions of outdoor concentration levels. In addition to the inhalation exposure assessments, several case studies were performed to evaluate potential multimedia exposures to utility trace

emissions through all exposure pathways (i.e., inhalation, ingestion, and dermal contact).

"Finally, the exposure assessments were combined with dose-response relationships to provide an estimate of potential public health risks. Due to the nature of the emissions (i.e., very low levels of substances emitted over a relatively long period of time), the primary health effects evaluated are potential increases in chronic cancer or non-cancer risks over a 70-year lifetime. For noncarcinogens, the predicted concentration levels due to generating unit emissions are compared to federal reference doses (RfDs) or reference concentrations (RfCs) for the substances of concern. These reference levels are defined as being levels of daily exposure that are likely to be without appreciable chronic deleterious effects, even for sensitive individuals in a population.

"For most of the carcinogens, the relevant unit risk factor tabulated by the U.S. EPA as of mid-1994 was used to estimate potential incremental cancer risk due to utility emissions of trace substances. The unit risk factor represents a plausible upper-bound estimate of the increased probability of contracting cancer due to a 70-year lifetime exposure to an inhalation concentration of 1 $\mu g/m^3$ of a given substance. In the case of arsenic, a revised unit risk factor was derived based on a re-analysis of existing and new occupational exposure data. The revised unit risk factor of 1.43×10^{-3} per $\mu g/m^3$ (one-third of that listed in 1994 in the EPA Integrated Risk Information System (IRIS) database) was used in this study to estimate arsenic inhalation cancer risks. In addition, risk estimates were carried out using the higher EPA IRIS value.

SYNOPSIS OF RESULTS

"The following highlights key research findings that contributed to the overall assessment of risks due to trace emissions from electric utility steam generating units, as well as the results of the risk assessment itself.

Concentrations of Trace Substances in Coal

"A data set based on U.S. Geological Survey information and coal cleaning data was developed to characterize

the concentrations of inorganic substances in coals, 'as fired,' at power plants. This database represents a significant improvement over previous coal characterizations in that it incorporates economic criteria (i.e., seam depth and quality) and the impact of coal cleaning processes in predicting 'as-fired' coal properties.

"In addition to this work, a measurement program was carried out to specifically examine mercury concentrations in 'as-fired' coal. Approximately 150 samples of delivered coal, representing 20 major seams and all coal ranks, were analyzed by atomic fluorescence to determine mercury concentrations. This analysis showed that concentrations of mercury in 'as-fired' or 'as-received' coal are about half of earlier estimates based on 'in-ground' coal samples.

Field Measurements and Data Correlations

"EPRI initiated its Field Chemical Emissions Monitoring (FCEM) program to rectify the lack of adequate field measurement data on trace substance emissions from operating power plants. FCEM provided the first such data for trace substances in power plant process and discharge streams. Initiated in May 1990 as part of the PISCES project, the FCEM program used EPA-recommended sampling analysis protocols (making modifications, as necessary), and acquired measurement data from 35 utility sites representing different combinations of boiler, fuel type, and environmental control devices. In addition, the U.S. Department of Energy (DOE) also conducted sampling and measurement programs at 8 utility plants, using similar protocols. The EPRI and DOE data encompass measurements for each major fuel type and boiler configuration, as well as all current SO_2, NO_x, and particulate control technologies. The resulting database represents the most up-to-date, complete, and accurate data set currently available for estimating trace substance emissions from the national population of steam electric generating units.

"For coal-fired units, guidelines were developed for extrapolating the measurement data to predict trace emissions from similar units. Three major groupings were defined in order to develop emission factors or

correlations that serve as the basis for predicting stack emissions for all coal-fired generating units.

"Particulate-phase inorganic substances. Based on the field data, these substances (e.g., arsenic, chromium) are well controlled by a particulate control device. In general, reductions of greater than 90 percent from levels in the incoming coal were achieved. Correlations were thus developed to estimate stack emissions based on the inlet coal concentration of each substance and the level of total particulate emissions.

"Volatile inorganic substances. These substances (including hydrochloric acid, mercury, and selenium) tend to be more volatile and not efficiently captured by particulate control devices. Based on the measurement data, the emissions of these substances could not be correlated to any specific factors and were therefore estimated using average removal efficiencies for each substance and control configuration.

"Organic compounds. These compounds are formed at very low levels during combustion and emitted in concentrations of parts per billion or lower. Emissions of organic compounds were estimated using the geometric means of measured emission factors, calculated from the field data, for each substance.

"For oil- and gas-fired power plants, available data are not yet adequate to estimate the trace substance concentrations in fuel burned at individual utility sites on a nationwide basis. Emissions for these plants were calculated using average emission factors (i.e., emissions per Btu of heat input), based on the field measurements, averaged across all measured units of the same configuration and fuel type. These data show that the emission factors for uncontrolled oil-fired power plants are about the same as for coal-fired plants with electrostatic precipitators.

Inhalation Exposure Assessment

"As noted above, EPRI developed an alternative measure of human exposure designed to provide a more realistic estimate of potential human health effects than the traditional 'Maximally Exposed Individual,' or MEI, approach. The 'Reasonably Exposed Individual,' or REI,

employed in this report still focuses on an individual living in the area of highest concentrations due to utility emissions. However, the REI methodology incorporates data on age-specific and activity-specific breathing rates and other exposure variables. In addition, the REI approach assumes that generation units do not continue to operate for a full 70 years from their respective start-up dates, but are replaced after an average operating span of 45 years with units in the same location that meet the EPA 1994 New Source Performance Standards (NSPS) for particulates.

"In general, inhalation exposures to carcinogens using the REI methodology are 2% to 19% of the exposure levels computed for the MEI. This difference is due primarily to assumptions regarding the amount of time individuals spend indoors and the amount of time spent residing in one location. For the noncarcinogens, REI exposures are 21% to 70% of those computed for the MEI. This difference is primarily due to assumptions regarding the amount of time spent indoors and the reduction in trace substance concentration levels in indoor environments.

Health Effects

"*Arsenic.* Based on new analyses of occupational exposure data, EPRI computed a revised unit risk factor for estimating increased cancer risks due to inhalation exposures to arsenic. The revised unit risk factor (1.43×10^{-3} per $\mu g/m^3$), which is used as the base case throughout this study, is one-third of the current EPA value. The revised value reflects a re-analysis of existing and new occupational exposure data for smelter workers exposed to arsenic in copper smelter dust. EPRI used the standard EPA risk assessment methodology to calculate the revised unit risk.

"Other important issues with respect to the toxicity of arsenic in power plant fly ash may not be addressed by the revised unit risk factor and remain the subject of ongoing research at EPRI and elsewhere. These issues include: (1) the importance with respect to health effects of differences in the valence state of arsenic found in copper smelter dust and that found in fly ash, (2) the comparative bioavailability of arsenic in fly ash vs. in other mixtures, and (3) the impact of metabolic detoxification processes at various arsenic

exposure levels. Although research is underway on these topics, they currently remain unresolved.

"*Mercury.* Recent data also may provide an improved basis for computing potential neurotoxic effects due to chronic exposures to mercury. EPA's current reference dose for methylmercury is based on an incident in Iraq involving acute exposures to very high methylmercury concentrations in grain. However, data sets based on populations exposed to mercury via fish ingestion may be more appropriate for evaluating health risks from utility mercury emissions in the United States. EPRI is currently assessing data on the neurological responses of children in New Zealand exposed to methylmercury via maternal fish ingestion to serve as an alternative basis for evaluating risk.

Inhalation Risk Assessment

"The results of research in a number of areas were brought together in a nationwide assessment of the potential health risks associated with trace substance emissions from electric utility steam generating units. In general, the analysis indicates that the cancer and noncancer inhalation risks to the general public due to trace substance emissions from utility generating units are small, as described in the following discussion.

"*Cancer Risk.* For the roughly 600 plants investigated, the expected increase in individual cancer risk, incorporating exposure assumptions associated with maximum exposure over a 70-year life span, did not exceed 1.7 in one million (1.7×10^{-6}). Out of this entire group of power plants, only 3 plants, or 0.5 percent, approach exposures leading to a cancer risk greater than one in one million (1×10^{-6}) for a maximally exposed individual (MEI).

"Incorporating more reasonable assumptions regarding individual exposure patterns results in the increased cancer risks for all plants being less than one in one million, and all but 2 plants (0.3 percent) being less than one in ten million (1×10^{-7}). Figure ES-1 [not included in this appendix] shows the distribution of increased cancer risk for a 'Reasonably Exposed Individual' (REI) due to utility trace substance emissions. As shown, the vast majority of plants (greater than 85 percent) are associated with increased

individual risk levels that are, at most, below 1 in 100 million (1×10^{-8}).

"For coal- and oil-fired power plants, across all coal ranks (i.e., bituminous, subbituminous, and lignite) and control configurations, arsenic and chromium were found to be the largest potential contributors to inhalation cancer risks from utilities.

"For plants fired only by gas, the median inhalation cancer risk is about an order of magnitude less than median risk levels for other fossil-fired plants, and the primary contributors to risk from gas plant emissions are chromium and formaldehyde.

"*Noncancer Risks.* Noncancer risks were evaluated based on comparisons with EPA-defined reference doses (RfD) or reference concentrations (RfC). When no EPA-listed value was available, an RfD or RfC was developed based on other available health standards. These RfD and RfC values reflect thresholds below which no adverse health effects are anticipated, even over continuous long-term exposures. For all of the plants, inhalation exposures to all of the noncarcinogens examined (including mercury) were well below the recommended threshold levels.

"*Sensitivity and Scenario Analyses.* Sensitivity analyses were conducted to clarify the impact of uncertainty in key parameters or modeling assumptions on the inhalation risk estimates. Based on extensive analyses, no single group of plants (as defined by plant configuration, operating characteristics, stack height, or fuel type) could be identified as consistently correlated with relatively high risk estimates. Rather, it was usually a unique combination of site- and plant-specific factors that led to higher relative risks for an individual plant.

"Finally, although variations in assumptions about future scenarios (e.g., load, fuel type, control configuration, etc.) can influence risk estimates for individual plants and the relative risks across multiple plants, in the aggregate, the alternative scenarios did not significantly affect the risk estimates.

Multimedia Risk Assessment

"EPRI conducted case studies of four power plants with measured emissions to estimate carcinogenic and noncarcinogenic multimedia risks from power plant emissions using the EPRI multimedia risk model, *TRUE* (Total Risk of Utility Emissions). Based on the four case studies, the estimated maximum incremental cancer risk due to exposures through all pathways (i.e., inhalation, ingestion, dermal contact) was below one in one million (1×10^{-6}) for all plants studied. For noncarcinogens, the multimedia analysis also showed all exposure levels to be below the relevant threshold levels (RfDs and RfCs) for adverse effects.

"*Mercury.* A key focus of the multimedia risk assessment was the potential health effects due to mercury emissions. The case study results suggest that risks due to power plant emissions of mercury are primarily driven by exposure through ingestion of fish in which mercury has accumulated as methylmercury. The current EPA Reference Dose for mercury is 0.3 µg per kg of body weight per day of methylmercury. Predicted methylmercury exposure levels due to mercury emissions from each of the four case study power plants are all less than 30 percent of federal reference levels.

"Although these results incorporate the best current understanding of mercury-related risks, the complex biogeochemistry of mercury, how it is transformed in the atmosphere and ecosystems, and what exposure and dose levels ultimately result in health effects are still not fully understood. As new and ongoing research contributes to our understanding of this chemical, potential impacts on the risk assessment results should be considered.

"*Radionuclides.* Exposures due to radionuclide emissions from fossil-fired generating units were also found to be small. Changes in the risk assessment methodology for radionuclides used by EPA resulted in risk levels below previous estimates made by EPA in its 1989 National Emissions Standards for Hazardous Air Pollutants (NESHAPS) for radionuclides. Specifically, improvements in estimating power plant radionuclide emissions (based on the average radioactivity of emitted particulate matter) resulted in predicted emissions that are one-third to one-tenth of previous

estimates. Changes in modeled deposition rates further reduced predicted exposure levels.

Impact of Current Control Technologies

"Trace metals in flue gas are normally condensed on fly ash particles and can be removed effectively by an efficient particulate collector. Mercury, present mainly in vapor form in the flue gas, is not collected effectively by particulate control devices such as electrostatic precipitators or baghouses. Studies to date to assess flue gas mercury removal methods, such as injection of activated carbon, show that the low mercury levels present in power plant flue gas are much more difficult to remove than the mercury emitted from waste incineration plants. Significantly more research is needed to evaluate these and other removal options in power plant settings.

SUMMARY

"This report is intended to provide insight into the best data and methods available for estimating health risks due to trace emissions from fossil-fuel-fired steam-electric generating units. To meet this goal, EPRI conducted extensive research aimed at improving the state-of-the-art in a number of areas, including:

- More appropriate fuel composition data
- More accurately measuring trace substance emissions from power plant stacks
- Improved methods for estimating emissions for the national capacity of power plants
- Development of alternative scenarios of future industry operations
- Updated health impact data
- Development of reasonable measures of human exposure and health risks

Although the research presented in this report provides a considerable improvement over previously available data and methods, important uncertainties remain. For example, more complete data are needed on: speciation

of arsenic, chromium, and mercury in stack emissions; the atmospheric chemistry of trace substances; and dose-response information incorporating bioavailability. However, the results presented herein suggest that trace substance emissions from electric utility steam generating units, after compliance with other provisions of the CAAA, will not pose significant long-term risks (either carcinogenic or noncarcinogenic) to human health."

EPA has reviewed the above report and has noted several differences in the approach and assumptions used by the Agency and the EPRI. EPRI used different cancer potencies for the three major trace metals: arsenic, chromium, and nickel. For nickel, which has a limited number of compounds known to be carcinogenic, EPRI assumed those nickel compounds emitted from utility power plants were not carcinogenic, whereas EPA assumed that various fractions (up to 100 percent) of the nickel was carcinogenic. For chromium, EPRI assumed that 5 percent of the total chromium was carcinogenic (the hexavalent form), and EPA assumed that 11 percent of the coal and 18 percent of the oil was carcinogenic. For arsenic, EPRI reported on some new data that indicated that arsenic was not as potent as the Agency had estimated; thus, EPRI used an unit risk estimate of 1.43×10^{-3}, which was about a factor of 3 lower than the 4.3×10^{-3} value used by EPA. (The Agency is currently reviewing this new data. Some of these differences are explained by the recent availability of speciation data that had not been seen by EPRI staff before their report was finished. In summary, EPRI applied potency estimates, for all three trace metals, that were lower than those used by EPA.

There were other significant differences. For instance, the Agency estimated the effects of long range transport (using the RELMAP model) for arsenic and projected these results onto other trace metals. The EPA also conducted long-range transport modeling for mercury. EPRI did not attempt this analysis. EPA conducted a radionuclide analysis for each utility plant in the United States, while EPRI used several model plants.[a] Both EPRI and EPA conducted multimedia exposure analyses for mercury and

---

[a] The EPRI model plant approach was similar to that used by the Agency in past analyses. However, choosing model plants tend to underestimate MIR levels, since the worst exposure scenarios cannot be known until all affected facilities are modeled. Modeling all the facilities is a large project. Because the Agency was investing in the resources to model all facilities for trace metals, it was decided to do a parallel effort for the radionuclide analysis to overcome the concern of potentially underestimating the MIR.

radionuclides; however, only the industry evaluated multimedia effects associated with emissions of arsenic, beryllium, cadmium, chromium, lead, nickel, vanadium, dioxins/furans, chlorine, and fluorine compounds. When conducting the mercury modeling analysis to estimate environmental fate and levels in various media, the Agency used model plants representing a range of sizes in typical scenarios, where the industry analyzed several typically sized plant in actual environmental settings. In addition, the EPRI estimated non-inhalation exposures to mercury. However, the EPA has not completed a human exposure assessment for mercury.

References

1. Letter and enclosure from Peck, Stephen C., Electric Power Research Institute, to Maxwell, William H., EPA:ESD. September 15, 1995. Transmittal of unlicensed Electric Utility Trace Substances Synthesis Report.

APPENDIX J - PARAMETER JUSTIFICATIONS, SCENARIO INDEPENDENT PARAMETERS

This page is intentionally blank.

DISTRIBUTION NOTATION

A comprehensive uncertainty analysis was not conducted as part of this study. Initially, preliminary parameter probability distributions were developed. These are listed in Appendicies J and K. These were not utilized in the generation of quantative exposure estimates. They are provided as a matter of interest for the reader.

Unless noted otherwise in the text, distribution notations are presented as follows.

Distribution	Description
Log (A,B)	Lognormal distribution with mean A and standard deviation B
Log*(A,B)	Lognormal distribution, but A and B are mean and standard deviation of underlying normal distribution.
Norm (A,B)	Normal distribution with mean A and standard deviation B
U (A,B)	Uniform distribution over the range (A,B)
T (A,B,C)	Triangular distribution over the range (A,C) with mode of B

J. SCENARIO INDEPENDENT PARAMETERS

This appendix describes the scenario-independent parameters used in the mercury modeling. Scenario independent parameters are variables whose values are independent of a particular site and are constant among various site-specific situations. Examples of scenario independent parameters are air density, the average height of an adult, or the average crop yield of a particular food item. These scenario independent parameters may be either chemical independent or chemical dependent. The following sections present the chemical independent and chemical dependent parameters used in this study.

J.1 CHEMICAL INDEPENDENT PARAMETERS

Chemical independent parameters are variables that remain constant despite the specific contaminant being evaluated. The chemical independent variables used in this study are described in the following sections.

J.1.1 Basic Constants

Table J-1 lists the chemical independent constants used in the study, their definitions, and values.

J.1.2 Agricultural Parameters

J.1.2.1 Interception Fraction.

Parameter: RPi

Definition: The fraction of the total deposition within a unit area that is initially intercepted by vegetation.

Units: unitless

Crop	Default Value	Distribution	Range
Leafy vegetables	0.15	Log (0.16, 0.10)	0.08 - 0.38
Legume vegetables	0.008	Log(0.008, 0.004)	0.005 - 0.01
Fruiting vegetables	0.05	Log(0.05, 0.05)	0.004 - 0.08
Rooting vegetables	0	N/A	N/A
Grains and cereals	0	N/A	N/A
Forage	0.47	Norm(0.47, 0.3)	0.02 - 0.89
Silage	0.44	Log (0.44, 0.3)	
Fruits	0.05	Log (0.05, 0.05)	0.004 - 0.08
Potatoes	0	N/A	N/A

Table J-1. Chemical Independent Constants

Parameter	Description	Value
R	ideal gas constant	8.21E-5 m^3-atm/mole-K
pa	air density	1.19E-3 g/cm^3
ua	viscosity of air	1.84E-4 g/cm-second
Psed	solids density	2.7 kg/L
Cdrag	drag coefficient	1.1E-3
κ	Von Karman's coefficient	7.40E-1
λ_2	boundary thickness	4.0

Technical Basis:

For leafy vegetables, Baes et al.[1] obtained an average interception fraction of 0.15 where it was emphasized that this value represents a theoretical average over the United States. This value was calculated assuming a logistic growth pattern for leafy vegetables and taking into account a distribution of field spacings.[1] The associated distribution and ranges shown in the previous table were calculated based on Baes's analyses by Belcher and Travis.[2]

For legumes and fruits, Belcher and Travis[2] used the exposed produce equation that relates the interception fraction to the standing crop biomass (also called productivity) and crop biomass values from Shor et al.,[3] to obtain the range of values given in the previous table. The values for fruiting vegetables are assumed to be the same as for fruits.

The distribution for forage is based on the work of Hoffman and Baes,[4] who determined that the values are normally distributed with the parameters presented in the previous table.

The value for silage was calculated in Baes et al.[1] and is based essentially on sorghum and corn plantings.[5,6]

Potatoes, root vegetables and grains are assumed to equal zero since the edible portion of the plant is protected from direct deposition (grains have a protective husk).

J.1.2.2 Length of Plant Exposure.

Parameter: TPi

Definition: The amount of time that the edible part of an exposed plant is exposed to direct deposition.

Units: years

Plant Type	Default Value (years)	Distribution	Range (years)
Leafy vegetables	0.157	U(0.082,0.247)	0.082- 0.247
Legume vegetables	0.123	U(0.082,0.247)	0.082- 0.247
Fruiting vegetables	0.123	U(0.082,0.247)	0.082 - 0.247
Forage	0.123	U(0.082,0.247)	0.082 - 0.247
Silage	0.123	U(0.082,0.247)	0.082 - 0.247
Fruits	0.123	U(0.082,0.247)	0.082 - 0.247

Technical Basis:

Bounding estimates were obtained by assuming an average time between successive harvests of 30 and 90 days. This range is based on the values in Baes et al.[1] of 60 to 90 days and the reported values by the South Coast Air Quality Management District (SCAQMD)[7] of 45 days for tomatoes and 30-85 days for lettuce.

The default value for leafy vegetables is the midpoint of the range for lettuce. The values for legumes, fruits and fruiting vegetables are based on the value of 45 days for tomatoes. The value for forage and silage is the average time between successive hay harvests and successive grazings by cattle.[1]

J.1.2.3 Plant Yield.

Parameter: YPi

Definition: Yield of the *i*th plant per unit area.

Units: kg (dry weight)/m^2

Type of Crop	Default Value (kg (dry weight)/m^2)	Range (kg (dry weight)/m^2)	Distribution
Leafy vegetables	0.177	0.091 - 0.353	Log (0.177, 0.086)
Legume vegetables	0.104	0.077 - 0.130	Log (0.104, 0.038)
Fruiting vegetables	0.107	0.012 - 0.253	Log(0.107, 0.093)

Type of Crop	Default Value (kg (dry weight)/m^2)	Range (kg (dry weight)/m^2)	Distribution
Rooting vegetables	0.334	0.090 - 0.434	Log(0.334, 0.142)
Grains and cereals	0.3	0.14 - 0.45	Log (0.30, 0.09)
Forage	0.31	0.02- 0.75	0.84482993969
Fruits	0.107	0.012 - 0.253	Log(0.107, 0.093)
Potatoes	0.48	0.405 - 0.555	Log (0.48, 0.106)
Silage	0.84	0.3- 1.34	Log(0.84,0.26)

Technical Basis:

The distributions and ranges shown for all but the silage values are those used in Belcher and Travis.[2] The distributions selected were chosen based on a probability plot for leafy vegetables with data in Shor et al.[3] The default values are the means of the distributions. Silage was not considered in Belcher and Travis,[2] but the same method by which the default values and distributions were calculated there were replicated using data from Shor et al.[3] for the purpose of this assessment.

J.1.2.4 Plant Ingestion by Animals.

Parameter: QPij

Definition: The daily consumption of plants by livestock.

Units: kg dry weight/day

Livestock Consumption of Plants	Default Value (kg dry weight/day)	Distribution	Range (kg dry weight/day)
Beef/Beef Liver			
grain	0.97	U(0.5,6.5)	0.5-6.5
forage	8.80	U(2.0,9.0)	2.0-9.0
silage	2.50	U(1,5)	1.0-5.0
Dairy			
grain	2.60	U(0.5,6.5)	0.5 - 6.5
forage	11.0	U(7,15)	7.0-15.0
silage	3.30	U(1,5)	1.0-5.0
Pork			
grain	3.0	U(2,4)	2.0-4.0

Livestock Consumption of Plants	Default Value (kg dry weight/day)	Distribution	Range (kg dry weight/day)
silage	1.3	U(0.5,3)	0.5-3.0
Sheep (lamb)			
forage	1.1	U(0,2)	0.0 - 2.0
Poultry/Eggs			
grain	0.08	U(0.04,0.10)	0.04-0.10

Technical Basis:

With the exception of the beef liver, egg and lamb-forage values, the default values are from U.S. EPA (1990).[8] The value for beef liver is assumed to be the same as for cattle, and the value for eggs is assumed to be the same as for poultry. The value for lamb-forage is from the National Academy of Sciences.[9]

The ranges shown are based on a combination of the ranges determined by Belcher and Travis,[2] the U.S. EPA[8] values, and the objective of capturing all of the most likely values.

Although lognormal distributions were chosen in Belcher and Travis,[2] this was not based on the actual distribution of the available data; that is, no probability plots were done. For that reason, uniform distributions are suggested here.

J.1.2.5 Soil Ingestion by Animals.

Parameter: QSj

Definition: Quantity of soil ingested daily by the a specific animal.

Units: kg/day

Technical Basis:

The values for beef cattle and dairy cattle are from McKone and Ryan.[10] The value for beef liver is assumed to be the same as for beef. The value for pork is the mean of the distributions used in Belcher and Travis[2] and are based on values in Fries.[11] The sheep value is from Fries.[12] The value for poultry is the mean of the distribution used in the Hanford Environmental Dose Reconstruction Project[13] (HEDR) and is based on values for free-ranging chickens. The range is that used in HEDR (1992).[13]

Livestock	Default Value (kg/day)	Range (kg/day)
Beef/beef liver	0.39	0.1 - 0.72
Dairy	0.41	0.1 - 0.72
Pork	0.034	0.0 - 0.0688
Sheep (lamb)	0.05	0.01 - 0.15
Poultry/eggs	0.009	0.006 - 0.012

For beef, dairy and pork, the ranges are from Belcher and Travis.[2]

The range for sheep is based on the values reported in Fries.[12] The lower end of the range is for sheep that are fed in a lot, in which case they eat little soil. The upper end is based on sheep grazing on poor pasture land.

J.2 CHEMICAL DEPENDENT PARAMETERS

Chemical dependent parameters are variables that change depending on the specific contaminant being evaluated. The chemical dependent variables used in this study are described in the following sections.

J.2.1 Basic Chemical Properties

The following sections list the chemical properties used in the study, their definitions, and values.

J.2.1.1 Molecular Weight.

Parameter: Mw

Definition: The mass in grams of one mole of molecules of a compound.

Units: g/mole

Chemical	Default Value (g/mole)
Hg^0, Hg^{2+}	201
Methylmercury	216
Methyl mercuric chloride	251
Mercuric chloride	272

J.2.1.2 Henry's Law Constant.

Parameter: H

Definition: Provides a measure of the extent of chemical partitioning between air and water at equilibrium.

Units: atm-m^3/mole

Chemical	Default Value (atm-m^3/mole)
Hg^0	$7.1x10^{-3}$
Hg^{2+} ($HgCl_2$)	$7.1x10^{-10}$
Methylmercury	$4.7x10^{-7}$

Technical Basis:

The higher the Henry's Law Constant, the more likely a chemical is to volatilize than to remain in the water. The value for Hg^0 is from Iverfeldt and Persson,[14] while the other values are from Lindquist and Rodhe.[15]

J.2.1. Soil-Water Partition Coefficient

Parameter: Kd

Definition: Equilibrium concentration in dry soil divided by concentration in water.

Units: mL/g

Chemical	Default Value (mL/g)
Hg^{2+}	53,700
Methylmercury	53,700

Technical Basis:

Values in the previous table are the geometric mean of calibrated values (see Appendix L).

J.2.1.4 Sediment-to-Water Partition Coefficient.

Parameter: Kdb

Definition: Equilibrium concentration in dry sediment divided by concentration in water.

Units: mL/g

Chemical	Default Value (mL/g)
Hg^{2+}	157,000
Methylmercury	157,000

Technical Basis:

Values in the previous table are the geometric mean of calibrated values (see Appendix L).

J.2.1.5 Suspended Sediment-Water Partition Coefficient.
Parameter: Kdw

Definition: Suspended sediment-water partition coefficient.

Units: L/kg

Chemical	Default Value (L/kg)	Range
Hg^{2+}	95000	1340-188,000
Methylmercury	650000	320,000 - 1,000,000

Technical Basis:

For divalent mercury, data were available from three studies, and are shown in Table J-2. The default value is the midpoint of the range. For methylmercury, the only data found that specifically address suspended material are those in Bloom et al.[16] In particular, they report that "Regardless of pH, for over three orders of magnitude, the log K_d for seston [suspended matter] was in the range of 5.5 to 6.0." The range listed in the previous table corresponds to this range. The midpoint of the observed range is used as the default value.

J.2.1.6 Soil and Water Loss Degradation Constants.
Parameter: ksg and kwg

Table J-2. Ranges of Values for Suspended Sediment-to-Water Partition Coefficient

Range (L/kg)	Reference
1380-188,000	Moore and Ramamodoray[17]
118,000	Glass et al.[18]
86,800-113,000	Robinson and Shuman[19]

Definition: Soil and water body loss of the contaminant due to biotic and abiotic degradation and aqueous hydrolysis, respectively.

Units: /yr

Chemical	Default Value (year)	Range
Hg^0	0.0	N/A
Hg^{2+}	0.0	N/A
Methylmercury	0.0	N/A

Technical Basis:

Data indicate that equilibrium is established between different species of mercury rather than a degradation/breakdown process. Parks et al.,[20] found that "In water, methylmercury and inorganic appear to be in quasi-equilibrium, as the methylmercury/total mercury ratio in river water is independent of contact time with sediments, the atmosphere, and the theoretical residence time of waters." For this reason, it appears reasonable simply to assume no net loss with time if any mercury species occurs in either soil or water.

J.2.1.7 Equilibrium Fraction for Chemical in Soil.

Parameter: fspecs

Definition: For all chemicals tied together in soil equilibrium, the fraction which is chemical *i* is given by fspec.

Units: unitless

Chemical	Default Value	Distribution
Hg^0	0	None
Hg^{2+}	0.98	T(0.9,0.98,0.9998)
Methylmercury	0.02	1 percent Hg^{2+}

Technical Basis:

Akagi et al.[21] reported methylmercury fractions of 0.02, 0.072 and 0.089 for sand, silt/woodchips, and woodchip sediments as compared to total mercury. Wilken and Hintelmann[22] reported that 0.10 of the total mercury in sediments from the River Elbe in Germany is methylated, although they pointed out that others had reported maximums of 0.01 and 0.02. Hildebrand et al.[23] found methylmercury fractions of 0.0002 - 0.0005 in sediments from the Holston River, VA.

The measurements in the previous table did not distinguish between Hg^{2+} and Hg^0 in the remaining fractions, leaving the partitioning of these species in soil uncertain. It is known that Hg^0 can be formed from reduction of Hg^{2+} in the soil environment, a fraction of which will volatilize and a fraction of which can be bound to organic matter. Both processes depend strongly on soil conditions.[24] At the redox potential normally found in soils, however, Hg^{2+} complexes are expected to be predominant than Hg^0.

Cappon[25] found that percent of methylmercury over total mercury for nonamended soils is 2.6 percent. This is an upper bound on values from unpublished data reported by several authors.[26]

J.2.1.8 Equilibrium Fraction for Chemical in Water.

Parameter: fspecw

Definition: For all chemicals tied together in water equilibrium, the fraction which is chemical *i* is given by fspecw.

Units: unitless

Chemical	Default Value	Distribution	Range
Hg^0	0.02	NA	0.007 - 0.04
Hg^{2+}	0.83	1 - (Methyl + Hg^0 %)[a]	0.31 - 0.96
Methylmercury	0.15	Log(0.14,1.0)	0.03 - 0.65

[a] The distribution is 1 minus the methylmercury concentration and elemental mercury concentration dissolved in the water.

Technical Basis:

The default value given for methylmercury is that suggested in U.S. EPA.[27] In well oxygenated water, the remaining fraction (i.e., non-methylated) will be mainly Hg^{2+} complexes.[24] There will be a small fraction of total mercury in water that will be Hg^0 due to reduction of Hg^{2+} by humic acid and microorganisms.[24,28]

Fitzgerald et al.[29] measured the concentration of total dissolved gaseous mercury in various lake waters and found in all cases that it consisted mainly of elemental mercury (> 97 percent). Much of these measurements were taken at both basins of Little Rock Lake, WI, from which total mercury concentrations for the acid-treatment and reference basins are known from the work of Watras and Bloom.[30] Comparing the concentrations within each basin gives a possible range for the percent mercury in water that is Hg^0 of 0.7 - 4 percent, the midpoint of which (2 percent) we use as the default equilibrium percentage of mercury in the water column that is elemental mercury.

There are a wealth of data on the Methylmercury/Total mercury in the water column. Table J-3 lists the values found reported in the literature. These values were used to determine the range given previously for methylmercury. The range for Hg^{2+} is then given by subtracting the contributions from methylmercury and elemental mercury from the total.

J.2.2 Biotransfer Factors

Biotransfer factors reflect the extent of chemical partitioning between a biological medium (plants, meats or fish) and an external medium (air, soil or water). The following sections describe the BCFs used in this study.

It is necessary to note the uncertainty inherent in determining BCFs for mercury species with regard to plant uptake. In general, there seems to be no consensus in the literature on plant bioconcentration factors for mercury, as values for each crop vary widely among studies. Further, in many studies the mercury speciation is not determined. In deriving BCFs for plant absorption of mercury species fromthe air and soil, it was, therefore sometimes necessary to make assumptions about certain behaviors ofmercury based on whatever information was at hand, as opposed to established scientific knowledg, which was lacking. These assumptions are described in each Technical Basis section

Table J-3. Reported Values for Fraction of Total Mercury that is Methylmercury in Water

Values	Reference
0.26, 0.11, 0.07, 0.07, 0.15	Bloom et al.[31]
0.01, 0.022, 0.019, 0.054, 0.055, 0.052, 0.049, 0.064	Parks et al.[20]
0.32, 0.48, 0.57	Akagi et al.[21]
0.12,0.05	Watras and Bloom[30]
<0.025	Bloom and Watras[32]
0.04-0.05	Lee et al.[33]
0.26-0.46	Kudo et al.[34]
0.01-0.89	Gill and Bruland[35]
0.036-0.273	Bloom and Effler[36]
0.036-0.053	Lee and Hultberg[37]

that follows, but it is useful at this time to identify some of the general uncertainties regarding plant uptake of mercury.

(1) Plants both absorb and release mercury to the environment. Hanson et al.[38] demonstrates clearly that at ambient air concentrations forest foliage usually acts as a source of elemental mercury to the atmosphere; deposition (plant absorption) only occurs above a "compensation concentration" at air mercury levels well above background. It is not yet known from where the mercury released by the plants originates (air uptake during periods of high mercury air concentrations, root uptake, Hg(II) absorption, etc.). Similarly, Mosbaek[39] found that for a given period of time more elemental mercury was released from a plant-soil system than was absorbed by the plant. These cases, however, in no way indicate that mercury is not bioconcentrated in plants; the above behaviors are consistent with mercury being collected by plants only to certain levels, after which any mercury absorbed is simply released.

(2) It is usually not known from where the mercury that is found in plants originated (air vs. soil). Only one study determined the fractions of total mercury in plants which came from air and soil[39]; in this study,

soil was isotopicly labelled with ^{203}Hg. After some time the specific activity in the plant was compared to that in the soil to ascertain how much of the mercury in the plant came from the soil. Although the experiment worked well, isotopic equilibrium in the soil was never achieved, and the number of plants studied was limited.

(3) The speciation of mercury in plants is often not known. If it is known, it is still very unclear as to how the speciation occurred. The plant speciation may be simply a result of direct uptake of different mercury species from the environment (but from air or soil?). It has been shown, however, that a few plants have the ability to change the species of mercury initially taken up from the environment.[40] Such behavior may have to be accounted for regarding plant uptake of mercury.

J.2.2.1 Plant-Soil BCF.

Parameter: BRi

Definition: The ratio of the contaminant concentration in plants (based on dry weight) to that in the soil.

Units: Unitless

Crop	Hg^{2+}		Methylmercury	
	Default Value	Distribution	Default Value	Distribution
Leafy vegetables	0	None	0	None
Legume vegetables	0.015	U(0.00026, 0.157)	0.031	U(0.0, 0.090)
Fruiting vegetables	0.018	U(0.007,0.059)	0.024	U(0.0,0.11)
Rooting vegetables	0.036	U(0.011, 0.073)	0.099	U(0.013,0.29)
Grains and cereals	0.0093	U(0.0024,0.057)	0.019[a]	U(0.0048,0.11)[a]
Forage	0	None	0	None
Fruits	0.018	U(0.007-0.059)	0.024	U(0.0,0.11)
Potatoes	0.1	U(0.05,0.2)	0.2[a]	U(0.1,0.4)[a]
Silage	0	None	0	None

[a] Hg^{2+} values multiplied by 2

Technical Basis:

Mosbaek[39] convincingly showed that for leafy, above-ground parts of plants virtually all of the mercury uptake was from air; therefore, for leafy vegetables, forage and silage no root uptake was modeled.

Values in Cappon[41,42] were the only data located which measured methylmercury concentrations in plants, and methylmercury plant-soil BCF's were determined for rooting vegetables, fruiting vegetables, and legumes. Values were determined for crops grown on compost[42] and sludge-treated soils,[41] and those values considering edible portions of plants are shown in Table J-4.

It has been shown, however, that mercury taken up into plants from the environment can be transformed into other mercury species, especially to organomercuric forms such as methylmercury.[43] The methylmercury in plants, therefore, may not have been directly absorbed from the environment. For the purposes of this study, considering root uptake, methylmercury concentrations in plants were treated as though they originated from the soil. It is also important to note that air-to-plant transfer may have occurred, but the Cappon[41,42] study was not designed to measure air-uptake.

Table J-5 shows additional soil-to-plant transfer coefficients for Hg^{2+} species (it was assumed that all the mercury in the soil is Hg^{2+}, which at worst would result in an error of a few percent in the Hg^{2+} soil-to-plant transfer coefficients) determined from a number of studies. Temple and Linzon[44] sampled garden produce in the vicinity of a chlor-alkali plant. Lenka et al.[45,46,47] also measured mercury concentrations in soil and plants near a chlor-alkali plant. Somu et al.[48] determined mercury uptake in wheat and beans grown on $HgCl_2$ contaminated soil. John[49] determined mercury concentrations in plants grown on soil artificially contaminated with $HgCl_2$. Wiersma et al.[50] measured soil and plant total mercury concentrations from major growing areas in the Netherlands. Belcher and Travis[2] compiled data from EPA.[51] Mosbaek[39] studied plant concentrations from soil and air uptake under background conditions. For studies reporting wet weight plant concentrations, wet weight to dry weight conversion factors in Baes et al.[1] were used to convert to dry weight based concentrations.

When possible, default values were chosen based on experiments under reasonable or background conditions, as opposed

Table J-4. Soil-to-Plant Transfer Coefficients for Mercury (from Cappon, 1987 and Cappon, 1981)

Crop	1987 Values		1981 Values	
	Hg^{2+}	Methylmercury	Hg^{2+}	Methylmercury
Rooting Vegetables				
Beet	0.055	0.227	0.017	0.11
Carrot	0.026	0.118	0.014	0.048
Onion, Yellow	0.073	0.288	0.053	0.042
Onion, Spanish	-	-	0.047	0.030
Red Radish	0.056	0.092	0.018	0.066
White Radish	-	-	0.011	0.060
Turnip	0.026	0.013	-	-
Fruiting Vegetables				
Cucumber, slicing	-	-	0.015	0
Cucumber, pickle	0.007	0	0.015	0.006
Pepper	0.019	0.022	0.016	0.042
Zucchini	0.021	0	0.014	0.018
Summer Squash	-	-	0.007	0
Acorn Squash	-	-	0.016	0.012
Spaghetti Squash	-	-	0.016	0.024
Pumpkin	-	-	0.008	0.006
Tomato	0.059	0.105	0.020	0.072
Legumes				
Green Bush Beans	0.011	0	0.014	0.020
Yellow Bush Beans	-	-	0.017	0.015
Lima Beans	-	-	0.017	0.090

Table J-5. Other Values for Soil-to-Plant Transfer Coefficients for Hg^{2+}

Crop	Values	References
Legume vegetables	0.157-1.79, 0.00026-0.0003, 0.0005, 0.003-0.03	Lenka et al.,[45,46,47] Somu et al.,[48] John,[49] Belcher and Travis[2]
Fruiting vegetables	0.013-0.33, 0.127-1.36, 0.0078-0.028	Temple and Linzon,[44] Lenka et al.,[45,46,47] Belcher and Travis[2]
Rooting vegetables	0.09-0.33, 0.090-0.149, 0.0065-0.013, 0.05-0.2, 1.6-1.9	Temple and Linzon,[44] Lenka et al.,[45,46,47] John,[49] Belcher and Travis,[2] Mosbaek[39]
Grains and cereals	0.0024-0.0093, 0.0033, 0.00038-0.057	Somu et al.,[48] John,[49] Belcher and Travis,[2]
Fruits	0.0078-0.028	Belcher and Travis[2]
Potatoes	0.05-0.2	Belcher and Travis[2]

to experiments where the soil was "spiked" with large amounts of mercury or measurements were taken from severely polluted areas. This is actually a conservative approach; although plants from mercury polluted areas will have greater contaminate levels, the efficiency of accumulation (quantified in the transfer coefficients) tends to decrease with increasing contaminate concentrations. Values from Cappon[42,41] were used when possible, since these experiments were conducted under reasonable garden conditions, edible portions of plants were analyzed separately, and different mercury species were measured. Cappon[41] analyzed plants grown in control soil (total mercury soil content of 120 ng/g with 4.2 percent methylmercury) in addition to the sludged soil (330 ng/g with 5.1 percent methylmercury, which is comparable to the 1987 soil levels of 430 ng/g with 5.3 percent methylmercury). The control soil data were not used since the methylmercury levels were often undetectable. Note that the compost and sludge-amended soils, although elevated in mercury, are nonetheless at reasonable concentrations. For fruiting vegetables, rooting vegetables and legumes values from Cappon[42] and values derived from the edible potions of plants grown on sludged soil from Cappon[41] were pooled and averaged; the results were used as the defaults for these plant types.

Default Hg^{2+} values for grains and cereals are from Somu;[48] the methylmercury values were assumed to be twice as great in accordance with the overall average trend noted in plants from the pooled Cappon data. The default values for fruits were assumed to be the same as for fruiting vegetables. The default Hg^{2+} value for potatoes was taken from Belcher and Travis;[2] the

methylmercury value for potatoes was assumed to be twice the Hg^{2+} value.

J.2.2.2 Air-Plant BCF.

Parameter: BI

Definition: The ratio of the contaminant concentration in plants (based on dry weight) to that in the air.

Units: Unitless

Crop	Hg^{2+}[a]		Methylmercury[a]	
	Default Value	Distribution	Default Value	Distribution
Leafy vegetables	18000	U[12000,24000]	5000	U[3300,6800]
Legume vegetables	1050	U[700,1400]	100	U[65,130]
Fruiting vegetables	22000	U[14000,29000]	1200	U[780,1600]
Rooting vegetables	0	NA	0	NA
Grains and cereals	1050	U[700,1400]	100	U[65,130]
Forage	18000	U[12000,24000]	5000	U[3300,6800]
Fruits	22000	U[14000,29000]	1200	U[780,1600]
Potatoes	0	NA	0	NA
Silage	18000	U[12000,24000]	5000	U[3300,6800]

[a] Based on elemental mercury air concentration, and speciation of divalent and methylmercury species based on Cappon.[41,42]

Technical Basis:

Mosbaek[39] determined that mercury concentration in the above-ground, leafy parts of plants is almost entirely the result of air-to-plant transfer of mercury. Cappon,[41,42] however, found only divalent and methylmercury in these types of plants. Fitzgerald[52] noted that up to 99 percent of the total airborne mercury is Hg^0 vapor. It was assumed that any atmospheric elemental mercury taken up by the plant is converted into Hg^{2+} and methylmercury in the plant tissue. This is not unreasonable: it has been shown that mercury taken up into plants from the environment can be transformed into other mercury species.[43]

A strong correlation between mercury soil concentration and concentration in rooting vegetables has been established,[45-47,49,53] and the Mosbaek study[39] demonstrated that much of the mercury in

rooting vegetables was from the soil. As a result, air-to-plant uptake of mercury was not modeled for rooting vegetables and potatoes.

For grains, fruits, legumes and fruiting vegetables, little correlation between mercury plant concentrations and either air or soil concentrations has been found; however, non-negligible concentrations of mercury species in these plants are routinely observed. For this reason, both air-to-plant and soil-to-plant uptake was modeled for these plants. Using a conservative approach, the transfer factors for each accumulation pathway were calculated as if all of the mercury in the plant came only from that pathway. This has the effect of possibly double-counting the amount of mercury in the plant tissue. There is a great deal of uncertainty due to the lack of applicable data.

The range of air-plant bioconcentration factors based on Mosbaek et al.[39] was found to be 15,000 - 31,000, based on total mercury concentration in the plant tissue. Mosbeak et al.[39] determined average mercury concentrations due to air uptake in lettuce, radish tops, and grass. Concentrations were converted to dry weight according to Baes et al.,[1] and the overall range of air-plant bioconcentration factors based on total mercury in the plant tissue was found to be 15,000 - 31,000. Air to plant bioconcentration factors can be derived from other studies only indirectly (by making a reasonable estimate of the air concentration and assuming all the mercury in plant tissue comes from air), and the values arrived at for various plant species generally fall into the previous range. Due to the limited data, it was decided to use the midpoint of the Mosbeak et al.[39] bioconcentration values (23,000) as the starting default for all plant species assumed to accumulate mercury from the air.

This approach was adjusted for the consideration of portions of grains and legumes that are not directly exposed to the atmosphere. Although atmospherically absorbed mercury can translocate throughout different portions of the plant, data indicate internal portions of grains and legumes (the edible portions) do not appear to accumulate mercury to the same degree as plant leaves or vines. Somu et al.,[48] John,[49] and Cappon[41] determined mercury concentrations from different portions of the same plants. Table J-6 below shows the relative concentrations of total mercury found in plant parts from the portions of these studies representative of noncontaminated conditions.

A clear trend of decreasing mercury concentrations is seen proceeding from leafy to seed portions of the plants. Based on these data, it was decided to decrease the default air-to-plant

Table J-6. Relative Concentration of Mercury in Different Parts of Edible Plants

Legumes	Beans (Somu et al.[48])	Peas (John[49])	Beans (Cappon[41])
vines		1.0	
stalks	1.0		
pods		0.045	1.0
seeds	0.060	0.0091	0.028 - 0.089
Grains	Wheat[48]	Oats[49]	
leaves		1.0	
stalks	1.0	0.063	
husks		0.61	
grain	0.14	0.051	

biconcentration factor of 23,000 by a factor of 20 (to 1200) to account for the decreasing accumulation of airborne mercury for the edible portions of these plants as compared to the leafy portions (for which the biconcentration factor of 23,000 is applicable). Airborne mercury uptake by fruits may also be overestimated with the default bioconcentration factor. However, no data are available to explore this possibility.

The product of the bioconcentration factors and the atmospheric mercury concentration is the total mercury in the plant tissue resulting from accumulation of airborne elemental mercury. Plant-specific speciation estimates from Cappon[41,42] were used to partition the total mercury bioconcentration factor (and corresponding range) in order to model the relative fractions of methylmercury and Hg^{2+} found in the plant; these are shown in Table J-7; note that the rest of the mercury was found to be divalent mercury.

Thus, for leafy, fruiting and legume vegetables, the default values for the bioconcentration of methylmercury based on the elemental mercury concentration in air were assumed to be 23,000 or 1200 multiplied by the average methylmercury percentages in Table J-6; the Hg^{2+} values were derived similarly (Hg^{2+} fraction x 23,000). The values for fruits were assumed to be the same as for fruiting vegetables. The values for forage and silage were assumed the same as for leafy vegetables, and the

Table J-7. Mercury Speciation in Various Plants

Plant Type	% Methylmercury Cappon[41]	% Methylmercury Cappon[42]
Leafy vegetables		
Head lettuce	8.8	21.4
Leaf lettuce	16.5	18
Spinach	19.8	23.1
Swiss chard, Fordhook	30.2	14.8
Swiss chard, Ruby Red	28.6	-
Broccoli[a]	33.1	17.8
Late Cabbage	28.8	-
Red Cabbage	22.4	-
Savoy King Cabbage	25.2	-
Jersey Wakefield Cabbage[a]	-	18
Cauliflower	21.2	-
Collards	22.8	-
Average	21.8	
Legume vegetables		
Green Bush Beans	0	7.2
Yellow Bush Beans	-	4.3
Lima Beans	-	22.4
Average	8.5	
Fruiting vegetables		
Cucumber, slicing	0	-
Cucumber, pickle	2.1	0
Pepper	12.5	6.1
Zucchini	6.7	0
Summer Squash	0	-
Acorn Squash	4.1	-
Spaghetti Squash	7.4	-
Pumpkin	4.0	-
Tomato	16.0	9.1
Average	5.2	

[a] These were classified as "cole" in Cappon.[42]

values for grains were assumed to be the same as for legumes (beans).

J.2.2.3 Animal BTF.

Parameter: BAj

Definition: The equilibrium concentration of a pollutant in an animal divided by the average daily intake of the pollutant.

Units: day/kg DW

Livestock	Default Value (day/kg DW)	Distribution
beef	0.02	U(0.0008,0.04)
beef liver	0.05	U(0.02,0.1)
dairy	0.02	U(0.003,0.09)
pork	0.00013	U(0.00005,0.00026)
poultry	0.11	U(0.094,0.13)
eggs	0.11	U(0.094,0.13)
lamb	0.09	U(0.009,0.3)

Technical Basis:

Biotransfer factors measure pollutant transfer from the environment to animal tissues and products. They are defined as the ratio of pollutant concentration in animal tissue to the daily pollutant intake of an animal. The biotransfer factors for mercury to cattle tissues were estimated based on data found in Vreman et al.,[54] and biotransfer factors for mercury to lamb were based on data found in van der Veen and Vreman.[55]

The data collected from Vreman et al.[54] and van der Veen and Vreman[55] are not from single pollutant and single route ingestion studies; rather, the animals in these studies were generally dosed with elevated levels of several metals in a single wafer. This is not the ideal set of studies for assessing the transfer of mercury primarily from ingested grass and soil. These studies, however are multiple dose and long-term experiments which should provide data more representative of the desired equilibrium situation than a single, very large dose experiment.

In two experiments, Vreman et al.[54] measured transfer of mercury from diet to tissues and milk of dairy cattle. In the first experiment 12 lactating cows/group were placed on pasture

in 2 groups for 3 months. The control group was fed uncontaminated wafers and, based on mercury levels in the pasture grass, were estimated to ingest 0.2 mg mercury/day. The exposed group received wafers treated with a solution of mercury acetate, lead, cadmium and arsenic pentoxide; the daily mercury ingestion rate for the exposed group was 1.7 mg/day. During the experiment mercury levels in milk were measured. After three months on test, four cows/group were slaughtered, and mercury levels were measured in liver, kidney and muscle samples. In the second study, lactating cows were kept indoors and divided into 4 groups of 8 for up to 28 months. In addition to the control group, the diets of 3 other groups were supplemented with the following: wafers containing the same metals (1.7 mg mercury/day), sludge delivering dietary levels of 3.1 mg mercury/day, and sludge delivering dietary levels of 1.2mg mercury/day. Two cows from each group were slaughtered at study termination (except for the group receiving 3.1 mg mercury/day from sludge in which only one cow was sacrificed). Mean milk mercury concentrations in the groups were reported, and mercury levels in the slaughtered cows were measured in liver, kidney and muscle samples.

Shown in Table J-8 are data from Vreman et al.[54] that are relevant to deriving beef and dairy biotransfer factors. The tissue mercury concentrations presented are in wet weight.

The data in Table J-8 can be easily converted into milk, beef and liver biotransfer factors by converting the tissue concentrations to dry weight and dividing the tissue concentrations by the daily intake of mercury (after converting the intake from mg/day to ug/day). The moisture content of the above tissues are reported in Baes et al. (1984): 0.87 for whole milk, 0.615 for beef and 0.70 for liver. The biotransfer factors derived are shown in Table J-9.

Using the number of animals sampled for each value in Table J-9, weighted averages for the Dairy, Beef and Beef Liver Biotransfer factors can be derived. These are chosen as the default values, with the ranges taken from Table J-9.

In a experiment very similar to Vreman et al.,[54] van der Veen and Vreman[55] measured transfer of mercury from diet to tissues of 10 week old fattening lambs. Two groups of 8 lambs were placed on pasture for 3 months. The control group was fed uncontaminated feed concentrate and based on mercury levels in the pasture grass and uncontaminated feed were estimated to ingest <0.02 mg mercury/Kg dry feed-day. The exposed group received feed concentrate treated with a solution of mercury acetate, lead, cadmium and arsenic pentoxide; the daily mercury

Table J-8. Mercury Concentrations in Specific Beef Tissue Media Per Test Group and Dose (from Vreman et al.[54])

Test Group	Dose (mg mercury/day)	Mercury in Milk (ug/Kg WW[A])	Mercury in Muscle (ug/Kg WW[A])	Mercury in Liver (ug/Kg WW[A])
Pasture Control	0.2	2.3	3	7
Pasture Treated	1.7	0.9	4	10
Indoor Control	0.2	<0.5	2	3
Indoor Wafer	1.7	0.6	2	26
Indoor High-Level Sludge	3.1	2.4	1	14
Indoor Low-Level Sludge	1.2	1.3	2	9

[A] Wet weight

Table J-9. Animal Biotransfer Factors Derived from Vreman et al.[54]

	Biotransfer Factor (day/kg DW)		
Test Group	Dairy	Beef	Beef Liver
Pasture Control	0.09	0.04	0.1
Pasture Treated	0.004	0.006	0.02
Indoor Control	0.02	0.03	0.05
Indoor Wafer	0.003	0.003	0.05
Indoor High-Level Sludge	0.006	0.0008	0.02
Indoor Low-Level Sludge	0.008	0.004	0.03

ingestion rate for the exposed group was 0.08 mg/Kg dry feed. Another four groups of 8 lambs were kept indoors and were fed hay and feed concentrate. A control group was fed uncontaminated feed concentrate, and were estimated to ingest <0.02 mg mercury/Kg dry feed-day. The 3 other groups were fed feed concentrate contaminated with, respectively, a soluble solution of the metals, harbor sludge and sewage sludge. Daily mercury ingestion rates for these groups ranged from 0.14 - 0.27 mg/Kg dry feed. After three months all lambs were slaughtered and mercury levels were measured in liver, kidney, brain and muscle samples.

Shown in Table J-10 are data from van der Veen and Vreman et al.[55] and the biotransfer factors derived from these data.

Table J-10. Mercury Concentrations and resulting BTFs in Lamb Muscle Tissue Per Test Group and Dose[55]

Test Group	Dose (mg mercury/Kg dry feed-day)	Feed Amount (Kg DW/day)	mercury in Muscle (ug/Kg WW)	Muscle Dry %	BTF[A] (day/Kg DW)
Pasture Control	<0.02	1.36	1	32.3	0.2
Pasture Treated	0.08	1.36	3	32.8	0.08
Indoor Control	<0.02	1.3	2	30.5	0.3
Indoor Wafer	0.14	1.28	1	29.5	0.02
Indoor High-Level Sludge	0.27	1.39	1	30.5	0.009
Indoor Low-Level Sludge	0.17	1.38	1	29.1	0.02

[A] Biotransfer Factor (BTF)

To calculate the biotransfer factors listed from the data in Table J-10, the daily mercury intake was calculated from the mercury concentration in dry feed and daily intake of dry feed. van der Veen and Vreman[55] reported the dry weight fractions of the muscle samples, and the mercury concentration in muscle was calculated on a dry weight basis. The biotransfer factor for each group of lambs was then determined. The average over all groups was chosen as the default value, with the ranges taken from Table J-10.

In U.S. EPA,[56] uptake slopes were developed for a number of pollutants found in sludge including mercury. For pork and poultry, U.S. EPA[56] reviewed the literature on concentrations of metals in meat from studies in which livestock were fed known concentrations of the metals in feed. These values were used to obtain the default values (after converting wet-weight values to dry-weight).

J.2.2 Fish Bioaccumulation Factor.

Parameter: Tier 3 Fish BAF (BAF_3)
Tier 4 Fish BAF (BAF_4)

Definition: The concentration of the methylmercury in fish divided by the concentration of total dissolved mercury in water

Units: L/kg

Fish Type		Percentiles (L/kg)		
	Default Value (L/kg)	5th Percentile	Median	95th Percentile
Trophic Level 3 Fish	66,200	6,400	662,000	684,000
Trophic Level 4 Fish	335,000	22,700	335,000	4,700,000

Technical Basis:

The methylmercury value is most important since virtually 100 percent of mercury in fish tissue is methylmercury. The BAFs for methylmercury is defined as the ratio of the methylmercury concentration in fish flesh divided by the concentration of total dissolved mercury (organic plus inorganic forms) in the water column. As virtually 100 percent of the mercury in fish flesh is in the methyl form, the definition of the BAF used here is equivalent to the definition of a total mercury BAF as found in the literature. The BAF represents the accumulation of mercury in fish of a specific trophic level from both water intake and predation on contaminated organisms, the latter being the dominant pathway. In this report BAFs for methylmercury are estimated for trophic level 3 (forage fish) and trophic level 4 (piscivorous fish) designated as BAF_3 and BAF_4, respectively. The BAFs are intended to be representative of the random selection of a fish from a random lake in a random geographical location.

The BAFs were estimated by probabilistic Monte Carlo simulation methods. Distributions were constructed from a limited number of available studies for BAF_3 and a predator-prey factor for trophic level 4 (PPF_4). PPF_4 represents the bioaccumulation of mercury for piscivorous trophic level 4 fish feeding on trophic level 3 fish. BAF_4 is the product of BAF_3 and PPF_4. Five studies were available for the estimation of BAF_3 with values ranging from 10,000 to 350,000. PPF_4 is based on 12 studies with values ranging from 1.2 to 15.5. A sensitivity analysis shows that BAF_3 has the greatest effect on the variance of the BAF_4 output, contributing 75 percent of the variance. A major source of variability in the BAF estimates is the dependence of PPF_4 and to some extent, BAF_3, on the age (and consequently the size) of the fish. Because fish accumulate mercury throughout their lives, the predator-prey and bioaccumulation factors increase with age, particularly for trophic level 4 fish. There is uncertainty as to whether a single BAF value is appropriate for derivation of water concentration when the fish-size range of the fish-consuming

populations is known. For example, kingfishers feed on smaller fish while human recreational anglers primarily consume large fish. Because of the large variance in the BAF distributions and the lack of distinction between uncertainty and variability, the current recommendation is to apply BAFs derived from valid data collected at the site of concern. Otherwise, it is recommended that the mean values of the BAF distributions, rather than upper or lower percentiles, be used for exposure assessment.

J.2.2.5 Plant Surface Loss Coefficient.

Parameter: kp

Definition: A measure of the loss of contaminants deposited on plant surfaces over time as a result of environmental processes.

Units: /yr

Chemical	Default Value (per year)	Distribution	Range
Hg^0	40.41	Log(40.41,17.39)	28.11 - 52.7
Hg^{2+}	40.41	Log(40.41,17.39)	28.11-52.7
Methylmercury	40.41	Log(40.41,17.39)	28.11-52.7

Technical Basis:

The values in the previous table were taken from Belcher and Travis,[2] although no speciation was provided. The values for all species were assumed to be the same. The default value is the mean of the lognormal distribution used in Belcher and Travis.[2] The choice of a lognormal distribution was based on the work of Miller and Hoffman.[57]

J.2.2.6 Fraction of Wet Deposition Adhering.

Parameter: Fw

Definition: Fraction of wet deposition that adheres to plant (i.e., is not washed off).

Units: unitless

Default Value	Distribution	Range
0.6	T (0.1,0.6,0.8)	0.1-0.8

Technical Basis:

The unitless parameter *Fw* represents the fraction of the pollutant in wet deposition that adheres to the plant, is not washed off by precipitation and is used to estimate plant pollutant levels. A value of 1 is the most conservative; this implies that all of the pollutant which deposits onto the plant via wet deposition will adhere to the plant. U.S. EPA[8] originally used a value of 0.02, which significantly diminishes the impact of this pathway. A more recent study by Hoffman et al.[58] suggests an answer between these extremes for both dissolved pollutants and suspended particulates in simulated rain drops.

Hoffman et al.[58] attempted to quantify the amount of radiolabeled beryllium (Be) and Iodine (I) as well as particles of sizes 3, 9, and 25 μm that adhered to three plant types (fescue, clover, and a typical weeded plot). The radiolabeled pollutants were dissolved or suspended in water, which was then showered upon the different types of vegetation to simulate precipitation. Two precipitation intensities were modeled in the experiment: moderate (1-4 cm/hour) and high (4-12 cm/hour). Due to experimental complications, total deposition and pollutant retention upon the vegetation were estimated by the authors; these estimates were termed the interception fraction in the Hoffman report. For example, in the experiment. Beryllium in the form of $BeCl_2$ was dissolved in the water and then showered upon the vegetation. For the moderate and high intensity precipitation events simulated, the mean interception fractions were estimated to be 0.28 and 0.15, respectively.

The 1993 Addendum to the Indirection Exposure Methodology[27] models deposition and retention as the product of the interception fraction (Rp_i) and *Fw*. In terms of the U.S. EPA model, the Hoffman report estimates the product $Rp_i x Fw$. To obtain estimates for *Fw*, the values reported in Hoffman et al.[58] were divided by the interception fraction for forage used in this assessment (0.47[1]). This provides estimates of 0.60 and 0.32 for *Fw* for the moderate and high precipitation intensities, respectively (see Table J-11).

Table J-11 shows the Hoffman et al.[58] estimates for the interception and adhesion of dissolved pollutants and suspended particles in simulated moderate and high intensity precipitation. Based on the Hoffman estimates and the assumption of an interception fraction for forage of 0.47, the *Fw* for the two

Table J-11. Values From Hoffman et al.[58] and the Values of *Fw* Estimated Using Those Values

Compound	Rp_i x Fw for Moderate Intensity	Rp_i x Fw for High Intensity	Fw Estimate for Moderate Intensity	Fw Estimate for High Intensity	Fw Mean
I	0.08	0.05	0.17	0.11	0.14
Beryllium	0.28	0.15	0.60	0.32	0.46
3 μm	0.30	0.24	0.64	0.51	0.58
9 μm	0.33	0.26	0.70	0.55	0.63
25 μm	0.37	0.31	0.79	0.66	0.72

pollutants and three particle sizes were estimated for the precipitation intensities studied, and the means were calculated. No attempt has been made to adjust the final estimate for frequency of the two precipitation intensities; however, since moderate precipitation intensities are more common, the unadjusted means are probably an underestimate.

The *Fw* estimated for beryllium was used as a surrogate for mercury. Be^{2+}, as a cation, is assumed to behave in a manner similar to Hg^{2+} during deposition. Because the moderate intensity is expected to be more common than the heavy intensity, an *Fw* of 0.60 is assumed to be a reasonable estimate of *Fw* for divalent mercury. This value is higher than the range of 0.1-0.3 presented in McKone and Ryan.[10] For beryllium, Hoffman noted the appearance of a strong attraction between the cation and the plant surface, which was assumed to be negatively charged. Beryllium is believed to adsorb to cation exchange sites in the leaf cuticle. Once dried on the plant surface, beryllium was not easily removed by subsequent precipitation events. Divalent mercury is assumed to exhibit a similar behavior. The range of 0.1-0.8 was used to estimate the sensitivity of this parameter.

The adjusted Hoffman data indicate that the greater the intensity of the precipitation, the smaller the *Fw* estimate for both dissolved pollutants and suspended particles. This is intuitively appealing given the understanding of the physical process. Hoffman et al.[58] noted that the intensity and amount of rainfall had approximately the same impact on the estimated values. It should also be noted that the data indicate that the value of *Fw* for pollutants that deposit as anions (e.g., I) may be significantly lower than cations.

J.3 REFERENCES

1. Baes, C.F., R.D. Sharp, A.L. Sjoreen, and R.W. Shor. *A Review and Analysis of Parameters for Assessing Transport of Environmentally Released Radionuclides Through Agriculture.* Prepared under contract No. DE-AC05-84OR21400. U.S. Department of Energy, Washington, D.C. 1984.

2. Belcher, G.D. and C.C. Travis. *Modeling Support for the Rura and Municipal Waste Combustion Projects: Final Report on Sensitivity and Uncertainty Analysis for the Terrestrial Food Chain Model.* Prepared for the U.S. EPA. 1989.

3. Shor, R.W. , C.F. Baes , and R.D. Sharp. *Agricultural Production in the United States by County: A Compilation of Information from the 1974 Census of Agriculture for Use in Terrestrial Food Chain Transport and Assessment Models.* Oak Ridge National Laboratory, ORNL-5786. 1982.

4. Hoffman, F.O. and D.F. Baes. *A Statistical Analysis of Selected Parameters for Predicting Food Chain Transport and Internal Dose of Radionucleotides.* ORNL/NUREG/TM-882. 1979.

5. Knott, J.E. *Handbook for Vegetable Growers.* J. Wiley and Sons, Inc., New York. 1957.

6. Rutledge, A.D. "Vegetable Garden Guide." Publication 447 (Revised) University of Tennessee Agricultural Extension Service, The University of Tennessee. 1979.

7. South Coast Air Quality Management District (SCAQMD). Multi-pathway Health Risk Assessment Input parameters. Guidance Document. 1988.

8. U.S. EPA. *Methodology for Assessing Health Risks Associated with Indirect Exposure to Combustor Emissions.* Office of Health and Environmental Assessment, Washington, D.C. EPA/600/6-90/003. 1990.

9. NAS (National Academy of Sciences). Predicting Feed Intake of Food-Producing Animals. National Research Council, Committee on Animal Nutrition, Washington, DC. 1987.

10. McKone, T.E. and P.B. Ryan. Human Exposure to Chemicals Through Food Chains: An Uncertainty Analysis. *Environ. Sci. Technol.* 23(9): 1154-1163. 1989.

11. Fries, G.F. Potential Polychlorinated Biphenyl Residues in Animal Products from Application of Contaminated Sewage Sludge to Land. J. Environ. Quality. 11: 14-20. 1982.

12. Fries, G.F. Potential Polychlorinated Biphenyl Residues in Animal Products from Application of Contaminated Sewage Sludge to Land. J. Environ. Quality. 11: 14-20. 1982.

13. Hanford Environmental Dose Reconstruction Project. *Parameters Used in Environmental Pathways (DESCARTES) and Radiological Dose (CIDER) Modules of the Hanford Environmental Dose Reconstruction Integrated Codes (HEDRICF) for the Air Pathway*, PNWD-2023 HEDR, Pacific Northwest Laboratories, September 1992.

14. Iverfeldt, A. and J. Persson. The solvation thermodynamics of methylmercury (II) species derived from measurements of the heat of solvation and the Henry's Law constant. *Inorganic Chimica Acta*, 103: 113-119. 1985.

15. Lindqvist, O., K. Johansson, M. Aastrup, A. Andersson, L. Bringmark, G. Hovsenius, L. Hakanson, A. Iverfeldt, M. Meili, and B. Timm. Mercury in the Swedish Environment - Recent Research on Causes, Consequences and Corrective Methods. *Water, Air and Soil Poll.* 55:(all chapters). 1991.

16. Bloom, N.S., C.J. Watras, and J.P. Hurley Impact of Acidification on the Methylmercury Cycle of Remote Seepage Lakes. *Water, Air, and Soil Poll.* 56: 477-491. 1991.

17. Moore, J.W. and S. Ramamoorthy. *Heavy Metal in Natural Waters – Applied Monitoring in Impact Assessment.* New York, Springer-Verlag. 1984.

18. Glass, G.E., J.A. Sorenson, K.W. Schmidt, and G.R. Rapp. New Source Identification of Mercury Contamination in the Great Lakes. Environmental Science and Technology 24:1059-1069. 1990.

19. Robinson, K.G. and M.S. Shuman. Determination of mercury in surface water using an optimized cold vapor spectrophotometric technique. *International Journal of Environmental Chemistry* 36:111-123. 1989.

20. Parks, J.W., A. Luitz, and J.A. Sutton. Water Column Methylmercury in the Wabigoon/English River-lake System: Factors Controlling Concentrations, Speciation, and Net Production. *Can. J. Fish. Aquat. Sci.* 46: 2184-2202. 1989.

21. Akagi H., D.C. Mortimer, and D.R. Miller. Mercury Methylation and Partition in Aquatic Systems. *Bull. Environ. Contam. Toxicol.* 23: 372-376. 1979.

22. Wilken, R.D. and H. Hintelmann. Mercury and Methylmercury in Sediments and Suspended Particles from the River Elbe, North Germany. *Water, Air, and Soil Poll.* 56: 427-437. 1991.

23. Hildebrand, S.G., R.H. Strand, and J.W. Huckabee. Mercury accumulation in fish and invertebrates of the North Fork Holston river, Virginia and Tennessee. J. Environ. Quan. 9:393-400. 1980.

24. Nriagu, J.O. *The Biogeochemistry of Mercury in the Environment.* Elsevier/North Holland. Biomedical Press: New York. 1979.

25. Cappon, C. Content and Chemical Form of mercury and selenium in soil, sludge and fertilizer materials. Water, Air, Soil Pollut 22:95-104. 1984.

26. Lindqvist, O., K. Johansson, M. Aastrup, A. Andersson, L. Bringmark, G. Hovsenius, L. Hakanson, A. Iverfeldt, M. Meili, and B. Timm. Mercury in the Swedish Environment - Recent Research on Causes, Consequences and Corrective Methods. *Water, Air and Soil Poll.* 55:(all chapters). 1991.

27. U.S. EPA. *Assessment of Mercury Occurence in Pristine Freshwater Ecosystems*, prepared by ABT Associates, Inc. Draft as of September 1993.

28. Alberts, J.J., J.E. Schindler, and R.W. Miller. Elemental Mercury Evolution Mediated by Humic Acid. *Science* 184: 895-897. 1974.

29. Fitzgerald, W.F., R.P. Mason, and G.M. Vandal. Atmospheric Cycling and Air-Water Exchange of Mercury over Mid-Continental Lacustrine Regions. *Water, Air, and Soil Pollution* 56: 745-767. 1991.

30. Watras, C.J. and N.S. Bloom. Mercury and Methylmercury in Individual Zooplankton: Implications for Bioaccumulation. *Limnol. Oceanogr.*37(6): 1313-1318. 1992.

31. Bloom, N.S. and C.J. Watras. Observations of Methylmercury in Precipitation. *The Sci. Tot. Environ.* 87/88: 199-207. 1989.

32.

33. Lee, Y., and H. Hultburg. Methylmercury in some Swedish Surface Waters. *Environ. Tocicol. Chem. 9*: 833-841.

34. Kudo et al. (1982). Reference to be added.

35. Gill, G. And K. Bruland. Mercury Speciation in surface freshwaters systems in California and other areas. Sci. Total Environ. 24:1392. 1990.

36. Bloom, N. and S.W. Effler. Water, Air, and Soil Poll. 53:251-265. 1990.

37. Lee, Y., and H. Hultburg. Methylmercury in some Swedish Surface Waters. *Environ. Toxicol. Chem.* 9: 833-841. 1990.

38. Hanson, P. J., S. E. Lindberg, K. H. Kim, J. G. Owens, and T. A. Tabberer, Air/surface exchange of mercury vapor in the forest canopy: I. Laboratory studies of foliar mercury vapor exchange. International Conference on Mercury as a Global Pollutant, July 10-14, Whistler, British Columbia, Canada. 1994.

39. Mosbaek, H., J. C. Tjell, and T. Sevel. Plant Uptake of Mercury in Background Areas. *Chemosphere* 17(6):1227-1236. 1988.

40. Fortmann, L. C., D. D. Gay, and K. O. Wirtz. Ethylmercury: Formation in Plant Tissues and Relation to Methylmercury Formation. U.S. EPA Ecological Research Series, EPA-600/3-78-037. 1978.

41. Cappon, C.J. Mercury and Selenium Content and Chemical Form in Vegetable Crops Grown on Sludge-Amended Soil. *Arch. Environm. Contam. Toxicol.* 10: 673-689. 1981.

42. Cappon, C.J. Uptake and Speciation of Mercury and Selenium in Vegetable CropsGrown on Compost-Treated Soil. *Water, Air, Soil Poll.* 34: 353-361. 1987.

43. Fortmann, L. C., D. D. Gay, and K. O. Wirtz. Ethylmercury: Formation in Plant Tissues and Relation to Methylmercury Formation. U.S. EPA Ecological Research Series, EPA-600/3-78-037. 1978.

44. Temple, P. J. and S. N. Linzon. Contamination of Vegetation, Soil, Snow and Garden Crops by Atmospheric Deposition of Mercury from a Chlor-Alkali Plant, in (1977) D. D. Hemphill [ed] Trace Substances in Environmental Health - XI, Univ Missouri, Columbia. p. 389-398. 1977.

45. Lenka, M., K. K. Panda, and B. B. Panda. Monitoring and Assessment of Mercury Pollution in the Vicinity of a Chloralkali Plant. IV. Bioconcentration of Mercury in *In Situ* Aquatic and Terrestrial Plants at Ganjam, India. *Arch. Environ. Contam. Toxicol.* 22:195-202. 1992.

46. Lenka, M., K.K. Panda, and B.B. Panda. Monitoring and Assessment of Mercury Pollution in the Vicinity of a Chloralkali Plant. II. Plant Availability, Tissue Concentration and Genotoxicity of Mercury from Agricultural Soil Contaminated with Solid Waste Assessed in Barley. *Environ. Poll.* 0269-7491/92. pp. 33-42. 1992.

47. Lenka, M., K.K. Panda, and B.B. Panda. Monitoring and Assessment of Mercury Pollution in the Vicinity of a Chlor-alkali Plant. IV. Bioconcentration of Mercury in In Situ Aquatic and Terrestrial Plants at Ganjam, India. *Arch. Environ. Contam. Toxicol.* 22:195-202. 1992.

48. Sumo, E., B.R. Singh, A.R. Selmer-Olsen, and K. Steenburg. Uptake of ^{203}Hg-labeled Mercury compounds by Wheat and Beans Grown on an oxisol. *Plant and Soil* 85: 347-355. 1985.

49. John, M.K. Mercury Uptake from Soil by Various Plant Species. *Bull. Environ. Contam. Toxicol.* 8(2): 77-80. 1972.

50. Wiersma, D., B. J. van Goor, and N. G. van der Veen. Cadmium, Lead, Mercury, and Arsenic Concentrations in Crops and Corresponding Soils in the Netherlands. *J. Agric. Food Chem.*, 34:1067-1074. 1986.

51. U.S. EPA. *Environmental profiles and hazard indices for constituents of municipal sludge: Mercury.* Washington, D.C.: Office of Water Regulations and Standards. 1985.

52. Fitzgerald, W. Cycling of mercury between the atmosphere and oceans, in: The Role of Air-Sea Exchange in Geochemical Cycling, NATO Advanced Science Institutes Series, P. Buat-Menard (Ed.), D. Reidel publishers, Dordrecht, pp 363-408. 1986.

53. Lindberg, S. E., D. R. Jackson, J. W. Huckabee, S. A. Janzen, M. J. Levin, and J. R. Lund. Atmospheric Emission and Plant Uptake of Mercury from Agricultural Soils near the Almaden Mercury Mine. *J. Environ. Qual.* 8(4):572-578. 1979.

54. Vreman, K., N.J. van der Veen, E.J. van der Molen and W.G. de Ruig. Transfer of cadmium, lead, mercury and arsenic from feed into milk and various tissues of dairy cows: chemical and pathological data. *Netherlands Journal of Agricultural Science* 34: 129-144. 1986.

55. van der Veen, N.G. and K. Vreman. Transfer of cadmium, lead, mercury and arsenic from feed into various organs and tissues of fattening lambs. *Netherlands Journal of Agricultural Science* 34: 145-153. 1986.

56. U.S. EPA. Technical Support document or Land Application of Sewage Sludge. Federal Register. 40 CFR Part 257 et al. Standards for the Use or Disposal of Sewage sludge; Final Rules. February 19, 1993.

57. Miller, C. And F. Hoffman. An examination of the environmental half-time for radionuclides deposited on vegetation. Health Physics 45:731. 1993.

58. Hoffman, F.O., K.M. Thiessen, M.L. Frank and B.G. Blaylock. Quantification of the interception and initial retention of radioactive contaminants deposited on pasture grass by simulated rain. *Atmospheric Environment*, 26A (18): 3313-3321. 1992.

This page is intentionally blank.

APPENDIX K - PARAMETER JUSTIFICATIONS SCENARIO-DEPENDENT PARAMETERS

This page is intentionally blank.

DISTRIBUTION NOTATION

A comprehensive uncertainty analysis was not conducted as part of this study. Initially, preliminary parameter probability distributions were developed. These are listed in Appendices J and K. These parameter probability distributions were not utilized to generate quantitative exposure estimates. They are provided as a matter of interest for the reader.

Unless noted otherwise in the text, distribution notations are presented as follows.

Distribution	Description
Log (A,B)	Lognormal distribution with mean A and standard deviation B
Log* (A,B)	Lognormal distribution, but A and B are mean and standard deviation of *underlying normal distribution.*
Norm (A,B)	Normal distribution with mean A and standard deviation B
U (A,B)	Uniform distribution over the range (A,B)
T (A,B,C)	Triangular distribution over the range (A,C) with mode of B

K. SCENARIO DEPENDENT PARAMETERS

This appendix describes the scenario dependent parameters used in the exposure modeling for the Mercury Study Report to Congress. Scenario dependent parameters are variables whose values are dependent on a particular site and may differ among various site-specific situations. For this assessment, three settings are being evaluated: (1) rural, (2) lacustrine, and (3) urban. The receptors differ for each of these scenarios, as do the parameters. These scenario dependent parameters may be either chemical independent or chemical dependent. The following sections present the chemical independent and chemical dependent parameters used in this assessment.

Chemical independent parameters are variables that remain constant despite the specific contaminant being evaluated. The chemical independent variables used in this assessment are described in the following sections.

Site physical data include information such as the environmental setting, vegetative cover, presence of surface water or groundwater, area of source and meteorological and climatological data. These parameters are described in the following sections.

K.1 Time of Concentration

Parameter: Tc

Definition: Number of years that the air concentration at the above level persists; equal to the facility lifetime for calculations from anthropogenic sources

Units: yrs

Scenario	Default Value(s) (years)	Distribution
All	30	None

Technical Basis:

The time of concentration is the same as the assumed facility lifetime. The generic value is 30 years. It is noted that this assumption is made only for estimation of soil concentrations. The water concentrations are calculated assuming

steady-state has been attained, with the flux due to runoff/erosion based on the 30-year soil concentrations.

K.2 Average Air Temperature

Parameter: Ta

Definition: Average air temperature of microscale area

Units: °C

Location	Default Value (Years value is based upon) (°C)	Distribution
Eastern Location	11.9 (25)	U (8,16)
Western Location	13.4 (47)	U (9,17)

Technical Basis:

The values for local airports are reported in the section "U.S. Local Climatological Data Summaries for 288 Primary Stations throughout the U.S." on CDROM by WeatherDisc Associates.[1] The distributions are arbitrary to explore the sensitivity of this parameter.

K.3 Watershed Area

Parameter: WAI

Definition: Area of contamination which drains into a water body

Units: Km^2

Location	Default Value (Km^2)
Eastern Location	37.3
Western Location	37.3

Technical Basis:

The values for the fish ingestion pathways are based on hypothetical watershed/waterbody surface area ratio of 15 and a lake diameter of 1.78 km. This parameter was used only to calculate the erosion and runoff load to the water body.

K.4 Average Annual Precipitation

Parameter: P

Definition: Average annual precipitation

Units: cm/yr

Location	Default Value (cm/yr)	Distribution
Eastern Location	102	T(82,102,122)
Western Location	21	T(1,21,41)

Technical Basis:

All values are for local airports as reported in the section "U.S. Local Climatological Data Summaries for 288 Primary Stations throughout the U.S." on CDRom by WeatherDisc Associates.[1] These were considered the "best estimates" of a triangular distribution, with a range of 20 in/yr above and below the mode.

K.5 Average Annual Irrigation

Parameter: I

Definition: Average annual irrigation of plants

Units: cm/yr

Location	Default Value (cm/yr)	Distribution
Eastern Location	12.5	U(0,25)
Western Location	57.5	U(50,65)

Technical Basis:

The ranges were approximated from Figure 4.25 in Baes et al.[2] The tentative default values are the midpoint of this range. It was assumed that both the farmer and home gardener will irrigate the same amount if they are in the same area of the country (i.e., irrigation rate does not depend on size of plot).

K.6 Average Annual Runoff

Parameter: Ro

Definition: Average annual runoff

Units: cm/yr

Location	Default Value (cm/yr)	Distribution
Eastern Location	18	U(9,27)
Western Location	1	U(0,2)

Technical Basis:

The default values for the eastern location are from Geraghty et al.[3] The total runoff values given in that report include groundwater recharge, direct runoff, and shallow interflow. Following U.S. EPA[4], this number was reduced by one-half to represent surface runoff. Because of the difficulty of hydrologic modeling in the western location, the PRZM-2 model[5] was used to estimate the runoff for this area. The estimated value was 1 cm/yr. The distributions are arbitrary to determine the sensitivity of this parameter.

K.7 Average Annual Evapotranspiration

Parameter: Ev

Definition: Average annual loss of water due to evaporation

Units: cm/yr

Location	Default Value (cm/yr)	Distribution
Eastern Location	65	U(60,70)
Western Location	13	U(8,18)

Technical Basis:

For the eastern location, the ranges are based on estimates from isopleths given in Figure 4.24 in Baes et al.[2] The values presented there were estimated based on local data (average temperature and precipitation) as well as the maximum possible sunshine for the area. The default value is the midpoint of this

range. For the western location, the model PRZM-2 was used to estimate the values given previously.

K.8 Wind Speed

Parameter: W

Definition: Wind speed

Units: m/s

Location	Default Value (m/s)	Distribution
Eastern Location	4.3	U(1,7)
Western Location	4.0	U(1,7)

Technical Basis:

All values were collected for local airports and reported in the section "U.S. Local Climatological Data Summaries for 288 Primary Stations throughout the U.S." on CDROM by WeatherDisc Associates.[1] The primary use of this parameter is for estimating volatilization from soil and water bodies. The distributions are arbitrary to explore the sensitivity of this parameter.

K.9 Soil Density

Parameter: BD

Definition: Soil density

Units: g/cm^3

Location	Default Value (g/cm^3)	Distribution	Range
All Sites	1.4	Log(1.4,0.15)	0.93-1.84

Technical Basis:

The distribution is from Belcher and Travis[6] and is based on a probability plot using data from Hoffman and Baes.[7] There is little variation in the parameter, despite the fact that more than 200 data points were used. The default value is the mean of the distribution.

K.10 Mixing Depth in Watershed Area

Parameter: Zd

Definition: The depth that contaminants are incorporated into soil (no tillage)

Units: cm

Location	Default Value (cm)	Distribution
All Sites	1.0	U(0.5,5)

Technical Basis:

The default value is based on U.S. EPA.[8] The distribution is arbitrary to determine the relative sensitivity of the parameter.

K.11 Mixing Depth for Soil Tillage

Parameter: Ztill

Definition: The depth that contaminants are incorporated into tilled soil

Units: cm

Location	Default Value (cm)	Distribution
All Sites	20	U(10,30)

Technical Basis:

The default value is based on U.S. EPA.[8] The distribution is arbitrary to determine the sensitivity of this parameter.

K.12 Soil Volumetric Water Content

Parameter: Theta,O

Definition: Amount of water that a given volume of soil can hold

Units: ml/cm^3

Location	Default Value (ml/cm^3)	Distribution
Eastern Location	0.30	U(0.15,0.42)
Western Location	0.36	U(0.15,0.42)

Technical Basis:

Values for water content can range from 0.003 to 0.40 ml/cm^3 depending on the type of soil.[7] Table K-1 demonstrates the dependency of values on the hydrologic soil type. These values were derived from the PATRIOT software system[9], which can be obtained from the Center for Exposure Assessment Modeling at the U.S. Environmental Protection Agency, Athens, Georgia.

Representative soil types for both sites are shown in Table K-2 and were determined from Carsel.[5] The soil types were used in conjunction with the previous table to determine the default value for the soil water content, with the value for the western location being the average of the values for types C and D. The distribution for all sites is a uniform distribution over the range over all soil types.

K.13 Soil Erosivity Factor

Parameter: R

Definition: Quantifies local rainfall's ability to cause erosion

Units: kg/km^2-yr

Location	Default Value (kg/km^2-yr)	Distribution
Eastern Location	200	U(100,300)
Western Location	53	U(30,75)

Technical Basis:

The ranges were determined based on an isopleth map for the region in USDA.[10] The upper and lower bounds were determined from this map by finding extremes within a 300-mile radius.

K.14 Soil Erodability Factor

Parameter: K

Table K-1. Water Content Per Soil Type

Soil Type	Water Content
A	0.15
B	0.22
C	0.30
D	0.42

Table K-2. Representative Soil Types For Each Site

Location	Soil Type
Eastern Location	C
Western Location	C/D

Definition: Quantifies soil's susceptibility to erosion

Units: tons/acre

Location	Default Value (tons/acre)	Distribution
Eastern Location	0.30	U(0.12,0.48)
Western Location	0.28	U(0.08,0.48)

Technical Basis:

Based on similar soil near the eastern location (loamy sand, loam, and silt loam) and using Table A2-2 in U.S. EPA[11], a range of 0.12 to 0.48 was obtained. A similar analyses has not been performed for the other sites, but the ranges listed in the previous table are apparently the maximum range possible based on Table A2-2 in U.S. EPA[8]; therefore, these ranges encompass all likely values and can be used for sensitivity analyses. The default values are the midpoint of these ranges.

K.15 Topographic Factor

Parameter: LS

Definition: Provides a measure of the length and steepness of the land slope

Units: unitless

Location	Default Value	Distribution
Eastern Location	2.5	U(0.25,5)
Western Location	0.4	U(0.1,1.2)

Technical Basis:

The length and steepness of the land slope substantially affect the rate of soil erosion. Table A2-3 in U.S. EPA[11] contains LS values for various slopes and slope lengths and was used in conjunction with United States Geological Survey (USGS) maps to obtain the ranges given in the previous table. A 1:24000 map was available for the humid/east/complex I site while only a 1:250000 USGS map was available for all other sites. The default value was chosen as representative of the most common slope and length in the area.

K.16 Cover Management Factor

Parameter: C

Definition: The ratio of soil loss from land cropped under local conditions to the corresponding loss from clean tilled fallow

Units: unitless

Location	Default Value
Eastern Location	0.006
Western Location	0.1

Technical Basis:

The lower end of the range for areas having forests (0.001) is the lower of two values suggested for woodlands in U.S. EPA.[12]

For those areas lacking forests (i.e., western site), the value of 0.1 given for grass in U.S. EPA[4] was used.

For the watershed, it was decided to use a cover fraction representative of undisturbed grass or forested areas, although high-end values were used. It was noted that the cover fraction can vary by several orders of magnitude, depending on the land use type and soil type. Table K-3 shows estimates of cover factor values for undisturbed forest land.[13] Based on the above values and the objectives of this exposure assessment, it was decided that the high-end values (of those above) would be appropriate; a nominal value of 0.006 (the midpoint of the high-end range) was chosen.

B.17 Sediment Delivery Ratio to Water Body

Parameter: Sdel

Definition: Sediment delivery ratio to water body

Units: unitless

Location	Default Value	Distribution
Both Locations	0.2	U(0.14,0.23)

Technical Basis:

The sediment delivery ratio is the fraction of soil eroded from the watershed that reaches the water body. It can be calculated based on the watershed surface area using an approach proposed by Vanoni[14]:

$$Sdel = a\ WA_L^{-b}$$

where WA_L is watershed area in m^2, b is an empirical slope coefficient (-0.125) and a is an empirical intercept coefficient that varies with watershed area. A graph of the sediment delivery ratio as a function of watershed area is given in the Water Quality Assessment Manual.[15]

Table K-3. Cover Factor Values of Undisturbed Forest Land (from WQAM, 1985; original citation Wischmeier and Smith[12])

Percent of Area Covered by Canopy of Trees and Undergrowth	Percent of Area Covered by Duff (litter) at least 5 cm deep	Cover Management Factor Value
75-100	90-100	0.0001-0.001
45-70	75-85	0.002-0.004
20-40	40-70	0.003-0.009

K.18 Pollutant Enrichment Factor

Parameter: EF

Definition: The pollutant enrichment factor accounts for the fact that the lighter particles susceptible to erosion tend to have a greater concentration of pollutants attached per mass than what the average soil concentration may suggest.

Units: unitless

Location	Default Value	Distribution
Both Locations	2	U(1.5,2.6)

Technical Basis:

Enrichment refers to the fact that erosion favors the lighter soil particles, which have higher surface area to volume ratios and are higher in organic matter content. Concentrations of hydrophobic pollutants would be expected to be higher in eroded soil as compared to in-situ soil. While enrichment is best ascertained with sampling or site-specific expertise, generally it has been assigned values in the range of 1 to 5 for organic matter, phosphorus, and other soil-bound constituents of concern. Mullins et al.[16] describe the following equation for calculating enrichment ratio for storm events:

$$EF = 2 + 0.2 \ln (X_e/A_w)$$

where X_e is the mass of soil eroded, in metric tons (1 metric ton = 1000 kg), and A_w is watershed area, in hectares (1 hectare = 10,000 m^2). Experience suggests that typical values range from 1.5 to 2.0, reflecting erosion events from 0.08 to 1.0 tonnes per hectare. A very large erosion event of 20 tonnes per hectare would

have a predicted enrichment ratio of 2.6. The default value assumed here is 2.

K.19 Water Body Surface Area

Parameter: Waw

Definition: Water body surface area

Units: km^2

Location	Default Value	Distribution
Both Locations	2.49	U(1.5,3)

Technical Basis:

For the purpose of this assessment, it was assumed that the hypothetical water body has a diameter of 1.78 km, from which the default surface area is calculated.

K.20 Water Body Volume

Parameter: Vw

Definition: Water body volume

Units: m^3

Location	Default Value	Distribution
Both Locations	1.24×10^7	Constant

Technical Basis:

For the purpose of this assessment, it was assumed that the hypothetical water body has a diameter of 1.78 km and mean depth of 5 m. The corresponding volume assuming a disk of height 5 m and radius 0.89 km is then given by 1.24×10^7 m^3 (using the formula $volume = \pi r^2 h$).

K.21 Long-Term Dilution Flow

Parameter: Q

Definition: Long term dilution flow

Units: m^3/yr

Location	Default Value (m^3/yr)
Eastern Location	$1.44x10^7$
Western Location	$1.44x10^5$

Technical Basis:

The long-term dilution flow can be estimated from Tables in U.S. EPA.[17] The values in in/yr are given in Table K-4. These were multiplied by the watershed area of $3.3x10^7$ m^2 to obtain the default values.

K.22 Suspended Solids Deposition Rate

Parameter: Ssdep

Definition: Suspended solids deposition rate

Units: m/day

Scenario	Default Value (m/day)
Both Locations	0.5

Technical Basis:

Stokes equation can be used to calculate the terminal velocity of a sediment particle settling through the water column, as described in Ambrose et al. (1988):

$$Vs = \frac{8.64g}{18\ E6}\ (FEp - FEw)\ dp^2$$

where:

Vs is Stokes velocity for a particle with diameter dp and density =FEp, m/day, g is acceleration of gravity =3D 981 cm/sec2, = E6 is absolute viscosity of water =3D 0.01 poise (g/cm3-sec) at 20 =F8C, = FEp is density of the solid, g/cm3, = FEw is density of water, 1.0 g/cm3, and dp is particle diameter, mm.

Table K-4. Long-Term Dilution Flow In In/Yr

Location	Value (in/yr)
Eastern Location	15
Western Location	0.15

Values of Vs for a range of particle sizes and densities are provided in Table 3.1. Deposition velocities should be set at or below the Stoke's velocity corresponding to the median suspended particle size, keeping in mind that pollutants tend to sorb more to the smaller silts and clays than to large silt and sand particles = 20. The deposition velocity here represents net deposition over time and so will be smaller for systems experiencing periodic scour = 20. The value chosen here is an order of magnitude below the Stoke's velocity calculated for medium silt particles.

K.23 Benthic Sediment Concentration

Parameter: BS

Definition: Benthic sediment concentration

Units: kg/L

Scenario	Default Value (kg/L)
Both Locations	1 kg/L

Technical Basis:

Benthic sediment concentration is related to the densities of sediment particles, water, and the bulk sediment:

$$Cs = \frac{FEp\ (FEb - FEw)}{(FEp - FEw)}$$

where

FEp is the particle density in g/cm3, FEw is the water density in g/cm3, and =FEB is the sediment bulk density in g/cm3.

Typical particle densities in sediments range between 2.6 and 2.7 k/cm3, and at 20 degrees Celsius water density is close to 1.0 g/cm3. For these properties, a bulk density value of 1.6 g/cm3 corresponds to a sediment concentration of 1.0 g/cm3 (or kg/L) and a porosity of 0.65, which represents consolidated benthic sediment. An analysis of 1680 measured bulk densities in marine sediments exhibited a range from 1.25 to 1.8 g/cm3 and an average particle density of 2.7.[18] Some waterbodies contain an upper unconsolidated layer of sediment with bulk densities of 1.1 to 1.3, which correspond to porosities of 0.94 to 0.82 and sediment concentrations of 0.16 to 0.48 g/cm3. In this study, we represent pollutant storage in consolidated beds.

K.24 Upper Benthic Sediment Depth

Parameter: Db

Definition: Benthic sediment concentration
Units: m

Scenario	Default Value (m)	Distribution
Both Locations	0.02	U(0.01,0.03)

Technical Basis:

The total benthic sediment depth can vary from essentially zero in rocky streams to hundreds of meters in oceans. In the lake environments being modeled here, the total benthic sediment depth usually exceeds a few centimeters. Here we are modeling only the upper layer that is in partial contact with the water column through physical mixing and bioturbation. Although bioturbation can descend to tens or even hundreds of centimeters, only the top few centimeters would be in significant contact with the water column. Because this model assumes chemical equilibrium between the upper sediment layer and the water column, a shallow depth of 2 cm was chosen.

K.25 Aquatic Plant Biomass

2 mg/L

Technical Basis:

Aquatic biomass can include phytoplankton and, in shallow areas, benthic algae and rooted aquatic plants. Phytoplankton biomass, as measured by chlorophyll a, can range from less than 1 E 6g/L in oligotrophic lakes to higher than 200 E 6g/L during

blooms = in eutrophic lakes. Given a typical carbon to chlorophyll ratio of 30 (Ambrose et al., 1988), and carbon to biomass ratio of approximately 0.4 [19], the range of aquatic phytoplankton biomass is from 0.08 to 15 mg/L. A yearly average chlorophyll a value of 25 E6g/L gives an estimated biomass of about 2 mg/L, which was used in this study.

K.26 Total Fish Biomass

Bioenergetics typically dictate that biomass declines each trophic level by a factor of 10. Trophic level 3 fish supported by 2 mg/L aquatic biomass, then, would be supported at about 0.02 mg/L. Additionally, trophic level 4 fish and fish supported by external energy sources (such as insects) can be present. A total fish biomass is estimated to be 0.05 mg/L.

K.27 References

1. WeatherDisc Associates. *U.S. Local Climatological Data Summaries for 288 Primary Stations throughout the U.S.*, on CDROM. 1992.

2. Baes, C.F., R.D. Sharp, A.L. Sjoreen, and R.W. Shor. *A Review and Analysis of Parameters for Assessing Transport of Environmentally Released Radionuclides through Agriculture.* Oak Ridge National Laboratory, ORNL-5786. 1984.

3. Geraghty, J. J., D. W. Miller, F. V. Der Leenden, and F. L. Troise, Water Atlas of the United States. A Water Information Center Publication, Port Washington, N.Y. 1973.

4. U.S. EPA. *Indirect Exposure Assessment Working Group Recommendations, DRAFT pending review.* 1993.

5. Carsel, R.F., C.N. Smith, L.A. Mulkey, J.D. Dean, and P. Jowise. User's Manual for the Pesticide Root Zone Model (PRZM) Release 1. U.S. EPA, Athens, GA. EPA-600/3-84-109. 1984.

6. Belcher, G.D. and C.C. Travis. *Modeling Support for the Rural and Municipal Waste Combustion Projects: Final Report on Sensitivity and Uncertainty Analysis for the Terrestrial Food Chain Model.* Prepared for the U.S. EPA. 1989.

7. Hoffman, F.O. and D.F. Baes. *A Statistical Analysis of Selected Parameters for Predicting Food Chain Transport and Internal Dose of Radionucleotides.* ORNL/NUREG/TM-882. 1979.

8. U.S. EPA. *Methodology for Estimating Health Risks from Indirect Exposure to Combustor Emissions.* Office of Health and Environmental Assessment, Washington, D.C. EPA/600/6-690/003. 1990.

9. Imhoff, J.C., P.R. Hummel, J.L. Kittle, and R.F. Carsel. PATRIOT - A Methodology and Decision Support System for Evaluating the Leaching Potential of Pesticides. EPA/600/S-93/010. U.S. Environmental Protection Agency, Athens, Georgia. 1994.

10. U.S. Department of Agriculture. *Handbook No. 537: Predicting Rainfall Erosion Losses.* U.S. Government Printing Office, Washington, D.C. 1978.

11. U.S. EPA. *Development of Risk Assessment Methodology for Land Application and Distribution and Marketing of Municipal Sludge.* Office of Health and Environmental Assessment, Washington, D.C. EPA/600/6-89/001. 1989.

12. U.S. EPA. *Superfund Exposure Assessment Manual.* Office of Remedial and Emergency Response, Washington, D.C. EPA/540/1086/060. 1988.

13. Wischmeier, W. and D. Smith. Predicting Rainfall and Erosion Losses: A Guide to Conservation Planning. U.S. Department of Agriculture, Agriculture Handbook No. 537. 1978.

14. Vanoni, V.A., *Sedimentation Engineering.* American Society of Civil Engineers, New York, NY. pp. 460-463. 1975.

15. Mills, W.B., et al. Water Quality Assessment: A Screening Procedure for Toxic and Conventional Pollutants in Surface and Ground Water. Part 1. EPA/600/6-85/002a. U.S. Environmental Protection Agency, Athens, Georgia. pp. 177,178. 1985.

16. Mullins, J.A., R.F. Carsel, J.E. Scarbrough, and A.M. Ivery. PRZM-2, A Model for Predicting Pesticide Fate in the Crop Root and Unsaturated Soil Zones: Users Manual for Release 2.0. EPA/600/R-93/046. U.S. Environmental Protection Agency, Athens, Georgia. p.6-22. 1993.

17. U.S. EPA. *Water Quality Assessment: A Screening Procedure for Toxic and Conventional Pollutants in Surface and Ground Water (Part 1).* Washington, D.C. EPA/600/6-85/002-A. 1985.

18. Richards, A.F., T.J. Hirst, and J.M. Parks. Bulk Density-Water Content Relationship in Marine Silts and Clays. Journal of Sedimentary Petrology, Vol.44, No.4, p 1004-1009. 1974.

19. Bowie, G.L. et al. Rates, Constants, and Kinetics Formulations in Surface Water Quality Modeling (Second Edition). EPA/600/3-85/040. U.S. EPA, Athens, GA. 1985.

APPENDIX L - MERCURY PARTITION COEFFICIENT CALIBRATIONS

This page is intentionally blank.

L.1 INTRODUCTION

For an assessment of mercury exposure, an accurate modelling of watershed chemistry is critical. One of the important parameters in this watershed chemistry model is the soil-water partition coefficient (K_d) and the benthic sediment-water partition coefficient (see Appendix M for a more complete description of the model). The method by which literature values were determined did not account completely for the watershed transport of mercury. As a consequence, a calibration effort was undertaken in which mercury watershed transport was assessed at specific sites and modeled in Addendum to the Methodology for Assessing Health Risks Associated with Indirect Exposure to Combustor Emissions (IEM2). To estimate a general effective K_d value for mercury, the model was calibrated at three sites. The geometric mean of the generated estimates was selected as the final value.

As noted by Dooley,[1] there is a difference of about three orders of magnitude between the reported K_d values for mercury in soil-water systems and those in water-suspended solid systems. Dooley indicated that this difference is not as large as other values in the literature suggest. In this appendix evidence is presented in support of this hypothesis by means of a series of calibrations of a watershed model. The calibrated partition coefficients are about one order of magnitude lower than the reported partition coefficients in water suspended solid systems.

L.2 BACKGROUND

L.2.1 Parameters and Coefficients

The parameters used to address mobility properties are among the most important in multimedia chemical fate and transport modeling. In many models, it is assumed that the total chemical mass is partitioned among several different compartments. A common assumption is that partitioning is linear; that is, the fraction in one compartment is directly proportional to the fraction in another compartment.

For soil-water systems, the constant of proportionality is called the partition or distribution coefficient and is usually denoted by K_d, with units of (mg/kg)/(mg/L) or L/kg. The partition coefficient is the ratio of the concentration sorbed onto soil particles to that dissolved in soil water at equilibrium; that is no net changes of amount of chemical in soil and water components. The adsorptive properties of a chemical can depend on a variety of environmental factors; e.g., pH of soil, amount of organic matter in the soil or water, percent of

sand, silt or clay in soil, other chemicals present and even the magnitude of the chemical concentration in the water itself. Because of the complicated nature of the sorptive process, it is not surprising that reported values for the linear partition coefficient can vary over many orders of magnitude for a given chemical.

More complicated methods than linear partitioning exist for addressing sorption. The nonlinear Freundlich equation is an example of a more complex model in which the soil concentration is assumed to be proportional to some power of the water concentration. The particular power, usually denoted *n* and called the Freundlich exponent, affords a wider range of data fitting capabilities, but as with the simpler approach and as noted by Buchter et al.[2], it does not provide much information about the actual processes involved.

For long-term (years) estimates, the simple linear approach is perhaps most applicable. The equilibrium assumptions necessary are more likely to be achieved over a long period of time, and the variation that could be observed and expected for short-term simulations are more likely to be adequately characterized by a single representative value. It is more appropriate to call such a partition coefficient an "effective" partition coefficient to reflect its strong empirical nature.

It is this kind of estimate that is appropriate for the methodology described in the Draft Addendum to the Methodology for Assessing Health Risks from Combustor Emissions.[3] The IEM2 model also requires partition coefficients for the suspended sediment-water and benthic sediment-water. The soil-water K_d is critical in determining the movement of mercury from land to water bodies, while the other coefficients partition the mercury once it arrives in the water body.

L.2.2 Mercury

Mercury (Hg) can exist in three oxidation states: Hg^0 (metallic or elemental), Hg_2^{2+} (mercurous), and Hg^{2+} (mercuric). The properties and behavior of mercury depend strongly on the oxidation state. Mercurous and mercuric mercury can form numerous inorganic and organic compounds; however, mercurous mercury is rarely stable under ordinary environmental conditions. Most of the mercury encountered in all environmental media except the atmosphere is in the form of inorganic mercuric salts and organomercurics. Organomercurics are defined by the presence of a covalent C-Hg bond. The compounds most likely to be found under environmental conditions are these: the mercuric salts $HgCl_2$, $Hg(OH)_2$ and HgS; the methylmercury (MHg) compounds CH_3HgCl

and CH_3HgOH; and, in small fractions, other organomercurics (e.g., dimethylmercury, phenylmercury and ethylmercury).

A number of methods can be used to determine mercury concentrations in environmental media. The concentrations of total mercury, elemental mercury, organic mercury compounds (especially methylmercury) and information on various Hg^{2+} compounds can be measured, although speciation among Hg^{2+} compounds is not usually attempted. Recently, significant improvements and standardizations in analytical methodologies enable reliable data on the concentration of methylmercury, elemental mercury and the Hg^{2+} fraction to be readily separated from the total mercury in environmental media. It is possible to further speciate the Hg^{2+} fraction into reactive, non-reactive and particle-bound compounds, but it is not generally possible to determine which Hg^{2+} species is present (e.g., HgS or $HgCl_2$).

Most of the mercury in soil is thought to be in the form of Hg^{2+} species. Soil conditions are typically favorable for the formation of inorganic Hg^{2+} compounds such as $HgCl_2$, $Hg(OH)_2$ and inorganic Hg^{2+} compounds complexed with organic anions).[4] Although inorganic Hg^{2+} compounds are quite soluble and thus theoretically mobile, they form complexes with soil organic matter (mainly fulvic and humic acids) and mineral colloids, with the former being the dominating process. This is due largely to the affinity of Hg^{2+} and its inorganic compounds for sulfur containing functional groups. This complexing behavior greatly limits the mobility of mercury in soil. Much of the mercury in soil is bound to bulk organic matter and is susceptible to elution in runoff only by being attached to suspended soil or humus. However, some Hg^{2+} will be absorbed onto dissolvable organic ligands and other forms of dissolved organic carbon (DOC) and may then partition to runoff in the dissolved phase. Hg^0 can be formed in soil by reduction of Hg^{2+} compounds/complexes mediated by humic substances .[5] This Hg^0 will eventually vaporize and re-enter the atmosphere. methylmercury can be formed by various microbial processes acting on Hg^{2+} substances. Generally, approximately 1 to 3 percent of the total mercury in surface soil is methylmercury, and as is the case for Hg^{2+} species, it will be largely bound to organic matter. The other 97-99 percent of total soil mercury can be considered largely Hg^{2+} complexes, although a small fraction of mercury in typical soil will be Hg^0.[6] The methylmercury percentage can exceed 3 percent[7] in garden soil with high organic content under slightly acidic conditions. Contaminated sediments may also contain higher methylmercury percentages compared to soils.[8,9]

Values for soil-water partition coefficients for mercury are rarely reported in the literature, regardless of species. Reported values for mercury range from 10 ml/g [10] to 408 ml/g [11]. For a Freundlich model, the partition coefficients range from 19 to 299 ml/g, with the Freundlich exponent ranging from 0.5 to 2.2.[2] Although there is considerable variability in these results, they suggest that typical values in soil-water systems are between 10 and 500 ml/g and are certainly less than 1000 ml/g. These values are based on laboratory experiments under conditions typically not representative of ambient mercury concentrations.

Values derived from measurement under real-world conditions are naturally most appropriate. A determination of the soil-water partition coefficient requires a measurement of speciated soil mercury concentration and the speciated soil water dissolved phase mercury concentration. Measurements of the speciated soil concentrations are typically reported in the literature, but speciated soil water dissolved phase mercury concentration are considerably harder to find.

Data on the benthic sediment-water K_d that are based on measurements under realistic conditions are scarce as well. Wiener et al.[12] studied mercury partitioning at Little Rock Lake, a clear water seepage lake in north-central Wisconsin. The mercury concentrations in the surficial sediment ranged from 10 to about 170 ng/g (dry weight). Assuming that the reactive mercury values reported represent dissolved Hg^{2+}, the dissolved water concentrations range from 0.29 to 0.59 ng/L. Using these values results in a range for the benthic sediment partition coefficients for this site from 16950 ml/g to 586200 ml/g. There appears to be at least as much uncertainty in the benthic K_d as the soil-water K_d.

In contrast, a number of values for the suspended-sediment K_d have been determined. These are for the most part based on measured data under realistic conditions, unlike the values for the soil-water and benthic-sediment partition coefficients (Appendix J). These values range from 10^3 ml/g[13] to 10^6 ml/g.[14]

Because of the need for realistic partition coefficients in the exposure assessment, several calibrations were performed and are described here. Studies were found that include data on the movement and partitioning of mercury in and around watersheds. The type of information available varies among these studies and can include soil, sediment, surface water, soil water, and runoff water mercury concentrations, as well as lake outflow, lake inflow (runoff and erosion) and sedimentation rates for mercury.

The main purposes of these calibrations are twofold: 1) to determine values for the soil-water partition coefficients and the benthic sediment-water partition coefficients that result in mercury to water transport and partitioning behavior that are in reasonable agreement with available mercury transport data; and 2) to confirm that the IEM2 model is capable of correctly predicting the complex process of mercury movement and partitioning in the soil and water environments with the use of realistic parameters. This is one of the most critical aspects of mercury behavior addressed in the exposure assessment.

The modelling results were not as sensitive to the suspended-sediment partition coefficients as the benthic sediment-water coefficients in predicting mercury behavior in the lakes considered in the calibrations, due to the clarity of the water bodies considered. There is also enough reliable information on the suspended-sediment partition coefficients to believe that the mid-point from measured values should reasonably predict mercury partitioning in this study (see Appendix J). Thus, the suspended-sediment partition coefficients were not used in the calibration process.

It is stressed that these calibrations are intended to be only semi-quantitative, with the degree of accuracy of the calibration determined qualitatively; the calibrated results are only to be "consistent with" available data. There are doubtless other possible calibrations. This problem is an intractable aspect of almost any calibration and is discussed in section L.4.

L.3 CALIBRATIONS

L.3.1 Description of Calibration Approach

For the model application described in chapter 7, the models were run in a "forward" fashion: the input parameters were specified, and the output values (e.g., media concentrations) were obtained. In the calibration effort described here, this process was reversed; the input parameters were modified so that certain output values were within specific ranges. The values for the partition coefficients that yielded acceptable output values were then used as representative values in the main report when the models were run in the "forward" fashion.

The watershed model used, IEM2, uses atmospheric chemical loads and perform to mass balances on a watershed soil element and a surface water element. This mass balance tracks all mercury specified in the background soil concentrations and the mercury deposition rates. The mass balances are performed for total mercury, which is assumed to speciate into three

components: Hg^0, Hg^{2+}, and methylmercury. The fraction of mercury in each of these components is specified for the soil and the surface water elements. Loadings and chemical properties are given for the individual mercury components, and the overall mercury transport and loss rates are calculated by the model. IEM2 first performs a terrestrial mass balance to obtain mercury concentrations in watershed soils. IEM2 next performs an aquatic mass balance driven by direct atmospheric deposition along with runoff and erosion fluxes (i.e., amount of the chemical transported from soil element to surface water element per unit time) from watershed soils. The water body output values of the IEM2 model are calculated based on the assumption that steady-state conditions (i.e., fluxes out of surface water element are equal to fluxes into element so that concentrations are independent of time) have been achieved.

There are two main assumptions made in these calibrations. The first is that the measured surface water concentrations are due to the estimated (or reported) fluxes to the water body. Other processes of mercury influx and outflux not considered here are assumed negligible. If these are significant, it could significantly modify the necessary calibrated values. Second, it is assumed that conditions are approximately at steady-state.

The calibrations were generally performed in three steps, depending on the particular data available. First the soil-water partition coefficients were adjusted until the soil-water concentration was within the target soil-water concentration range. Then the runoff/erosion parameters were adjusted until the fluxes to the water body were within the target range of values. Finally, the benthic sediment partition coefficients were adjusted until the water concentrations and benthic sediment concentrations were both within acceptable range (increasing the benthic sediment partition coefficient reduces the water concentration and increases the benthic sediment concentration).

L.3.2 Parameters Constant for All Calibrations

Table L-1 shows the values for parameters that were the same for all calibrations.

L.3.3 Calibration Results

L.3.3.1 Swedish Composite Lake. In a series of papers, Meili investigated the mercury cycle through Swedish boreal forest watersheds and lakes.[15,16,17] The data in these papers, which consist of a combination of summary values for Swedish lakes and predicted values, were used to construct a model

Table L-1. Parameters Constant for All Calibrations

Chemical-Dependent Parameters	Hg^0	Hg^{2+}	Methylmercury
Molecular weight (g/mole)	201	201	216
Henry's Constant (atm-m^3/mole)	$7.3x10^{-3}$	$7.3x10^{-10}$	$4.7x10^{-7}$
Soil-water partition coefficient (ml/g)	130[a]	Calibrated	Calibrated
Benthic-sediment partition coefficient	130[a]	Calibrated	Calibrated
Suspended-sediment partition coefficient	1[a]	$9.50x10^4$ [b]	$6.50x10^5$ [b]
Equilibrium fraction in soil	*0*	0.98	0.02
Equilibrium fraction in water	0.02	0.83	0.15
Constants	**Value**	**Comment**	
Ideal gas constant (m-atm/mole-K)	$8.21x10^{-5}$	Used for volatilization from soil and surface water	
Air density (g/cm^3)	$1.19x10^{-3}$	Used for water body calculations	
Solids density (kg/L = g/cm^3)	2.70	Used to estimate speciation in waterbody and concentration in benthos	
Drag coefficient	$1.10x10^{-3}$	Used for water body volatilization calculations	
Von Karman's Coefficient	$7.40x10^{-1}$	Used for water body volatilization calculations	
Dimensionless boundary thickness	4.00	Used for water body volatilization calculations	
Run Options	**Value**	**Comment**	
Water body type	1	Stagnant ponds, lakes	
Suspended solids options switch	0	Use given sediment deposition rate to calculate suspended solids concentration	
Equilibrium speciation option	1	Species are tied together in equilibrium	

[a] Because it is assumed that the equilibrium fraction of elemental mercury in soil is 0 (see Appendix J), the soil-water partition coefficient does not affect the calculations. Similarly, due to the low assumed equilibrium fraction in surface water the other partition coefficients for elemental mercury does not significantly affect calculations and so it is not varied from the value shown here.

[b] The suspended sediment partition coefficients were not as influential on the results used in the calibrations here, based on the initial sensitivity analyses. For this reason, they were assigned the values given in Appendix J. These values are based on these studies: Moore and Ramamodoray,[13] and Robinson and Shuman.[18]

Swedish lake, from which many of the necessary IEM2 parameters could be approximated. The output values in Meili[15,17] that were used as target values in the calibrations are shown in Table L-2. Table L-3 shows the input values, excluding the partition coefficients, used in the IEM2 model for the calibrations.

Because there is considerable uncertainty about the degree of volatilization from the surface water body, two separate calibrations were performed. In the first, volatilization from the surface water body was considered as a loss process. In the second, no volatilization was assumed. The latter is consistent with assumptions in Meili et al.[17] where volatilization was not considered due to uncertainty. The calibration of the soil-water partition coefficients is the same in both calibrations because it is not affected byloss processes from the surface water body.

The first step was to calibrate the soil-water partition coefficients so that the predicted total mercury soil-water concentration was within range of the target values (3.75 to 5 ng/l). Then the erosion parameters were modified so that the fluxes to the water body from runoff and erosion agreed. In the IEM2 model, the various erosion parameters (sediment delivery ratio, pollutant enrichment factor, erosivity factor, erodability factor, topographic factor, cover management factor) are multiplied together to obtain an estimate of the annual amount of soil erosion; thus, there are many different possible combinations of various values for these parameters that can yield the same general erosion rate. Finally, the benthic sediment partition coefficients were modified so that the predicted surface water and benthic sediment concentrations were consistent with the values reported in Meili et al.[16] The results of both calibrations are shown in Table L-4.

Although there is general agreement with the target outfluxes, the high benthic sediment concentration suggests that the assumption of no significant volatilization from the surface water may not be true, unless there are processes not addressed here that serve to prevent the predicted high benthic sediment concentrations from occurring.

In summary, using the available data on 88 lakes in Sweden, the IEM2 watershed model was calibrated using these available data. The calibrated values of the benthic-sediment partition coefficients depend on the significance of the volatilization pathway from the water body. The calibrated benthic-sediment

Table L-2. Target Values for Swedish Lake Calibration

Output Parameter	Value	Comment
Mercury Concentration in lake (ng/L)	2-3	For clearwater lake; Table I of Meili[19]
Runoff load of mercury to lake, ug/m^2/yr or g/yr[a]	4-8 Central Sweden, 6-11 Southern Sweden	
Mercury Concentration in Runoff (ng/L)	3.7	Based on mercury/Carbon ratio of 0.25 ug/g in runoff water and organic carbon concentration of 15 g/m^3.[20]
Outflow of mercury from lake, ug/m^2/yr or g/yr[a]	2-5 Central Sweden, 3-7 Southern Sweden	
Sedimentation of mercury in lake, ug/m^2/yr or g/yr[a]	7-20 Central Sweden, 10-30 Southern Sweden	
Ratio of runoff load and direct deposition	0.6	For clearwater lakes Meili[21]
Surface sediment concentration, ng/g	150-460	Range from Table I in Meili et al.[22] and p.441 for characteristics of 25 study lakes in 1986
Mass balance of Loss Processes	% Sedimentation	% Outflow
Central Sweden	80	20
Southern Sweden	79	21

[a] Fluxes are given per unit lake surface area.[23] Using the assumed surface area of 1 km^2 for a typical lake gives an estimate of the flux in grams per year.

partition coefficients were found to agree with the overall range reported in Wiener et al..[12]

L.3.3.2 Fen at Tivedan National Park, Sweden. Aastrup et al.[26], describe mercury transport within a small segment (6 percent) of a larger watershed area. The results presented in this paper were used for calibrating the parameters involved in estimating the runoff of mercury from the watershed.

The study area was described as a minicatchment watershed consisting of a small forested catchment in the Tivedan National

Table L-3. Site-Specific Parameter Values Used in Swedish Composite Lake Calibrations (Excluding Partition Coefficients)

Parameter	Value	Comment
Mercury deposition rate (ug/m^2/yr)	12.5	Average of values for Central and Southern Sweden (Range 7-25)
Irrigation Rate (cm/yr)	0	Assumed negligible
Time of Concentration (years)	1	Fluxes estimated in Meili et al. are presented on a yearly basis
Average air temperature (C)	4	Based on mean air temperature if 1-7[24]
Average water temperature	4	Assumed to be the same as average air temperature
Average annual precipitation (cm/yr)	75	Average of central and southern Sweden[21]
Average annual runoff (cm/yr)	40	Annual area-specific runoff water discharge for central and southern Sweden[21]
Average annual evapotranspiration (cm/yr)	17.5	Rough estimate (this is only used for estimating leaching loss rate)
Average wind speed (m/s)	3.5	Rough estimate (this is only used for volatilization)
Soil Erosion Parameters		
Practice Support Factor	1	Cover management factor is used to incorporate this.
Sediment delivery ratio (unitless)	0.2	Typical value
Pollutant enrichment factor (unitless)	2	Typical value
Erosivity factor (/yr)	175	Rough estimate based on U.S. values (values range from 100 to 300)
Erodability factor (tons/acre)	0.28	Typical value (U.S. values range from 0.28 to 0.3)
Topographic factor (unitless)	2.5	Value for a location in the upper northeast, which is assumed to be roughly similar to the Swedish area
Cover management factor (unitless)	0.006	Forest value
Watershed Parameters		
Watershed area (km^2)	4	Mean of lakes in Meili et al.[15,17]
Bulk soil density (g/cm^3)	1.4	Typical value.
Watershed soil mixing depth (cm)	1	Value suggested for non-tilled soil[3]
Soil moisture content (unitless)	0.3	Typical value
Background soil concentration (ng/g)	100	Average of mean reported in Jensen and Jensen[25] for Swedish soils of 76 ng/g and weighted average for soil layers in Swedish soil of 125 ng/g[26]

Table L-3. Continued

Parameter	Value	Comment
Water body parameters		
Sediment deposition rate (m/day)	0.5	Rough mean of typical values[27]
Benthic sediment concentration (kg/L)	1	Rough mean of typical values[27]
Upper benthic depth (m)	0.02	Typical value[27]
Water body surface area (km^2)	1	Value for clearwater lake in Meili[28]
Water column volume (m^3)	$6x10^6$	Based on area of 1 km^2, depth of 6 m[21]
Long term dilution flow (m^3/yr)	$2x10^6$	Based on volume of lake and mean water residence time of 3 years[21]

Table L-4. Summary of Composite Swedish Lake Calibrations

Calibration Parameters	Volatilization from Surface Water Assumed	No Volatilization from Surface Water Assumed	Target Calibration Value
Soil-Water partition coefficients for Hg^{2+} and methylmercury (ml/g)	22500	22500	NA
Topographic factor (unitless)	0.8	0.8	NA
Pollutant enrichment factor (unitless)	1.0	1.0	NA
Sediment delivery ratio (unitless)	0.10	0.10	NA
Soil erosivity factor (kg/km^2-yr)	125	125	NA
Benthic Sediment Partition Coefficients for Hg^{2+} and methylmercury (ml/g)	155000	350000	NA
Output Parameters			
Total mercury Soil Concentration after one year	101	101	100
Total mercury Soil-Water Concentration (ng/l)	4.47	4.47	3.75 Central 5 Southern
Total Load to water body from runoff/erosion (g/yr)	8.53	8.53	4-8 Central 6-11 Southern

Table L-4. Continued

Calibration Parameters	Volatilization from Surface Water Assumed	No Volatilization from Surface Water Assumed	Target Calibration Value
% Erosion	18	18	NA
% Runoff	82	82	NA
Steady-state Total Water Column Concentration (ng/l)	3.07	3.00	2-3
Steady-state outflows from water body (g/yr)			
Volatilization	8.72 (40%)	0 (0%)	NA
Sedimentation	6.79 (32%)	15 (71 %)	7-20 Central 10-30 Southern
Dilution flow	6.12 (28%)	6 (29%)	2-5 Central 3-7 Southern
Concentration in Benthos (ng/g)	460	1020	150-460

Park located in southern Sweden. The mercury budget was estimated for a till formation on a slope, making up a funnel-shaped minicatchment of 0.014 km^2. This area drains into a fen (low land covered wholly or partly with water unless artificially drained). Elevation in the minicatchment ranges from approximately 1.5 m at the point farthest from the fen to 0 m at the fen itself. The catchment was divided into three areas: an upper level with shallow soils, an intermediate area, and a waterlogged area.

Mercury concentrations were reported for different soil layers. It was noted that 41 percent of the total mercury estimated (8.8 kg/km^2) was found in the highest humic layer. Table L-5 shows the total mercury found in each soil layer analyzed.

Also reported were estimates of mercury concentrations in soilwater and groundwater. There was a large amount of variation in the measured values. The values included in Table L-6 generally have a standard deviation as large as the mean, even for those with as many as 30 samples.

The soilwater mercury concentration calculated in the IEM2 model is assumed to be the dissolved mercury, and hence does not consist of any particulate-bound mercury. For the purpose of the calibration effort, it was decided that this calculated quantity would be bounded above by the values for Hg-II (sum of reactive and unreactive mercury) reported in Aastrup et al. and shown in Table L-6. These values, estimated in accordance with the standard Swedish sampling program (Chapter 2 in Lindquist et al.[29]), are the sum of the dissolved Hg^{2+} plus some reactive particle associations and some humic matter associations which may fall under particulate mercury (Hg-IIa and Hg-IIb). The difference between total mercury concentration (Hg-tot) and Hg-II was assumed to be Hg^{2+} strongly bound to particulates (i.e., not dissolved).

The fluxes out of the minicatchment area were estimated from Figure 4 (page 165) in Aastrup et al.[26] (as well as Figure 2 in Johansson et al.[30]). The flux to the fen from the top 20 cm of soil is 2.6 $g/km^2/yr$. Because the fluxes are normalized to the minicatchment area, multiplying by the area (0.014 km^2) yields a total flux of 0.0364 g/yr. Similarly, for the top 8 cm (called the mor layer, which consists of humic matter distinct from mineral soil), the flux is 1.5 $g/km^2/yr$, corresponding to a total flux of 0.02 g/yr.

Table L-5. Soil Layers and mercury Concentrations Reported in Aastrup et al.[10]

Soil Layer	Assumed Thickness (cm)	Mercury Content (ng/g)	Total Mercury (g)
Mor	8	250	50
E-Horizon	6	27	9
upper B-horizon	6	58	34
lower B-horizon	NA	23	23
C-horizon	NA	6	8
Total		NA	124

Two separate calibrations were performed. In the first, the top 20 cm was treated as a single layer, while in the second only the mor layer was used. The parameters, their values, and the rationale for their selection are shown in Table L-7. Table L-8 shows the results for the both calibrations.

Despite the low values used for the default soil erosion parameters, the loss due to erosion becomes significant when the effective partition coefficient is increased. Whether this was actually true at the Tividen site is not certain. Nevertheless, the calibration for the mor layer alone provides an upper bound for the partition coefficient, as the predicted soil-water concentration lies at the lower end of the observed range.

L.3.3.3 Composite Minnesota Lake. These calibrations are based on the Minnesota lake characterization presented in Sorensen et al.[31] based on 80 lake watersheds. Mercury concentrations in precipitation, lake water and sediment were measured and analyzed along with watershed data for 80 lake watersheds in the study region of northeastern Minnesota. The summary values are shown in Table L-9. Median values were used when possible because a number of large watersheds/ waterbodies biased the mean values. The values used in the IEM2 model are shown in Table L-10.

The median value for evaporation reported in Sorensen et al.[31] was 47.6; however, this results in a negative net leach rate since leach rate is proportional to *Precipitation + Irrigation - Runoff - Evapotranspiration*. For this reason, the evapotranspiration was set so that leach rate is 0. This has

Table L-6. Soilwater Mercury Concentrations Reported in Aastrup et al.[26]

Soil Layer	Total Mercury (ng/L)				Hg-II[a] (ng/L)				Hg-IIa[b] (ng/L)			
	Mean	Std.Dev.	Minimum	Maximum	Mean	Std.Dev.	Minimum	Maximum	Mean	Std.Dev.	Minimum	Maximum
0-8 cm	11.9	12.7	1.9	39.6	4.1	3.7	0.9	10.3	1.4	1.1	0.5	3.4
8-20 cm	13.6	13.7	1.9	48.4	4.3	4.8	0.5	20.2	1.5	1.1	0	4.2
20-50 cm	15.1	12.9	0.6	52.1	4.1	4.6	0.1	19.5	1.3	0.8	0	3.8
50-100 cm	9.9	8.8	0.7	39.2	3.3	4.9	0	27.6	1.1	0.9	0	3.8
100-165 cm	6.8	3.7	1.5	12.5	0.9	0.5	0.3	1.7	0.5	0.4	0	1.4

[a] Hg-II - Reactive and non-reactive mercury fraction of total mercury.
[b] Hg-IIa - Reactive, acid labile, inorganic fraction of total mercury.

Table L-7. Model Parameter Values Estimated from Aastrup et al.[26]

Parameter	Value	Comment
Mercury Deposition Rate (ug/m^2/yr)	20	Value assumed in Aastrup et al.[26]
Approximate Estimated background soil concentration (ng/g) in soil layer of consideration	125 for Combined mor, E and upper B 250 for mor alone	Weighted average soil concentration for mor, E-horizon, and upper B-horizon soil layers.
Time period of consideration (yr)	1.3	16 months, which was the length of the study period in Aastrup et al.[26]
Mixing Depth (cm)	20 cm for combined mor, E and upper B 8 cm for mor alone	Depths reported in Aastrup et al[26]
Estimated precipitation (cm/yr)	120	Estimated from Figure 3, page 163 in Aastrup et al.[32]
Estimated runoff (cm/yr)	58.7 for Mor, E and upper B 37.7 for mor alone	Figure 3, page 163 in Aastrup et al[32]
Evapotranspiration (cm/yr)	34 for mor, E and upper B 38.5 for mor alone	Value set so that precipitation minus runoff minus evapotranspiration is equal to estimated leach rate from soil layer considered (Figure 3 in Aastrup et al.[26]. Leach rate is 26.7 cm/yr from top 20 cm, 42.8 cm/yr from top 8 cm (mor layer).
Average Air Temperature (C)	4	Estimate of average Swedish temperatures[15]
Average Wind speed (m/s)	3.5	Rough estimate
Bulk Soil Density (g/cm^3)	1.4	There is usually little variation in this parameter across the U.S.; Swedish soils assumed to be similar
Soil Moisture Content	0.30	Rough midpoint of typical values; there is usually little variation across U.S. soils.
Erosivity factor (/yr)	175	Rough average of typical values.
Erodability factor (tons/acre)	0.28	There was little variation for U.S. Sites (0.28-0.30).
Topographic factor (unitless)	0.19	Computed using method of Arnold et al.[33] using slope of area
Cover management factor (unitless)	0.006	Typical forest value

Table L-8. Calibrated Values for Soil-Water Partition Coefficients for Combined Soil Layers and Mor Layer Alone

Parameter	Combined Mor, E and Upper B Horizon		Mor Soil Layer Alone	
	Value	Target Calibration Value	Value	Target Calibration Value
Soil-Water Partition Coefficient (ml/g) for Hg^{2+} and methylmercury	38000	NA	250,000	NA
Total Mercury Soil Concentration (ng/g)	125	125	250	250
Total Mercury Soil-Water Concentration (ng/L)	3.29	0.5 - 20.2 (mean 4.2)	1	0.9 - 10.3 (mean 4.1)
Total Load to Water body from Catchment Region Considered (g/yr)	0.036	0.036	0.02	0.02
% Erosion	24.4	NA	77	NA
% Runoff	75.6	NA	23	NA

Table L-9. Parameter Values for 80 Minnesota Lakes Reported in Sorensen et al.[31]

Parameter	Median	Range/Comment
Lake concentration (ng/L)	2.30	0.90-7.00
Total organic carbon as C in surface water (mg/L)	6.76	3.53-14.3
Annual Direct deposition onto lake (ug/m^2/yr)	12.7	10.4-15.4
Deposition immediate ug/m^2 (calculated deposition falling directly on lake surface plus calculated runoff from immediate watershed (assuming 100% mercury transport to lake)	24.8	14.8-58.4
Indirect/Direct Deposition to Water Body	0.95 (calculated using median values, but not necessarily the median)	This is a value calculated here by assuming that the difference between the "deposition immediate" and the direct deposition onto the lake is the flux from the immediate watershed (which turns out to be 12.1 ug/m^2/yr). Dividing this by the direct deposition gives this ratio.
Median surface sediment concentration (ng/g)	154	34-753
Lake surface area (Ha)	328	24-89400
Immediate watershed area (Ha)	650	55-168000
Site elevation (m)	432	388-587
Topographic high immediate (m)	476	378-664
Annual precipitation (m/yr)	0.665	0.560-0.762
Annual evaporation, land (m/yr)	0.476	0.446-0.506
Annual runoff (m/yr)	0.196	0.103-0.315
Lake renewal time (yr)	49.1	5.85-202
Total renewal time (yr)	2.18	0.01-45.4
Mean depth (m)	5.70	1.08-29.0
Lake volume (m^3)	$1.5x10^7$	$4.35x10^5$ - $5.47x10^9$
% Forest	83	46.2-94.7
% Water	16.2	4.10-38.5

Table L-10. Parameter Values Used in Composite Minnesota Lake Calibrations (Excluding Partition Coefficients)

Parameter	Value	Comment
Mercury deposition rate (ug/m^2/yr)	12.7	Median of values reported in Table III of Sorensen et al,[34]
Irrigation Rate (cm/yr)	0	Assume it is negligible
Time of Concentration (years)	1	Used only in calculating soil concentrations.
Average air temperature (C)	5	Mean for Minnesota
Average water temperature	5	Assumed to be the same as average air temperature
Average annual precipitation (cm/yr)	66.5	Median of values reported in Table III of Sorensen et. al.[34]
Average annual runoff (cm/yr)	19.6	Median of values reported in Table III of Sorensen et. al.[34]
Average annual evapotranspiration (cm/yr)	46.9	Set to precipitation *minus* runoff
Average wind speed (m/s)	3.5[a]	Rough estimate; this is only used for volatilization.
Soil Erosion Parameters		
Practice Support Factor	1	Cover management factor is used to incorporate this.
Sediment delivery ratio (unitless)	0.2	Typical value
Pollutant enrichment factor (unitless)	2	Typical value
Erosivity factor (/yr)	175	Rough estimate based on U.S. values; values range from 100 to 300
Erodability factor (tons/acre)	0.28	Typical value (U.S. values range from 0.28 to 0.3)
Topographic factor (unitless)	2.45	This is actually a calibrated value so that indirect/direct ratio matched a value consistent with the values reported in Sorensen et al.[31]
Cover management factor (unitless)	0.01	Forest value
Watershed Parameters		
Watershed area (km^2)	6.5	Based on median value of 650 hectares reported in Table III in Sorensen et al.[31]
Bulk soil density (g/cm^3)	1.4	Typical value

Table L-10. Continued

Parameter	Value	Comment
Watershed soil mixing depth (cm)	1	Standard value. Variations in the mixing depth will contribute to the overall uncertainty, but the value is deemed appropriate given the qualitative nature of the current calibration efforts.
Soil moisture content (unitless)	0.3	Typical value (usually relatively little variation)
Background soil concentration (ng/g)	87	Average of values reported in Sorensen et al.;[35] values ranged from 12 to 220 ng/g.
Water body parameters		
Sediment deposition rate (m/day)	0.5	Rough mean of typical values[27]
Benthic sediment concentration (kg/L)	1	Rough mean of typical values[27]
Upper benthic depth (m)	0.02	Typical value[27]
Water body surface area (km^2)	3.28	Based on median value of 328 hectares reported in Table III in Sorensen et al.[31]
Water column volume (m^3)	$1.5x10^7$	Median value reported in Table III in Sorensen et al.[31]
Long term dilution flow (m^3/yr)	$6.88x10^6$	Based on volume of lake and median total renewal time of 2.18 years (Table III of Sorensen et al.[31]).

[a] The wind speed was also set to zero for a calibration run in which no volatilization occurs.

little practical affect on predicted values because the background soil concentration is not subject to these loss processes.

Although no values are reported for the soil-water concentrations in Sorensen et al.[31] the values reported in Aastrup et al.[26] for Swedish soil indicate that they may be approximated by the surface water concentration. The target value for this effort was the median of the surface water concentrations reported in Sorensen et al.[31] of 2.3 ng/l.

After the soilwater concentrations were calibrated, the topographic factor, used in estimating soil erosion, was set so that the indirect/direct ratio was consistent with that estimated from Sorensen et al..[31]

As in the calibrations performed for the composite Swedish lake, two separate calibrations were performed, one with and one without volatilization from the surface water body. The results of the calibrations are shown in Table L-11. These two calibrations provide a range for the benthic sediment concentrations.

Despite the uncertainties introduced by using a composite lake, the results are in general agreement with previous calibrations. As for the composite Swedish lake, the benthic-sediment partition coefficients had to be substantially increased if volatilization from the surface water body was not considered as a loss process.

L.4 LIMITATIONS AND UNCERTAINTIES

The calibrated partition coefficients derived here are intended to represent long-term retention properties of the watershed systems for which they were derived. An obvious limitation with any calibration effort is that there may be other calibrations that also give the same qualitative agreement but have significantly different values for the calibrated parameters. The likelihood of such alternative calibrations is increased when large data gaps exist. Because the calibrations were performed in a sequence of steps, these possibilities are discussed in turn for each step in the calibration process used here.

The soil-to-water partition coefficient calibrations seem the most defensible because there is relatively little involved in calculating soilwater concentrations. Furthermore, only a relatively simple argument is required in order to suggest that

Table L-11. Results for Composite Minnesota Lake Calibrations

Parameter	Volatilization from Surface Water Assumed	No Volatilization from Surface Water Assumed	Target Calibration Value
Effective Soil-Water Partition Coefficient (ml/g) for Hg^{2+} and methylmercury	38200	38200	NA
Effective Benthic Sediment Partition Coefficient (ml/g) for Hg^{2+} and Methylmercury	100500	149600	NA
Total Mercury Soil Concentration after one year (ng/g)	87.8	87.8	87
Total Mercury Soilwater Concentration (ng/L)	2.3	2.3	2.30
Indirect/Direct Ratio	0.95	0.95	0.95
Total Load to Water body from Catchment Region Considered (g/yr)	39.7	39.7	NA
% Erosion	92.36	92.36	NA
% Runoff	7.64	7.64	NA
Total Water column concentration (ng/L)	2.3	2.3	2.3
Steady-state outflows (g/yr)			
Volatilization	21.4 (26%)	0	
Sedimentation	44.0 (54%)	65.4 (80%)	
Dilution	15.7 (20%)	15.7 (20%)	
Total Mercury Concentration in Benthos (ng/g)	214	318	154 (Range 34-753)

the typically reported values for the mercury partition coefficients in soil-water systems are questionable. In the IEM2 model, the total concentration of each mercury component in soil is assumed to reach equilibrium between its particulate and aqueous phases. The concentration of species *i* dissolved in pore water is given by the following equation:

$$C_{ds,i} = \frac{Sc_i \, BD}{\theta_s + Kd_{s,i} \, BD} \qquad (1)$$

The concentration in particulate phase is defined in equation (2).

$$C_{ps,i} = C_{ds,i}\, Kd_{s,i} = \frac{Sc_i\, Kd_{s,i}\, BD}{\theta_s + Kd_{s,i}\, BD} \qquad (2)$$

where:

Sc_i	=	total soil concentration of component "i" (µg/g)
θ_s	=	volumetric soil water content (L_{water}/L)
$Kd_{s,i}$	=	soil/water partition coefficient for component "i" (L/kg = ml/g)
BD	=	soil bulk density (g/cm^3)
$C_{st,i}$	=	total soil concentration of component "i" (mg/L)
$C_{ds,i}$	=	concentration of "i" dissolved in pore water (mg/L_{water})
$C_{ps,i}$	=	concentration of "i" in particulate phase (mg/kg)

The total soil concentration in ug/g is given by this equation.

$$SC_i = \left(\frac{\theta_s}{BD} + Kd_{s,i} \right) C_{ds,i} \qquad (3)$$

The value for the partition coefficient to achieve a given soil-water concentration is , thus,

$$Kd_{s,i} = \frac{SC_i}{C_{ds,i}} - \frac{\theta_s}{BD} \qquad (4)$$

If the mercury soil-water concentrations reported in Meili et al.[16] are accurate, then these values indicate that the mercury in the soil-water represents only a small fraction of the total mercury per volume. For example, if a typical total soil concentration of 100 ng/g (0.10 ug/g) were completely dissolved in a liter of water, and assuming a typical soil density of 1.4 g/cm^3, the resulting water concentration would be 100000 ng/L (100 ug/L). This is to be compared to the reported soil-water concentrations in the range of 1-10 ng/L. Thus, at most about 0.01 percent can be dissolved to achieve the values observed, and the rest must be bound to particulates in the soil matrix. Even assuming a volumetric soil water content of 1, using equation (4) above the partition coefficient must be about 10^4 ml/g in order to have a dissolved water concentration of 10 ng/L. Achieving soil-water concentrations of 2 ng/L requires a partition coefficient of slightly less than $5x10^4$ ml/g.

Because adequate speciation estimates were not available, there is uncertainty in the values for the partition coefficients for methylmercury. For the purpose of this effort they were assumed to be the same as for Hg^{2+}. In sediment, values between about 2 percent and 9 percent methylmercury have been reported[36] for sand, silt/woodchips and woodchip sediments. Cappon[37] found that percent methylmercury for nonamended soils was about 2.6 percent (this is an upper bound on values from unpublished data reported by several authors as cited in *Water, Air and Soil Pollution* 1991[38]). If the speciation in soil-water is similar to that sorbed onto soil particles, then the partition coefficients for methylmercury would be similar to those for Hg^{2+}. Although there is considerable variability in the percent of total mercury that is methylmercury in surface waters, the latest estimates (Bloom et al.[14]; Watras and Bloom[39] range from 5 to 25 percent methylmercury. If the fraction in soil water is slightly larger than that sorbed onto soil particles, as the data would indicate, then the required calibrated partition coefficient for methylmercury would be correspondingly lower than that for Hg^{2+} derived above. This is because the fraction dissolved for methylmercury would be higher than that for Hg^{2+}. However, for the purpose of this calibration effort, it was felt that the data were not adequate to justify separate calibrations for both Hg^{2+} and methylmercury. The result of this assumption is that the amount of methylmercury in the flux to the water body from runoff may be underestimated and amount in soil erosion overestimated.

Calculation of the flux to the water body boils down to determining the a set of adequate erosion/runoff parameters. The total load due to runoff and erosion, denoted here by $L_{E/R,i}$ (g/yr), is given by equation (5).

$$L_{R/E,i} = WA_L \left(R\ C_{ds,i}\ 10^{-2} + X_e\ SD\ ER\ C_{ps,i}\ 10^{-3} \right. \quad \textbf{(5)}$$

where:

$L_{E/R,i}$	=	load to water body from surface runoff and soil erosion for component *i* (g/yr)
WA_L	=	watershed surface area (m^2)
R	=	average annual runoff (cm/yr)
$C_{ds,i}$	=	concentration of "i" dissolved in pore water (mg/L_{water})
X_e	=	unit soil loss ($kg/m^2/yr$)
SD	=	sediment delivery ratio (unitless)
ER	=	contaminant enrichment ratio (unitless)
$C_{ps,i}$	=	concentration of "i" in particulate phase (mg/kg)

The unit soil loss rate is given by equation (6).

$$X_e = R\_\ K\ LS\ C\ PS\ \frac{907.18}{0.00407} \quad (6)$$

where

R_	=	soil erosivity factor (kg/km^2/yr)
K	=	soil erodability factor (tons/acre)
LS	=	topographic factor (unitless)
C	=	cover management factor (unitless)
PS	=	support practice factor (unitless)

Values for the site-specific average annual runoff were available for the sites considered. Values for the soil erosion parameters (R_, K, LS, C, PS, SD, ER) were not available. This was further complicated by the composite nature of the sites considered for the calibration efforts. For this reason, the erosion parameters were calibrated so that the ultimate total fluxes to the water body were consistent with measured data.

The calibrated benthic sediment partition coefficients are consistent with values reported elsewhere (e.g., Wiener et al.[12]). Because there is apparently considerable uncertainty as to the degree of volatilization from surface water bodies, two different calibrations were performed, when possible. In the first the volatilization was assumed to contribute to the total loss rate from the surface water using a generic set of the relevant parameters (e.g., equilibrium speciation of the mercury species in water,wind speed). Another calibration was also performed assuming that volatilization was negligible. The differences in the calibrated partition coefficients are well within the range of the usual variation of the partition coefficients themselves. Calibration without volatilization requires that sedimentation play a larger role as a loss process. The higher benthic sediment partition coefficients needed to achieve this effect, while resulting in high benthic sediment concentrations, provide upper bounds on the partition coefficients for the site under consideration.

L.5 CONCLUSIONS

Calibrations of the IEM2 model were performed using three data sets, with the partition coefficients serving as the primary calibration parameters. Due to uncertainty as to the exact degree of volatilization from the surface water body, two separate calibrations were performed with and without volatilization. The calibrated partition coefficients are shown in Table L-12.

Table L-12. Summary of Calibration Results

	Composite Swedish Lake		Fen in Tivedan Park, Sweden		Composite Minnesota Lake		Geometric Mean of Calibrated Values
	Volatilization Included	Volatilization not Included	Combined Soil Layers	Top layer alone	Volatilization Included	Volatilization not Included	
Soil-Water Partition Coefficients for Hg^{2+} and Methylmercury (ml/g)	$2.3x10^4$	$2.3x10^4$	$3.8x10^4$	$2.5 x10^5$	$3.8x10^4$	$3.8x10^4$	$5.37x10^4$
Benthic Sediment Partition Coefficients for Hg^{2+} and Methylmercury (ml/g)	$1.5x10^5$	$2.7x10^5$	N/A	N/A	$1.0x10^5$	$1.5x10^5$	$1.57x10^5$

The significance of volatilization as a mercury loss process from water bodies is currently unclear. The results derived here show that the assumption that volatilization is negligible, while it can be modelled by increasing the benthic sediment partition coefficients, results in benthic sediment concentrations that are near or above the upper end of the measured values. This suggests that volatilization may in fact be nonnegligible.

Despite acknowledged uncertainties and limitations, the results derived here support the use of soil-to-water partition coefficients that are higher than previously published values, when the equilibrium assumption is considered appropriate. The effective partition coefficients (soil and benthic) determined from these calibrations are similar to values found for suspended-sediment partition coefficients, for which much reliable data are available. Additionally, it was confirmed that the IEM2 model could predict mercury movement and partitioning in the soil and water environments with the use of realistic modeling parameters. Thus, we have established that applying this part of the IEM2 model using partition coefficients representative of those in Table L-12 can be expected to result in reasonable predictions of mercury movement and behavior in and out of watersheds.

That soil-water partition coefficients larger than previously published values would be necessary is consistent with the growing concern that watershed soils may be serving as a significant repository for mercury. This repository can potentially act as a source of mercury to water bodies long after enhanced mercury deposition has occurred.

L.6 REFERENCES

1. Dooley, J. H. Natural Sources of Mercury in the Kirkwood-Cohansey Aquifer System of the New Jersey Coastal Plain. New Jersey Geological Survey, Report 27. 1992.

2. Buchter, B., B. Davidoff, M.C. Amacher, C. Hinz, I.K. Iskandar, and H.M. Selim. Correlation of Freundlich K_d and retention parameters with soils and elements. *Soil Science* 148:370-379. 1989.

3. U.S. EPA. External Review Draft addendum to Methodology for Assessing Health Risks Associated with Indirect Exposure to Combustor Emissions. EPA/600-93/003 November 1993.

4. Schuster, E. The Behavior of Mercury in the Soil with Special Emphasis on Complexations and Adsorption Processes – a Review of the Literature. *Water Air Soil Pollution.* Vol. 56:(667-680) 1991.

5. Nriagu, J.O. The Biogeochemistry of Mercury in the Environment. Elsevier/North Holland. Biomedical Press: New York. 1979.

6. Revis, N.W., T.R. Osborne, G. Holdsworth, and C. Hadden. Mercury in Soil: A Method for Assessing Acceptable Limits. *Arch. Environ. Contam. Toxicol.* 19:221-226. 1990.

7. Cappon, C.J. Uptake and Speciation of Mercury and Selenium in Vegetable CropsGrown on Compost-Treated Soil. *Water, Air, Soil Poll.* 34:353-361. 1987.

8. Wilken, R.D. and H. Hintelmann. Mercury and Methylmercury in Sediments and Suspended particles from the River Elbe, North Germany. *Water, Air and Soil Poll.* 56:427-437. 1991.

9. Parks, J.W., A. Lutz, and J.A. Sutton. Water Column Methylmercury in the Wabigoon/ English River-Lake System: Factors Controlling Concentrations, Speciation, and Net Production. *Can. J. Fisher. Aq. Sci.* 46:2184-2202. 1989.

10. Baes, C.F., R.D. Sharp, A.L. Sjoreen, and R.W. Shor. *A Review and Analysis of Parameters for Assessing Transport of Environmentally Released Radionuclides Through Agriculture.* Prepared under contract No. DE-AC05-84OR21400. U.S. Department of Energy, Washington, D.C. 1984.

11. Rai, D. and J.M. Zachara. Chemical attenuations, coefficients and constants in leachate migration, v.1, A Critical Review. EA-3356, v.1, Research Pro. 1984.

12. Wiener, J.G., W.F. Fitzgerald, C.J. Watras, and R.G. Rada. Partitioning and Bioavailibility of Mercury in an Experimentally Acidified Wisconsin Lake, *Environmental Toxicology and Chemistry*, Vol.9, pp. 909-918. 1990.

13. Moore, J.W. and S. Ramomodoray. *Heavy Metal in Natural Waters - Applied Monitoring in Impact Assessment.* New York, Springer-Varlag. 1984.

14. Bloom, N.S., C.J. Watras, and J.P. Hurley. Impact of Acidification on the Methylmercury Cycle of Remote Seepage Lakes. *Water, Air, and Soil Poll.* 56:477-491. 1991.

15. Meili, M. The Coupling of Mercury and Organic Matter in the Biogeochemical Cycle - Towards a Mechanistic Model for the Boreal Forest Zone, *Water, Air, and Soil Pollution* 56:333-347. 1991.

16. Meili, M., A. Iverfeldt and L. Hakanson. Mercury in the Surface Water of Swedish Forest Lakes - Concentrations, Speciation and Controlling Factors, *Water, Air, and Soil Pollution* 56:439-453. 1991.

17. Meili, M. Fluxes, Pools, and Turnover of Mercury in Swedish Forest Lakes, *Water, Air, and Soil Pollution* 56:719-717. 1991.

18. Robinson, K.G. and M.S. Shuman. Determination of mercury in surface waters using an optimized cold vapor spectrophotometric technique. *International Journal of Environmental Chemistry* 36:111-123. 1989.

19. Ref. 17, p. 723.

20. Ref. 17, Table I.

21. Ref. 17, p. 724

22. Ref. 16, Table I and p. 441.

23. Ref. 17, p. 722.

24. Ref. 6, p. 337.

25. Jensen, A. and Jensen, A. Historical deposition rates of mercury in Scandavia estimated by dating and measurement of mercury in cores of peat bogs, *Water, Air, and Soil Pollution* 56:759-777.

26. Aastrup, M., J. Johnson, E. Bringmark, I. Bringmark, and A. Iverfeldt. Occurrence and Transport of Mercury within a Small Catchment Area, *Water, Air, and Soil Pollution* 56: 155-167. 1991.

27. U.S. EPA. Personal communication with R.A. Ambrose, U.S. EPA, Athens, GA. 1994.

28. Ref. 17, Table II, p. 723.

29. Lindqvist, O., K. Johansson, M. Aastrup, A. Andersson, L. Bringmark, G. Hovsenius, L. Hakanson, A. Iverfeldt, M. Meili, and B. Timm. Mercury in the Swedish Environment - Recent Research on Causes, Consequences and Corrective Methods. *Water, Air and Soil Poll.* 55:(all chapters). 1991.

30. Johansson, K., M. Aastrup, A. Andersson, L. Bringmark, and A. Iverfeldt. Mercury in Swedish Forest Soils and Waters - Assessment of Critical Load, *Water, Air, and Soil Pollution* 56:267-281. 1991.

31. Sorensen, J., G.E. Glass, K.W. Schmidt, J.K Huber, and G.R. Rapp, Jr. Airborne Mercury Deposition and Watershed Characteristics in Relation to Mercury Concentrations in Water, Sediment, Plankton, and Fish of Eighty Northern Minnesota Lakes, *Environ. Sci. Technol.* 24:1716-1727. 1990.

32. Ref. 26, Figure 3, p.163.

33. Arnold, J.G., J. Williams, A. Nicks, and N. Sammons. SWRBB: A Basin-Scale Simulation Model for Soil and Water Resources Management, Texas A & M University Press, College Station, Texas. 1990.

34. Ref. 31, Table III.

35. Ref. 31, p.1724.

36. Akagi H., D.C. Mortimer, and D.R. Miller. Mercury Methylation and Partition in Aquatic Systems. *Bull. Environ. Contam. Toxicol.* 23:372-376. 1979.

37. Cappon, C. Content and Chemical Form of mercury and selenium in soil, sludge and fertilizer materials. Water, Air, Soil Pollut 22:95-104. 1984.

38. *Water, Air and Soil Pollution*, 56, 1991.

39. Watras, C.J. and N.S. Bloom. Mercury and Methylmercury in Individual Zooplankton: Implications for Bioaccumulation. *Limnol. Oceanogr.* 37(6):1313-1318. 1992.

This page is intentionally blank.

Appendix M: Description of Exposure Models

This page is intentionally blank.

M.1 DESCRIPTION OF RELMAP MERCURY MODELING

M.1.1 History and Background Information

During the mid-1970's, SRI International developed a Lagrangian puff air pollution model called the European Regional Model of Air Pollution (EURMAP) for the Federal Environment Office of the Federal Republic of Germany.[1] This regional model simulated monthly sulfur dioxide (SO_2) and sulfate (SO_4^{2-}) concentrations, wet and dry deposition patterns, and generated matrices of international exchanges of sulfur for 13 countries of western and central Europe. In the late-1970's, the U.S. EPA sponsored SRI International to adapt and apply EURMAP to eastern North America. The adapted version of this model, called Eastern North American Model of Air Pollution (ENAMAP), also calculated monthly SO_2 and SO_4^{2-} concentrations, wet and dry deposition patterns, and generated matrices of interregional exchanges of sulfur for a user-defined configuration of regions.[2,3] In the early-1980's, U.S. EPA modified and improved the ENAMAP model to increase its flexibility and scientific credibility.

By 1985, simple parameterizations of processes involving fine (diameters < 2.5 μm) and coarse (2.5 μm < diameters < 10.0 μm) particulate matter were incorporated into the model. This version of the model, renamed the Regional Lagrangian Model of Air Pollution (RELMAP), is capable of simulating concentrations and wet and dry deposition patterns of SO_2, SO_4^{2-} and fine and coarse particulate matter and can also generate source-receptor matrices for user defined regions. In addition to the main model program, the complete RELMAP modeling system includes 19 preprocessing programs that prepare gridded meteorological and emissions data for use in the main program. The RELMAP code was developed using FORTRAN on a Sperry-UNIVAC 1100/82 computing system. It has since been migrated and adapted to operate on other computing systems. Currently, the RELMAP is operated by U.S. EPA's Atmospheric Research and Exposure Assessment Laboratory on DEC VAX and CRAY computing systems, and a test version has recently been installed on a DEC 3000 AXP (Alpha) workstation. The simulations for the Mercury Study Report to Congress were performed on a CRAY Y-MP supercomputer at the National Environmental Supercomputing Center. A complete scientific specification of the RELMAP as used at U.S. EPA for atmospheric sulfur modeling is provided in RELMAP: *A Regional Lagrangian Model of Air Pollution - User's Guide*.[4] Section M.1.2.1 discusses the modifications made to the original sulfur version of RELMAP to enable the simulation of atmospheric mercury.

M.1.2 RELMAP Modeling Strategy for Atmospheric Mercury

M.1.2.1 Introduction. Previous versions of RELMAP have been described by Eder et al.[4] and Clark et al.[5] The goal of the current effort was to model the emission, transport, and fate of airborne mercury over the continental U.S. for the year of 1989. Modifications to the RELMAP for atmospheric mercury simulation were heavily based on recent Lagrangian model developments in Europe.[6] The mercury version of RELMAP was developed to handle three species of mercury: elemental (Hg^0), divalent (the mercuric ion, Hg^{2+}) and particulate mercury (Hg_{part}), and also carbon soot. Recent experimental work indicates that ozone[7] and carbon soot[8,9,10] are both important in determining the wet deposition of Hg^0. Carbon soot, or total carbon aerosol, was included as a modeled pollutant in the mercury version of RELMAP to provide necessary information for the Hg^0 wet deposition parameterization. Observed O_3 air concentration data were obtained from the Agency's Aerometric Information Retrieval System (AIRS) data base, and it was not necessary to include O_3 as an explicitly modeled pollutant. Observed O_3 air concentration data were objectively interpolated in time and space for each 3-hour timestep of the model simulation to produce grids of O_3 air concentration. A minimum O_3 air concentration value of 20 ppb was imposed. Methylmercury was not included in the mercury version of RELMAP because it is not yet known if it has a primary natural or anthropogenic source, or if it is produced in the atmosphere.

RELMAP may be run in either of two modes. In the field mode, wet deposition, dry deposition, and air concentrations are computed at user-defined time intervals. In the source-receptor mode, RELMAP also computes the contribution of each source cell to the deposition and concentration at each receptor cell. For mercury, only the field mode of RELMAP operation was used. With over 10,000 model cells in the high-resolution receptor grid and a significant fraction of these cells also emitting mercury, the data accounting task of a source-receptor run for all mercury sources could not be performed with the computing resources and time available.

Unless specified otherwise in the following sections, the modeling concepts and parameterizations described by Eder et al.[4] were preserved for the RELMAP mercury modeling study.

M.1.2.2 Physical Model Structure. Because of the long atmospheric residence time of mercury, long range transport of the majority of mercury emitted was expected. RELMAP simulations were originally limited to the area bounded by 25 and 55 degrees

north latitude and 60 and 105 degrees west longitude and had a minimum spatial resolution of 1 degree in both latitude and longitude. For this study, the western limit of the RELMAP modeling domain was moved out to 130 degrees west longitude, and the modeling grid resolution was reduced to ½ degree longitude by ⅓ degree latitude (approximately 40 km square) to provide high-resolution coverage over the entire continental U.S.

Since the descriptive document by Eder et al.[4] was produced, the original 3-layer puff structure of the RELMAP has been replaced by a 4-layer structure. The following model layer definitions were used for the RELMAP mercury simulations:

Layer 1 top - 30 to 50 meters above the surface (season-dependent)
Layer 2 top - 200 meters above the surface
Layer 3 top - 700 meters above the surface
Layer 4 top - 700 to 1500 meters above the surface (month-dependent)

M.1.2.3 Mercury Emissions. Point source emissions were introduced into model layer 2 to account for the effective stack height of the point source type in question. Effective stack height is the actual stack height plus the estimated plume rise. The layer of emission is inconsequential during the daytime when complete vertical mixing is imposed throughout the 4 layers. At night, since there is no vertical mixing, area source emissions to layer 1 are subject to dry deposition while point source emissions to layer 2 are not. Large industrial emission sources and sources with very hot stack emissions tend to have a larger plume rise, and their effective stack heights might actually be larger than the top of layer 2. Since, however the layers of the pollutant puffs remain vertically aligned during advection, the only significant process effected by the layer of emission is nighttime dry deposition.

For the RELMAP mercury modeling study, the point sources were assigned particular mercury speciation profiles. These speciation profiles defined the estimated fraction of mercury emitted as Hg^0, Hg^{2+}, or Hg_{part}. Since there remains considerable uncertainty as to the actual speciation factors for each point source type, an alternate emission speciation was simulated in addition to the base speciation in order to test the sensitivity of the RELMAP results to the speciation profiles used. The base-case and alternate speciation profiles used for this study are shown in Table M-1. Gridded fields of total Hg^0, Hg^{2+} and Hg_{part} point source emission rates and Hg^0 area source emission rates were produced and used as input to the RELMAP model simulation.

Table M-1. Emission Speciation Profiles for the Point Source Types Defined

Point Source Type	Base-Case Speciation (%)			Alternate Speciation (%)		
	Hg^0 [a]	Hg^{2+} [b]	Hg_p [c]	Hg^0 [a]	Hg^{2+} [b]	Hg_p [c]
Electric Utility Boilers	50	30	20	50	0	50

[a] Hg^0 symbolizes elemental mercury
[b] Hg^{2+} symbolizes divalent mercury
[c] Hg_p symbolizes particle bound mercury

Global-scale natural and recycled anthropogenic emissions were accounted for by assuming an ambient atmospheric concentration of Hg^0 gas of 1.6 ng/m^3. This use of a constant background concentration to account for global-scale natural and anthropogenic emissions is the same technique used by Petersen et al.[6] The deposition parameterizations described in section M.1.3.1 were used to simulate the scavenging of Hg^0 from this constant ambient concentration throughout the entire 3-dimensional model domain. The result was used as an estimate of the deposition of mercury from all natural sources and anthropogenic sources outside the model domain.

M.1.2.4 Carbon Aerosol Emissions. Penner et al.[11] concluded that total carbon air concentrations are highly correlated with sulfur dioxide (SO_2) air concentrations from minor sources. They concluded that the emissions of total carbon and SO_2 from minor point sources are correlated as well, since both pollutants result from the combustion of fossil fuel. Their data indicate a 35 percent proportionality constant for total carbon air concentrations versus SO_2 air concentrations. The RELMAP mercury model estimated total carbon aerosol emissions using this 35 percent proportionality constant and SO_2 emissions data for minor sources obtained by the National Acidic Precipitation Assessment Program (NAPAP) for the year 1988. Much of these SO_2 emissions data had been previously analyzed for use by the Regional Acid Deposition Model (RADM). For the portion of the RELMAP mercury model domain not covered by the RADM domain, state by state totals of SO_2 emissions were apportioned to the county level on the basis of weekday vehicle-miles-traveled data since recent air measurement studies have indicated that aerosol elemental carbon can be attributed mainly to transportation source types.[12] The county level data were then apportioned by

area to the individual RELMAP grid cells. Total carbon soot was assumed to be emitted into the lowest layer of the model.

M.1.2.5 Ozone Concentration. Ozone concentration data were obtained from U.S. EPA's Aerometric Information Retrieval System (AIRS) and the Acidmodes experimental air sampling network. AIRS and Acidmodes data were available hourly. Any observations of ozone concentration below 20 ppb were treated as missing. For each RELMAP grid cell, the ozone concentrations were computed for the two mid-day time steps by using the mean concentration value during two corresponding time periods (1000-1300 and 1400-1600 local time). The mean of these two mid-day values was used to estimate the ozone concentration for the time steps after 1600 local time and before 1000 local time the next morning. This previous-day average was used at night since ground-level ozone data are not valid for the levels aloft, where the wet removal of elemental mercury was assumed to be occurring. Finally, an objective interpolation scheme was used to produce complete ozone concentration grids for each time step, with a minimum value of 20 ppb imposed.

M.1.2.6 Lagrangian Transport and Deposition. In the model, each pollutant puff begins with an initial mass equal to the total emission rate of all sources in the source cell multiplied by the model time-step length. For mercury, as for most other pollutants, emission rates for each source cell were defined from input data, and a time step of three hours was used. The initial horizontal area of each puff was set to 1200 km^2, instead of the standard initial size of 2500 km^2, in order to accommodate the finer grid resolution used for the mercury modeling study; however, the standard horizontal expansion rate of 339 km^2 per hour was not changed. Although each puff was defined with four separate vertical layers, each layer of an individual puff was advected through the model cell array by the same wind velocity field. Thus, the layers of each puff always remained vertically stacked. Wind field initialization data for a National Weather Service prognostic model, the Nested Grid Model (NGM), were obtained from the NOAA Atmospheric Research Laboratory for the entire year of 1989. Wind analyses for the σ_p=0.897 vertical level of the NGM were used to define the translation of the puffs across the model grid, except during the months of January, February, and December, when the σ_p=0.943 vertical level was used to reflect a more shallow mixed layer. σ_p is a pressure-based vertical coordinate equal to $(p-p_{top})/(p_{surface}-p_{top})$.

Pollutant mass was removed from each puff by the processes of wet deposition, dry deposition, diffusive air exchange between the surface-based mixed layer and the free atmosphere and, in the

case of reactive species, chemical transformation. The model parameterizations for these processes are discussed in Section M.1.3. Precipitation data for the entire year of 1989, obtained from the National Climatic Data Center, were used to estimate the wet removal of all pollutant species modeled. Wet and dry deposition mass totals were accumulated and average surface-level concentrations were calculated on a monthly basis for each model cell designated as a receptor. Except for cells in the far southwest and eastern corners of the model domain where there were no wind data, all cells were designated as receptors for the mercury simulation. When the mass of pollutant on a puff declines through deposition, vertical diffusion or transformation to a user-defined minimum value, or when a puff moves out of the model grid, the puff and its pollutant load is no longer tracked. The amount of pollutant in the terminated puff is taken into account in monthly mass balance calculations so that the integrity of the model simulation is assured. Output data from the model includes monthly wet and dry deposition totals and monthly average air concentration for each modeled pollutant, in every receptor cell.

M.1.3 Model Parameterizations

M.1.3.1 Chemical Transformation and Wet Deposition. The simplest type of pollutant to model with RELMAP is the inert type. To model inert pollutants, one can simply omit chemical transformation calculations for them, and not be concerned with chemical interactions with the other chemical species in the model. In the mercury version of RELMAP, particulate mercury and total carbon were each modeled explicitly as inert pollutant species. Reactive pollutants are normally handled by a chemical transformation algorithm. RELMAP was originally developed to simulate sulfur deposition, and the algorithm for transformation of sulfur dioxide to sulfate was independent of wet deposition. For gaseous mercury, however, the situation is more complex. Since there are no gaseous chemical reactions of mercury in the atmosphere which appear to be significant[6], for this modeling study mercury was assumed to be reactive only in the aqueous medium. Elemental mercury has a very low solubility in water, while oxidized forms of mercury and particle bound mercury readily find their way into the aqueous medium through dissolution and particle scavenging, respectively. Worldwide observations of atmospheric mercury, however, indicate that particulate mercury is generally a minor constituent of the total mercury loading[9] and that gaseous elemental mercury (Hg^0) is, by far, the major component. Swedish measurements of large north-to-south gradients of mercury concentration in rainwater without corresponding gradients of atmospheric mercury concentration

suggest the presence of physical and chemical interactions with other pollutants in the precipitation scavenging process.[9] Aqueous chemical reactions incorporated into the mercury version of RELMAP were based on research efforts in Sweden [7,10,13-17]

Unlike other pollutants that have been modeled with RELMAP, mercury has wet deposition and chemical transformation processes that are interdependent. A combined transformation/wet-removal scheme proposed by Petersen et al.[6] was used. In this scheme, the following aqueous chemical processes were modeled when and where precipitation is present.

1) oxidation of dissolved Hg^0 by ozone yielding Hg^{2+}
2) catalytic reduction of this Hg^{2+} by sulfite ions
3) adsorption of Hg^{2+} onto carbon soot particles suspended in the aqueous medium

$$W(Hg^0) = \frac{k_1}{k_2} \cdot \frac{1}{H_{Hg}} \cdot [O_3]_{aq} \cdot (1 + K_3 \cdot \frac{c_{soot}}{r})$$

Petersen et al.[6] shows that these three simultaneous reactions can be considered in the formulation of a scavenging ratio for elemental mercury gas as follows:
where,

k_1 is the second order rate constant for the aqueous oxidation of Hg^0 by O_3 equal to 4.7×10^7 $M^{-1}s^{-1}$,

k_2 is the first order rate constant for the aqueous reduction of Hg^{2+} by sulfite ions equal to 4.0×10^{-4} s^{-1},

H_{Hg} is the dimensionless Henry's Law coefficient for Hg^0 (0.18 in winter, 0.22 in spring and autumn, and 0.25 in summer as calculated from Sanemasa),[18]

$[O_3]_{aq}$ is the aqueous concentration of ozone,

K_3 is a model specific adsorption equilibrium constant (5.0×10^{-6} m^4g^{-1}),

c_{soot} is the total carbon soot aqueous concentration, and r is the assumed mean radius of soot particles (5.0×10^{-7} m).

$[O_3]_{aq}$ is obtained from this equation.

$$[O_3]_{aq} = \frac{[O_3]_{gas}}{H_{O3}}$$

where H_{O3} is the dimensionless Henry's Law coefficient for ozone (0.448 in winter, 0.382 in spring and autumn, and 0.317 in summer as calculated from Seinfeld).[19] c_{soot} is obtained from the simulated atmospheric concentration of total carbon aerosol using a scavenging ratio of 5.0×10^5.

The model used by Petersen et al.[6] defined one-layer cylindrical puffs, and the Hg^0 scavenging layer was defined as the entire vertical extent of the model. The RELMAP defines 4-layer puffs to allow special treatment of surface-layer and nocturnal inversion-layer processes. It was believed that, due to the low solubility of Hg^0 in water, the scavenging process outlined above would only take place effectively in the cloud regime, where the water droplet surface-area to volume ratio is high, and not in falling raindrops. Thus the Hg^0 wet scavenging process was applied only in the top two layers on RELMAP, which extends from 200 meters above the surface to the model top.

For the modeling study described in Petersen et al.[6], the wet deposition of Hg^{2+} was treated separately from that of Hg^0. Obviously, any Hg^{2+} dissolved into the water droplet directly from the air could affect the reduction-oxidation balance between the total concentration of Hg^0 and Hg^{2+} in the droplet. Since the solubility and scavenging ratio for Hg^{2+} is much larger than that for Hg^0, and since air concentrations of Hg^0 are typically larger than those of Hg^{2+}, separate treatment of Hg^{2+} wet deposition was deemed acceptable. Thus, process 2 above was only considered as a moderating factor for the oxidation of dissolved Hg^0.

There was no attempt to develop a new interacting chemical mechanism for simultaneous Hg^0 and Hg^{2+} wet deposition. Although Hg^{2+} was recognized as a reactive species in aqueous phase redox reactions, it was, in essence, modeled as an inert species just like particulate mercury and total carbon soot. With the rapid rate at which the aqueous Hg^{2+} reduction reaction is believed to occur in the presence of sulfite, it is possible that an interactive cloud-water chemical mechanism might produce significant conversion of scavenged Hg^{2+} to Hg^0, with possible release of that Hg^0 into the gaseous medium.

Wet deposition of Hg^{2+}, particulate mercury, and total carbon soot in the mercury version of RELMAP were modeled with the same scavenging ratios used by Petersen et al.[6] The gaseous

nitric acid scavenging ratio of 1.6×10^{-6} has been applied for Hg^{2+} since the water solubilities of these two pollutant species are similar. For particulate mercury, a scavenging ratio of 5.0×10^{-5} was used, based on experiences in long-range modeling of lead in northern Europe. As previously mentioned, a scavenging ratio of 5.0×10^{-5} was also used for total carbon soot. These scavenging ratios for Hg^{2+}, particulate mercury, and total carbon soot were applied to all four layers of the RELMAP in the calculation of pollutant mass scavenging by precipitation.

M.1.3.2 Dry Deposition. Recent experimental data indicate that elemental mercury vapor does not exhibit a net dry depositional flux to vegetation until the atmospheric concentration exceeds a rather high compensation point of around 10 ng/m^3.[20] This compensation point is apparently dependent on the surface or vegetation type and represents a balance between emission from humic soils and dry deposition to leaf surfaces.[21] Since the emission of mercury from soils was accounted for with a global-scale ambient concentration and not an actual emission of Hg^0, for consistency, there was no explicit simulation of the dry deposition of Hg^0.

For Hg^{2+} during daylight hours, a dry deposition velocity table previously developed based on HNO_3 data was used.[22,23] The dry deposition characteristics of HNO_3 and Hg^{2+} should be similar since their water solubilities are similar. This dry deposition velocity data, shown in Table M-2, provided season-dependent values for 11 land-use types under six different Pasquill stability categories. Based on the predominant land-use type and climatological Pasquill stability estimate of each RELMAP grid cell, and the season for the month being modeled, the dry deposition velocity values shown in Table M-2 were used for the daytime only. For nighttime, a value of 0.3 cm/s was used for all grid cells since the RELMAP does not have the capability of applying land-use dependent dry deposition at night. Since the nighttime dry deposition was applied only to the lowest layer of the model and no vertical mixing is assumed for nighttime hours, all Hg^{2+} modeled to be quickly depleted from the lowest model layer by larger dry deposition velocities.

For Hg_{part}, Petersen et al.[6] used a dry deposition velocity of 0.2 cm/s at all times and locations. Lindberg et al.[24] (1991) suggests that the dry deposition of Hg_{part} seems to be dependent on foliar activity. During the daylight hours of spring, summer, and autumn, a dry deposition velocity of 0.11 cm/s was used for Hg_{part}, except for model cells with predominant surface characteristics of water, barren, and rocky terrain where 0.02 cm/s was used. At night and at all hours during the winter,

Table M-2. Dry Deposition Velocity (cm/s) for Divalent Mercury (Hg^{2+})

Season	Land-Use Category	Pasquill Stability Category					
		A	B	C	D	E	F
Winter	Urban	4.83	4.80	4.61	4.30	2.79	0.36
	Agricultural	1.32	1.30	1.20	1.05	0.46	0.15
	Range	1.89	1.86	1.73	1.52	0.73	0.19
	Deciduous Forest	3.61	3.57	3.34	3.02	1.68	0.29
	Coniferous Forest	3.61	3.57	3.34	3.02	1.68	0.29
	Mixed Forest/Wetland	3.49	3.46	3.27	2.99	1.77	0.29
	Water	1.09	1.07	0.98	0.85	0.38	0.13
	Barren Land	1.16	1.14	1.06	0.92	0.39	0.31
	Non-forested Wetland	2.02	2.00	1.89	1.70	0.96	0.21
	Mixed Agricultural/Range	1.62	1.60	1.48	1.30	0.60	0.17
	Rocky Open Areas	1.98	1.95	1.81	1.58	0.73	0.20
Spring	Urban	4.59	4.54	4.35	4.05	2.49	0.36
	Agricultural	1.60	1.56	1.46	1.28	0.53	0.18
	Range	1.49	1.46	1.36	1.19	0.48	0.17
	Deciduous Forest	3.42	3.36	3.13	2.81	1.42	0.29
	Coniferous Forest	3.42	3.36	3.13	2.81	1.42	0.29
	Mixed Forest/Wetland	3.28	3.23	3.05	2.78	1.55	0.29
	Water	0.98	0.96	0.89	0.77	0.31	0.13
	Barren Land	1.05	1.04	0.97	0.85	0.30	0.13
	Non-forested Wetland	1.85	1.82	1.73	1.56	0.84	0.21
	Mixed Agricultural/Range	1.60	1.56	1.46	1.28	0.53	0.18
	Rocky Open Areas	1.84	1.81	1.67	1.46	0.58	0.20
Summer	Urban	4.47	4.41	4.12	3.73	2.07	0.36
	Agricultural	2.29	2.25	2.04	1.76	0.72	0.24
	Range	1.67	1.64	1.48	1.26	0.41	0.19
	Deciduous Forest	3.32	3.26	2.95	2.57	1.04	0.29
	Coniferous Forest	3.32	3.26	2.95	2.57	1.04	0.29
	Mixed Forest/Wetland	3.17	3.12	2.86	2.53	1.27	0.29
	Water	0.92	0.90	0.81	0.69	0.22	0.13
	Barren Land	0.98	0.98	0.89	0.76	0.23	0.13
	Non-forested Wetland	1.91	1.88	1.73	1.52	0.77	0.22
	Mixed Agricultural/Range	1.90	1.87	1.69	1.44	0.52	0.21
	Rocky Open Areas	1.95	1.91	1.71	1.46	0.42	0.21
Autumn	Urban	4.64	4.59	4.35	4.05	2.49	0.36
	Agricultural	2.02	1.98	1.81	1.60	0.73	0.21
	Range	1.78	1.74	1.59	1.40	0.60	0.19
	Deciduous Forest	3.46	3.40	3.13	2.81	1.42	0.29
	Coniferous Forest	3.46	3.40	3.13	2.81	1.42	0.29
	Mixed Forest/Wetland	3.32	3.27	3.05	2.78	1.55	0.29
	Water	1.00	0.98	0.89	0.77	0.31	0.13
	Barren Land	1.07	1.06	0.97	0.85	0.30	0.13
	Non-forested Wetland	1.88	1.86	1.73	1.56	0.84	0.21
	Mixed Agricultural/Range	1.93	1.90	1.74	1.53	0.68	0.20
	Rocky Open Areas	1.97	1.94	1.76	1.54	0.63	0.20

all cells used 0.02 cm/s as the dry deposition velocity for Hg_{part}. Lindberg et al.[24] suggested a value of 0.003 cm/s for non-vegetated land, but since the RELMAP can not model land-use dependent dry deposition at night, the value of 0.02 cm/s was used for these cells by necessity.

For total carbon soot, daytime dry deposition velocities were calculated using a FORTRAN subroutine developed by the California Air Resources Board.[25] A particle density of 1.0 g/cm^3 and radius of 0.5 μm was assumed. Table M-3 shows the wind speed (u) used for each Pasquill stability category in the calculation of deposition velocity from the CARB subroutine, while Table M-4 shows the roughness length (z_0) used for each land-use category. For nighttime, a dry deposition velocity of 0.07 cm/s was used for all seasons and land-use types.

The RELMAP assumes instantaneous vertical mixing of all pollutants through the entire depth of the model. For grid cells with significant emission rates, this results in an underestimation of the ground-level concentration and therefore an underestimation of the dry deposition rate for mercury species emitted near the ground. To remedy this, the model used a local dry deposition factor for Hg_{part} in a similar manner as Petersen et al.[6] This local deposition factor was 0.5, meaning that one-half of the Hg_{part} emissions from a grid cell were assumed to dry deposit within that grid cell by processes not otherwise simulated by the dry deposition parameterization. There was no application of a local deposition factor for Hg^{2+} since the majority of its emission was assumed to be from elevated point dry deposition factor for Hg_{part} in a similar manner as Petersen et al.[6] This local deposition factor was 0.5, meaning that one-half of the Hg_{part} emissions from a grid cell were assumed to dry deposit within that grid cell by processes not otherwise simulated by the dry deposition parameterization. There was no application of a local deposition factor for Hg^{2+} since the majority of its emission was assumed to be from elevated point sources.

M.1.3.3 Vertical Exchange of Mass with the Free Atmosphere. Due to the long atmospheric lifetime of mercury, the RELMAP was adapted to allow a treatment of the exchange of mass between the surface-based mixed layer and the free atmosphere above. As a first approximation, a pollutant depletion rate of 5 percent per 3-hour timestep was chosen to represent this diffusive mass exchange. When compounded over a 24-hour period, this depletion rate removes 33.6 percent of an inert, non-depositing pollutant.

Table M-3. Wind Speeds Used for Each Pasquill Stability Category in the CARB Subroutine Calculations

Stability Category	Wind Speed (m/s)
A	10.0
B	5.0
C	5.0
D	2.5
E	2.5
F	1.0

Table M-4. Roughness Length Used for Each Land-Use Category in the CARB Subroutine Calculations

Land-Use Category	Roughness Length (meters)	
	autumn-winter	spring-summer
Urban	0.5	0.5
Agricultural	0.15	0.05
Range	0.12	0.1
Deciduous Forest	0.5	0.5
Coniferous Forest	0.5	0.5
Mixed Forest/Wetland	0.4	0.4
Water	10^{-6}	10^{-6}
Barren Land	0.1	0.1
Non-forested Wetland	0.2	0.2
Mixed Agricultural/Range	0.135	0.075
Rocky Open Areas	0.1	0.1

Since all three forms of the modeling mercury deposit to the surface to some degree, their effective diffusion rate out of the top of the model is less than 33.6 percent per day.

M.1.4 Discussion of RELMAP Modeling Uncertainties

M.1.4.1 Vertical Model Domain. The RELMAP model top is defined to be the maximum vertical extent of the convectively

driven mixed layer. Monthly values defined from mixed-layer-height climatology are rough estimates of a meteorological phenomenon that may not exist in many situations. Although a surface-based mixed layer may be well defined, pollutants that persist in the atmosphere for long periods of time are certain to mix to some degree into the free atmosphere above the mixed-layer top. Chlorofluorocarbon (CFC) compounds are an extreme example of this possibility. Elemental mercury deposits relatively slowly through precipitation processes due to its low water solubility, and its dry deposition appears to be minimal since it is in vapor form under normal atmospheric conditions. In fact, pollutant mass balance accounting information from the RELMAP mercury simulation indicated that approximately 75 percent of all elemental mercury emitted was transported out of the model domain before it was wet or dry deposited. Elemental mercury appears to be quite persistent in the atmosphere.

Since the RELMAP does not simulate the flux of air or pollutant through the height of the mixed layer, which is fixed for each monthly simulation, the use of horizontally divergent/convergent wind fields to define the motion of the pollutant puffs can sometimes result in unrealistic instantaneous concentration fields. Horizontally convergent winds will tend to concentrate puffs at the point of convergence, resulting in high modeled concentrations when the effects of the puffs are summed together. Ordinarily, horizontal convergence in the surface-based mixed layer would push the mixed-layer top higher into the atmosphere as a result of the incompressible nature of air in general atmospheric motion. This higher mixed-layer top would compensate for the greater pollutant mass loading per unit area from the converging puffs, keeping the resulting pollutant concentration more constant. The RELMAP was not designed to provide instantaneous realizations of pollutant concentration fields. Rather, it was designed for seasonal and annual simulations where the total effects of convergent and divergent wind fields can balance one another. There does exist some uncertainty, however, as to whether this balance actually occurs in all situations.

M.1.4.2 Aqueous Chemistry. The aqueous reduction-oxidation chemistry mechanism in the mercury version of RELMAP was applied only to the Hg^0 dissolved from the ambient air into the water droplet. Where significant concentrations of Hg^{2+} from emissions exist in the ambient air, this Hg^{2+} could be dissolved into the water droplet along with the Hg^0 and inhibit the scavenging of Hg^0. The RELMAP results described above indicate that Hg^{2+} air concentrations are certainly lower than those for Hg^0 at the

length scales of the RELMAP grid cells; however, the magnitude of the effect of ambient Hg^{2+} on the Hg^0 oxidation scavenging is not yet well understood.

Another source of modeling uncertainty in aqueous chemistry relates to the fact that the aqueous chemical mechanisms were invoked only when and where precipitation was known to occur, and precipitation fields were only defined over land areas where precipitation observations were available. Significant wet transformation and removal of mercury may occur over oceanic areas were precipitation observations are not available, and it is possible that significant aqueous chemistry is occurring in non-precipitating clouds.

M.1.4.3 Transport and Diffusion. Since the RELMAP simulates transport and diffusion only in the surface-based mixed layer and vertical wind shear is small when the mixed-layer is well defined, under ideal conditions transport and diffusion are handled adequately. When the surface-based mixed layer is not well defined, vertical gradients in the speed and/or direction of the wind may be present which cannot be represented by the motion of individual Lagrangian puffs whose layers remain vertically stacked. There are two techniques that might be used to represent vertical wind shear in the RELMAP: puff splitting and wind-shear-dependent puff expansion. Due to computational limits and scheduling constraints, these were not attempted. The most complete solution to the problem of vertical wind shear is the use of a Eulerian reference frame for numerical modeling. The Atmospheric Characterization and Modeling Division of U.S. EPA's Atmospheric Research and Exposure Assessment Laboratory has proposed the development of a Toxics Linear Chemistry Model (TLCM) using the Eulerian reference frame of the Regional Acid Deposition Model (RADM). The TLCM could be operational within two years.

M.1.4.4 Boundary Fluxes of Pollutants. Due to the fact that RELMAP simulates atmospheric pollutant loading as the combined effect of a population of discrete Lagrangian puffs, and the fact that elemental mercury gas has a long residence time in the atmosphere, natural mercury emissions from the oceans and land surfaces could not be explicitly modeled. Given the general west-to-east wind flow at the latitudes of the continental U.S., simulated puffs of natural mercury emissions could be emitted from all grid cells, but their effects would be artificially concentrated in the eastern sections of the model domain. The only puffs that could impact the western areas would be those originating from the far western grid cells, while the eastern areas could be impacted by puffs from all parts of the model

domain. The use of a Eulerian-type model would allow the definition of boundary fluxes of pollutant based on larger-scale model results or assumed background concentration levels.

M.1.5 Verification of Mercury RELMAP Results

In general, the EPA modelers believed that the RELMAP would tend: 1) to overestimate Hg values in urban areas; and 2) to underestimate Hg values in rural areas and in the urban center of larger cities. There was limited data available to check the model and confirm those beliefs. The discussion below summarizes the the limited comparison between model predictedions and measured data. [Note that measured Hg values will have some uncertainty associated with each reported value.] Overall, the RELMAP seems to over- and underestimate Hg values within a factor of 2 and was relatively unbiased in its predictions..

M.1.5.1 Verification of Mercury Concentration Estimates.

The RELMAP-simulated Hg0 and Hg2+ air concentrations taken together with the assumed background Hg0 concentration of 1.6 ng/m^3 agree well with observations of vapor-phase Hg air concentration in Minnesota[26], in Vermont[27] and in Wisconsin[28]. These observations showed that annual average vapor-phase Hg concentrations were near the levels found over other remote locations in the northern hemisphere, from 1.6 to 2.0 ng/m^3. The RELMAP simulation indicated 1.64 ng/m^3 in Minnesota, 1.67 ng/m^3 in Wisconsin and 1.70 ng/m^3 in Vermont. Measurements taken for a two-week period at three sites in Broward County, Florida[29], show slightly elevated vapor-phase Hg air concentrations for two of those sites downwind of industrial activities. These two sites had average vapor-phase Hg air concentrations of 3.3 and 2.8 ng/m^3. The RELMAP simulation results for the Fort Lauderdale area show only about a 0.2 ng/m^3 elevation of the annual average vapor-phase Hg (Hg0 plus Hg2+) concentration over the 1.6 ng/m^3 background value assumed. However, the measurements in Broward County did not extend for a significant portion of the year and there was no discrimination between Hg0 and Hg2+ forms. The third site for their observations had an average vapor-phase air concentration of 1.8 ng/m^3, exactly what the RELMAP simulation suggests. Obviously, a more comprehensive air monitoring program is required before an evaluation of the RELMAP results for Florida can be performed.

The maximum annual average HgP (particulate mercury) concentrations from the RELMAP simulation are around 50-100 pg/m3 (0.05-0.1 ng/m^3) in the urban centers of the Northeast. A study in urban Detroit during March of 1992 found an average HgP concentrations over an 18-day period of 94 pg/m^3.[19] The RELMAP

simulation suggests an annual average HgP concentration in the Detroit area of about 50 pg/m3. Average HgP concentrations of between 34 and 51 pg/m3 were measured in Broward County, Florida, at three sites from 25 August to 7 September of 1993.[29] The RELMAP simulation showed an average annual concentration of about 50 pg/m3 for HgP around the city of Fort Lauderdale. Researchers have found annual average HgP air concentrations of 10.5 pg/m3 in Pellston, Michigan, 22.4 pg/m3 in South Haven, Michigan, and 21.9 pg/m3 in Ann Arbor, Michigan, from April 1993 to April 1994, and 11.2 pg/m3 in Underhill, Vermont, for the year of 1993.[8] The RELMAP simulation results agree quite well with these observations also, with 10 to 20 pg/m3 indicated for Pellston and Underhill, and 20 to 50 pg/m3 indicated for South Haven and Ann Arbor.

M.1.5.2 Verification of Mercury Wet Deposition Results. Measurements of mercury wet deposition at three locations in northeastern Minnesota during 1989 indicated annual wet deposition rates of 6.5 ug/m^2 at Duluth, 13.5 ug/m^2 at Marcell and 41.9 ug/m^2 at Ely.[30] A later study measuring annual wet deposition of Hg during 1990, 1991 and 1992 at Ely, Duluth and seven other sites in Minnesota, upper Michigan and northeastern North Dakota found all annual wet deposition totals to be within the range of 3.8 to 9.7 ug/m^2.[31] The RELMAP simulation indicated a range of 1.7 to 10.9 ug/m^2. Measurements at Little Rock Lake, in northern Wisconsin, of Hg in snow during February and March, 1989, and in rain from May to August, 1989, have been used to estimate annual Hg depositions in rain and snow of 4.5 and 2.3 ug/m^2, respectively.[26] This suggests a total annual Hg wet deposition of 6.8 ug/m^2 at Little Rock Lake, while the RELMAP simulation showed 5.8 ug/m^2. Measurements at Presque Isle, also in northern Wisconsin, from 1993 to 1994 indicated a wet deposition rate for total Hg of 5.2 ug/m^2/yr,[28] only slightly less than the RELMAP simulation of 5.7 ug/m^2/yr.

There were also some Hg wet deposition measurement programs conducted during the early 1990's in somewhat less remote sites in Michigan and Vermont. Observations during two years of event precipitation sampling at three sites in Michigan show evidence for a north-to-south gradient in Hg wet deposition.[32] The total Hg wet deposition observed for the two years at South Haven, in the southwest part of the state, were 9.45 and 12.67 ug/m^2, while the RELMAP simulation showed 13.98 ug/m^2. At Pellston, in the northern part of the lower peninsula of Michigan, the wet deposition was 5.79 and 5.54 ug/m^2, while the RELMAP showed 8.12 ug/m^2. At Dexter, in southeast Michigan just west of Detroit, the observed wet deposition was 8.66 and 9.11 ug/m^2. The RELMAP simulation showed 24.74 ug/m^2 for the grid cell containing

Dexter, but this grid cell also contains the city of Detroit. The RELMAP 40-km horizontal grid is unable to resolve urban-scale gradients. The higher second-year wet deposition at South Haven has been attributed to increased precipitation rate, and measurements at Underhill, Vermont[27], are cited as further evidence of the importance of precipitation amount.[32] From December 1992 to December 1993, the average volume-weighted Hg concentration at Underhill (8.3 ng/L) was similar to that observed at Pellston (7.9 ng/L). However, with more precipitation during that period, the total Hg wet deposition at Underhill was 9.26 ug/m^2, significantly higher than at Pellston. The RELMAP simulation for Underhill shows 17.41 ug/m^2, again due to influences from a nearby city, Burlington, VT.

The very large total Hg wet deposition values (>50 ug/m^2) from the RELMAP simulation for some of the larger urban centers in the Ohio Valley and Northeast regions can not be evaluated thoroughly due to a lack of long-term precipitation event sampling at those locations. RELMAP results of around 50 ug/m^2 along the east coast of south Florida can be compared to observed data. Precipitation event sampling was performed from 19 August to 7 September of 1993 at 4 sites in Broward County, Florida, in and around the city of Fort Lauderdale.[29] During the 20-day sampling period, total Hg mean concentrations in precipitation were 35, 57, 40 and 46 ng/L at the 4 sites. Given the average annual precipitation of 150 cm per year typical of that area, the resulting annual wet deposition estimates at these 4 sites are 52.5, 85.5, 60 and 69 ug/m^2. Since most of the annual rainfall in Broward County occurs in warm tropical conditions of the March to October wet season, this extrapolation from 20 days during the wet season to an annual estimate may be considered reasonable. However, additional urban measurement studies will certainly be required to allow any credible evaluation of RELMAP wet deposition results in heavily populated, industrialized areas.

M.2 Description of COMPDEP Air Dispersion Model

M.2.1 Description of the COMPDEP Air Quality Model

General references for this section are Overcamp[33], Rao,[34] and U.S. EPA.[35]

The COMPDEP model uses hourly meteorological data to estimate air concentrations and deposition fluxes from a point source. In this section a summary description of the model is presented. In Section M.2.2.1, specific modifications made for this assessment are discussed.

M.2.1.1 Atmospheric Stability and System Used in COMPDEP. After pollutants are emitted from a source, they are diluted with ambient air. The degree of dispersion is a function of wind speed and the level of turbulence. In general, higher wind speeds or turbulence result in lower air concentrations. The amount of turbulence is quantified in terms of the atmospheric stability. A stable atmosphere is one that suppresses vertical motions, hence mitigating turbulence, while an unstable atmosphere is one that enhances turbulence. Atmospheric turbulence *per se* is difficult and expensive to measure[36], and it is usually estimated from other more easily measurable quantities. In particular, the stability of the atmosphere is typically characterized by the vertical temperature profile of the atmosphere.

For an isolated parcel of air in which no heat is transferred in or out (adiabatic), one can show using the first law of thermodynamic and the hydrostatic equation[37] that there is a 1 degree (C) decrease for every 100 m increase in altitude, and a 1 degree increase for every 100 m decrease. This is called the adiabatic lapse rate.

The atmosphere is not adiabatic as it is both heated and cooled. This results in temperature profiles that differ from the adiabatic profile, and it is this difference that is ultimately responsible for a given atmospheric stability. The three broad classes of stability and their associated temperature profiles are summarized in Table M-5.

It should be noted that any time the temperature increases with altitude, the atmospheric condition is termed an inversion. Because of the associated stability, inversions tend to decrease.[38]

The most widely used scheme of atmospheric stability classification, and that used in COMPDEP, was developed by Pasquill[39] and modified by Gifford[40]. There are six stability classes, denoted with the letters A through F. In general, classes A through C indicate unstable conditions, D is roughly neutral, and classes E and F represent stable conditions. Table M-6, from Hanna et al.[41], originally from Gifford[42], shows the criteria for the different classes.

The meteorological conditions that are used to determine the stability class are shown in Table M-7. From this table, it can be seen that extremely unstable conditions (class A) occur during the day with light winds and moderate to strong solar radiation

Table M-5. Classes of Atmospheric Stability and Associated Vertical Temperature Distribution

Vertical Temperature Profile	General Result	Class of Stability
Increases with height, or decreases less rapidly than adiabatic lapse rate	Vertical motions inhibited	Stable
Nearly identical with adiabatic rate	No significant buoyant forces	Neutral
Decreases with height faster than adiabatic lapse rate	Vertical motions enhanced	Unstable

Table M-6 Pasquill Turbulence Types and Corresponding Atmospheric Conditions[42]

Pasquill Turbulence Type	Atmospheric Stability Conditions
A	Extremely unstable
B	Moderately unstable
C	Slightly unstable
D	Neutral[a]
E	Slightly stable
F	Moderately stable

[a] Applicable to heavy overcast day or night.

(necessary conditions for the formation of an unstable temperature profile.[33] Conversely, extremely stable conditions can occur only at night with clear skies and light winds. Hanna et al. note that some have filled in the blank in Table M-7 with a "G" class, but this has not received wide acceptance.[41]

Other stability classification schemes exist. For example, M.E. Smith[43] proposed a classification scheme that is based on wind direction, and Cramer[44] advocated a method based on observed wind fluctuations at a height of 10m (often referred to the Brookhaven National Laboratory, or BNL, stability classes). In addition, Irwin[45] proposed a method of allowing for a continuum of stability, as opposed to a discrete approach such as the Pasquill method. Use of the Pasquill letter classes is common due to their ease of use, and because they have produced satisfactory results.

Table M-7. Meteorological Conditions Defining Pasquill Turbulence Types[42]

	Daytime Solar Radiation			Nighttime conditions	
Surface wind speed (m/sec)	Strong	Moderate	Slight	Mostly Overcast	Mostly Clear
<2	A	A-B	B		
2-3	A-B	B	C	E	F
3-4	B	B-C	C	D	E
4-6	C	C-D	D	D	D
>6	C	D	D	D	D

For this assessment, the stability classes for each hour were estimated with the RAMMET program[46], using hourly surface meteorological data.

Estimation of wind speed is important because higher wind speeds result in greater dispersion and hence reduced concentrations of pollutants. Frictional forces cause the surface wind speed, which is usually the value available, to be lower than the speed at the stack top. A power law wind speed profile is typically used to calculate the change of wind speed with height, and takes the following form:

$$\frac{u_s}{u_{ref}} = \left(\frac{z_s}{z_{ref}} \right)^p$$

where, u_{ref} = wind speed at the reference height
z_{ref} = reference height
u_s = wind speed at the release height
z_s = release height
p = wind speed profile exponent (dependent on atmospheric stability and is between 0 and 1). In general, a reference anemometer height of 10 m, the standard height for measurement of wind speed and direction by the National Weather Service, is used.[33]

The wind profile exponents used in COMPDEP are given in Table M-8. These are the default values for rural settings in U.S. EPA[35] and are based on Irwin[45]. Although default values for urban settings are available in U.S. EPA[35] as well, due to limitations of the COMPDEP model it was decided that their use was not warranted for this assessment. The default values for urban settings were about twice as high as the rural ones for classes A, B, and C, which resulted in higher wind speeds at the stack top.

Directional shear with height is not included, which means that the direction of flow is assumed to be the same at all heights over the region. The taller the effective height of a source, the larger the expected error in direction of plume transport.[47]

M.2.1.2 Plume Rise. A general principle, borne out by the analytic solutions of the diffusion algorithms and known since at least 1917[48], is that the maximum ground level concentration is inversely proportional to the height of release.[36] Due to the buoyant properties of the stack gases and the velocity of the stack gases emitted, the height of release from a modeling perspective is usually higher than the actual physical height of the stack. This height is called the effective stack height and is the sum of the physical stack height and the rise of the plume.

Due to the sensitivity of the maximum concentrations to the effective stack height, and because the maximum downwind concentration has been historically the output of interest for regulatory agencies, numerous methods exist for estimating plume rise in a variety of conditions. Overcamp[33] noted that over 50 different plume rise formulas had been published by 1977, and Pasquill[49] observed that there are many rival formulae from which to choose.

The method used in COMPDEP is based on Briggs[50,51,52] and Bowers et al.[53] With this approach, it must be determined whether thermal buoyancy or vertical momentum is dominating the plume's motion. Estimates of the buoyancy flux (F_b, units of m^4/s^3) and momentum flux (F_m, units of m^4/s^2) are based on Briggs[54]:

Table M-8. Wind Profile Exponents Used In The Assessment

Stability Category	Wind Profile Exponent
A	0.07
B	0.07
C	0.10
D	0.15
E	0.35
F	0.55

$$F_b = g\ v_s\ d_s^2 \left(\frac{T_s - T_a}{4T_s} \right)$$

$$F_m = v_s^2\ d_s^2\ \frac{T_a}{4T_s}$$

where, g = acceleration due to gravity (9.80616 m/s^2)
v_s = stack gas exit velocity (m/s)
d_s = stack diameter (m)
T_s = stack gas temperature (K)
T_a = ambient air temperature (K).

If the stack gas temperature is less than or equal to the ambient air temperature, it is assumed that plume rise is dominated by momentum, in which case the effective stack height is given by this formula:

$$h_e = h_s + \begin{cases} 3d_s \dfrac{v_s}{u_s} & \textit{Unstable or neutral} \\ \min\left\{ 1.5 \left(\dfrac{F_m}{u_s \sqrt{s}} \right)^{1/3},\ 3d_s \dfrac{v_s}{u_s} \right\} & \textit{Stable} \end{cases}$$

where, h_s = actual physical stack height (m)
s = stability parameter[41,51] and is only used in calculations for stable conditions (classes E and F):

$$s = \frac{g}{T_a} \begin{cases} 0.020 & StabilityClassE \\ 0.035 & StabilityClassF \end{cases}$$

where the constants 0.02 and 0.035 are default approximations of the derivative of the ambient potential temperature with respect to height.

If the stack gas temperature is greater than the ambient air temperature, then the determination of which force is dominating is made by calculating a critical crossover temperature difference DT_c above which it is assumed that buoyancy dominates. This critical value depends on the stack gas temperature, atmospheric stability, and the magnitude of the buoyant flux itself in a chain of empirical formulas[50-54] as follows:

$$\Delta T_c = \begin{cases} 0.0297 T_s \dfrac{v_s^{1/3}}{d_s^{2/3}} & Unstable\ or\ neutral, F_b<55 \\ 0.00575 T_s \dfrac{v_s^{2/3}}{d_s^{1/3}} & Unstable\ or\ neutral, F_b \geq 55 \\ 0.019582 T_s v_s \sqrt{s} & Stable \end{cases}$$

$$h_e = h_s + \begin{cases} 21.425 \dfrac{F_b^{3/4}}{u_s} & Unstable\ or\ neutral, F_b<55 \\ 38.71 \dfrac{F_b^{3/5}}{u_s} & Unstable\ or\ neutral, F_b \geq 55 \\ 2.6 \left(\dfrac{F_b}{u_s\ s} \right)^{1/3} & Stable \end{cases}$$

If the difference between the stack gas temperature and the ambient air is less than the critical temperature, then it is assumed that momentum dominates, and the equations above are used. Otherwise, the effective stack height is given by these equations:

$$x_f = \begin{cases} 49\ F_b^{5/8} & \textit{Buoyancy rise, Unstable or neutral, } F_b<55 \\ 119\ F_b^{2/5} & \textit{Buoyancy rise, Unstable or neutral, } F_b \geq 55 \\ 2.0715 \dfrac{u_s}{\sqrt{s}} & \textit{Buoyancy rise, Stable} \\ 0 & \textit{Momentum rise, all stability classes} \end{cases}$$

Past a certain distance the plume is assumed to stop rising. This distance is called the distance to final rise (x_f) and is calculated in a similar method as for the plume rise. The calculation is dependent on which force dominates, the atmospheric stability class, and the magnitude of the buoyant flux. It is estimated by the following:

The estimated distance-dependent plume rise is the minimum of the effective stack height for final rise and the height based on that for buoyancy-dominated conditions.[55] The distance-dependent plume effective stack height $h_e(x)$ is this:

$$h_e(x) = \min \left\{ h_e \ ,\ h_s + 1.60 \left(F_b^{1/3} \ \frac{x^{2/3}}{u_s} \right) \right\}$$

This is sometimes referred to as the "2/3 law" of plume rise[51] and follows from the assumptions that buoyancy is conserved and that the initial plume momentum is negligible for a very buoyant plume in unstratified surroundings. It is claimed[56,57] that the constant 1.60, based on the best fit to data in Table II of Briggs[51], can be expected to be accurate within 40 percent with variations due to downwash or local terrain effects.

M.2.1.3 Estimation of Air Concentration Accounting for Plume Depletion. The method used is that developed in Rao.34 All estimations of concentration and deposition originate from the steady-state form of the atmospheric advection-diffusion equation:

$$U\ C_x = K_y\ C_{yy} + K_z\ C_{zz} + W\ C_z$$

where, $C(x,y,z)$ = pollutant concentration at (x,y,z)

x = downwind distance
y = horizontal crosswind distance
z = vertical distance
U = the constant average wind speed for the hour
W = the gravitational settling velocity (cm/g)
K_y = the eddy diffusivity in the crosswind direction
K_z = the eddy diffusivity in the vertical directions

For a continuous point source of strength Q located at (0,0,H), the assumed boundary conditions are defined by this equation:

$$C(0,y,z) = \frac{Q}{U}\,\delta(y)\,\delta(z-H)$$

$$C(\infty,y,z) = C(x,\pm\infty,z) = C(x,y,\infty) = 0$$

$$\left[K_z C_z + WC\right]_{z=0} = \left[V_d C\right]_{z=0}$$

where, U = wind speed (m/s)
V_d = depositional velocity (cm/s)
H = height above the ground

The first condition is the limiting condition of the mass continuity equation at the source, with d being the Dirac delta "function". This condition is implicated by the assumption that the source is coming from an infinitely small point located at height H above the ground.

The second condition (actually three separate boundary conditions) is equivalent to the assumption that for all times the concentration of the pollutant is zero infinitely far away from the source in all directions.

The final condition is the one that accounts for possible depletion of the plume. It is the mathematical formulation of the assumption that at ground level (z=0) the sum of the turbulent transfer of pollutant down the concentration gradient (K_z C_z) and the downward settling flux due to the particles' weight (W C) is balanced by the net flux of material to the surface resulting from an exchange between the atmosphere and the surface.[58] The deposition velocity V_d is the parameter that is assumed to characterize the interaction between the diffusing pollutant and the surface. If the deposition velocity is 0, then the lower boundary acts as a perfect reflector. If it is infinite, it acts as a perfect sink. If the deposition velocity

is equal to the settling velocity, then the net deposition due to vertical diffusion is zero. For gases and small particles, the settling velocity is approximately 0, while for particles the settling and deposition velocities are estimated using the CARB algorithms[59] that represent empirical relationships for transfer resistances as a function of particle size, density, surface roughness, and friction velocity.

It is not difficult to derive an analytic expression for the solution of the advection-diffusion equation satisfying the boundary conditions above, with the solution involving nothing more complicated than exponential and error functions.

The eddy diffusion coefficients are expressed in terms of the standard deviations of the crosswind and vertical Gaussian concentration distributions (s_y and s_z, respectively), for which extensive empirical data exist. In particular, for Fickian diffusion34 the relationships are these:

$$K_y = \sigma_y^2(x) \frac{U}{2x} \quad , \quad K_z = \sigma_z^2(x) \frac{U}{2x}$$

In practice the dependence of the standard deviations on the downwind distance is not usually explicitly noted. Also, as is standard in the atmospheric dispersion literature, the partial differential equation is solved as if the eddy diffusion coefficients do not depend on the downwind distance x. In fact, the solution to the advection-diffusion equation would be different were this dependence considered, with the magnitude of difference between the two solutions depending on how "nonconstant" the standard deviations are with respect to x (i.e., on the magnitude of the derivative of the eddy diffusion coefficients with respect to x).

It is assumed that the plume is allowed to travel in a potentially vertically bounded layer called the mixing layer (sometimes called the Ekman layer).[49] The height of this layer is called the mixing height, denoted here by L. If the effective stack height exceeds the mixing height, then the plume is assumed to fully penetrate the elevated inversion and the ground level concentration is set to zero. The mixing height is estimated based on twice-daily mixing heights using the RAMMET program, which uses the Holzworth[60] procedures. These mixing heights are considered representative in rural areas only during periods of instability or neutral stability (stability classes A-D). The applicability of the Holzworth method to rural areas with stable atmospheric conditions is considered questionable, because the

minimum mixing heights include the heat island effect for urban areas. In this case, unlimited vertical mixing is assumed.

Depending on the atmospheric stability class and mixing layer depth, the air concentration was estimated in three different ways, all of which are derived from the analytic solution of the original advection-diffusion equation above. The methods are summarized in Table M-9.

Only the vertical diffusion field was modified by deposition, and for deposition velocities on the order of a few centimeters per second, the shape of the vertical concentration profile was modified only slightly.[34]

M.2.1.4 Estimation of the Atmospheric Dispersion Parameters. The dispersion parameters s_y and s_z were estimated using equations that approximately fit the Pasquill-Gifford curves[61] These equations approximately fit the Pasquill-Gifford curves[61] and were based on a rural setting:

$$\sigma_y = 465.11628\ x\ \tan(\vartheta(x))$$

where x is the downwind distance (in km), and

$$\vartheta(x) = 0.017453293(\ c - d\ \ln x).$$

The parameters c and d depend on the stability class and are given in Table M-10. The vertical dispersion parameter is estimated by

$$\sigma_z = a\ x^b$$

where the parameters a and b depend on the stability class, and are given in Table M-11.

M.2.1.5 Deposition Processes. COMPDEP addresses both wet and dry deposition, taking into account the fraction of an hour during which precipitation occurs.

Table M-9. The Three Main Cases for Determining Air Concentration With Plume Depletion Effects

Condition	Criteria of Determination	Method of Solution
Stable or unlimited mixing	Pasquill classes E or F or unstable/neutral and L>5000 m	Analytic solution used.
Unstable/neutral, non-uniform mixing	Pasquill classes A-D,s_z <1.6 L and L<5000 m	Multiple eddy reflections from both the ground and stable layer aloft (plume is "trapped")
Unstable/neutral, limited and uniform mixing	Pasquill classes A-D,s_z >1.6 L and L<5000 m	Non-uniform vertical term integrated with limited mixing from height 0 to infinity

Table M-10. Parameters Used to Calculate Horizontal Dispersion Parameter s_y in COMPDEP[61]

Pasquill Stability Class	c	d
A	24.1670	2.5334
B	18.3330	1.8096
C	12.5000	1.0857
D	8.3330	0.72382
E	6.2500	0.54287
F	4.1667	0.36191

The air concentrations are calculated accounting for plume depletion from dry deposition. The dry deposition rate, in g/m^2/time, is given by the product of the deposition velocity, the air concentration and the fraction of the hour during which precipitation does not occur. For particles, the settling and deposition velocities were estimated using the CARB algorithms[59] that represent empirical relationships for transfer resistances as a function of particle size, density, surface roughness and friction velocity. In general, the deposition velocity has values that can range from zero up to 180 cm/s.[62] COMPDEP calculates the annual wet deposition flux according to the method developed by Slinn[63] and later modified by PEI and Cramer.[64] The scavenging

Table M-11. Parameters Used to Calculate Vertical Dispersion Parameter s_z in COMPDEP[61]

Pasquill Stability Class	x (km)	a	b
A[a]	<0.10	122.800	0.94470
	0.10 - 0.15	158.080	1.05420
	0.16 - 0.20	170.220	1.09320
	0.21 - 0.25	179.520	1.1262
	0.26 - 0.30	217.410	1.26440
	0.31 - 0.40	258.890	1.40940
	0.41 - 0.50	346.750	1.72830
	0.51 - 3.11	453.850	2.1160
	>3.11	[b]	[b]
B[a]	<0.20	90.673	0.93198
	0.21 - 0.40	98.483	0.98332
	>0.40	109.300	1.09710
C[a]	All	61.141	0.91465
D[a]	<0.30	34.459	0.86974
	0.31 - 1.00	32.093	0.81066
	1.01 - 3.00	32.093	0.64403
	3.01 - 10.00	33.504	0.60486
	10.01 - 30.00	36.650	0.56589
	>30.00	44.053	0.51179
E[a]	<0.10	24.260	0.83660
	0.11 - 0.30	23.331	0.81956
	0.31 - 1.00	21.628	0.75660
	1.01 - 2.00	21.628	0.63077
	2.01 - 4.00	22.534	0.57154
	4.01 - 10.00	24.703	0.50527
	10.01 - 20.00	26.970	0.46713
	20.01 - 40.00	35.420	0.37615
	>40.00	47.618	0.29592
F[a]	<0.20	15.209	0.81558
	0.21 - 0.70	14.457	0.78407

Table M-11. Continued

Pasquill Stability Class	x (km)	a	b
	0.71 - 1.00	13.953	0.68465
	1.01 - 2.00	13.953	0.63227
	2.01 - 3.00	14.823	0.54503
	3.01 - 7.00	16.187	0.46490
	7.01 - 15.00	17.386	0.41507
	15.01 - 30.00	22.651	0.32681
	30.01 - 60.00	27.074	0.27436
	> 60.00	34.219	0.21716

[a] If the calculated value of s_z exceeds 5000 m, then it is set to 5000 m.
[b] s_z is set to 5000 m.

process consists of repeated exposures of particles and gases to cloud or precipitation elements with some chance of collection on the element for each exposure.[65] This has been addressed historically as a first order decay process with decay constant L, called the scavenging coefficient (units of inverse time). The concentration at any distance x downwind is then given by $C(x,y,z)\ exp(-L\ t)$, where $C(x,y,z)$ is the (steady-state) concentration without scavenging and t is the time since precipitation began.[41] For the purpose of modelling, t was replaced with x/u_s (the travel time to the receptor); thus, the decay is essentially accounting for previous scavenging upwind of the receptor.

The wet deposition flux Dyw at a given location is

$$Dyw = \Lambda \int_0^z C(x,y,z)\ e^{-\Lambda\ t} dz$$

where z is the height from which the precipitation falls. Because it was assumed that the effects of dry deposition and gravitational settling are negligible compared with precipitation scavenging, the concentration used was that without deposition effects (deposition and settling velocities set to zero). To facilitate evaluation of the integral, it was extended to infinity as an approximation. The deposition flux for a given hour then reduces to this equation:

$$Dyw = f \Lambda Q R_{DW} e^{-\Lambda \frac{x}{u_s}}$$

where, f = the fraction of the hour that precipitation occurs

R_{DW} = the integrated vertical relative concentration (unit source strength) without depletion effects

R_{DW} can be calculated by these equations:

$$R_{DW} = \begin{cases} \dfrac{\exp\left(-0.5\ y^2/\sigma_y^2\right)}{u_s \sigma_y \sqrt{2\pi}} & \textit{Simple or intermediate terrain} \\ \dfrac{1}{2\pi u_s x/16} & \textit{Complex terrain (sector-averaged)} \end{cases}$$

As noted in PEI and Cramer[64], there are several assumptions in deriving the equation for wet deposition.

1) The intensity of precipitation is constant over the entire path between the source and receptor.

2) The precipitation originates at a level above the top of the plume so that hydrometeors (i.e., products formed by condensation of water vapor) pass vertically through the entire plume.

3) The time duration of the precipitation over the entire path between the source and the receptor point is such that exactly f (f is defined as the fraction of the hour in which precipitation occurs) of the hourly emission is subject to a constant intensity for the entire travel time required to traverse the distance between the source and the receptor. The remaining fraction is subject only to dry deposition processes.

In COMPDEP, the scavenging coefficient may be intensity- and particle-size dependent, in which case the total wet deposition is the sum of the contributions of each category particle size category. For particles, example scavenging coefficients are from PEI and Cramer[64] and are shown in Table M-12. Only a small fraction of the pollutants of concern for this exposure assessment

Table M-12. Example of Precipitation Scavenging Coefficients (per second) in COMPDEP

Precipitation Intensity	Particle Size Category (mM)		
	Less than 2	2 to 10	Greater than 10
Heavy	1.46E-03	4.64E-03	9.69E-03
Moderate	5.60E-04	8.93E-04	9.69E-03
Light	2.20E-04	1.80E-04	9.69E-03

are particulate or particulate-bound. Estimation of the scavenging coefficients for vapor phase pollutants are discussed in Section M.2.2.1.

M.2.1.6 Treatment of Terrain. The "COMP" in the name COMPDEP refers to the capability of the model to estimate concentrations and deposition at receptor locations at or above stack top. This can be done in three ways: (1) the effective stack height may be modified based on the receptor height; (2) the concentrations may be reduced by a height-dependent correction factor for receptors above the stack top; and (3) sector-averaging is used for receptors above stack top.

The method of adjusting the effective stack height H_t is based on models developed by Briggs[66] and Egan[67]. With this method the amount of reduction depends on the receptor height and empirical terrain adjustment factors.

$$H_t = \max\{H - r_h \cdot (1 - ter),\ H \cdot ter,\ H_{min}\}$$

where, H = the effective stack height calculated without considering terrain

r_h = the height of the receptor above the stack base

ter = stability-class dependent terrain adjustment factor

H_{min} = the minimum distance between the plume centerline and ground.

Following standard practice, $H_{min}=10$ m.

The terrain adjustment factors used in the exposure assessment are consistent with the method of Egan[67] and are shown in Table M-13. By choosing these terrain factors in neutral and unstable conditions the effective stack height is reduced by $r_h/2$

Table M-13. Terrain Adjustment Factors Used in Calculating Terrain-Dependent Effective Stack Height

Pasquill Stability Class	Terrain Adjustment Factor (unitless)
A	0.5
B	0.5
C	0.5
D	0.5
E	0
F	0

or *H/2*, whichever is smaller. It should be noted that Briggs[66] suggests that the stack height be reduced by r_h or *H/2*, whichever is smaller. Briggs' method will result in slightly higher ground-level concentrations for the surface of small hills.[41] It should also be noted that the reduction by *H/2* is based on potential flow theory and wind-tunnel experiments.[41] Both Egan's and Briggs' methods assume terrain factors of zero for stable conditions, in which case it is assumed that the plume maintains a constant elevation (and so the effective height is reduced by the receptor height).

For receptors whose ground level elevation exceeds the effective stack height, the concentrations and deposition rates are multiplied by a "correction" factor *corr*, given by this:

$$corr = \begin{cases} (400 - Diff)/400 & 0 < Diff < 400m \text{ and Stable conditions} \\ 0 & Diff \geq 400m \text{ and Stable conditions} \\ 1 & \text{Unstable or neutral conditions} \end{cases}$$

where *Diff* is the difference between receptor ground level elevation and the effective stack height. Thus, in stable conditions (Pasquill stability classes E or F) the concentrations and deposition rates were assumed to be zero if the receptor is 400 m above the effective stack height. Although the exact origin of this method is not clear, it is used in the Valley dispersion model (one of the precursors of COMPDEP), where it is observed that the application of the correction factor in stable conditions should not be inferred to represent pollutant decay or penetration into the terrain. This is an empirical scheme intended as a general representation of the blocking of air flow by significant terrain features. Furthermore, the concentrations

calculated for the leeward side of a substantial hill will not reflect this attenuation upwind, and so such concentrations should be considered suspect.

By setting the correction factor to one in unstable or neutral atmospheric stability conditions, the plume was assumed to parallel the terrain feature at the terrain-dependent effect stack height as calculated above.

For terrain above the effective stack height, sector averaging was used to calculate the air concentration and was subsequently used for deposition. This assumes that there is no crosswind variation in concentration within an angular sector equal to the resolution of the wind direction data (22.5 degrees for this assessment). It should be noted that there was no technical basis for using sector averaging for terrain above stack height rather than point estimates for the horizontal dispersion parameters. This decision was made consequent to personal communication with Donna Schwede (7-20-94).

M.2.1.7 Downwash. Usually, emissions from an industrial source will rise due to a combination of their initial vertical momentum and buoyancy. Under certain peculiar conditions, however, they may be trapped in either the wake of the stack or nearby building, resulting in increased concentrations. Two types of these phenomena are addressed in COMPDEP: stack-tip downwash and building downwash (building wake effects).

Stack-tip Downwash. In practice, it has been observed that if the stack exit velocity is low relative to the wind speed, then the stack emissions may be pulled into the low pressure cavity in the wake of the stack. The emissions are pulled down and may not rise further, resulting in higher ground level concentrations than if plume rise had occurred. In COMPDEP, this phenomenon was assumed to occur when the ratio of the stack exit velocity to the wind speed at stack top was below 1.5. This value, which has survived without modification for 25 years, is that recommended by Briggs[50] and is based on wind tunnel experiments by Sherlock and Stalker.[68] It should be noted that very buoyant sources may accelerate fast enough to avoid any significant downwash.[33,50]

If stack-tip downwash occurs, then the physical stack height used is that of Briggs[69]:

$$h_s' = h_s + 2d_s \left(\frac{v_s}{u_s} - 1.5 \right)$$

From the above equation it can be seen that the maximum amount the stack height will be reduced by this method is three times the diameter of the stack.

Building Downwash. Building downwash can occur when the stack emittants are captured in the wake of a nearby building. A long-standing rule-of-thumb is that building effects should not occur if the stack height is at least 2.5 times the height of any adjacent building. Because this was considered overly restrictive (from a design perspective) for tall, thin buildings, Briggs[66] proposed a modification of this rule in which building downwash was assumed not to occur if the stack height was greater than the sum of the building height and 1.5 times the minimum of the building height and width.

In the use of COMPDEP for the mercury assessment, building downwash was considered if the plume height, calculated from the sum of the stack height and the distance-dependent plume rise at a distance of two building heights, was greater than either (a) 2.5 times the building height, or (b) the sum of the building height and 1.5 times the building width. If wake effects were predicted, then the effective stack height was reduced by reducing the estimated plume rise. First a distance-dependent plume rise is estimated based on momentum-dominated conditions.[53]

$$\Delta h_p = \begin{cases} \max\left[\dfrac{3v_s d_s}{u_s}, \left(\dfrac{3F_m\, x}{\beta_j^2 u_s^2}\right)^{1/3}\right] & \textit{Unstable or neutral} \\ \max\left[\dfrac{3v_s d_s}{u_s}, \left(3F_m \dfrac{\sin(x\sqrt{s}/u_s)}{\beta_j^2 u_s \sqrt{s}}\right)^{1/3}\right] & \textit{Stable} \end{cases}$$

The effective stack height was then set to the maximum of this value and the distance-dependent buoyancy-dominated effective stack height:

$$h_e = h_s + \max\left\{\Delta h_p \;,\; 1.60\left(F_b^{1/3}\frac{x^{2/3}}{u_s}\right)\right\}$$

The dispersion parameters were also modified based on the dimensions of the building. These modifications are based on Huber and Snyder building downwash procedures[70,71] and are principally based on the results of wind-tunnel experiments using a model building with a crosswind double that of the building height. Because the atmospheric turbulence simulated in the wind-tunnel experiments was intermediate (between a slightly unstable Pasquill C category and neutral D), the data upon which the formulas were based reflect a specific stability, building shape, and orientation with respect to the mean wind direction.[72]

The basic idea was to estimate modified lateral and vertical dispersion parameters, and then use the minimum of these and the dispersion parameters estimated without wake effects. In general, the ratio of the building width to building height plays a key role.

Setting

$$\sigma_y' = \begin{cases} 0.35h_1 + 0.067(x-3h_2) & \text{if } 3h_m \le x \le 10h_m \\ \sigma_y(x+x_y) & \text{if } x \ge 10h_m \end{cases}$$

where h_m is the minimum of the building width and height, and h_1 and h_2 are given by

$$h_1 = \begin{cases} h_b & \text{if } w_b/h_b > 5 \\ w_b & \text{else} \end{cases}$$

and

$$h_2 = \begin{cases} w_b & \text{if } w_b/h_b < 1 \\ h_b & \text{else} \end{cases}$$

and x_y is the lateral virtual distance, given by

$$x_y = \left(\frac{c_w w_b + c_h h_b}{p} \right)^{1/q} - h_m$$

where the coefficients p and q depend on the stability class, and the coefficients c_w and c_h are given by:

$$c_w = \begin{cases} 0.85 & if\ w_b/h_b<1 \\ 0.35 & if\ 1\le w_b/h_b\le 5 \\ 0 & if\ w_b/h_b>5 \end{cases}$$

and

$$c_h = \begin{cases} 0 & if\ w_b/h_b<1 \\ 0.5 & if\ 1\le w_b/h_b\le 5 \\ 0.85 & if\ w_b/h_b>5 \end{cases}$$

The virtual source location was calculated by requiring that $s_y'(10\ h_1) = .35\ h_1 + 0.5\ h_2$.[73]

Table M-14 presents the coefficients used to calculate lateral virtual distances.

The vertical dispersion term is modified similarly.

$$\sigma_z' = \begin{cases} 0.7h_m + 0.067(x-3h_m) & if\ 3h_m\le x\le 10h_m \\ \sigma_z(x+x_z) & if\ x\ge 10h_m \end{cases}$$

where h_m is the minimum of the building width and height, and x_z is the vertical virtual distance, given by

$$x_z = \left(\frac{1.2h_m}{a}\right)^{1/b} - h_m$$

where the coefficients a and b are given in Table M-11 above. The virtual source location x_z is calculated by requiring that $s_z'(10\ h_m) = 1.2\ h_m$[74], and is added in order to account for the enhanced initial plume growth caused by the building wake.[75]

M.2.1.8 Buoyancy-Induced Dispersion. It has been observed that the initial dispersion of plumes may be augmented by turbulent motion of the plume and turbulent entrainment of ambient air. This is addressed by increasing the calculated standard deviations in the crosswind and vertical directions using the method of Pasquill:[76]

Table M-14. Coefficients Used to Calculate Lateral Virtual Distances for Pasquill Dispersion Rates

Pasquill Stability Class	p	q
A	209.14	0.890
B	154.46	0.902
C	103.26	0.917
D	68.26	0.919
E	51.06	0.921
F	33.92	0.919

$$\sigma_{ze} = \left(\sigma_z^2 + \left(\frac{\Delta h}{3.5} \right)^2 \right)^{1/2}$$

$$\sigma_{ye} = \left(\sigma_y^2 + \left(\frac{\Delta h}{3.5} \right)^2 \right)^{1/2}$$

where, s_{ye} = the effective standard deviation of lateral concentration distributions (m) for buoyancy-induced dispersion

σ_{ze} = the effective standard deviation of vertical concentration distributions (m) for buoyancy-induced dispersion

s_y = the standard deviation of lateral concentration distributions (m) without buoyancy effects

s_z = the standard deviation of vertical concentration distributions (m) without buoyancy effects,

Dh = the estimated plume rise (m).

M.2.1.9 Meteorological Data. COMPDEP uses hourly meteorological data to estimate hourly concentrations and deposition rates. If wet deposition is not to be modeled, then the only data file required is one containing hourly values for average wind speed, wind direction, Pasquill stability class, mixing height, and ambient air temperature.

If wet deposition is to be modeled, then a data file containing a summary of the hourly precipitation intensities and fraction of hour for which precipitation occurred is also

required. COMPDEP only considers four precipitation intensity classes. These are summarized in Table M-15.

M.2.2 Application of the COMPDEP Model for the Exposure Assessment

To estimate local mercury concentrations in environmental media, hypothetical sources (model plants) were designed using available information. Each model plant/control scenario/ emission speciation estimate was placed in the hypothetical locations. In this section modifications made to the COMPDEP model for this exposure assessment, as well as parameter values used are discussed.

M.2.2.1 Modifications of COMPDEP for the Exposure Assessment. Several modifications were made to COMPDEP in order to address more effectively the atmospheric deposition of mercury species. These modifications were necessary, because mercury exists primarily in the vapor phase, and the previous version of COMPDEP (version 93340) could not estimate deposition for vapor.

Specification of Vapor phase/Particle-Bound Phase Ratio. This modification consisted of adjusting COMPDEP to allow the user to specify the fractions of the emissions of a particular pollutant that are in vapor phase and particle-bound phase. The modification was necessary because the transport properties of the two phases can be quite different and the forms of mercury considered in this report are primarily in the vapor phase.

Dry Deposition of Vapor Phase Contaminants. The mercury species assumed to be emitted (elemental and divalent mercury) are predominantly in the vapor phase; however, the algorithms in COMPDEP for calculating deposition velocities can only be used for particles. For this reason, COMPDEP was modified so that, for the vapor phase fraction of a pollutant, the user can specify atmospheric stability class-dependent deposition velocities. These were used in the concentration algorithms with plume depletion, with the gravitational settling velocity set to zero as is recommended for gases.34 Section M.2.2.3 gives a description of the deposition velocities used in the exposure assessment.

Wet Deposition of Vapor Phase Contaminants. To estimate wet deposition COMPDEP requires a scavenging coefficient for each pollutant. This scavenging coefficient can depend on the precipitation intensity and particle size. No values are given for gases, for which the scavenging coefficient will depend strongly on the chemical properties of the pollutant in the vapor phase (e.g., solubility).

Table M-15. Precipitation Intensities Considered by COMPDEP

Intensity Class	Precipitation Rate (in/hr)
0	0
1	trace to 0.10
2	0.11 to 0.30
3	greater than 0.30

Modifications were made to COMPDEP to enable the user to specify a unitless washout ratio W for the vapor phase portion of the pollutant. The washout ratio is the ratio of the concentration in air to the concentration in precipitation.

Connection Between the Washout Ratio and Scavenging Coefficient. By definition, the washout ratio W is the ratio of the concentration in surface-level precipitation to the concentration in surface level air.[63] Let C_w and C_a denote the concentrations in surface-level precipitation and surface-level air, respectively (units of g/m^3). Then

$$W = \frac{C_w}{C_a}$$

Using the scavenging coefficient to estimate air concentration during periods of precipitation, the concentration in air is given by this equation:

$$C_a = C\ (x, y, z_s)\ e^{-\lambda t}$$

where, z_s = height of the receptor (m)
x = downwind distance to the receptor
y = crosswind distances to the receptor (m),
t = travel time (seconds) to the receptor
L = scavenging coefficient (units of inverse seconds).

The concentration in precipitation can be approximated by the wet deposition flux divided by the precipitation rate for the time period:

$$C_w = \frac{\Lambda \int_{z_s}^{H} C\ (x,y,z)\ e^{-\Lambda t}\ dz}{P}$$

where, H = height from which the precipitation falls (m) and
P = precipitation rate (m/s).

The washout ratio is then given by these formulae:

$$\frac{\int C\ (x,y,z)\ e^{-\Lambda t}\ dz}{C\ (x,y,z_s)\ e^{-\Lambda t}} = \frac{\Lambda \int_{z_s}^{H} C\ (x,y,z)\ dz}{P\ C\ (x,y,z_s)} = \frac{(\Lambda H)(1/H) \int_{z_s}^{H} C\ (x,y,z)\ dz}{P\ C\ (x,y,z_s)} =$$

where Overline{$C(x,y)$} is the vertically averaged air concentration at (x,y). Assuming that Overline{$C(x,y)$} is approximately equal to $C(x,y,z_s)$, and that the height H is the mixing height H_L, the equation reduces to

$$W = \frac{\Lambda H_L}{P}$$

and conversely

$$\Lambda = \frac{W P}{H_L}$$

Because only the intensity classes (0-3) of the precipitation were assumed to be in the precipitation data file, the user must specify the representative precipitation rate for each intensity class.

For a discussion of the washout ratios used in this study see M.2.2.3.

M.1.2.2 Meteorological Data and Receptor Locations Relative to Local Source. For both of the locations, meteorological data

were obtained for one year (1989). The types of data files and their use are described in Table M-16.

M.2.2.3 Vapor Deposition Parameters Dry Deposition Velocities. The dry deposition velocities for divalent vapor were based on those used by the RELMAP model and were estimated based on assumed similar deposition properties of nitric acid. Deposition velocities depend on the season, land use, time of day, and stability class. Table M-17 shows the seasonally-averaged deposition velocities as a function of land-use. Dry deposition rate is proportional to the dry deposition velocities. In order to address the fact that deposition is lower during nighttime conditions, it was assumed that the deposition velocity for divalent vapor was 0.3 cm/s for stability classes D-F, which occur primarily at night, and 1 cm/s for stability classes A-C.

Washout Ratios. For this assessment, it was assumed that both elemental and divalent mercury species would be deposited via wet deposition. Because of its higher solubility, the divalent form would be washed out at significantly higher rates. The washout ratio is a function of the concentration, total carbon, and ozone air distribution. For divalent vapor, a washout ratio of 1.6×10^6 was used, while for the elemental phase a value of 1.6×10^4 was used; this was roughly the average of the washout ratio for elemental vapor for both locations (see Section M.1).

In order to calculate the scavenging coefficient, the precipitation rate for the hour is required. In the precipitation data file, the precipitation rate is classified as either none, light (trace to 0.1 in/hr), moderate (0.11 to 0.3 in/hr), or heavy (greater than 0.3 in/hr). Thus, a representative precipitation rate is required and is specified by the version of COMPDEP modified for this assessment. For the light and moderate categories, the midpoint of the range was used, while for the heavy category the representative rate was assumed equal to 0.3 in/hr.

An informal examination of the scavenging coefficients computed for divalent vapor (using the representative rates discussed above) showed that they were in the same range as the upper end scavenging coefficients for particles as estimated by PEI and Cramer.[64] Table M-16 presents divalent mercury vapor deposition velocities. It was assumed that the elemental mercury vapor has a dry deposition velocity of zero.

Table M-16. Description of Meteorological Files Used to Make Input Files for COMPDEP

Data File	Use
Hourly surface observations (CD144)	Used by RAMMET program to create meteorological data file. Used by ORNL precipitation preprocessor to create precipitation data file for wet deposition calculations.
Mixing Height Data file	Used by RAMMET to create meteorological data file.

Table M-17. Divalent Mercury Vapor Seasonally-Averaged Deposition Velocities (cm/s)

Land-use	Pasquill Stability Class					
	A	B	C	D	E	F
Urban	4.63	4.59	4.36	4.03	2.46	0.36
Agricultural	1.81	1.77	1.63	1.42	0.61	0.20
Range	1.71	1.68	1.54	1.34	0.56	0.19
Deciduous Forest	3.45	3.40	3.14	2.80	1.39	0.29
Coniferous Forest	3.45	3.40	3.14	2.80	1.39	0.29
Mixed forest/wetland	3.32	3.27	3.06	2.77	1.54	0.29
Water	1.00	0.98	0.89	0.77	0.31	0.13
Barren Land	1.07	1.06	0.97	0.85	0.31	0.18
Non-forested wetland	1.92	1.89	1.77	1.59	0.85	0.21
Mixed agric./rangeland	1.76	1.73	1.59	1.39	0.58	0.19
Rocky open areas	1.94	1.90	1.74	1.51	0.59	0.20

M.2.2.4 Other Parameters Used in Air Modeling. This section presents the values for all parameters not already discussed that were used in the air modeling for all of the model plants. These are given in Tables M-18 to M-20.

M.3 Description of the IEM2 Indirect Exposure Methodology

Atmospheric mercury concentrations and deposition rates estimated from RELMAP and COMPDEP drive the calculations of mercury in watershed soils and surface waters. The soil and water concentrations, in turn, drive calculations of concentrations in the associated biota and fish, which humans and other animals are assumed to consume. These "indirect" exposure

Table M-18. Air Modeling Parameter Values Used In the Exposure Assessment: Generic Parameters

Parameter	Value Used in Exposure Assessment
Particle Density (g/cm^3)	1.8
Surface Roughness Length (m)[a]	0.30
Anemometer Height (m)	10
Wind Speed Profile Exponents	
Stability Class A	0.07
Stability Class B	0.07
Stability Class C	0.10
Stability Class D	0.15
Stability Class E	0.35
Stability Class F	0.55
Terrain Adjustment Factors	
Stability Class A	0.5
Stability Class B	0.5
Stability Class C	0.5
Stability Class D	0.5
Stability Class E	0
Stability Class F	0
Distance Limit for Plume Centerline (m)	10
Model Run Options	
Terrain Adjustment	Yes
Stack-tip Downwash	No
Building Wake Effects	No
Transitional Plume Rise	Yes
Buoyancy-induced dispersion	Yes
Calms Processing Option	No

[a] This is used to estimate deposition velocities for particles.

Table M-19. Model Plant Parameter Values Used in COMPDEP

Plant Type	Stack Height (ft)	Stack Diameter (ft)	Stack Exit Temperature (F)	Stack Exit Velocity (m/s)	Total Mercury Emission Rate (kg/yr)
Large Municipal Waste Combustor	230	10	285	21.9	1330
Small Municipal Waste Combustor	140	5	375	21.9	170
Continuous Medical Waste Incinerator	40	3	1500	7.3	80
Intermittent Medical Waste Incinerator	40	1	1500	7.3	2.4
Large Coal-fired Utility Boiler	732	27	273	31.1	230
Medium Coal-fired Utility Boiler	465	18	275	26.7	90
Small Coal-fired Utility Boiler	266	12	295	6.6	10
Medium Oil-fired Utility Boiler	290	14	322	20.7	2
Chlor-alkali Plant	10	1	Ambient[a]	0.1	380
Primary Copper Smelter	505	15	430	6	536
Primary Lead Smelter	350	20	347	2.80	2680

[a] Average annual temperature was used (see Appendix B).

Table M-20. Model Plant Mercury Speciation of Emissions

Plant Type	Speciation of Emissions			Speciation of Emissions: "Error-Bounding Estimate"		
	% Elemental Mercury Vapor	% Divalent Mercury Vapor	% Divalent Particulate	% Elemental Mercury Vapor	% Divalent Mercury Vapor	% Divalent Particulate
Large Coal-fired Utility Boiler	50	30	20	85.00	15.00	0.00
Medium Coal-fired Utility Boiler	50	30	20	85.00	15.00	0.00
Small Coal-fired Utility Boiler	50	30	20	85.00	15.00	0.00
Medium Oil-fired Utility Boiler	50	30	20	85.00	15.00	0.00

calculations were modified from the Indirect Exposure Document[77] as updated in an Addendum (in preparation). Relevant sections of the updated methodology, IEM2, are described below. The equations were implemented in a spreadsheet and parameterized.

IEM2 uses atmospheric chemical loadings to perform mass balances on a watershed soil element and a surface water element, as illustrated in Figure M-1. The mass balances were performed for total mercury, which was assumed to speciate into three components: Hg^0, Hg(II), and methylmercury. The fraction of mercury in each of these components was specified for the soil and the surface water elements. Loadings and chemical properties were given for the individual mercury components, and the overall mercury transport and loss rates are calculated by the methodology.

IEM2 first performs a terrestrial mass balance to obtain mercury concentrations in watershed soils. Soil concentrations were used along with vapor concentrations and deposition rates to calculate concentrations in various food plants. These were used, in turn, to calculate concentrations in animals. IEM2 next performs an aquatic mass balance driven by direct atmospheric deposition along with runoff and erosion loads from wateshed soils. Methylmercury concentrations in fish were derived from total dissolved water concentrations using bioaccumulation factors (BAF).

IEM2 was developed to handle individual chemicals, or chemicals linked by kinetic transformation reactions. The kinetic transformation rates affecting mercury components in soil, water, and sediments – oxidation, reduction, methylation, and demethylation – were considered too uncertain to implement in this study. For this study, the methodology was expanded to handle multiple chemical components in a steady-state relationship. The fraction of each chemical component in the soil and water column was specified by the user. The methodology predicts the total chemical concentration in watershed soils and the water body based on loading and dissipation rates specified for each of the components.

The nature of this methodology is basically steady with respect to time and homogeneous with respect to space. While it tracks the buildup of watershed soil concentrations over the years given a steady depositional load and long-term average hydrological behavior, it does not respond to unsteady loading or meteorological events. There are, thus, limitations on the analysis and interpretations imposed by these simplifications.

Figure M-1. Overview of the IEM2 Watershed Modules

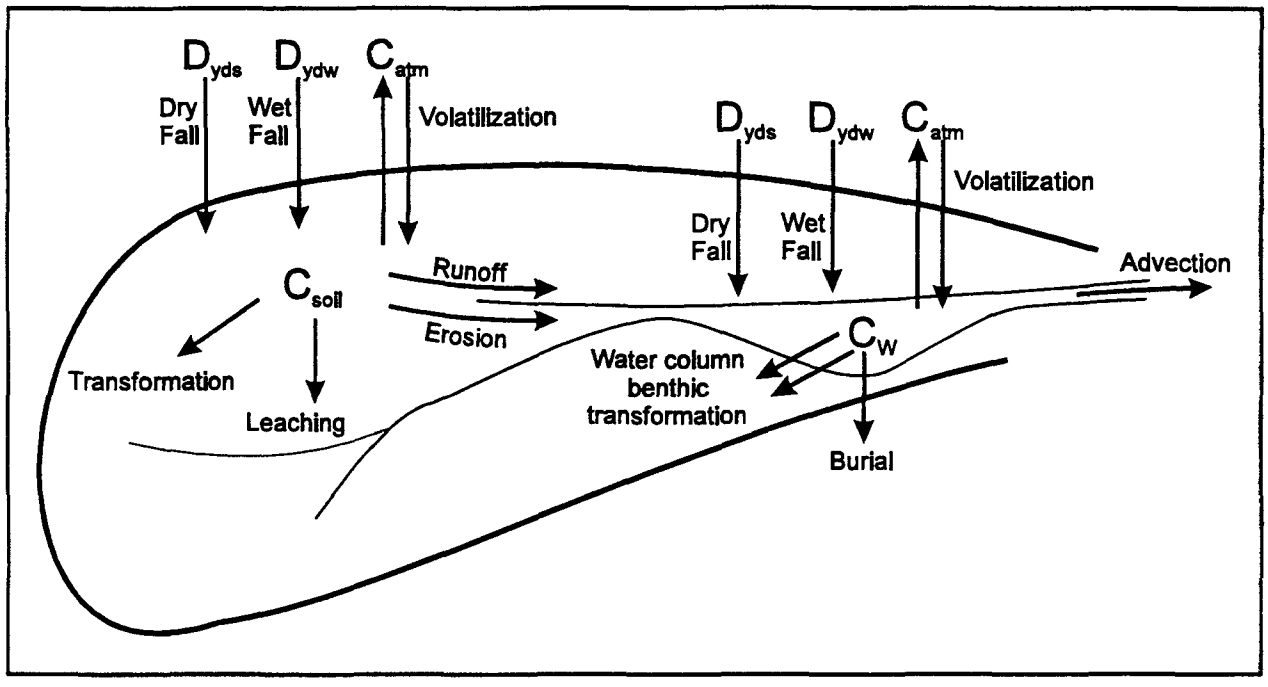

Definitions for Figure M-1

C_{soil}	chemical concentration in upper soil	mg/L
C_w	chemical concentration in water body	mg/L
C_{atm}	vapor phase chemical concentration in air $\mu g/m^3$	
D_{yds}	average dry deposition to watershed	mg/yr
D_{yws}	average wet deposition to watershed	mg/yr

The methodology cannot be used to predict the response to reduction or elimination of loadings. The model's calculations of average water body concentrations are less reliable for unsteady environments, such as streams, than for more steady environments, such as lakes.

M.3.1 The Terrestrial Equations

The IEM2 framework for estimating watershed soil impacts from stack emissions calculates surface soil concentrations, including dissolved and sorbed phases, as illustrated in Figure M-2. The model accounts for three routes of contaminant entry into the soil: deposition of particle-bound contaminant through dryfall; deposition through wetfall; and diffusion of vapor phase contaminant into the soil surface. The model also accounts for five dissipation processes that remove contaminants from the surface soils: decay of total contaminants (sorbed + dissolved) within the soil horizon; volatilization (diffusion of gas phase out of the soil surface); runoff of dissolved phase from the soil surface; leaching of the dissolved phase through the soil horizon; and erosion of particulate phase from the soil surface. Key assumptions in the watershed soil impact algorithm were these:

- Soil concentrations within a depositional area are assumed to be uniform within the area, and can be estimated by the following key parameters: dry and wet contaminant deposition rates, a wind-driven gaseous exchange rate with the atmosphere, a soil dissipation rate, a soil bulk density, and a soil mixing depth.

- The partitioning of the contaminant within the soil/water matrices can be described by partition coefficients.

M.3.1.1 Chemical Mass Balance in Watershed Soils. A mass balance equation can be written for total mercury in watershed soils, balancing areal deposition fluxes with chemical loss processes:

$$Sc = \frac{L_W}{ks\ Z\ BD}\ (1 - e^{-ks\ Tc})\ 100 + C_{sb}$$

Figure M-2. Overview of the IEM2 Soils Processes

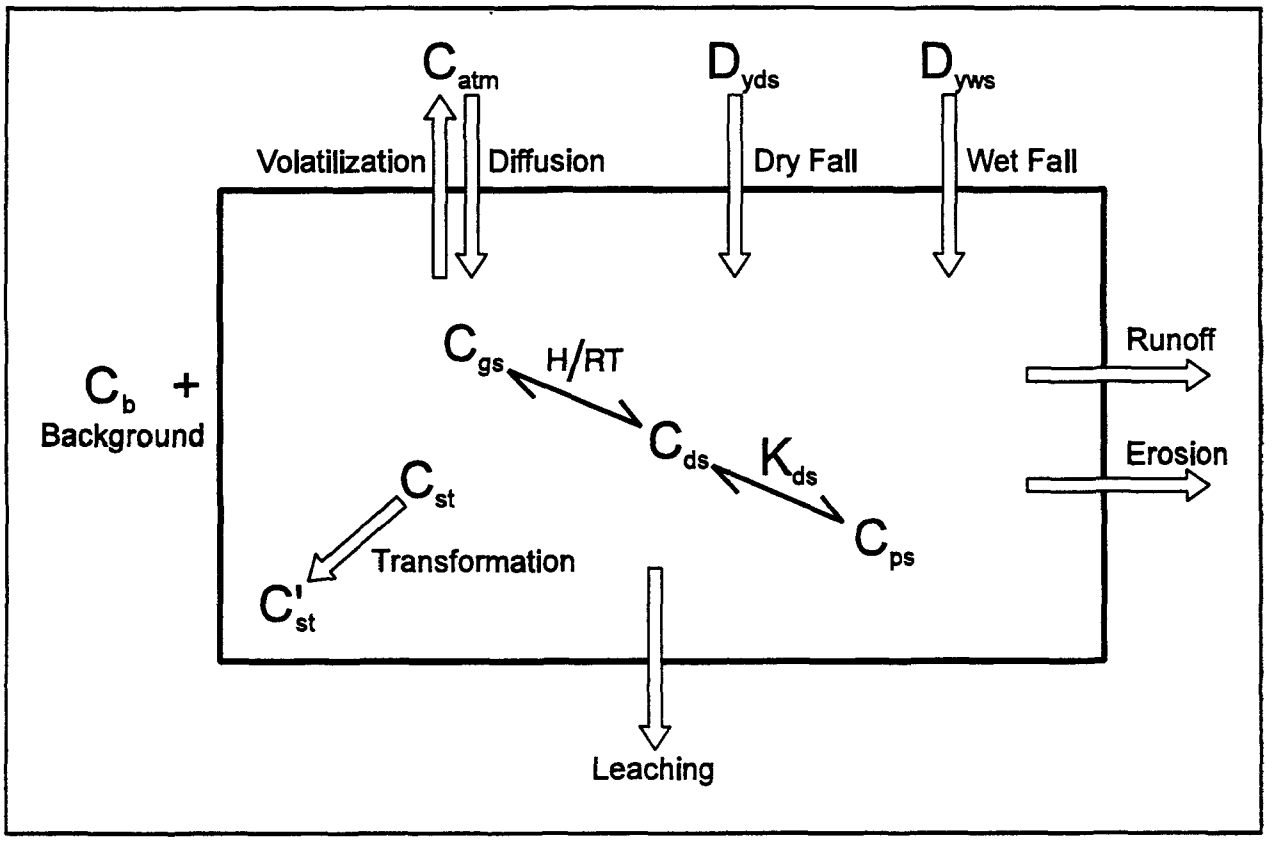

Definitions for Figure M-2

C_{atm}	vapor phase chemical concentration in air	$\mu g/m^3$
D_{yds}	average dry deposition to watershed	mg/yr
D_{yws}	average wet deposition to watershed	mg/yr
C_{st}	total chemical concentration in soil	mg/L
C_{st}'	reaction product concentration in soil	mg/L
C_b	background chemical concentration in soil	mg/L
C_{gs}	chemical concentration in soil gas	$\mu g/m^3$
C_{ds}	chemical concentration in soil water	mg/L
C_{ps}	chemical concentration on soil particles	$\mu g/g$
H	Henry's Law constant	atm-m^3/mole
R	universal gas constant	atm-m^3/mole-°K
T	temperature	°K
K_{ds}	soil/water partition coefficient	L/kg

where:

Sc	=	average watershed soil concentration after time period of deposition (µg pollutant/g soil)
L_w	=	yearly average load of pollutant to watershed on an areal basic (g pollutant/m^2-yr)
ks	=	total chemical loss rate constant from soil (yr^{-1})
Tc	=	total time period over which deposition has occurred (yr)
Z	=	representative watershed mixing depth to which deposited pollutant is incorporated (cm)
BD	=	representative watershed soil bulk density (g/cm^3)
100	=	units conversion factor (µg-m^2/g-cm^2)
C_{sb}	=	background "natural" soil concentration (µg pollutant/g soil)

The first term in the equation represents the steady-state concentration achieved after a sufficient period of constant loading. The exponential term gives the fraction of the steady-state response achieved after Tc years of loading. The final term gives the natural background concentration found in soils. The background soil concentration of mercury was assumed to be negligible in this study. The major terms in this equation are discussed in sections below.

M.3.1.2 Equilibrium Speciation in Watershed Soils. Total mercury in the soil was assumed to be distributed among three components – Hg^0, Hg(II), and methylmercury. The steady-state fraction of the total in each component is specified by the user, so that:

$$Sc_{Hg^0} = Sc \cdot f_{s1}$$

$$Sc_{Hg(II)} = Sc \cdot f_{s2}$$

$$Sc_{MeHg} = Sc \cdot f_{s3}$$

where:

Sc	=	soil concentration of total mercury (µg pollutant/g soil)
Sc_{Hg0}	=	soil concentration of elemental mercury (µg pollutant/g soil)

$Sc_{Hg(II)}$ = soil concentration of divalent mercury (µg pollutant/g soil)
Sc_{MeHg} = soil concentration of methylmercury (µg pollutant /g soil)
f_{s1} = fraction of soil concentration that is elemental mercury
f_{s2} = fraction of soil concentration that is divalent mercury
f_{s3} = fraction of soil concentration that is methylmercury

The total concentration of each mercury component in soil was assumed to reach equilibrium between its particulate and aqueous phases according to the following equations:

$$C_{st,i} = Sc_i \, BD$$

$$C_{ps,i} = C_{ds,i} \, Kd_{s,i}$$

$$C_{ps,i} = \frac{Sc_i \, Kd_{s,i} \, BD}{\theta_s + Kd_{s,i} \, BD}$$

$$C_{ds,i} = \frac{Sc_i \, BD}{\theta_s + Kd_{s,i} \, BD}$$

Where:
Sc_i = total soil concentration of component "i" (µg/g)
θ_s = volumetric soil water content (L_{water}/L)
$Kd_{s,i}$ = soil/water partition coefficient for component "i" (L/kg)
BD = soil bulk density (g/cm^3)
$C_{st,i}$ = total soil concentration of component "i" (mg/L)
$C_{ds,i}$ = concentration of "i" dissolved in pore water (mg/L)
$C_{ps,i}$ = concentration of "i" in particulate phase (mg/kg)

A derivation of the soil equilibrium equations is given in Section M.3.3.2.

M.3.1.3 Loads to Watershed Soils. The total pollutant load term L_W in the mass balance equation is the sum of the loadings for each component "i." Component loadings include wetfall and

dryfall fluxes, atmospheric diffusion fluxes and internal transformation loads:

$$L_{W,i} = Dydw_i + Dyww_i + L_{Is,i} + L_{DIF,i}$$

where:

$Dydw_i$ = yearly average dry depositional flux of component "i" (g/m^2-yr)

$Dyww_i$ = yearly average wet depositional flux of component "i" (g/m^2-yr)

$L_{Is,i}$ = internal transformation load of component "i" per areal basis (g/m^2-yr)

$L_{DIF,i}$ = atmospheric diffusion flux of component "i" to soil (g/m^2-yr)

Internal transformation loads are set to 0 in the equilibrium component approach. Wet and dry depositional fluxes were determined by measurement or by air modeling and were specified as input to this model. The load due to vapor diffusion is given as the following:

$$L_{DIF,i} = 0.31536\ K_{t,i}\ C_{atm,i}$$

where:

$L_{DIF,i}$ = atmospheric diffusion flux of component "i" to soil (g/m^2-yr)

$K_{t,i}$ = gas phase mass transfer coefficient for component "i" (cm/s; see Eq [4-6], IED)

$C_{atm,i}$ = gas phase atmospheric concentration for component "i" ($\mu g/m^3$)

M.3.1.4 Loss Processes in Watershed Soils

The total chemical loss rate constant ks in the soil mass balance equation is the weighted sum of the chemical loss rate constants for each component "i":

$$ks = \sum_i ks_i \cdot f_{si}$$

where:

ks_i = total soil loss constant for component "i" (yr^{-1})

f_{si} = fraction of soil concentration that is component "i" (i.e., elemental, divalent, and methylmercury)

The total chemical loss rate constant for component "i" is due to several physical and chemical processes:

$$ks_i = ksl_i + kse_i + ksr_i + ksg_i + ksv_i$$

where:

ks_i	=	soil loss constant for component "i" due to all processes (yr^{-1})
ksl_i	=	soil loss constant due to leaching (yr^{-1})
kse_i	=	soil loss constant due to erosion (yr^{-1})
ksr_i	=	soil loss constant due to runoff (yr^{-1})
ksg_i	=	soil loss constant due to chemical transformation/ degradation (yr^{-1})
ksv_i	=	soil loss constant due to volatilization (yr^{-1})

The degradation constant, ksg_i, is set to 0 in the equilibrium component approach. The other four constants are given by these equations:

$$ksl_i = \frac{P + I - Ro - EV}{\theta_s Z}\left(\frac{1}{1.0 + Kd_{s,i}\, BD/\theta_s}\right)$$

$$kse_i = \frac{0.1\, X_e\, SD\, ER}{BD\, Z}\left(\frac{Kd_{s,i}\, BD}{\theta_s + Kd_{s,i}\, BD}\right)$$

$$ksr_i = \frac{Ro}{\theta_s Z}\left(\frac{1}{1 + Kd_{s,i}\, BD/\theta_s}\right)$$

$$ksv_i = Ke_i\, Kt_i$$

where:

P	=	average annual precipitation (cm/yr)
I	=	average annual irrigation (cm/yr)
Ro	=	average annual runoff (cm/yr)
Ev	=	average annual evapotranspiration (cm/yr)
θ_s	=	volumetric water content (dimensionless; cm^3/cm^3)
Z	=	watershed mixing zone depth (cm)
BD	=	soil bulk density (g/cm^3)
SD	=	sediment delivery ratio
ER	=	contaminant enrichment ratio
$Kd_{s,i}$	=	soil-water partition coefficient for component "i" (cm^3/g)

X_e = unit soil loss (kg/m^2-yr; see Eq [9-3][78])
Ke_i = equilibrium coefficient for component "i" (s/cm-yr); see Eq [4-5][79])
Kt_i = gas phase mass transfer coefficient for component "i" (cm/s; see Eq [4-6][79])
0.1 = units conversion factor

Sc is the concentration resulting from contaminated particles depositing on and mixing with surface soils. For mercury components, where $Kd_{s,i}$ values are large, Sc_i was essentially equal to the sorbed concentration, $C_{ps,i}$, and the dissolved phase concentration, $C_{ds,i}$, was small. Mercury components depositing as particles were assumed to reequilibrate in the soil/soil water system (see the state equations above). In the listing of state equations, the reequilibrated sorbed phase concentration, $C_{ps,i}$, and the dissolved phase concentration, $C_{ds,i}$, were used to estimate loads to the water body due to soil erosion and surface runoff, respectively.

M.3.2 The Aquatic Equations.

The following framework for estimating surface water impacts from stack emissions estimates water column as well as bed sediment concentrations. Water column concentrations included dissolved, sorbed to suspended sediments and total (sorbed plus dissolved, or total contaminant divided by total water volume). This framework also provides three concentrations for the bed sediments: dissolved in pore water, sorbed to bed sediments, and total. The model accounts for five routes of contaminant entry into the water body: erosion of chemical sorbed to soil particles; runoff of dissolved chemical in runoff water; deposition of particle-bound contaminant through wetfall and dryfall; and diffusion of vapor phase contaminants into the water body. The model also accounts for four dissipation processes that remove contaminants from the water column and/or bed sediment reservoirs: decay of total contaminants (sorbed + dissolved) within the water column; decay of total contaminants (sorbed + dissolved) within the bed sediment; volatilization of dissolved phase out of the water column; and removal of total contaminant via "burial" from the surficial bed sediment layer. This burial rate constant is a function of the deposition of sediments from the water column to the bed; it accounts for the fact that much of the soil eroding into a water body annually becomes bottom sediment rather than suspended sediment. The impact to the water body was assumed to be uniform. This tends to be more realistic for smaller water bodies as compared to large river systems. Key assumptions in the surface water impact algorithm are the following.

- The partitioning of the contaminant within the sediment/water matrices - suspended solids in the water column, and bed sediments in the benthos of the water body - can be described by partition coefficients.

- One route of entry into the surface water body is direct deposition. A second route of entry is contaminant dissolved in annual surface runoff. This is estimated as a function of the contaminant dissolved in soil water and annual water runoff. A third route of entry is via soil erosion. A sorbed concentration of contaminant in soil, together with an annual soil erosion estimate, a sediment delivery ratio and an enrichment ratio, can be used to describe the delivery of contaminant to the water body via soil erosion. A sediment delivery ratio serves to reduce the total potential amount of soil erosion (where the total potential equals a unit erosion rate in kg/m^2 multiplied by the watershed area, in m^2) reaching the water body recognizing that most of the erosion within a watershed during a year deposits prior to reaching the water body. The enrichment ratio accounts for the fact that eroding soils tend to be lighter in texture, be more abundant in surface area, and have higher organic carbon. All these characteristics lead to concentrations in eroded soils that tend to be higher in concentration as compared to in *situ* soils. A fourth and final route of entry is via diffusion in the gaseous phase. The dissolved concentration in a water body is driven toward equilibrium with the vapor phase concentration above the water body. At equilibrium, gaseous diffusion into the water body is matched by volatilization out of the water body. Gaseous diffusion is estimated with a transfer rate (determined internally given user inputs) and a vapor phase air concentration. This air concentration is specified by the user and is an output of the atmospheric transport model.

- For the surface water solution algorithm, it is assumed that equilibrium is maintained between contaminants within the water column and contaminants in surficial bed sediments. Equilibrium is established when the dissolved phase concentration in the water column is equal to the dissolved phase concentration within the surficial bed sediments. This condition is imposed by the water body equations.

- A rate of contaminant "burial" in bed sediments is estimated as a function of the rate at which sediments deposit from the water column onto the surficial sediment layer. This burial represents a permanent sink, recognizing that a portion of the eroded soil and sorbed contaminant becomes bottom sediment while the remainder becomes suspended sediment. This solution assumes that there will be a net depositional loss, even though resuspension and redeposition of sediments is ongoing, particularly with moving water bodies. For cases where the net deposition rate is zero, there will be no burial loss calculated.

- Separate water column and benthic decay rate constants allow for the consideration of decay mechanisms that remove contaminants from the water body, optionally linking them through internal loading to a reaction product. For the equilibrium component approach to mercury, decay constants are set to 0.

Figure M-3 displays the framework for this analysis, with a listing of the ten concentrations that were part of the solution algorithm. In the following sections, the mass balance equations and the equilibrium state equations that link the concentrations are developed.

M.3.2.1 Chemical Mass Balance in the Water Body. Taking Figure M-4 as a control volume for the water body, it can be seen that a steady-state mass balance equation can be written that balances chemical loadings with outflow and loss:

$$C_{wtot} = \frac{L_T}{Vf_x \, f_{water} \, d_z/d_w + k_{wt} \, V_z}$$

where:

C_{wtot} = total water body concentration, including water column and benthic sediment (mg/L)

L_T = total chemical load into water body, including deposition, runoff, erosion, atmospheric diffusion, and internal chemical transformation (g/yr)

Vf_x = average volumetric flow rate through water body (m^3/yr)

Figure M-3. Overview of the IEM2 Water Body Processes

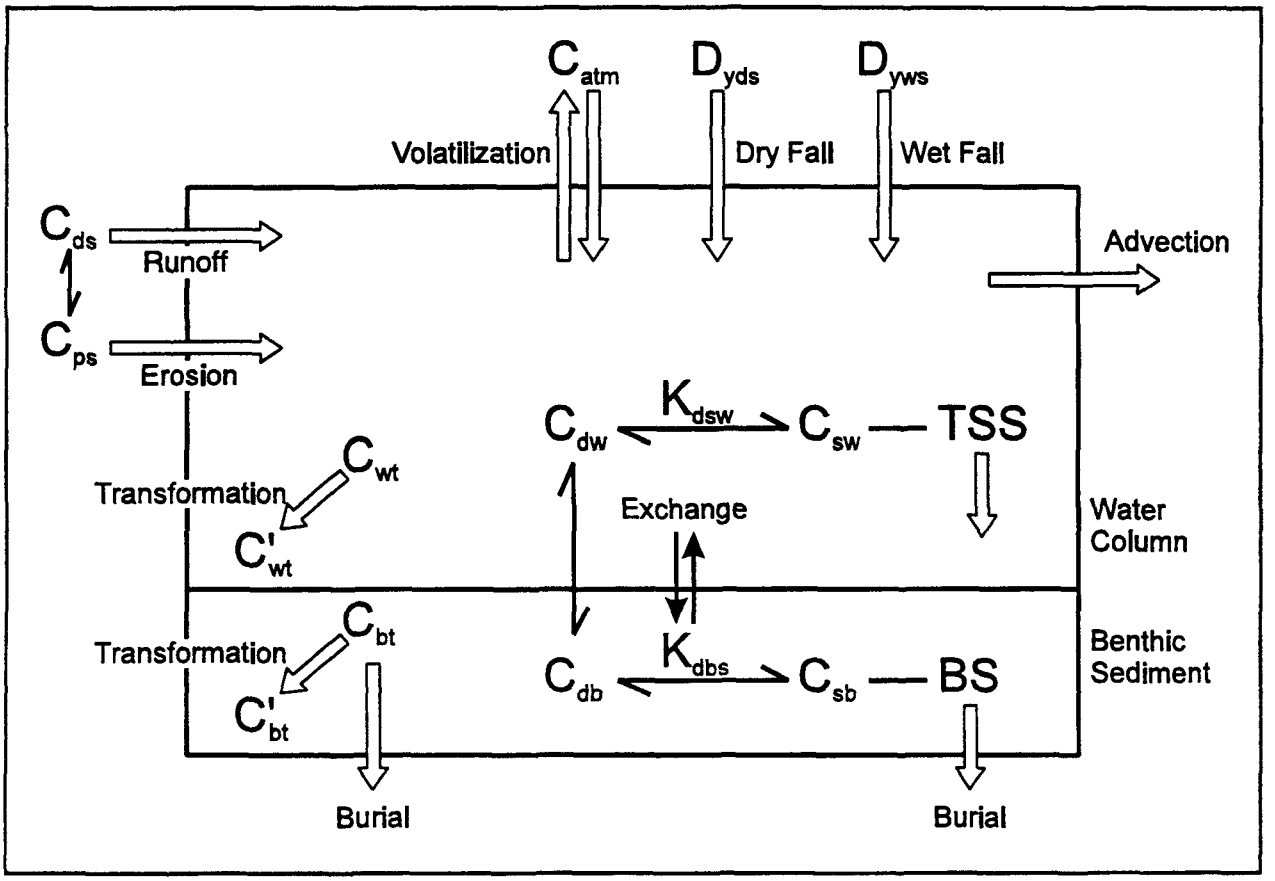

Definitions for Figure M-3

C_{ds}	concentration dissolved in soil water	mg/L
C_{ps}	concentration sorbed to soil	mg/kg
D_{yds}	yearly dry deposition to surface water	mg/yr
D_{yws}	yearly wet deposition to surface water	mg/yr
C_{atm}	vapor phase atmospheric concentration	$\mu g/m^3$
C_{wt}	total concentration in water column	mg/L
C_{wtot}	total water concentration in surface water system, including water column plus benthic sediment (not shown in figure)	mg/L
C_{dw}	dissolved phase water concentration	mg/L
C_{sw}	sorbed phase water concentration	mg/kg
C_{bt}	total concentration in bottom sediment	mg/L
C_{db}	concentration dissolved in bed sediment pore water	mg/L
C_{sb}	concentration sorbed to bottom sediments	mg/kg

Figure M-4. IEM2 Steady State Sediment Balance in Water Bodies

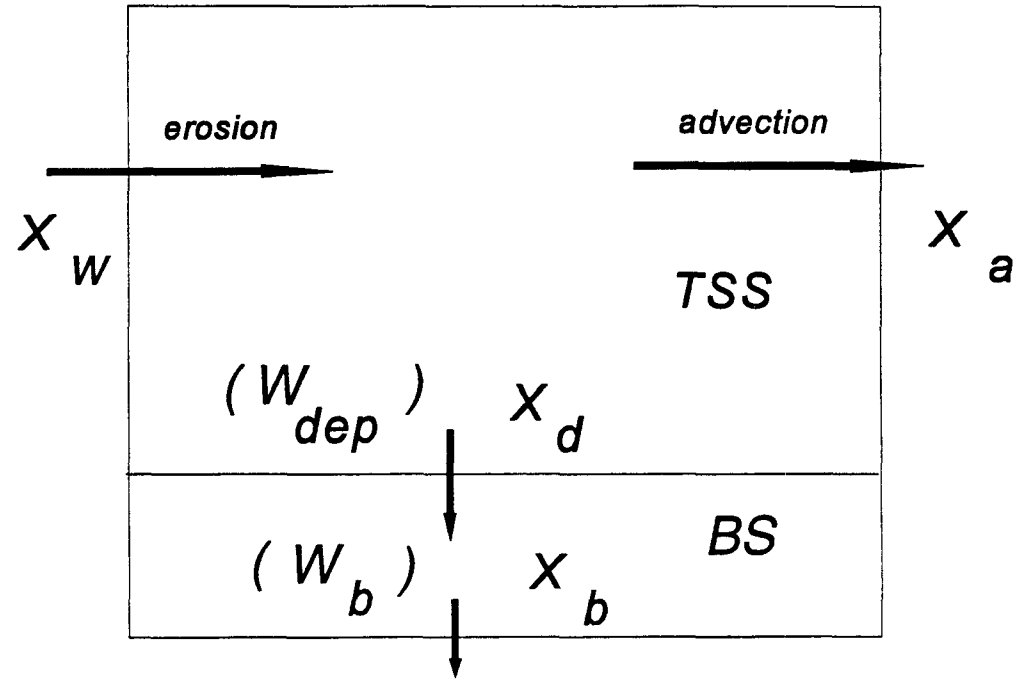

Definitions for Figure M-4

X_w	soil erosion input from depositional area	g/yr
X_a	advective loss from water body	g/yr
X_d	deposition onto bottom sediment	g/yr
X_b	burial below bottom sediment layer	g/yr
TSS	suspended solids concentration	mg/L
BS	bottom sediments concentration	g/L
W_{dep}	rate of deposition onto bed sediment	m/yr
W_b	rate of burial	m/yr

V_z = total volume of water body or water body segment being considered, including water column and benthic sediment (m^3)
k_{wt} = total first order dissipation rate constant, including water column and benthic degradation, volatilization, and burial (yr^{-1})
f_{water} = fraction of total water body contaminant concentration that occurs in the water column
d_w = depth of the water column (m)
d_z = total depth of water body, d_w+d_b (m)

The first term in the denominator accounts for the advective flow of chemical from the water column, while the second term accounts for loss processes from the bed and water column. This mass balance equation is derived in Section M.3.3.3. The terms in this equation are discussed in sections below.

M.3.2.2 Sediment Mass Balance in the Water Body. Before calculating chemical fate, a mass balance equation for sediments in the water body must be solved. Taking Figure M-4 as a control volume for the water body, it can be seen that a steady-state mass balance equation can be written that balances sediment loadings with outflow and loss:

$$TSS = \frac{X_e \, WA_L \, SD \, 10^3}{Vf_x + W_{dep} \, WA_w}$$

where:
TSS = suspended solids concentration (mg/L)
X_e = unit soil erosion flux, calculated in the soils section from the USLE equation (kg/m^2-yr)
WA_L = watershed surface area (m^2)
SD = watershed sediment delivery ratio (unitless)
Vf_x = average volumetric flow rate through water body (m^3/yr)
W_{dep} = suspended solids deposition rate (m/yr)
WA_w = water body surface area (m^2)
10^3 = units conversion factor

The first term in the denominator accounts for the advective flow of sediment from the water column, while the second term accounts for depositional loss from the water column. This mass balance equation is derived in Section M.3.3.3. The terms in this equation are discussed in sections below.

In the second part of the solids balance, the mass deposited to the bed, X_d, was set equal to the mass buried, X_b. Solving for the burial rate gives the following:

$$W_b = W_{dep} \frac{TSS\ 10^{-6}}{BS}$$

where:

W_b	=	burial rate (m/yr)
W_{dep}	=	deposition rate (m/yr)
TSS	=	suspended solids concentration (mg/L)
BS	=	benthic solids concentration (kg/L)
10^{-6}	=	conversion factor (kg/mg)

Finally, the benthic porosity, the volume of water per volume of benthic space, was calculated from the benthic solids concentration and sediment density:

$$\theta_{bs} = 1 - BS/\rho_s$$

where:

θ_{bs}	=	benthic porosity (L/L)
BS	=	benthic solids concentration (kg/L)
ρ_s	=	solids density, 2.65 kg/L

For input benthic solids concentrations between 0.5 and 1.5 kg/L, benthic porosity ranged between 0.8 and 0.4.

The suspended solids, benthic solids, and benthic porosity were used in the chemical equilibrium speciation equations. The burial rate was used in the chemical burial equation. These equations are developed below.

M.3.2.3 Equilibrium Speciation in Water Body. Total mercury in the water body is assumed to be distributed among three components – Hg^0, Hg(II), and methylmercury. The steady-state fraction of the total in each component in the water column is specified by the user using the following relationship:

$$C_{wt,Hg^0} = C_{wt} \cdot f_{w1}$$

$$C_{wt,Hg(II)} = C_{wt} \cdot f_{w2}$$

$$C_{wt,MeHg} = C_{wt} \cdot f_{w3}$$

where:

C_{wt}	=	water column concentration of total mercury (µg/L)
$C_{wt,Hg0}$	=	water column concentration of elemental mercury (µg/L)
$C_{wt,Hg(II)}$	=	water column concentration of divalent mercury (µg/L)
$C_{wt,MeHg}$	=	water column concentration of methylmercury (µg/L)
f_{w1}	=	fraction of water column concentration that is elemental mercury
f_{w2}	=	fraction of water column concentration that is divalent mercury
f_{w3}	=	fraction of water column concentration that is methylmercury

The total concentration of each mercury component in the water body, $C_{wtot,i}$, was assumed to reach equilibrium between the benthic and water column compartments and between its particulate and aqueous phases within each compartment. $C_{wtot,i}$ gives the mass per volume of the entire water body, including both water column and benthic sediment. The water column concentration, $C_{wt,i}$, was based on the water column volume; the benthic concentration, $C_{bt,i}$, was based on the benthic volume. The equilibrium relationships are given by the following equations, which are derived in Section M.3.3.4.

Surface Water System –

$$C_{wtot,i} = C_{wt,i} \cdot d_w/d_z + C_{bt,i} \cdot d_b/d_z$$

$$= \textit{see mass balance equation}$$

$$f_{water,i} = \frac{(1 + Kd_{sw,i} \cdot TSS \cdot 10^{-6}) \cdot d_w/d_z}{(1 + Kd_{sw,i} \cdot TSS \cdot 10^{-6}) \cdot d_w/d_z + (\theta_{bs} + Kd_{bs,i} \cdot BS) \cdot d_b/d_z}$$

$$f_{benth,i} = \frac{(\theta_{bs} + Kd_{bs,i} \cdot BS) \cdot d_b/d_z}{(1 + Kd_{sw,i} \cdot TSS \cdot 10^{-6}) \cdot d_w/d_z + (\theta_{bs} + Kd_{bs,i} \cdot BS) \cdot d_b/d_z}$$

Water Column –

$$C_{wt,i} = f_{water,i} \cdot C_{wtot,i} \cdot d_z/d_w$$

$$C_{dw,i} = C_{wt,i} \cdot f_{dw,i} = C_{wt,i}\left[\frac{1}{1 + Kd_{sw,i} \cdot TSS \cdot 10^{-6}}\right]$$

$$C_{sw,i} = Kd_{sw,i} \cdot C_{dw,i}$$

Bed Sediment —

$$C_{bt,i} = f_{benth,i} \cdot C_{wtot,i} \cdot d_z / d_b$$

$$C_{db,i} = C_{bt,i} \cdot f_{db,i} / \theta_{bs} = C_{bt,i}\left[\frac{1}{\theta_{bs} + Kd_{bs,i} \cdot BS}\right]$$

$$C_{sb,i} = Kd_{bs,i} \cdot C_{db,i}$$

Note that by substituting the relationship between $C_{wt,i}$ and $C_{wtot,i}$ into the expression for $C_{bt,i}$, one can obtain benthic concentrations as a function of water column concentrations:

$$C_{bt,i} = C_{wt,i} \cdot \frac{\theta_{bs} + Kd_{bs,i} \cdot BS}{1 + Kd_{sw,i} \cdot TSS \cdot 10^{-6}}$$

$$C_{db,i} = C_{dw,i}$$

$$C_{sb,i} = C_{ps,i} \cdot Kd_{bs,i} / Kd_{sw,i}$$

where:

θ_{bs} = bed sediment porosity (L_{water}/L)
$Kd_{sw,i}$ = suspended sediment/surface water partition coefficient for component "i" (L/kg)
$Kd_{bs,i}$ = bottom sediment/pore water partition coefficient for component "i" (L/kg)
TSS = total suspended solids (mg/L)
BS = bed sediment concentration (g/cm^3)
d_w = depth of the water column (m)
d_b = depth of the upper benthic layer (m)
d_z = total depth of water body, d_w+d_b (m)

$f_{water,i}$ = fraction of total water body component "i" concentration that occurs in the water column

$f_{benth,i}$ = fraction of total water body component "i" concentration that occurs in the bed sediment

$f_{dw,i}$ = fraction of water column component "i" concentration that is dissolved

$f_{db,i}$ = fraction of bed sediment component "i" concentration that is dissolved

M.3.2.4 Loads To The Water Body. The total chemical load term L_T in the mass balance equation is the sum of the loadings for each component "i." Component loadings included wet and dry deposition, impervious and pervious runoff, erosion, atmospheric diffusion, and internal transformation:

$$L_{T,i} = L_{Dep,i} + L_{RI,i} + L_{R,i} + L_{E,i} + L_{Dif,i} + L_{I,i}$$

where:

$L_{T,i}$ = total component "i" load to the water body (g/yr)

$L_{Dep,i}$ = deposition of particle bound component "i" (g/yr)

$L_{RI,i}$ = runoff load from impervious surfaces (g/yr)

$L_{R,i}$ = runoff load from pervious surfaces (g/yr)

$L_{E,i}$ = soil erosion load (g/yr)

$L_{Dif,i}$ = diffusion of vapor phase component "i" (g/yr)

$L_{I,i}$ = internal transformation load, equal to 0 for equilibrium mercury chemistry (g/yr)

The runoff and erosion loads required estimation of average contaminant concentration in watershed soils that comprise the depositional area. These concentrations were developed in terrestrial sections above.

Load due to direct deposition – The load to surface waters via direct deposition is solved as follows:

$$L_{Dep,i} = (Dyds_i + Dyws_i)\ WA_w$$

where:

$L_{Dep,i}$ = direct component "i" deposition load (g/yr)

$Dyds_i$ = yearly dry deposition rate of component "i" onto surface water body (g pollutant/m^2-yr)

$Dyws_i$ = yearly wet deposition rate of component "i" onto surface water body (g pollutant/m^2-yr)

WA_w = water body area (m^2)

Load due to impervious surface runoff – A fraction of the wet and dry chemical deposition in the watershed will be to impervious surfaces. Dry deposition may accumulate and be washed off during rain events. If the impervious surface includes gutters, the pollutant load will be transported to surface waters, bypassing the watershed soils. The average load from such impervious surfaces is given by this equation:

$$L_{RI,i} = (D_{yww,i} + D_{ydw,i})\ WA_I$$

where:

$L_{RI,i}$ = impervious surface runoff load for component "i" (g/yr)
WA_I = impervious watershed area receiving pollutant deposition (m^2)
$D_{yww,i}$ = yearly wet deposition flux of component "i" onto the watershed (g/m^2-yr)
$D_{ydw,i}$ = yearly dry deposition flux of component "i" onto the watershed (g/m^2-yr)

Load due to pervious surface runoff – Most of the chemical deposition to a watershed will be to pervious soil surfaces. These loads are accounted for in the soil mass balance equation. During periodic runoff events, dissolved chemical concentrations in the soil are transported to surface waters as given by this equation:

$$L_{R,i} = Ro\ (WA_L - WA_I) \left[\frac{Sc_i\ BD}{\theta_s + Kd_{s,i}\ BD} \right] 10^{-2}$$

where:

$L_{R,i}$ = pervious surface runoff load for component "i" (g/yr)
Ro = average annual runoff (cm/yr)
Sc_i = component "i" concentration in watershed soils (µg/g)
BD = soil bulk density (g/cm^3)
θ_s = volumetric soil water content (cm^3/cm^3)
$Kd_{s,i}$ = soil-water partition coefficient for component "i" (L/kg or cm^3/g)
WA_L = total watershed area receiving pollutant deposition (m^2)
WA_I = impervious watershed area receiving pollutant deposition (m^2)
10^{-2} = units conversion factor (g^2/kg-µg)

Load due to soil erosion – During periodic erosion events, particulate chemical concentrations in the soil are transported to surface waters as described by this relationship:

$$L_{E,i} = X_e \ (WA_L - WA_I) \ SD \ ER \left| \frac{Sc_i \ Kd_{s,i} \ BD}{\theta_s + Kd_{s,i} \ BD} \right| 10^{-3}$$

where:

$L_{E,i}$	=	soil erosion load for component "i" (g/yr)
X_e	=	unit soil loss (kg/m^2-yr)
Sc_i	=	component "i" concentration in watershed soils (µg/g)
BD	=	soil bulk density (g/cm^3)
θ_s	=	volumetric soil water content (cm^3/cm^3)
$Kd_{s,i}$	=	soil-water partition coefficient for component "i" (L/kg or cm^3/g)
WA_L	=	total watershed area receiving pollutant deposition (m^2)
WA_I	=	impervious watershed area receiving pollutant deposition (m^2)
SD	=	watershed sediment delivery ratio (unitless)
ER	=	soil enrichment ratio (unitless)
10^{-3}	=	units conversion factor (g-cm^2/µg-m^2)

Load due to gaseous diffusion – The change in the total water concentration over time due to volatilization is given by this:

$$\frac{\partial C_{wtot,i}}{\partial t}\Big|_{volat} = -\frac{K_{v,i}}{D}\left(f_{water,i} f_{dw,i} C_{wtot,i} - \frac{C_{atm,i} \ 10^{-6}}{H_i / RT_k} \right)$$

where:

$C_{wtot,i}$	=	total water body component "i" concentration (mg/L)
$K_{v,i}$	=	overall component "i" transfer rate (m/yr)
D	=	depth of water body (m)
$f_{water,i}$	=	fraction of total water body component "i" concentration that occurs in the water column
$f_{dw,i}$	=	fraction of water column component "i" concentration that is dissolved
$C_{atm,i}$	=	component "i" vapor phase air concentration over water body (µg/m^3)
H_i	=	component "i" Henry's Constant (atm-m^3/mole)
R	=	universal gas constant, 8.206*10^{-5} atm-m^3/mole-K

T_k = water body temperature (°K)
10^{-6} = units conversion factor

This treatment of volatilization is based on the well-known two-film theory[80], as implemented in standard chemical fate models.[81,82] The right side of the volatilization equation contains two terms. The first term constitutes a first order loss rate of aqueous contaminant, which is covered in more detail below. The second term in the volatilization equation describes diffusion of gas-phase contaminant from the atmosphere into the water body. Because this term is independent of water body contaminant concentration, it can be treated as an external load. As formulated above, this term has units of mg/L-yr. It must be converted to loading units by multiplying by the water column volume, V. Noting that V/D is equal to the surface water area WA_w, we see that the atmospheric diffusion load is given as this:

$$L_{Dif,i} = \frac{K_{v,i}\, C_{atm,i}\, WA_w\, 10^{-6}}{H_i / R T_k}$$

where:

$L_{Dif,i}$ = diffusion of vapor phase component "i" (g/yr)
$K_{v,i}$ = the overall component "i" transfer rate (m/yr)
WA_w = surface water body area (m^2)
$C_{atm,i}$ = component "i" vapor phase air concentration over water body ($\mu g/m^3$)
H_i = component "i" Henry's Constant (atm-m^3/mole)
R = universal gas constant (8.206 x 10^{-5} atm-m^3/mole-°K)
T_k = water body temperature (°K)
10^{-6} = units conversion factor

M.3.2.5 Advective Flow From The Water Body. The first term in the denominator of the chemical mass balance equation accounts for advective flow from the water body. It is the product of the average annual volumetric flow rate, Vf_x; the fraction of the chemical in the water body that is present in the water column, f_{water}; and the adjustment factor d_z/d_w, which normalizes the outflowing chemical concentration to a water column volume basis. An impacted water body derives its annual flow from its watershed or effective drainage area. Flow and watershed area, then, are related, and compatible values should be specified by the user. Given the area of drainage, one way to estimate annual flow volume is to multiply total drainage area (in length squared units) by a unit surface water runoff (in length per time). *The Water Atlas of the United States*[83] provides maps with isolines of

annual average surface water runoff, which is defined as all flow contributions to surface water bodies, including direct runoff, shallow interflow, and groundwater recharge. The values ranged from 5 to 40 in/yr in various parts of the United States.

M.3.2.6 Chemical Dissipation Within The Water Body. The second term in the denominator of the chemical mass balance equation accounts for dissipation within the water body. It is the product of the water body volume, V_t, and the total first order dissipation rate constant, k_{wt}. The water body volume, in units of m^3, together with the annual flow rate, in m^3/yr, determines the average residence time of a pollutant traveling through the water body. The residence time for Lake Erie is about 10 years, for example, while for the larger Lake Superior it is estimated to be 200 years. For a swiftly moving river, on the other hand, the residence time can be on the order of hours (1 hour = 0.00011 yr). Larger volumes and residence times allow the internal dissipation processes to have a larger effect on pollutant concentration, while smaller volumes and residence times lessen the effect. It is necessary to specify reasonable volumes for the type of surface water body being represented. In addition, compatible values for related water body parameters, such as surface area, WA_w must be used. The water body volume divided by the surface area gives the average depth, which can vary from a fraction of a meter for small streams to a few meters for shallow reservoirs to tens of meters for deep lakes.

The total dissipation rate constant, k_{wt}, applies to the total water body concentration, C_{wtot}, and is the weighted sum of the chemical loss rate constants for each component "i":

$$k_{wt} = \sum_i k_{wt,i} \cdot f_{wi}$$

where:

ks_i = total soil loss constant for component "i" (yr^{-1})
f_{si} = fraction of soil concentration that is component "i" (i.e., elemental, divalent, and methylmercury)

The total chemical loss rate constant for component "i" includes processes affecting any of the chemical phases – dissolved or sorbed in the water column or benthic sediments. Volatilization, water column and benthic degradation, and burial are considered in this relationship:

$$k_{wt,i} = f_{water,i}\, k_{gw,i} + f_{benth,i}\, k_{gb,i} + f_{water,i}\, k_{v,i} + f_{benth,i}\, k_{b,i}$$

where:

$k_{wt,i}$ = overall total water body dissipation rate constant for component "i" (yr^{-1})

$k_{gw,i}$ = water column degradation or transformation rate constant for component "i" (yr^{-1})

$k_{gb,i}$ = benthic degradation or transformation rate constant for component "i" (yr^{-1})

$k_{v,i}$ = water column volatilization rate constant (yr^{-1})

$k_{b,i}$ = benthic burial rate constant for component "i" (yr^{-1})

$f_{water,i}$ = fraction of total water body component "i" concentration that occurs in the water column

$f_{benth,i}$ = fraction of total water body component "i" concentration that occurs in the benthic sediment

These processes are described below.

Chemical/Biological Degradation – Contaminants can be degraded and transformed by a number of processes in the water column or in the benthic sediment. Mercury components are subject to oxidation, reduction, and methylation. In the equilibrium approach taken here, the transformation rates were set to 0 and the fraction of total chemical in each component was specified directly.

Volatilization – Volatile chemicals can move between the water column and the overlying air, as described by Equation (3-41). The right side of this equation contains two terms. The second term describes diffusion into the water from the atmosphere and was treated as an external load. The first term, $(K_{v,i}f_{water,i}f_{dw,i}C_{wtot,i}/D)$, constitutes a first order loss rate of aqueous contaminant. This term includes the quantity $f_{water,i}f_{dw,i}C_{wtot,i}$, which is equal to the water column dissolved phase concentration $C_{dw,i}$ and which is subject to volatilization loss. The rate constant for volatilization from the water column, $k_{v,i}$, is given as this:

$$k_{v,i} = \frac{K_{v,i}\, f_{dw,i}}{D}$$

where:

$k_{v,i}$ = water column volatilization loss rate constant for component "i" (yr^{-1})

$K_{v,i}$ = overall transfer rate, or conductivity for component "i" (m/yr)

$f_{dw,i}$ = fraction of component "i" in the water column that is dissolved
D = water body depth (m)

The overall transfer rate, $K_{v,i}$ or conductivity, was determined by the two-layer resistance model.[80,81,82] The two-resistance method assumes that two "stagnant films" are bounded on either side by well mixed compartments. Concentration differences serve as the driving force for the water layer diffusion. Pressure differences drive the diffusion for the air layer. From mass balance considerations, it is obvious that the same mass must pass through both films; thus, the two resistances combine in series, so that the conductivity is the reciprocal of the total resistance:

$$K_{v,i} = (R_{L,i} + R_{G,i})^{-1} = \left(K_{L,i}^{-1} + \left(K_{G,i} \frac{H_i}{R\ T_K} \right)^{-1} \right)^{-1}$$

where:
$R_{L,i}$ = liquid phase resistance (year/m)
$K_{L,i}$ = liquid phase transfer coefficient (m/year)
$R_{G,i}$ = gas phase resistance (year/m)
$K_{G,i}$ = gas phase transfer coefficient (m/year)
R = universal gas constant (atm-m^3/mole-°K)
H_i = Henry's law constant for component "i" (atm-m^3/mole)
T_k = water body temperature (°K)

The value of $K_{v,i}$, the conductivity, depends on the intensity of turbulence in a water body and in the overlying atmosphere. As the Henry's Law coefficient increases, the conductivity tends to be increasingly influenced by the intensity of turbulence in water. As the Henry's Law coefficient decreases, the value of the conductivity tends to be increasingly influenced by the intensity of atmospheric turbulence.

Because Henry's Law coefficient generally increases with increasing vapor pressure of a compound and generally decreases with increasing solubility of a compound, highly volatile low solubility compounds are most likely to exhibit mass transfer limitations in water, and relatively nonvolatile high solubility compounds are more likely to exhibit mass transfer limitations in the air. Volatilization is usually of relatively less magnitude in lakes and reservoirs than in rivers and streams.

The estimated volatilization rate constant was for a nominal temperature of 20°C. It is adjusted for the actual water temperature using the equation:

$$K_{v,i,T} = K_{v,i,20}\ \theta^{(T-20)}$$

where:

θ	=	temperature correction factor, set to 1.026.
T	=	water body temperature (°C)

There have been a variety of methods proposed to compute the liquid ($K_{L,i}$) and gas phase ($K_{G,i}$) transfer coefficients. The particular method that was used in the exposure assessment is the O'Connor-Dobbins[84] method.

The liquid and gas film transfer coefficients computed under this option vary with the type of water body. The type of water body was specified as one of the surface water constants and can either be a flowing stream, river or estuary, or a stagnant pond or lake. The primary difference is that in a flowing water body, the turbulence is primarily a function of the stream velocity, while for stagnant water bodies, wind shear may dominate. The formulations used to compute the transfer coefficients vary with the water body type, as shown below.

Flowing Stream or River – For a flowing system, the transfer coefficients are controlled by flow-induced turbulence. For these systems, the liquid film transfer coefficient (K_L) was computed using the O'Connor-Dobbins[84] formula:

$$K_{L,i} = \left(\frac{10^{-4}\ D_{w,i}\ u}{d_w} \right)^{1/2} (3.15x10^{7})$$

where:

$K_{L,i}$	=	liquid phase transfer coefficient for component "i" (m/year)
u	=	current velocity (m/s)
$D_{w,i}$	=	diffusivity of the component "i" in water (cm^2/s)
d_w	=	water depth (m)
10^{-4}	=	units conversion factor
$3.15x10^{7}$	=	units conversion factor

The gas transfer coefficient (K_G) was assumed constant at 36500 m/yr for flowing systems.

Quiescent Lake or Pond – For a stagnant system, the transfer coefficients are controlled by wind-induced turbulence. For stagnant systems, the liquid film transfer coefficient (K_L) was computed using the O'Connor[85] equations:

$$K_{L,i} = u^* \left(\frac{\rho_a}{\rho_w} \right)^{0.5} \left(\frac{k^{0.33}}{\lambda_2} \right) Sc_{w,i}^{-0.67} (3.15x10^7)$$

$$K_{G,i} = u^* \left(\frac{k^{0.33}}{\lambda_2} \right) Sc_{a,i}^{-0.67} (3.15x10^7)$$

where:

$$u^* = C_d^{0.5} W$$

$$Sc_{a,i} = \frac{\mu_a}{\rho_a D_{a,i}} = \frac{\nu_a}{D_{a,i}}$$

$$D_{a,i} = \frac{1.9}{MW_i^{2/3}}$$

$$\nu_a = (1.32 + 0.009 T_a) \times 10^{-1}$$

$$Sc_{w,i} = \frac{\mu_w}{\rho_w D_{w,i}}$$

$$D_{w,i} = \frac{22\times10^{-5}}{MW_i^{2/3}}$$

$$\rho_w = 1 - 8.8\times10^{-5}\, T_w$$

$$\log(\mu_w) = \left[\frac{1301}{998.333 + 8.1855\,(T_w-20) + 0.00585\,(T_w-20)^2}\right] - 3.0233$$

and:

u^*	=	shear velocity (m/s)
C_d	=	drag coefficient (= 0.0011)
W	=	wind velocity, 10 m above water surface (m/s)
ρ_a	=	density of air corresponding to the water temperature (g/cm^3)
ρ_w	=	density of water corresponding to the water temperature (g/cm^3)
k	=	von Karman's constant (= 0.4)
λ_2	=	dimensionless viscous sublayer thickness (= 4)
$Sc_{a,i}$	=	air Schmidt number for component "i" (dimensionless)
$Sc_{w,i}$	=	water Schmidt number for component "i" (dimensionless)
$D_{a,i}$	=	diffusivity of component "i" in air (cm^2/sec)
$D_{w,i}$	=	diffusivity of component "i" in water (cm^2/sec)
μ_a	=	viscosity of air corresponding to the air temperature (g/cm-s)
μ_w	=	viscosity of water corresponding to the water temperature (g/cm-s)
ν_a	=	dynamic viscosity of air (cm^2/sec)
MW_i	=	molecular weight of component "i"
T_a	=	air temperature (°C)
T_w	=	water temperature (°C)
3.15×10^7	=	units conversion factor

Deposition and Burial – The benthic burial rate, W_b, was determined as a function of user input variables as part of the sediment balance. This burial rate is used to determine the mass loss of contaminant from the benthic sediment layer. As seen in Figure M.3, the burial loss rate was applied to the total benthic contaminant concentration, C_{bt}. The water body contaminant burial loss rate was solved by equating the mass loss rate of total water body chemical with mass loss rate of benthic chemical:

$$C_{wtot,i}\ V_t\ k_{b,i} = C_{bt,i}\ V_b\ \frac{W_b}{d_b}$$

where:

$C_{wtot,i}$ = total water body component "i" concentration, including water column and benthic sediment (mg/L)
V_t = total volume of water body or water body segment being considered, including water column and benthic sediment (m^3)
$k_{b,i}$ = first order burial rate constant for total component "i" (yr^{-1})
$C_{bt,i}$ = total benthic component "i" concentration (mg/L)
V_b = volume of upper benthic sediment layer (m^3)
d_b = depth of the upper benthic sediment layer (m)
W_b = benthic burial rate (m/yr)

From the equilibrium state equations, it is seen that the total benthic contaminant concentration, $C_{bt,i}$, can be expressed as a function of the total water body concentration, $C_{wtot,i}$. Solving for the total chemical burial rate gives this:

$$k_{b,i} = f_{benth,i}\ \frac{W_{b,i}}{d_b}$$

where:

$f_{benth,i}$ = fraction of total water body component "i" concentration that occurs in the bed sediment
d_b = depth of the upper benthic sediment layer (m)
W_b = burial rate (m/yr)

M.3.3 Derivation of Select Equations

In this section, some of the equations in Sections M.3.1 and M.3.2 are derived. A summary of notation is given in Section M.3.4.

M.3.3.1 Terrestrial Mass Balance Relationships. Taking Figure M-2 as a control volume for the watershed soil, a mass balance equation can be written. Contaminant concentration is expressed per unit mass of soil. The change in concentration per unit time is equal to the loading rate per unit soil mass minus the total loss rate:

$$\frac{dSc}{dt} = \frac{L_W \cdot A_s}{BD \cdot V_s} - ks \cdot Sc$$
$$= \frac{100 L_W}{BD \cdot Z} - ks \cdot Sc$$

This is a first order, ordinary differential equation with this general solution:

$$Sc = \frac{100 L_W}{ks \cdot BD \cdot Z} + C_x e^{-ks \cdot t}$$

where C_x is an unknown constant. Applying the condition Sc=0 at t=0 gives the following:

$$Sc = \frac{100 L_W}{ks \cdot BD \cdot Z} \left(1 - e^{-ks \cdot t}\right)$$

If a stable natural background concentration exists in the soil that is independent of the loading and loss processes, then this C_{sb} can be added to the above solution to obtain the overall concentration.

M.3.3.2 Terrestrial Equilibrium Relationships. Within the soil, the dissolved chemical concentration equilibrium with the sorbed concentration is defined by a partition coefficient:

$$C_{ps,i} = C_{ds,i} \cdot Kd_{s,i}$$

Assuming that the soil gas phase is negligible on a mass basis, the total soil chemical concentration is composed of dissolved chemical plus sorbed chemical:

$$C_{st,i} = C_{ds,i}\theta_s + C_{ps,i} \cdot BD$$

Substituting the partitioning relationship between dissolved and sorbed chemical, one gets the total soil chemical concentration:

$$C_{st,i} = C_{ds,i}\left(\theta_s + Kd_{s,i} \cdot BD\right)$$

The fraction of chemical dissolved in the soil water is the following:

$$f_{ds,i} = \frac{C_{ds,i} \cdot \theta_s}{C_{st,i}} = \frac{\theta_s}{\theta_s + Kd_{s,i} \cdot BD}$$

The fraction of chemical sorbed in the soil is $1-f_{ds,i}$:

$$f_{ps,i} = \frac{Kd_{s,i} \cdot BD}{\theta_s + Kd_{s,i} \cdot BD}$$

The concentration of chemical dissolved in the soil water is derived as follows:

$$C_{ds,i} = \frac{f_{ds,i} \cdot Sc_i \cdot BD}{\theta_s} = \frac{Sc_i \cdot BD}{\theta_s + Kd_{s,i} \cdot BD}$$

and the concentration of chemical sorbed to the soil is this:

$$C_{ps,i} = f_{ps,i} \cdot Sc_i = \frac{Sc_i \cdot Kd_{s,i} \cdot BD}{\theta_s + Kd_{s,i} \cdot BD}$$

M.3.3.3 Surface Water Mass Balance Relationships. Taking Figure M-3 as a control volume for the water body, at steady-state total chemical loading equals the sum of chemical outflow and chemical loss. The chemical outflow is the product of the volumetric flow rate and the water column concentration:

$$Outflow = Vf_x \cdot C_{wt}$$

The fraction of the total water body chemical concentration that is in the water column is defined in this way:

$$f_{water} = \frac{C_{wt} \cdot d_w / d_z}{C_{wtot}}$$

The outflow can, thus, be given in terms of the total water body concentration:

$$Outflow = Vf_x \cdot f_{water} \cdot C_{wtot} \cdot d_z / d_w$$

The chemical loss can also be given in terms of the total water body concentration:

$$Loss = k_{wt} \cdot C_{wtot} \cdot V_z$$

Equating loading to outflow plus loss, and solving for the total water body concentration gives this:

$$C_{wtot} = \frac{L_T}{Vf_x \, f_{water} \, d_z/d_w + \; k_{wt} \, V_z}$$

In a similar manner, the mass balance equation for sediment in the water body can be derived. Taking Figure M-4 as a control volume, the soil eroding into the water body, X_w, equals the sum of the amount depositing into the upper bed, X_d, and the advective loss from the water column, X_a. X_w is the product of the areal soil erosion flux, the watershed surface area, and the watershed sediment delivery ratio, with a factor converting kg to mg:

$$X_w = X_e \cdot WA_L \cdot SD \cdot 10^3$$

X_d is the product of the suspended solids concentration and the deposition rate:

$$X_d = W_{dep} \cdot WA_w \cdot TSS$$

X_a is the product of the suspended solids concentration and the volumetric flow rate:

$$X_a = Vf_x \cdot TSS$$

Substituting these relationships into the solids mass balance and solving for the suspended solids concentration in the water column gives this equation:

$$TSS = \frac{X_e \, WA_L \, SD \, 10^3}{Vf_x + W_{dep} \, WA_w}$$

M.3.3.4 Surface Water Equilibrium Relationships. Within the water column, the dissolved chemical concentration equilibrium with the sorbed concentration is defined by a partition coefficient:

$$C_{sw,i} = C_{dw,i} \cdot Kd_{sw,i}$$

The total chemical concentration in the water column is composed of dissolved chemical plus sorbed chemical:

$$C_{wt,i} = C_{dw,i} + C_{sw,i} \cdot TSS \cdot 10^{-6}$$

Substituting the partitioning relationship between dissolved and sorbed chemical, the total chemical concentration is calculated as this:

$$C_{wt,i} = C_{dw,i}\left(1 + Kd_{sw,i} \cdot TSS \cdot 10^{-6}\right)$$

The fraction of chemical dissolved in the water column becomes the following:

$$f_{dw,i} = \frac{C_{dw,i}}{C_{wt,i}} = \frac{1}{1 + Kd_{sw,i} \cdot TSS \cdot 10^{-6}}$$

Within the bed sediment, the dissolved chemical concentration equilibrium with the sorbed concentration is defined by a partition coefficient:

$$C_{db,i} = C_{sb,i} \cdot Kd_{bs,i}$$

The total benthic chemical concentration is composed of dissolved chemical plus sorbed chemical:

$$C_{bt,i} = C_{db,i}\theta_{bs} + C_{sb,i} \cdot BS$$

Substituting the partitioning relationship between dissolved and sorbed chemical, one calculates the total benthic chemical concentration:

$$C_{bt,i} = C_{db,i}\left(\theta_{bs} + Kd_{bs,i} \cdot BS\right)$$

The fraction of chemical dissolved in the benthic pore water is the following:

$$f_{db,i} = \frac{C_{db,i} \cdot \theta_{bs}}{C_{bt,i}} = \frac{\theta_{bs}}{\theta_{bs} + Kd_{bs,i} \cdot BS}$$

The total chemical concentration on a total water body basis is the sum of the water column and the benthic concentrations, weighted by the respective volumes is given by these relationships:

$$C_{wtot,i} = C_{wt,i} \cdot \frac{V_w}{V_z} + C_{bt,i} \cdot \frac{V_b}{V_z} = C_{wt,i} \cdot \frac{d_w}{d_z} + C_{bt,i} \cdot \frac{d_b}{d_z}$$

Substituting in the relationships for $C_{wt,i}$ and $C_{bt,i}$, and noting that at equilibrium $C_{dw,i} = C_{db,i}$, one obtains the total water body concentration as a function of the dissolved water column concentration:

$$C_{wtot,i} = C_{dw,i}\left[(1 + Kd_{sw,i}\cdot TSS\cdot 10^{-6})\cdot d_w/d_z + (\theta_{bs} + Kd_{bs,i}BS)\cdot d_b/d_z\right]$$

The fraction of the chemical that is in the water column is defined as this:

$$f_{water,i} = \frac{C_{wt,i}\cdot d_w/d_z}{C_{wtot,i}}$$

Substituting in the relationships for $C_{wt,i}$ and $C_{wtot,i}$, one obtains expressions for $f_{water,i}$ and $f_{benth,i}$ as functions of environmental and chemical properties:

$$f_{water,i} = \frac{(1 + Kd_{sw,i}\cdot TSS\cdot 10^{-6})\cdot d_w/d_z}{(1 + Kd_{sw,i}\cdot TSS\cdot 10^{-6})\cdot d_w/d_z + (\theta_{bs} + Kd_{bs,i}\cdot BS)\cdot d_b/d_z}$$

$$f_{benth,i} = \frac{(\theta_{bs} + Kd_{bs,i}\cdot BS)\cdot d_b/d_z}{(1 + Kd_{sw,i}\cdot TSS\cdot 10^{-6})\cdot d_w/d_z + (\theta_{bs} + Kd_{bs,i}\cdot BS)\cdot d_b/d_z}$$

M.3.4 Summary of Notation

A_s = surface area of watershed soil element (m^2)

BD = representative watershed soil bulk density (g/cm^3)
BS = benthic solids concentration (kg/L)

$C_{atm,i}$ = component "i" vapor phase air concentration over watershed ($\mu g/m^3$)
$C_{bt,i}$ = total benthic component "i" concentration (mg/L)
C_d = drag coefficient (= 0.0011)
$C_{ds,i}$ = concentration of "i" dissolved in pore water (mg/L)
$C_{ps,i}$ = concentration of "i" in particulate phase (mg/kg)
C_{sb} = background "natural" soil concentration (µg pollutant/g soil)
$C_{st,i}$ = total soil concentration of component "i" (mg/L)
C_{wt} = water column concentration of total mercury (µg/L)
$C_{wt,Hg0}$ = water column concentration of elemental mercury (µg/L)
$C_{wt,Hg(II)}$ = water column concentration of divalent mercury (µg/L)
$C_{wt,MeHg}$ = water column concentration of methylmercury (µg/L)
$C_{wtot,i}$ = total water body component "i" concentration, including water column and benthic sediment (mg/L)
C_{wtot} = total water body concentration, including water column and benthic sediment (mg/L)

d_b = depth of the upper benthic sediment layer (m)
d_w = depth of the water column (m)
d_z = total depth of water body, d_w+d_b (m)
D = depth of water body (m)
$D_{a,i}$ = diffusivity of component "i" in air (cm^2/sec)
$D_{w,i}$ = diffusivity of component "i" in water (cm^2/sec)
$Dyds_i$ = yearly dry deposition rate of component "i" onto surface water body (g pollutant/m^2-yr)
$Dydw_i$ = yearly average dry depositional flux of component "i" onto watershed (g/m^2-yr)
$Dyws_i$ = yearly wet deposition rate of component "i" onto surface water body (g pollutant/m^2-yr)
$Dyww_i$ = yearly average wet depositional flux of component "i" onto watershed (g/m^2-yr)

ER = soil enrichment ratio (unitless)
Ev = average annual evapotranspiration (cm/yr)

$f_{benth,i}$ = fraction of total water body component "i" concentration that occurs in the benthic sediment

$f_{db,i}$ = fraction of bed sediment component "i" concentration that is dissolved

$f_{ds,i}$ = fraction of soil component "i" concentration that is dissolved

$f_{dw,i}$ = fraction of water column component "i" concentration that is dissolved

$f_{ps,i}$ = fraction of soil component "i" concentration that is sorbed

f_{si} = fraction of soil concentration that is component "i" (i.e., elemental, divalent, and methylmercury)

f_{s1} = fraction of soil concentration that is elemental mercury

f_{s2} = fraction of soil concentration that is divalent mercury

f_{s3} = fraction of soil concentration that is methylmercury

$f_{water,i}$ = fraction of total water body component "i" concentration that occurs in the water column

f_{w1} = fraction of water column concentration that is elemental mercury

f_{w2} = fraction of water column concentration that is divalent mercury

f_{w3} = fraction of water column concentration that is methylmercury

H_i = Henry's law constant for component "i" (atm-m^3/mole)

I = average annual irrigation (cm/yr)

$k_{b,i}$ = benthic burial rate constant for component "i" (yr^{-1})

$k_{gb,i}$ = benthic degradation or transformation rate constant for component "i" (yr^{-1})

$k_{gw,i}$ = water column degradation or transformation rate constant for component "i" (yr^{-1})

$k_{v,i}$ = water column volatilization loss rate constant for component "i" (yr^{-1})

k_{wt} = total first order dissipation rate constant, including water column and benthic degradation, volatilization, and burial (yr^{-1})

$k_{wt,i}$ = overall total water body dissipation rate constant for component "i" (yr^{-1})

ks = total chemical loss rate constant from soil (yr^{-1})

ks_i = soil loss constant for component "i" due to all processes (yr^{-1})

ksl_i = soil loss constant due to leaching (yr^{-1})

kse_i = soil loss constant due to erosion (yr^{-1})

ksr_i = soil loss constant due to runoff (yr^{-1})

ksg_i = soil loss constant due to chemical transformation/ degradation (yr^{-1})

ksv_i = soil loss constant due to volatilization (yr^{-1})

$K_{G,i}$ = gas phase transfer coefficient (m/year)

$K_{L,i}$ = liquid phase transfer coefficient for component "i" (m/year)

$K_{t,i}$ = gas phase mass transfer coefficient for component "i" (cm/s; see Eq [4-6], IED)

$K_{w,i}$ = overall transfer rate, or conductivity for component "i" (m/yr)

$Kd_{bs,i}$ = bottom sediment/pore water partition coefficient for component "i" (L/kg)

$Kd_{s,i}$ = soil-water partition coefficient for component "i" (L/kg or cm^3/g)

$Kd_{sw,i}$ = suspended sediment/surface water partition coefficient for component "i" (L/kg)

Ke_i = equilibrium coefficient for component "i" (s/cm/yr); see Eq [4-5], IED)

Kt_i = gas phase mass transfer coefficient for compone "i" (cm/s; see Eq [4-6], IED)

$L_{Dep,i}$ = deposition of particle bound component "i" (g

$L_{DIF,i}$ = atmospheric diffusion flux of component "i" soil (g/m^2-yr)

$L_{Dif,i}$ = diffusion of vapor phase component "i" (g/yr)

$L_{E,i}$ = soil erosion load for component "i" (g/yr)

$L_{I,i}$ = internal transformation load, equal to 0 f equilibrium mercury chemistry (g/yr)

$L_{Is,i}$ = internal transformation load of componen areal basis (g/m^2-yr)

$L_{R,i}$ = pervious surface runoff load for compon (g/yr)

$L_{RI,i}$ = runoff load from impervious surfaces (total chemical load into water body,

L_T = deposition, runoff, erosion, atmosphe diffusion, and internal chemical tra (g/yr)

$L_{T,i}$ = total component "i" load to the wat

L_W = yearly average load of pollutant t an areal basis(g pollutant/m^2-yr)

MW_i = molecular weight of component "i"

P = average annual precipitation (cm/yr)

R = universal gas constant (8.206×10^{-5} atm-m^3/mole-°K)

$R_{G,i}$ = gas phase resistance (year/m)

$R_{L,i}$ = liquid phase resistance (year/m)

Ro = average annual runoff (cm/yr)

Sc = average watershed soil concentration after time period of deposition (µg pollutant/g soil)

$Sc_{a,i}$ = air Schmidt number for component "i" concentration in watershed (dimensionless)

Sc_i = total component "i" concentration in watershed soils (µg/g)

Sc_{Hg0} = soil concentration of elemental mercury (µg pollutant/g soil)

$Sc_{Hg(II)}$ = soil concentration of divalent mercury (µg pollutant/g soil)

Sc_{MeHg} = soil concentration of methylmercury (µg pollutant /g soil)

$Sc_{w,i}$ = water Schmidt number for component "i" (dimensionless)

SD = watershed sediment delivery ratio (unitless)

T_a = air temperature (°C)

T_k = water body temperature (°K)

T_w = water temperature (°C)

TC = total time period over which deposition has occurred (yr)

TSS = suspended solids concentration (mg/L)

u = current velocity (m/s)

u^* = shear velocity (m/s)

V_b = volume of upper benthic sediment layer (m^3)

= volume of watershed soil layer (m^3)

= volume of water column (m^3)

= volume of water body or water body segment being considered, including water column and benthic sediment (m^3)

W = total volume of water body

W_2 = average volumetric flow rate through water body (m^3/yr)

W_{10} = wind velocity, 10 m above water surface (m/s)

Z_b = benthic burial rate (m/yr)

Z_s = suspended solids deposition rate (m/yr)

A_i = impervious watershed area receiving pollutant deposition (m^2)

ks_i = soil loss constant for component "i" due to all processes (yr^{-1})

ksl_i = soil loss constant due to leaching (yr^{-1})

kse_i = soil loss constant due to erosion (yr^{-1})

ksr_i = soil loss constant due to runoff (yr^{-1})

ksg_i = soil loss constant due to chemical transformation/ degradation (yr^{-1})

ksv_i = soil loss constant due to volatilization (yr^{-1})

$K_{G,i}$ = gas phase transfer coefficient (m/year)

$K_{L,i}$ = liquid phase transfer coefficient for component "i" (m/year)

$K_{t,i}$ = gas phase mass transfer coefficient for component "i" (cm/s; see Eq [4-6], IED)

$K_{v,i}$ = overall transfer rate, or conductivity for component "i" (m/yr)

$Kd_{bs,i}$ = bottom sediment/pore water partition coefficient for component "i" (L/kg)

$Kd_{s,i}$ = soil-water partition coefficient for component "i" (L/kg or cm^3/g)

$Kd_{sw,i}$ = suspended sediment/surface water partition coefficient for component "i" (L/kg)

Ke_i = equilibrium coefficient for component "i" (s/cm/yr); see Eq [4-5], IED)

Kt_i = gas phase mass transfer coefficient for component "i" (cm/s; see Eq [4-6], IED)

$L_{Dep,i}$ = deposition of particle bound component "i" (g/yr)

$L_{DIF,i}$ = atmospheric diffusion flux of component "i" to soil (g/m^2-yr)

$L_{Dif,i}$ = diffusion of vapor phase component "i" (g/yr)

$L_{E,i}$ = soil erosion load for component "i" (g/yr)

$L_{I,i}$ = internal transformation load, equal to 0 for equilibrium mercury chemistry (g/yr)

$L_{Is,i}$ = internal transformation load of component "i" per areal basis (g/m^2-yr)

$L_{R,i}$ = pervious surface runoff load for component "i" (g/yr)

$L_{RI,i}$ = runoff load from impervious surfaces (g/yr)

L_T = total chemical load into water body, including deposition, runoff, erosion, atmospheric diffusion, and internal chemical transformation (g/yr)

$L_{T,i}$ = total component "i" load to the water body (g/yr)

L_W = yearly average load of pollutant to watershed on an areal basis(g pollutant/m^2-yr)

MW_i = molecular weight of component "i"

P = average annual precipitation (cm/yr)

R = universal gas constant (8.206×10^{-5} atm-m^3/mole-°K)

$R_{G,i}$ = gas phase resistance (year/m)

$R_{L,i}$ = liquid phase resistance (year/m)

Ro = average annual runoff (cm/yr)

Sc = average watershed soil concentration after time period of deposition (µg pollutant/g soil)

$Sc_{a,i}$ = air Schmidt number for component "i" (dimensionless)

Sc_i = total component "i" concentration in watershed soils (µg/g)

Sc_{Hg0} = soil concentration of elemental mercury (µg pollutant/g soil)

$Sc_{Hg(II)}$ = soil concentration of divalent mercury (µg pollutant/g soil)

Sc_{MeHg} = soil concentration of methylmercury (µg pollutant /g soil)

$Sc_{w,i}$ = water Schmidt number for component "i" (dimensionless)

SD = watershed sediment delivery ratio (unitless)

T_a = air temperature (°C)

T_k = water body temperature (°K)

T_w = water temperature (°C)

Tc = total time period over which deposition has occurred (yr)

TSS = suspended solids concentration (mg/L)

u = current velocity (m/s)

u^* = shear velocity (m/s)

V_b = volume of upper benthic sediment layer (m^3)

V_s = volume of watershed soil layer (m^3)

V_w = volume of water column (m^3)

V_z = total volume of water body or water body segment being considered, including water column and benthic sediment (m^3)

Vf_x = average volumetric flow rate through water body (m^3/yr)

W = wind velocity, 10 m above water surface (m/s)

W_b = benthic burial rate (m/yr)

W_{dep} = suspended solids deposition rate (m/yr)

WA_I = impervious watershed area receiving pollutant deposition (m^2)

WA_L = total watershed area receiving pollutant deposition (m^2)

WA_w = water body surface area (m^2)

X_e = unit soil erosion flux, calculated in the soils section from the Universal Soil Loss Equation (USLE); see Eq [9-3], IED (kg/m^2-yr)

Z = representative watershed mixing depth to which deposited pollutant is incorporated (cm)

k = von Karman's constant (= 0.4)

λ_2 = dimensionless viscous sublayer thickness (= 4)

μ_a = viscosity of air corresponding to the air temperature (g/cm-s)

μ_w = viscosity of water corresponding to the water temperature (g/cm-s)

ρ_a = density of air corresponding to the water temperature (g/cm^3)

ρ_s = solids density, 2.65 kg/L

ρ_w = density of water corresponding to the water temperature (g/cm^3)

ν_a = dynamic viscosity of air (cm^2/sec)

θ = temperature correction factor, set to 1.026.

θ_s = volumetric soil water content (L_{water}/L)

θ_{bs} = bed sediment porosity (L_{water}/L)

M.4 References

1. Johnson, W. B., D. E. Wolf, and R. L. Mancuso, Long-term regional patterns and transfrontier exchanges of airborne sulfur pollution in Europe. *Atmospheric Environment* 12: 511-527. 1978.

2. Bhumralkar, C. M., R. L. Mancuso, D. E. Wolf, R. H. Thuillier, K. D. Nitz, and W. B. Johnson, Adaptation and application of a long-term air pollution model ENAMAP-1 to Eastern North America. Final Report, EPA-600/4-80/039, U.S. Environmental Protection Agency, Research Triangle Park, NC. 1980.

3. Johnson, W. B., 1983. Interregional exchanges of air pollution: Model types and applications. *Journal of the Air Pollution Control Association* 33: 563-574. 1983.

4. Eder, B. K., D. H. Coventry, T. L. Clark, and C. E. Bollinger, RELMAP: A regional Lagrangian model of air pollution - users guide. Project Report, EPA/600/8-86/013, U.S. Environmental Protection Agency, Research Triangle Park, NC. 1986.

5. Clark, T. L., P. Blakely, and G. Mapp, Model calculations of the annual atmospheric deposition of toxic metals to Lake Michigan. 85th Annual Meeting of the Air and Water Management Assoc., Kansas City, MO, June 23-37. 1992.

6. Petersen, G., Å. Iverfeldt and J. Munthe, Atmospheric mercury species over Central and Northern Europe. Model calculations and comparison with observations from the Nordic Air and Precipitation Network for 1987 and 1988. *Atmospheric Environment* 29:47-68. 1995.

7. Munthe, J., The aqueous oxidation of elemental mercury by ozone. *Atmospheric Environment* 26A: 1461-1468. 1992.

8. Brosset, C. and E. Lord, Mercury in Precipitation and Ambient Air. A New Scenario. *Water, Air and Soil Pollution* 56:493-506. 1991.

9. Iverfeldt, Å., Occupance and Turnover of Atmospheric Mercury over the Nordic Countries. *Water, Air and Soil Pollution* 56:251-265. 1991.

10. Lindqvist, O., K. Johansson, M. Aastrup, A. Andersson, L. Bringmark, G. Hovsenius, L. Håkanson, Å. Iverfeldt, M. Meili, and B. Timm, Mercury in the Swedish environment. Transformation and deposition processes. *Water, Air and Soil Pollution* 55:49-63. 1991.

11. Penner, J. E., H. Eddleman and T. Novakov, Towards the development of a global inventory for black carbon emissions. *Atmospheric Environment* 27A:1277-1295. 1993.

12. Keeler, G. J., S. M. Japar, W. W. Brachaczek, R. A. Gorse, Jr., J. M. Norbeck and W. R. Pierson, The sources of aerosol elemental carbon at Allegheny Mountain. *Atmospheric Environment* 24A:2795-2805. 1990.

13. Iverfeldt, Å., and O. Lindqvist, Atmospheric oxidation of elemental mercury by ozone in the aqueous phase. *Atmospheric Environment* 20:1567-1573. 1986.

14. Munthe, J., Z. F. Xiao and O. Lindqvist, The aqueous reduction of divalent mercury by sulfite. *Water, Air and Soil Pollution,* 56:621-630. 1991.

15. Munthe, J. and W. McElroy, Some aqueous reactions of potential importance in the atmospheric chemistry of mercury. *Atmospheric Environment* 26A: 553-557. 1992.

16. Schroeder, W. H. and R. A. Jackson, Environmental measurements with an atmospheric mercury monitor having speciation capabilities. *Chemosphere* 16:183-199. 1987.

17. Schroeder, W. H., G. Yarwood and H. Niki., Transformation processes involving mercury species in the atmosphere - Results from a literature survey. Wat. Air Soil Pollut. 56:653-666. 1991.

18. Sanemasa, I., The solubility of elemental mercury vapor in water. *Bulletin of the Chemical Society of Japan,* 48:1795-1798. 1975.

19. Seinfeld, J. H., Atmospheric Chemistry and Physics of Air Pollution, John Wiley and Sons, New York, NY. 1986.

20. Hanson, P.•J., S. E. Lindberg, K. H. Kim, J. G. Owens, and T. A. Tabberer, Air/surface exchange of mercury vapor in the forest canopy: I. Laboratory studies of foliar mercury vapor exchange. International Conference on Mercury as a Global Pollutant, July 10-14, Whistler, British Columbia, Canada. 1994.

21. Lindberg, S. E., T. P. Meyers, G. E. Taylor, Jr., R. R. Turner and W. H. Schroeder, Atmosphere-surface exchange of mercury in a forest: Results of modeling and gradient approaches. *Journal of Geophysical Research* 97:2519-2528. 1992.

22. Walcek, C. J., R. A. Brost, J. S. Chang and M. L. Wesely, SO_2, sulfate and HNO_3 deposition velocities computed using regional land use and meteorological data. *Atmospheric Environment* 20:949-964. 1985.

23. Wesely, M. L., 1986. On the parameterization of dry deposition of acidifying substances for regional models. Internal Report (Nov. 1986): Interagency Agreement DW89930060-01 to the U.S. Department of Energy, U.S. Environmental Protection Agency, Atmospheric Sciences Research Laboratory, Research Triangle Park, NC.

24. Lindberg, S. E., R. R. Turner, T. P. Meyers, G. E. Taylor, Jr. and W. H. Schroeder, Atmospheric concentrations and deposition of mercury to a deciduous forest at Walker Branch Watershed, Tennessee, USA. *Water, Air and Soil Pollution* 56:577-594. 1991.

25. Deposition rate calculations for air toxics source assessments. Report dated September 16, 1987, by California Air Resources Board, 6 pp. 1987.

26. Fitzgerald, W. F., R. P. Mason and G. M. Vandal., Atmospheric cycling and air-water exchange of mercury over mid-continental lacustrine regions. Wat. Air Soil Pollut. 56:745-767. 1991.

27. Burke, J., M. Hoyer, G. Keeler and T. Scherbatskoy., Wet deposition of mercury and ambient mercury concentrations at a site in the Lake Champlain basin. Wat. Air Soil Pollut. 80:353-362. 1995.

28. Lamborg, C. H., W. F. Fitzgerald, G. M. Vandal and K. R. Rolfhus., Atmospheric mercury in northern Wisconsin: Sources and species. Wat. Air Soil Pollut. 80:189-198. 1995.

29. Dvonch, J. T., A. F. Vette, G. J. Keeler, G. Evans and R. Stevens., An intensive multi-site pilot study investigating atmospheric mercury in Broward County, Florida. Wat. Air Soil Pollut. 80:169-178. 1995.

30. Glass, G. E., J. A. Sorenson K. W. Schmidt, G. R. Rapp, Jr., D. Yap and D. Fraser., Mercury deposition and sources for the upper Great Lakes region. Wat. Air Soil Pollut. 56:235-249. 1991.

31. Sorenson, J. A., G. E. Glass and K. W. Schmidt., Regional patterns of wet mercury deposition. Environ. Sci. Technol. 28:2025- 2032. 1994.

32. Hoyer, M., J. Burke and G. Keeler., Atmospheric sources, transport and deposition of mercury in Michigan: Two years of event precipitation. Wat. Air Soil Pollut. 80:199-208. 1995.

33. Overcamp, T.J. *Modelling of Air Quality for Industrial Pollution Control,* Appendix from a Continuing Education Short course taught at Clemson University on December 7, 1977.

34. Rao, K.S. Analytical solutions of a gradient-transfer model for plume deposition and sedimentation. NOAA-TM-ERL ARL-109. U.S. National Oceanic and Atmospheric Administration, Silver Spring, MD. 1981.

35. U.S. EPA, *User's Guide for the Industrial Source Complex (ISC2) Dispersion Models, Volume II - Description of Model Algorithms,* EPA-450/4-92-008b, Research Triangle Park, North Carolina 27711. 1992.

36. Randerson, D., D. Randerson, editor, *Atmospheric Science and Power Production,* DOE/TIC-27601. 1984.

37. Hanna, S.R., G.A. Briggs, and R.P. Hosker, Jr. Handbook on Atmospheric Diffusion, DOE/TIC-11223. Pp. 2-3. 1982.

38. Wark, K. and C.F. Warner *Air Pollution Its Origin and Control,* Harper Collins. 1981.

39. Pasquill, F. The Estimation of Dispersion of Windborne Material, *Meteorol.Mag.*, 90:33-49. 1961.

40. Gifford, F.A. 1961. Use of routine meteorological observations for estimating atmospheric dispersion. Nuclear Safety, 2, No. 4, 47-51.

41. Hanna, S.R., G.A. Briggs, and R.P. Hosker, Jr. Handbook on Atmospheric Diffusion, DOE/TIC-11223. 1982.

42. Gifford, F.A. Turbulent Diffusion Typing Schemes - A Review, *Nucl.Saf.*, 17:68-86. 1976.

43. Smith, M.E., The Forecasting of Micrometerological Variables, *Meteorol. Monogr.*, 4:50-55. 1951.

44. Cramer, H.E. A Practical Method for Estimating the Dispersal of Atmospheric Contaminants, in *Proceedings of the First National Conference on Applied Meteorology,* Sec. C, pp. C-33-C-35, American Meteorological Society, Hartford, Conn. 1957.

45. Irwin, J. Estimating Plume Dispersion: A Recommended Generalized Scheme, in *Proceedings of the Fourth Symposium on Turbulence, Diffusion, and Air Pollution,* Jan. 15-18, 1979, Reno, Nev., pp. 62-69, American Meteorological Society, Boston, Mass. 1979.

46. Catalano, J.A., D.B. Turner, and J.H. Novak. *User's Guide for RAM — Second Edition.* EPA/600/8-87/046, U.S. EPA, Research Triangle Park, North Carolina. 1987.

47. Pierce, T.E. and D.B. Turner, User's Guide for MPTER: A multiple point Gaussian dispersion algorithm with optional terrain adjustment. EPA-600/8-80-016. U.S. E.P.A., Research Triangle Park, N.C. 1980

48. Wells, A.E. , Results of Recent Investigations of the Smelter Smoke Problem, *Ind. Eng. Chem,* 9:640-646. 1917.

49. Pasquill, F., *Atmospheric Diffusion, the Dispersion of Windborne Material from Industrial and other Sources,* Ellis Horwood, New York. 1974.

50. Briggs, G.A. *Plume Rise*, AEC Critical Review Series, TID - 25075, National Technical Information Service, Springfield, VA., 81 pp. 1969.

51. Briggs, G.A. Some recent analyses of plume rise observation, Paper presented at the Second International Clean Air Congress of the International Union of Air Pollution Prevention Associations, Washington, D.C., December 6-11, 1970.

52. Briggs, G.A. Discussion on Chimney Plumes in Neutral and Stable Surroundings. *Atmos. Environ.* 6:507-510. 1972.

53. Bowers, J.R., J.R. Bjorkland and C.S. Cheney. Industrial Source Complex (ISC) Dispersion Model User's Guide. Volume I, EPA-450/4-79-030, U.S. EPA, Research Triangle Park, North Carolina. 1979.

54. Briggs, G.A., Plume Rise predications, in *Lectures on Air Pollution and Environmental Impact Analysis,* American Meteorological Society, Boston, Massachusetts. 1975.

55. Ref. 52, p. 1030.

56. Ref. 41, p. 14.

57. Fay, J.A., M. Escudier, and D.P. Hoult, A Correlation of Field Observations of Plume Rise, Fluid Mechanics Laboratory Publication No. 69-4, Massachusetts Institute of Technology. 1969.

58. Rao, K.S. and L. Satterfield. A study of the probable environmental impact of fugitive coal dust emissions at the Ravenswood Power Plant, New York. ATDL Contribution 80/26, NOAA, Oak Ridge, TN. 1980.

59. Subroutines for Calculating Dry Deposition Velocities Using Sehmel's Curves. Prepared by Bart Croes, California Air Resources Board. 1986.

60. Holzworth,G.C., Mixing Heights, Wind Speeds and Potential for Urban Air Pollution Throughout the Contiguous United States. Publication No.AP-101, U.S. EPA, Research Triangle Park, North Carolina 27711. 1972.

61. Turner, D.B., *Workbook of Atmospheric Dispersion Estimates.* Public Health Service Publication No. 999-AP-26, U.S. E.P.A., Research Triangle Park, N.C. 1970.

62. Sehmel,G.A., Deposition and Resuspension, in *Atmospheric Science and Power Production,* D. Randerson (Ed.), DOE/TIC-27601. 1984.

63. Slinn, W.G.N. Precipitation Scavenging, in Atmospheric Science and Power Production, D. Randerson, ed. DOE/TIC-27601. 1984.

64. PEI Associates, Inc, and H.E. Cramer Company, Inc., Air quality modeling analysis of municipal waste combustors. Prepared for Monitoring and Data Analysis Division, Office of Air Quality Planning and Standards, Research Triangle Park, North Carolina 27711. 1986.

65. Engelmann, R.J. The Calculation of Precipitation Scavenging, in *Meteorology and Atomic Energy 1968,* D.H. Slade, editir. U.S. Atomic Energy Commission. 1968.

66. Briggs, G.A., *Diffusion Estimation for Small Emissions,* Atmospheric Turbulance and Diffusion Laboratory, Contribution File No. 79, Oak Ridge, Tennessee. 1973.

67. Egan, B.A., Turbulent Diffusion in Complex Terrain, in *Lectures on Air Pollution and Environmental Impacts Analysis,* pp. 112-135, D.Haugen (Ed.), American Meteorological Society, Boston, Mass. 1975.

68. Sherlock, R.H. and E.A. Stalker, A Study of Flow Phenomena in the Wake of Smoke Stack, *Engineering Research Bulletin* 29, University of Michigan, Ann Arbor. 1941.

69. Briggs, G.A., Diffusion Estimation for Small Emissions. In ERL, ARL USAEC Report ATDL-106. U.S. Atomic Energy Commission, Oak Ridge, Tennessee. 1974.

70. Huber, A.H. Incorporating Building/Terrain Wake Effects on Stack Effluents, in *Preprints of Joint Conference on Applications of Air Pollution Meteorology,* Salt Lake City, Nov. 29-Dec.2, pp. 353-356, American Meteorological Society, Boston, Mass. 1977.

71. Hubert, A.H. and W.H. Snyder (1976). Building Waste Effects on Short Stack Effluents, in *Third Symposium on Atmospheric Turbulence, Diffusion, and Air Quality,* Raliegh, NC, Oct. 19-22, pp. 235-242, American Meteorological Society, Bostan, Mass.

72. Ref. 35, p. 1-20.

73. Ref. 36, p. 303.

74. Ref. 36, p. 303.

75. Ref. 35, p. 1-24.

76. Pasquill, F., *Atmospheric Dispersion Parameters in Gaussian Plume Modeling: Part II. Possible Requirements for Change in Turner Workbook Values,* Report EPA-600/4-760306, U.S. EPA. 1976.

77. U.S. EPA. *Methodology for Assessing Health Risks Associated with Indirect Exposure to Combustor Emissions.* Interim Final. Office of Health and Environmental Assessment, Cincinnati, Ohio. EPA/600/6-90/003. 1990.

78. Wischmeier, W.H. and D.D. Smith., *Predicting Rainfall Erosion Losses — A Guide to Conservation Planning.* USDA Handbook No. 537. 1978.

79. Travis, C.C., C.F. Baes, III, L.W. Barnthouse, et al., *Exposure Assessment Methodology and Reference Environments for Synfuel Risk Analysis.* Oak Ridge National Laboratory. ORNL/TM-8672. Prepared for U.S. Environmental Protection Agency, Office of Research and Development. 1983.

80. Whitman, R.G., A Preliminary Experimental Confirmation of the Two-Film Theory of Gas Absorption. Chem. Metallurg. Eng. 29:146-148. 1923.

81. Burns, L.A., D.M. Cline, and R.R. Lassiter. Exposure Analysis Modeling System (EXAMS): User Manual and System Documentation, U.S. Environmental Protection Agency, Athens, GA. EPA-600/3-82-023. 1982.

82. Ambrose, R.B. et al. WASP4, A Hydrodynamic and Water Quality Model--Model Theory, User's Manual, and Programmer's Guide. U.S. Environmental Protection Agency, Athens, GA. EPA/600/3-87-039. 1988.

83. Geraghty, J.J., D.W. Miller, F.V. Der Leenden, and F.L. Troise, *Water Atlas of the United States,* A Water Information Ceter Publication, Port Washington, N.Y. 1973.

84. O'Connor, D.J. and W.E. Dobbins., Mechanism of Reaeration in Natural Streams, ASCE Transactions, pp. 641-684, Paper No. 2934. 1958.

85. O'Connor, D.J., Wind Effects on Gas-Liquid Transfer Coefficients. Journal of Environmental Engineering, Volume 109, Number 9, pp. 731-752. 1983.

TECHNICAL REPORT DATA

(Please read Instructions on reverse before completing)

1 REPORT NO	2.	3. RECIPIENT'S ACCESSION NO.
EPA-453/R-96-013c		

4 TITLE AND SUBTITLE	5. REPORT DATE
Study of Hazardous Air Pollutant Emissions from Electric Utility Steam Generating Units -- Interim Final Report Volume 3. Appendices H - M	October 1996
	6 PERFORMING ORGANIZATION CODE
7 AUTHOR(S)	8. PERFORMING ORGANIZATION REPORT NO
9 PERFORMING ORGANIZATION NAME AND ADDRESS U.S. Environmental Protection Agency Emission Standards Division/Air Quality Strategies and Standards Division Office of Air Quality Planning and Standards Research Triangle Park, NC 27711	10. PROGRAM ELEMENT NO.
	11 CONTRACT/GRANT NO
12 SPONSORING AGENCY NAME AND ADDRESS	13. TYPE OF REPORT AND PERIOD COVERED
	14 SPONSORING AGENCY CODE
15 SUPPLEMENTARY NOTES	

16 ABSTRACT

This report has been prepared pursuant to section 112(n)(1)(A) of the Clean Air Act, and provides the Congress and the public with information regarding the emissions, fate, and transport of utility HAPs. The primary components of this report are: (1) a description of the industry; (2) an analysis of emissions data; (3) an assessment of hazards and risks due to inhalation exposures to numerous HAPs (excluding mercury); (4) an assessment of risks due to multipathway (inhalation plus non-inhalation) exposure to radionuclides; and (5) a discussion of alternative control strategies. The assessment for mercury includes a description of emissions, deposition estimates, control technologies, and a dispersion and fate modeling assessment which includes predicted levels in various media based on modeling from four representative utility plants using hypothetical scenarios. The EPA plans to publish a final report at a later date which will include (1) a more complete assessment of the exposures, hazards, and risks; (2) conclusions, as appropriate and feasible, regarding the significance of the risks and impacts to public health; and (3) a determination as to whether regulation of utility HAPs is appropriate and necessary.

17 KEY WORDS AND DOCUMENT ANALYSIS

a DESCRIPTORS	b IDENTIFIERS/OPEN ENDED TERMS	c. COSATI Field/Group
Air Pollution Atmospheric Dispersion Modeling Electric Utility Steam Generating Units Hazardous Air Pollutants/Air Toxics	Air Pollution Control	

18. DISTRIBUTION STATEMENT	19. SECURITY CLASS *(Report)*	21. NO. OF PAGES
Release Unlimited	Unclassified	286
	20. SECURITY CLASS *(Page)*	22. PRICE
	Unclassified	